REPORT DOCUMENTATION PAGE

1a. REPORT SECURITY CLASSIFICATION Unclassified	1b. RESTRICTIVE MARKINGS None
2a. SECURITY CLASSIFICATION AUTHORITY	3. DISTRIBUTION/AVAILABILITY OF REPORT Approved for public release; distribution is unlimited.
2b. DECLASSIFICATION/DOWNGRADING SCHEDULE	
4. PERFORMING ORGANIZATION REPORT NUMBER(S) NORDA Technical Note 370	5. MONITORING ORGANIZATION REPORT NUMBER(S) NORDA Technical Note 370
6. NAME OF PERFORMING ORGANIZATION Naval Ocean Research and Development Activity	7a. NAME OF MONITORING ORGANIZATION Naval Ocean Research and Development Activity
6c. ADDRESS *(City, State, and ZIP Code)* Ocean Science Directorate NSTL, Mississippi 39529-5004	7b. ADDRESS *(City, State, and ZIP Code)* Ocean Science Directorate NSTL, Mississippi 39529-5004
8a. NAME OF FUNDING/SPONSORING ORGANIZATION Naval Ocean Research and Development Activity 8b. OFFICE SYMBOL *(If applicable)*	9. PROCUREMENT INSTRUMENT IDENTIFICATION NUMBER
8c. ADDRESS *(City, State, and ZIP Code)* Ocean Science Directorate NSTL, Mississippi 39529-5004	10. SOURCE OF FUNDING NOS. PROGRAM ELEMENT NO.: 61153N PROJECT NO.: 3205, 3208 TASK NO.: 3GO, 3HO WORK UNIT NO.: 13217E/132 37D/13317G 13217J/132 37F/13317V
11. TITLE *(Include Security Classification)* Inverted Echo Sounder Data Near the New England Seamounts 1985-1986	
12. PERSONAL AUTHOR(S) Zachariah R. Hallock and William J. Teague	
13a. TYPE OF REPORT Final	13b. TIME COVERED From _____ To _____
14. DATE OF REPORT *(Yr., Mo., Day)* September 1987	15. PAGE COUNT 165
16. SUPPLEMENTARY NOTATION	

17. COSATI CODES			18. SUBJECT TERMS *(Continue on reverse if necessary and identify by block number)*
FIELD	GROUP	SUB. GR.	GEOSAT, topography, satellite, echo sounders, AXBT probes, thermocline depth, moored instrumentation, LORAN

19. ABSTRACT *(Continue on reverse if necessary and identify by block number)*

A major component of the field activities for the Northwest Atlantic Regional Energetics Experiment (REX) is focused on collecting and analyzing data from inverted echo sounders (IESs). These instruments provide information concerning the height of the sea surface, as well as information concerning movement of the Gulf Stream and mesoscale features in the REX area. In this report the collection, processing, and preliminary analysis of the IES data and the associated ship expendable bathythermograph and conductivity-temperature-depth data are described, and various plots are presented. These data are generally of good quality and constitute a significant contribution to our understanding of Gulf Stream dynamics.

20. DISTRIBUTION/AVAILABILITY OF ABSTRACT UNCLASSIFIED/UNLIMITED ☐ SAME AS RPT. ■ DTIC USERS ☐	21. ABSTRACT SECURITY CLASSIFICATION Unclassified
22a. NAME OF RESPONSIBLE INDIVIDUAL Zachariah R. Hallock	22b. TELEPHONE NUMBER *(Include Area Code)* (601) 688-5242 22c. OFFICE SYMBOL Code 331

DD FORM 1473, 83 APR EDITION OF 1 JAN 73 IS OBSOLETE.

Naval Ocean Research and
Development Activity
NSTL, Mississippi 39529-5004

NORDA Technical Note 370
September, 1987

Inverted Echo Sounder Data Near the New England Seamounts 1985–1986

Zachariah R. Hallock
William J. Teague
Oceanography Division
Ocean Science Directorate

Executive Summary

A major component of the field activities for the Northwest Atlantic Regional Energetics Experiment (REX) is focused on collecting and analyzing data from inverted echo sounders (IESs). These instruments provide information concerning the height of the sea surface, as well as information concerning movement of the Gulf Stream and mesoscale features in the REX area. In this report the collection, processing, and preliminary analysis of the IES data and the associated ship expendable bathythermograph and conductivity-temperature-depth data are described, and various plots are presented. These data are generally of good quality and constitute a significant contribution to our understanding of Gulf Stream dynamics.

Acknowledgments

Field instruction and assistance, provided by Dr. Randy Watts, Mr. Gerry Chaplin, and Mr. Mike Mulroney of the University of Rhode Island in the deployment and recovery of inverted echo sounders, were invaluable and are greatly appreciated. Support from Mr. Steve Sova and Mr. Richard Myrick of NORDA, Mr. Lou Banchero, formerly of NORDA, and Dr. Laury Miller of NOAA NGS are gratefully acknowledged. Thanks are extended to the crew of the U.S.N.S. *Bartlett*, who made this data collection effort possible. Data reduction and plotting were primarily done by Ms. Jan Dastugue of Planning Systems, Incorporated. This work was supported by the Office of Naval Research under Program Element 61153N, Dr. H. C. Eppert, Jr., Program Manager, as part of the basic research project, Ocean Dynamics from Altimetry.

Contents

Inverted Echo Sounder Data Near the New England Seamounts 1985–1986

Introduction

Developing a suitable satellite system for the global observation of the world's oceans is rapidly becoming a major thrust within the oceanographic research and development communities. Much of this effort within the U.S. Navy is appropriately focused upon mission planning for the Navy satellite systems scheduled for launch during the next decade. A major focal point for interim activity, however, is the U.S. Navy GEOdesy SATellite, launched in March 1985, and the associated Northwest Atlantic Regional Energetics Experiment (REX) (Mitchell et al., 1985). The REX represents the first concurrent application of several developing oceanographic techniques. The goal is to increase the fundamental, process-oriented knowledge of the dynamics and energetics of the Gulf Stream and associated rings. The major experiment (Fig. 1) centers around the analysis of:

- topographic data from the U.S. Navy GEOSAT;
- long time series of sea surface and thermocline fluctuations collected via arrays of Inverted Echo Sounders with Pressure Gauges (IES/PG);
- extensive Airborne Expendable Bathythermograph (AXBT) surveys;
- regional eddy-resolving numerical model results (using much of the data as model input and as a means of refining model dynamics).

Field activities for the REX focus on collecting and analyzing data from regional AXBT surveys (using the Naval Research Laboratory's P-3 aircraft) and from arrays of bottom-moored IES/PGs deployed slightly up- and downstream of the New England Seamount Chain (Mitchell and Hallock, 1984). Figure 2 shows the arrays of IES/PGs, which were deployed by NORDA across the mean axis of the Gulf Stream in June 1985, and were recovered in July 1986 during a joint NORDA-University of Rhode Island (URI) effort. Of the 13 NORDA instruments, 12 were successfully recovered (one instrument not recovered was located, but would not release its anchor) along with 10 URI IESs. Another NORDA IES deployment is scheduled for the same region in August 1987. Thus far, four AXBT surveys have been made: May, August, and December 1985 (Mitchell et al., 1987; Teague et al., 1987; Hallock et al., 1987), and December 1986 (report in progress). Additional AXBT surveys are planned during 1987–1988. This report describes the IES data and the complementary ship-acquired data in detail.

Background

The capability to monitor and describe fluctuations in oceanic mesoscale features, such as the Gulf Stream and associated rings and eddies, is essential for understanding the evolution of such features. Traditionally, this has been accomplished with hydrographic surveys which are limited to relatively short time intervals with current meter moorings that are expensive and exclude the upper layers of the ocean in high-energy regions. More recently, satellite infrared imagery has provided series of synoptic pictures of sea-surface temperature where major mesoscale features can often be seen in great detail. The latter technique sees only the surface signature; however, experience has shown that sea-surface temperature often provides a distorted picture of dynamically significant features and, in some cases, fails to see them at all.

In the past decade an elegant, new technique for obtaining time series of changes in first-mode baroclinic features has evolved as the inverted echo sounder (IES). The IES is a bottom-moored, upward-looking echo sounder, which records time series of round-trip acoustic travel time (TT) to the sea surface. The entire mooring configuration is compact, weighs about 250 lb in air, and extends 2 m above the bottom. Changes in the thermal structure of the intervening water column (i.e., raising or lowering of the thermocline) and, to a lesser extent, changes in sea-surface height, result in changes in TT. Changes in the depth of the thermocline are indicative of movement of such mesoscale ocean features, as eddies or current meanders.

The method of acoustically monitoring the depth of the thermocline was first proposed by H. T. Rossby (1969). The first scientific use of the IES was related by Watts and Rossby (1977). Many experiments using IESs have subsequently been undertaken by Watts and his associates.

Until about 1983, IESs were obtainable through URI but were not commercially available. Subsequently, the Sea Data Corporation (SDC) of Newton,

Massachusetts, became the first to offer the IES to the general oceanographic community. NORDA made the first major purchase of 15 units in 1984, which were used in a field program in the eastern Gulf Stream region (Mitchell et al., 1985). The IESs procured by NORDA also incorporate precision pressure sensors, temperature sensors, and ambient noise receivers to provide additional data with TT.

The IES is moored with an expendable anchor that is jettisoned by an acoustically operated release mechanism. In principle, IES deployment and recovery procedures are similar to those used for current-meter moorings. The moorings, however, are usually much larger than an IES, so fewer current-meter mooring deployments (e.g., 1–5) than IES deployments are feasible for a given cruise. Consequently, many IESs can be deployed or recovered on a single cruise (up to about 25), since deployment requires only about 1 hour and recovery about 3 hours. Deployment and recovery procedures are discussed by Teague and Hallock (1987). The analysis and interpretation of IES observations are discussed elsewhere (Hallock, 1987; Watts and Rossby, 1977).

Instrument Description

The Sea Data Model 1665 IES (Fig. 3) weighs about 150 lb in air; the anchor adds about 100 lb. The IES electronics package is housed in a 17-inch-diameter glass sphere near the top of the fiberglass shroud. Additional flotation (a 13-inch sphere) is located in the lower part. The anchor line (¼-inch nylon braid) is shackled to several links of stainless steel chain, which is, in turn, secured to a hinged pin in an assembly (known as a release block) on the bottom of the shroud. Electrical connections run through the large sphere to the release block and to the transducer, which is located on the top of the shroud. When deployed, the IES floats about 1 m above the bottom with its transducer pointed upward. Tethered to the protective bale around the transducer, a 10-inch glass sphere floats about 10 m above the IES. The 10-inch sphere contains a radio beacon and strobe, which are activated whenever the sphere is rotated from its deployed position. During normal operation, the IES samples pressure, temperature, ambient noise, and a burst of up to 24 travel times over a period of several minutes during each sampling interval (e.g., 1 hour).

The 1665 IES uses the Paroscientific 10,000 psi DIGIQUARTZ quartz pressure sensor for extreme pressure accuracy and resolution. The pressure channel measures with a resolution of about 1:1,000,000 (0.01 psi or about 0.6 mb). Ambient noise is measured through a single WOTAN (Weather Observation Through Ambient Noise) channel at 10 kHz. Temperature is measured with a 0.1°C interchangeable thermistor, which has an overall accuracy of 0.15°C and a resolution of about 0.0007°C.

IES Data Processing

IES data are internally recorded on cassette tapes. These tapes are normally removed from the instrument at sea. At NORDA, data are transferred in hexidecimal format from the tapes to disk files on the Code 331 VAX 11/750 via the communications program VAXNET in conjunction with an SDC Asynchronous Reader Interface (ARI) connected to an SDC Model 12B Reader. Engineering data, recorded every 4 hours, are then separated from the IES data record. Engineering data include system voltages, currents, and other information useful for tracking the performance of the IES. The ASCII-encoded hexidecimal data are decoded and stored in a disk file in VFEB format, a standard format used by the Physical Oceanography Branch at NORDA. Each sample in this raw, unedited file consists of 28 variables: time, pressure, temperature, ambient noise, and 24 travel times. Appropriate calibrations are applied and the results written to another VFEB file consisting of five variables for each sample: time, pressure, temperature, ambient noise, and a single travel time.

For the data described in this report, single travel times were computed from three consecutive bursts (72 realizations) using the mode of the Rayleigh distribution (Watts and Rossby, 1977). Using three bursts instead of one reduced much of the noise in the data, which resulted from a travel-time detector problem that caused an abnormally high number of late or missed echoes (this detector problem is now believed to be fixed, but has not been field tested).

Pressure and temperature data were relatively clean and were despiked using a first difference test. Eight primary tidal constituents (O1, K1, Q1, P1, M2, K2, N2, and S2) were then subtracted from the pressure series. Resulting detided pressure data were then plotted, and any remaining pressure spikes were manually removed from the original pressure series. Amplitudes and phases of each tidal constituent provided a cross check on the absolute time attached to each record. To determine the long-term sensor drift, an exponential function was fitted to the low-pass filtered pressure series. The resulting exponential trend was subtracted from the unfiltered series.

Travel-time records contained noisy segments, which were identified by examining high-pass-filtered travel-time data. Questionable points and segments were removed from the original series.

Calibration and utility of the ambient noise measurements are uncertain at this time. No further reference is made to the ambient noise measurements in this report.

Final processed data are stored in VFEB format. Plots of the IES pressure, temperature, and travel time are presented in Figures 4–15, 16–27, and 28–39, respectively. Times and positions of the IES/PGs are given in Table 1.

Table 1. Times and positions of the IES/PGs.

IES No.	Latitude (N)	Longitude (W)	Depth (m)	Deployed	Recovered
IES85001	39°13.9′	067°28.5′	3580	30 May 85	10 July 86
IES85002	38°48.6′	067°33.3′	4125	30 May 85	10 July 86
IES85003	38°36.0′	067°02.8′	4465	31 May 85	11 July 86
IES85004	38°09.9′	067°09.9′	4620	31 May 85	11 July 86
IES85005	37°57.7′	066°39.3′	4765	1 June 85	11 July 86
IES85006	37°31.7′	066°47.6′	4910	1 June 85	12 July 86
IES85007	37°18.0′	066°17.3′	4950	1 June 85	11 July 86
IES85008	Not Recovered				
IES85009	40°23.4′	057°40.4′	5125	3 June 85	4 July 86
IES85010	40°01.3′	058°01.1′	5140	4 June 85	3 July 86
IES85011	39°40.0′	057°38.8′	5180	4 June 85	30 June 86
IES85012	39°18.1′	057°59.7′	5170	4 June 85	30 June 86
IES85013	38°58.5′	057°27.8′	5200	5 June 85	29 June 86

Table 2. Locations and times of casts.

CTD No.	Julian Day	Time (Z)	Latitude (N)	Longitude (W)	Cast Depth (m)
1001	150	0436	39°19.3′	67°28.7′	1213
2002	151	0403	38°47.4′	67°33.9′	2007
3003	151	1125	38°37.5′	67°2.2′	2001
4004	151	1910	39°9.0′	67°2.2′	712
7005	152	1409	37°19.1′	66°17.5′	2998
8006	154	1752	40°45.3′	57°59.8′	2013
9007	154	2343	40°24.3′	57°41.1′	2054
10008	155	0545	40°1.2′	57°59.2′	693
11009	155	1118	39°39.7′	57°36.1′	1994
12010	155	1813	39°16.9′	57°58.6′	2008
13011	155	2212	38°57.4′	57°39.7′	1987
4012	159	2142	38°12.5′	67°5.9′	1483

CTD Data Collection and Processing

CTD (conductivity-temperature-depth) data were acquired only during the deployment cruise. Location of the CTD stations is shown in Figure 40. A Neil Brown Instrument System, Inc. (NBIS) Mark III CTD unit was used for profiling conductivity and temperature versus pressure. Data were acquired at approximately 30 Hz as the CTD underwater unit was lowered at about 60 m/min. Data were recorded in full on nine-track digital tape and analog (audio) tape, and at about one sample per meter on diskette. Temperature, conductivity, and salinity profiles were plotted for all stations aboard ship for quality control.

Salinities of water samples obtained with a rosette sampler were determined using a Guildline salinometer according to the practical salinity scale 1978 algorithm (Lewis, 1980). CTD-obtained salinities, which were 0.018 psu lower than the salinities obtained from the water samples, were corrected accordingly. Accuracies of about 0.005 psu in salinity, 0.005°C in temperature, and 5 dbar in pressure are claimed.

Final data processing was performed at NORDA on the Physical Oceanography Branch's VAX 11/750 computer. All data were processed from the analog tapes because the digital tape recorder had a faulty buffer. Data processing consisted of editing, calibrating, matching temperature and conductivity response times, low-pass filtering and reducing to 1-m vertical levels, and computing derived quantities (salinity, density, Brunt-Vaisala frequency, and sound speed). A three-point matching filter (Fofonoff et al., 1974) with a time constant of 60 msec was used to compensate for the difference in response time between temperature and conductivity sensors. Some salinity spiking still exists in strong gradient regions. Both raw and final processed data are stored in VFEB format.

Graphs of the data (at 1-m levels) are presented in Figures 41–52 for quality assessment and analyses. Locations and times of the casts are given in Table 2.

XBT Data Collection and Processing

During the IES deployment cruise, XBT data (Fig. 53) were acquired with Sippican T-7 probes using a microcomputer (Hewlett-Packard 9825T) data acquisition system developed at NORDA (Holland et al., 1980). This system digitizes and records temperatures at 20 Hz for 2.5 minutes, which corresponds to a profile at a depth of about 950 m. Immediately following each drop, the data are recorded on cassette tape, and temperature is plotted versus depth.

During the IES recovery cruise, XBT data (Fig. 54) were acquired again with Sippican T-7 probes; however, a Bathy Systems data acquisition system using a Hewlett-Packard 85 computer was used. This system digitizes and records temperatures at 10 Hz to a depth of about 900 m. Similarly, following each drop, the data are recorded on cassette tape, and temperature is plotted versus depth.

Final data processing was performed at NORDA on the VAX 11/750 computer. All data were transferred from the cassettes to disk files on the VAX. The data were then converted to physical units (meters and degrees Celsius), edited for spikes, and processed to 2-m levels. Manufacturer's standard conversion formulas were used to convert the voltage to temperature, and the time to depth. Raw data and final processed data are stored in VFEB format. Plots of the data are presented in Figures 55–104 for the IES deployment cruise and in Figures 105–139 for the IES recovery cruise. Times and locations of the drops are given for the deployment cruise in Table 3 and for the recovery cruise in Table 4.

Discussion

IES Temperatures

The IES temperature records exhibit significant variability about their averages, which range from 2.14 to 2.39°C. The root-mean-square (RMS) amplitude

Table 3. Times and locations of drops for the deployment cruise.

XBT No.	Julian Day	Time (Z)	Latitude (N)	Longitude (W)	Cast Depth (m)
1	150	2129	39°14.1′	67°27.7′	800
4	151	1351	38°29.0′	67°4.8′	800
5	151	1506	38°17.9′	67°6.3′	800
6	151	2057	38°9.0′	67°0.6′	800
7	151	2212	38°6.5′	66°45.0′	800
8	152	0120	37°58.4′	66°39.8′	800
9	152	0319	37°50.0′	66°43.5′	800
10	152	0428	37°40.5′	66°45.5′	800
11	152	0740	37°32.6′	66°47.3′	800
12	152	0910	37°27.7′	66°36.0′	800
13	152	1015	37°22.1′	66°26.6′	800
14	152	1410	37°18.6′	66°17.3′	800
15	154	2032	40°33.7′	57°50.2′	800
16	155	0247	40°11.7′	57°52.9′	800
17	155	0801	39°50.0′	57°51.5′	800
18	155	0812	39°48.3′	57°50.2′	800
19	155	1408	39°29.2′	57°48.4′	800
20	155	2003	39°11.0′	57°53.8′	800
21	155	2056	39°4.0′	57°46.5′	800
Begin Section 1					
22	156	0300	38°58.4′	57°21.2′	800
23	156	0330	38°54.8′	57°21.5′	800
24	156	0400	38°49.3′	57°22.4′	800
25	156	0430	38°46.6′	57°22.9′	800
26	156	0500	38°42.6′	57°24.0′	800
27	156	0530	38°38.2′	57°25.4′	800
28	156	0600	38°33.7′	57°27.1′	800
29	156	0630	38°29.3′	57°29.0′	800
30	156	0700	38°24.8′	57°30.8′	800
31	156	0730	38°20.5′	57°32.6′	800
32	156	0800	38°16.9′	57°35.6′	800
End Section 1					
Begin Section 2					
33	156	0945	38°19.2′	57°55.2′	800
34	156	1015	38°23.8′	57°55.7′	800
35	156	1045	38°28.7′	57°56.3′	800
36	156	1115	38°33.5′	57°56.6′	800
37	156	1145	38°38.5′	57°56.8′	800
38	156	1215	38°43.3′	57°56.5′	800
39	156	1245	38°48.2′	57°55.9′	800
40	156	1315	38°52.9′	57°55.2′	800
41	156	1345	38°57.6′	57°54.6′	800
42	156	1415	39°2.5′	57°54.6′	800
43	156	1445	39°7.0′	57°54.5′	800
44	156	1515	39°11.8′	57°54.5′	800
45	156	1545	39°16.4′	57°54.6′	800
47	156	1619	39°21.8′	57°54.6′	800
48	156	1645	39°26.3′	57°54.5′	800
49	156	1715	39°30.7′	57°54.5′	800
End Section 2					
50	156	1800	39°29.5′	58°2.0′	800
51	156	2100	39°22.1′	58°37.5′	800
52	157	0000	39°16.1′	59°15.5′	800
53	157	0202	39°13.7′	59°40.5′	800
54	157	0401	39°14.8′	59°53.7′	800
55	157	0602	39°15.1′	60°31.7′	800
56	157	0800	39°16.0′	60°56.9′	800
57	157	1000	39°12.0′	61°20.4′	800
58	157	1200	39°4.6′	61°38.5′	800
59	157	1500	38°58.3′	62°0.8′	800
60	157	1729	38°47.2′	62°4.9′	800
61	157	1931	38°38.3′	62°7.6′	800
62	157	2138	38°30.7′	62°13.8′	800
63	158	0000	38°25.6′	62°21.3′	800
64	158	0300	38°22.0′	62°30.5′	800
65	158	0307	38°20.4′	62°31.0′	800
67	158	0900	38°8.3′	62°53.7′	800
68	158	1202	38°7.3′	63°9.2′	800
69	158	1501	38°10.3′	63°32.2′	800
70	158	1800	38°12.6′	63°54.6′	800
71	158	2100	38°12.5′	64°16.8′	800
72	159	0000	38°22.3′	64°35.5′	800
73	159	0300	38°33.7′	64°53.8′	800
74	159	0600	38°29.2′	65°27.6′	800
75	159	0901	38°21.6′	65°47.7′	800
76	159	1200	38°19.7′	66°12.6′	800
77	159	1500	38°21.2′	66°37.8′	800
Begin Section 3					
78	159	1948	38°20.6′	67°9.2′	800
80	159	2042	38°15.1′	67°9.8′	800
81	159	2128	38°10.1′	67°10.2′	800
82	160	0102	38°5.0′	67°4.3′	800
83	160	0146	37°59.9′	67°5.6′	800
84	160	0229	37°55.0′	67°2.6′	800
85	160	0311	37°50.0′	66°59.6′	800
86	160	0352	37°45.0′	66°57.2′	800
87	160	0443	37°40.0′	66°53.9′	800
89	160	0547	37°33.3′	66°49.0′	800
Begin Section 4					
90	160	0632	37°32.1′	66°46.6′	800
End Section 3					
91	160	0746	37°38.8′	66°40.0′	800
92	160	0831	37°43.8′	66°33.9′	800
93	160	0902	37°48.5′	66°34.1′	800
94	160	0946	37°53.1′	66°38.4′	800
95	160	1018	37°58.0′	66°40.0′	800
96	160	1047	38°3.0′	66°41.2′	800
97	160	1118	38°8.0′	66°42.5′	800
98	160	1150	38°13.4′	66°45.0′	800
99	160	1230	38°18.0′	66°47.7′	800
100	160	1302	38°22.7′	66°48.4′	800
101	160	1347	38°27.9′	66°51.4′	800
102	160	1505	38°33.1′	66°59.1′	800
103	160	1635	38°38.0′	67°7.2′	800
104	160	1807	38°42.7′	67°21.5′	800
106	160	2033	38°49.4′	67°35.2′	800
107	160	2046	38°49.9′	67°36.8′	800
End Section 4					

about the mean ranges from 0.012 to 0.04°C. With the exception of IES001 the amplitudes are similar. They are slightly higher in the eastern array (IES009–IES013) than in the western array. The most energetic fluctuations in temperature appear to be several-day events interposed with relatively quiescent periods. IES001, however, shows about a three-fold increase in amplitude over the other records in the western

Table 4. Times and locations of the drops for the recovery cruise.

XBT No.	Julian Day	Time (Z)	Latitude (N)	Longitude (W)	Cast Depth (m)
1	172	1400	35°31.6′	73°23.1′	499
2	172	1415	35°31.8′	73°23.7′	793
3	174	0019	37°33.6′	70°58.0′	793
4	174	0214	37°48.7′	70°40.5′	793
5	174	0435	38°9.2′	70°25.5′	793
6	174	0744	38°0.5′	70°23.3′	485
7	174	0846	37°53.9′	70°16.5′	793
8	174	1130	37°47.4′	70°10.8′	793
9	174	1423	37°39.8′	70°6.2′	793
10	174	1526	37°31.7′	70°5.1′	793
11	174	1628	37°24.1′	70°0.6′	793
13	174	2248	37°9.8′	69°53.7′	285
113	174	2250	37°9.8′	69°53.7′	793
14	175	1632	37°31.0′	71°22.0′	793
15	175	1823	37°43.4′	71°29.3′	793
16	175	2030	37°54.5′	71°33.1′	793
17	176	0048	37°57.0′	71°52.5′	793
18	176	0259	38°5.0′	72°6.0′	793
19	177	1552	36°56.0′	71°52.8′	793
20	177	2100	36°58.3′	70°42.4′	793
21	178	0125	36°55.9′	69°45.0′	793
22	178	0433	36°41.1′	69°36.8′	793
23	178	0748	36°25.9′	69°29.2′	793
24	178	1346	37°0.5′	69°1.1′	793
25	178	2230	37°30.8′	67°37.2′	793
26	179	0121	37°46.4′	66°53.4′	793
27	179	0331	37°50.8′	66°20.2′	793
28	179	0520	37°56.7′	65°49.4′	793
29	179	0924	38°17.6′	64°39.6′	793
30	179	1330	38°38.6′	63°37.8′	793
31	179	1730	38°53.5′	62°43.1′	793
33	179	2129	39°12.7′	61°51.3′	793
34	179	2333	39°18.6′	61°25.6′	793
35	180	0303	39°21.5′	60°37.2′	793
36	180	0705	39°19.5′	59°32.2′	793
37	180	1105	39°11.4′	58°21.9′	793
38	180	1712	38°57.1′	57°28.4′	793
39	181	0000	39°7.4′	57°44.1′	793
40	181	0243	39°18.0′	57°59.8′	793
41	181	0618	39°28.5′	57°45.3′	793
42	181	0725	39°39.7′	57°38.0′	793
43	182	0821	39°27.3′	57°45.9′	793
44	182	1807	39°43.0′	57°59.1′	793
45	182	1910	39°34.0′	57°54.8′	793
46	182	2016	39°25.0′	57°50.0′	793
47	182	2126	39°15.7′	57°48.0′	793
48	182	2237	39°6.4′	57°42.4′	793
49	184	0329	40°1.9′	58°1.6′	129
149	184	0331	40°1.9′	58°1.6′	793
50	184	1415	40°1.6′	58°0.6′	219
51	184	1423	40°1.7′	58°0.7′	793
52	184	2356	40°44.8′	58°0.4′	539
53	185	0834	40°24.0′	57°41.0′	793
54	191	1605	39°21.7′	67°41.3′	793
55	191	1814	39°13.5′	67°28.0′	793
56	191	2136	39°0.9′	67°34.3′	793
57	191	2248	38°48.6′	67°33.1′	793
58	192	0203	38°42.0′	67°16.6′	793
59	192	0322	38°35.9′	67°2.4′	793
60	192	0735	38°15.5′	67°6.9′	793
61	192	0828	38°9.6′	67°8.3′	793
62	192	1126	38°5.3′	66°54.5′	793
63	192	1245	37°58.1′	66°39.7′	793
64	192	1940	37°18.0′	66°17.6′	793
65	193	0053	37°31.7′	66°47.8′	793
66	193	1629	37°34.1′	69°17.7′	793
67	193	2129	37°55.5′	69°22.2′	793
68	194	0022	38°5.9′	69°32.5′	793
69	194	1222	37°6.5′	70°26.5′	405
70	194	1232	37°5.8′	70°27.7′	793

array. The increase may be associated with bottom topography at this location.

IES Pressures

Semidiurnal and diurnal tidal components, with amplitudes of about 1 dbar, dominate the unfiltered pressure series (Figs. 4–15). After removal of periods shorter than about 40 hours, variability of several days to several weeks prevails (Figs. 140–151). In several records (e.g., IES004) seasonal-to-annual trends appear; these trends are questionable, since they are of the same time scale as the sensor drift described above. Several energetic events appear (e.g., IES006 near days 345 and 535), which were at first suspect. The nearly simultaneous occurrence of such features near the start of records IES009 and IES010 suggests that they are real, but that their cause is not clear. The weekly to monthly excursions are most likely associated with barotropic mesoscale changes. Low-level (0.05–0.10 dbar), three- to five-day oscillations throughout the presssure records may be associated with atmospheric events.

IES Travel Times

The dominant signal in the travel times is the baroclinic mesoscale variability. This signal is caused primarily by the meandering of the Gulf Stream and the passage of rings and eddies. Also evident are tidal frequency fluctuations with amplitudes of about 10% of that of the mesoscale signal. During a number of periods of up to two days' duration, no good echoes were received, resulting in broad spikes (e.g., IES001 near day 475). Since some of these spikes appear simultaneously in two or more adjacent records, they are probably the result of elevated noise levels during storms. These erroneous data are to be manually edited prior to analysis. The general character of the mesoscale variability seen in the travel-time records indicates vigorous Gulf Stream meandering over the entire domain of the IES arrays.

CTD Profiles

During the 1985 deployment, attempts were made to acquire CTD data at each IES site. The first three digits of the station coincide with the IES that has the same number. Wind and current conditions prevented successful casts at sites 5, 6, and 10 (a successful cast is one to a depth of at least 1200 m). The data that were acquired are of good quality, despite some problems during processing. Its primary use will be in IES calibration.

XBT Profiles

During the 1985 deployment, 100 good XBT profiles were acquired. Some of these profiles were used to locate the Gulf Stream and did not necessarily form part of a planned pattern. Some XBT drops were made at the IES sites to complement or to substitute for the CTD casts. Two continuous transects of the axis of the Gulf Stream were made in each of the two deployment areas. The drop separation was about 9 km and the sections were about 100 km long. The data from these four transects were contoured and appear as sections 1–4 (Figs. 152–155). Each shows the Gulf Stream, and dynamic computations imply a surface geostrophic current of about 200 cm/sec, which is consistent with ship-drift observations.

During the 1986 recovery cruise 70 good XBT profiles were acquired. Virtually all were for IES calibration and for Gulf Stream location, and no extensive transects were made. In addition to their primary purposes as stated, XBT observations from both cruises will be used to enhance regional statistics of hydrographic variability.

References

Fofonoff, N. P., S. P. Hayes, and R. D. Millard, Jr. (1974). WHOI/Neil Brown CTD Microprofiler: *Methods of Calibration and Data Handling*. Woods Hole Oceanographic Institution, Woods Hole, Massachusetts, Technical Report WHOI 74-89.

Hallock, Z. R. (in press). Regional Characteristics for Interpreting Inverted Echo Sounder (IES) Observations. *Journal of Atmospheric and Oceanic Technology* 4 (2), pp. 298–304.

Hallock, Z. R., W. J. Teague, J. L. Mitchell, and J. M. Dastugue (1987). REX AXBT *Data in the Northwest Atlantic, December 1985*. Naval Ocean Research and Development Activity, NSTL, Mississippi, NORDA Report 198.

Holland, C. R., R. T. Miles, and R. A. Brown (1982). *Operation and Maintenance Manual for the Expendable Probes Data Acquisition System*. Naval Ocean Research and Development Activity, NSTL, Mississippi, NORDA Technical Note 127.

Lewis, E. L. (1980). The Practical Salinity Scale 1978 and Its Antecedents. IEEE, *Journal of Oceanic Engineering* OE-5 pp. 3-8.

Mitchell, J. L. and Z. R. Hallock (1984). Plans for Oceanography from the U.S. Navy GEOSAT. *Proceedings of the Pacific Congress on Marine Technology* (PACON '84), April 24–27, Honolulu, Hawaii.

Mitchell, J. L., Z. R. Hallock, and J. D. Thompson (1983). The REX and the U.S. Navy GEOSAT. *Naval Research Reviews*, Office of Naval Research, Three/1985, Vol. XXXVII, pp. 16–23.

Mitchell, J. L., W. J. Teague, and Z. R. Hallock (1987). REX AXBT *Data in the Northwest Atlantic, May 1985*, Naval Ocean Research and Development Activity, NSTL, Mississippi, NORDA Report 196.

Rossby, H. T. (1969). On Monitoring Depth Variations of the Main Thermocline Acoustically. *Journal of Geophysical Research* 74:5542–5546.

Teague, W. J., Z. R. Hallock, J. L. Mitchell, and J. M. Dastugue (in press). REX AXBT *Data in the Northwest Atlantic, August 1985*. Naval Ocean Research and Development Activity, NSTL, Mississippi, NORDA Report 197.

Teague, W. J. and Z. R. Hallock (in press). *Deployment and Recovery Procedures for Inverted Echo Sounders*, Naval Ocean Research and Development Activity, NSTL, Mississippi, NORDA Technical Note 366.

Watts, D. R. and H. T. Rossby (1977). Measuring Dynamic Heights with Inverted Echo Sounders: Results from MODE. *Journal of Physical Oceanography* 7:345–358.

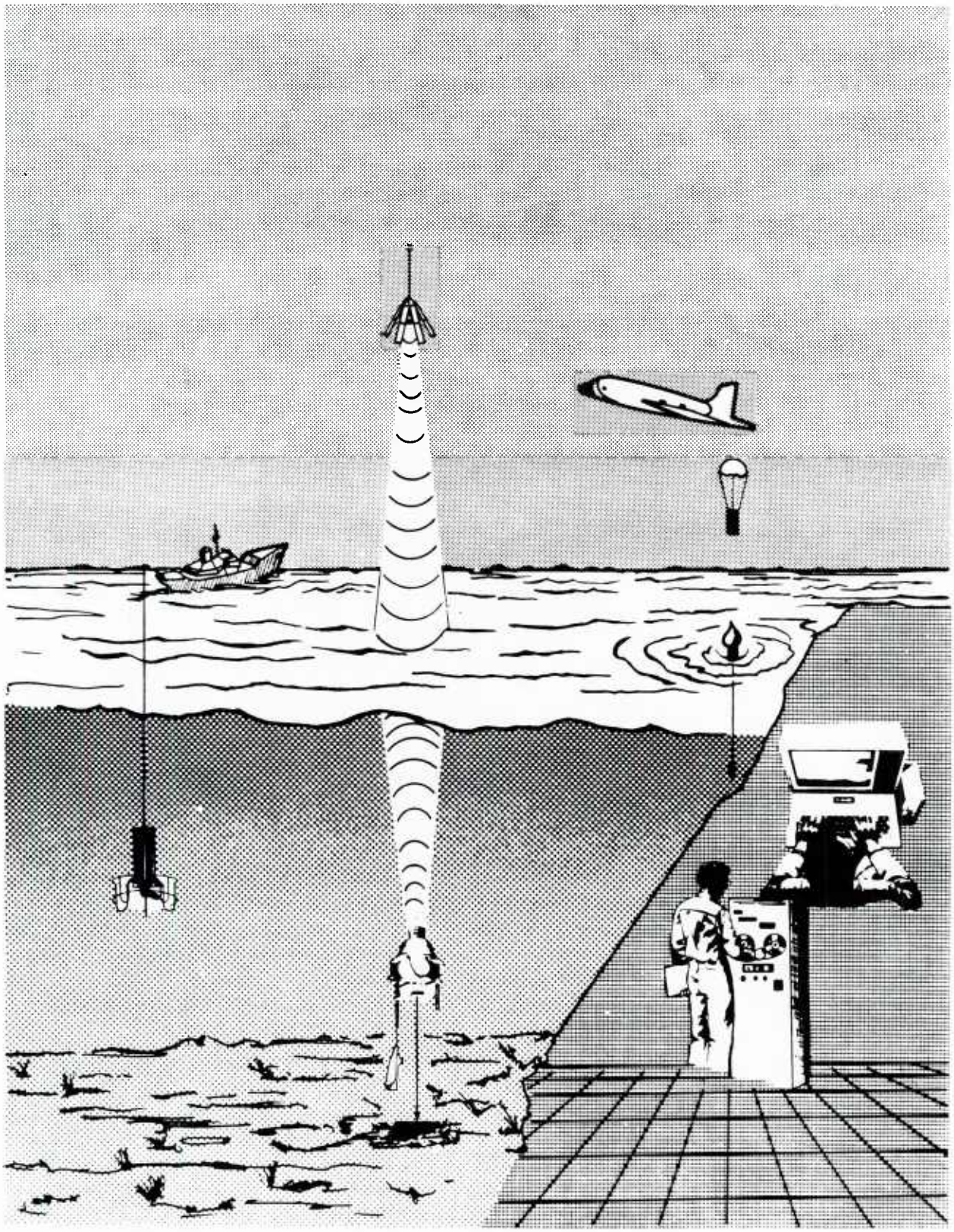

Figure 1. Artist's concept of the NW Atlantic Regional Energetics Experiment (REX). The major components of the REX are sea surface topography provided by the U.S. Navy GEOSAT, field data collected from bottom-moored Inverted Echo Sounders with Pressure Gauges (IES/PG) and regional AXBT surveys, and extensive regional numerical modeling studies.

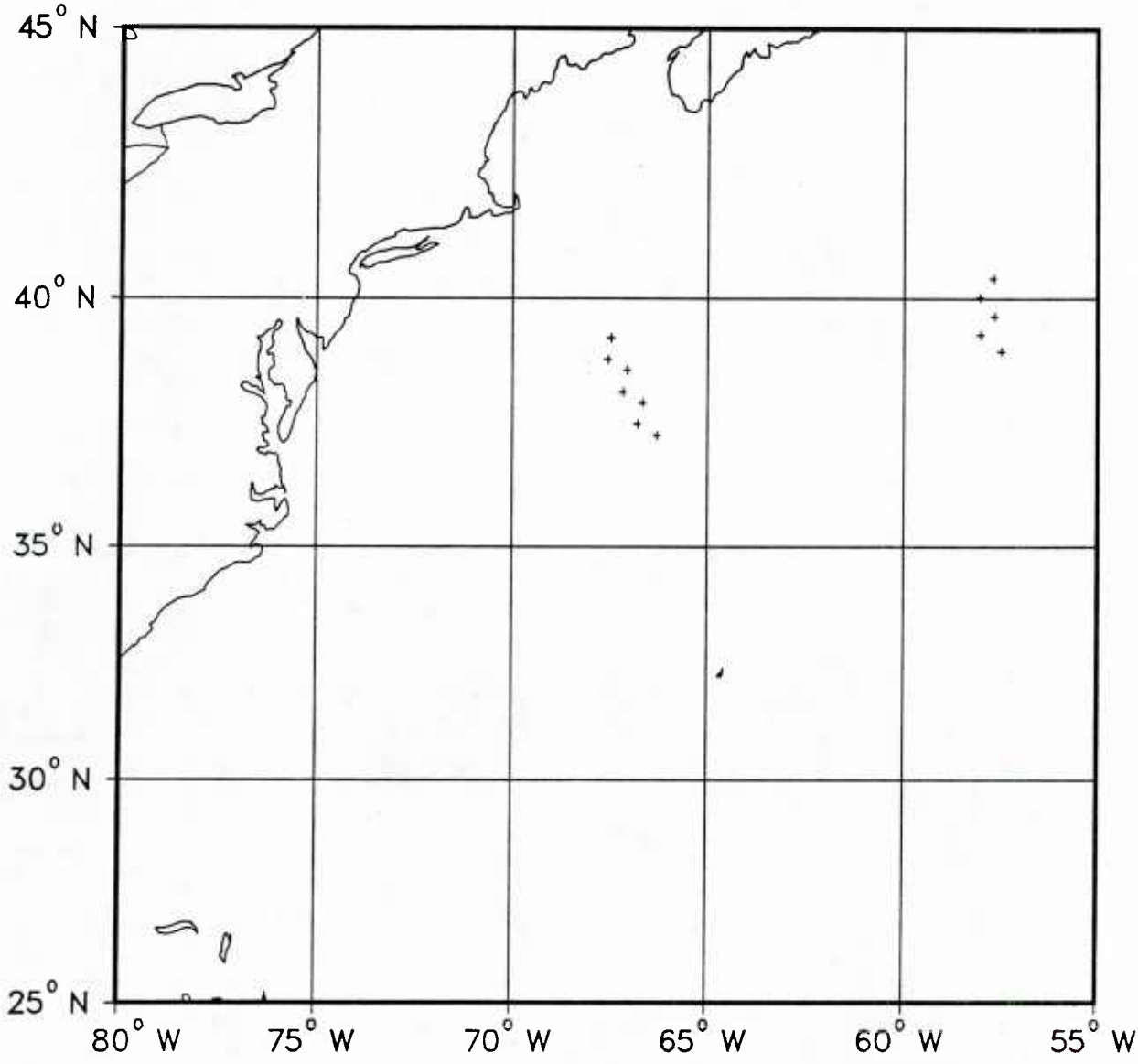

Figure 2. Inverted Echo Sounder locations.

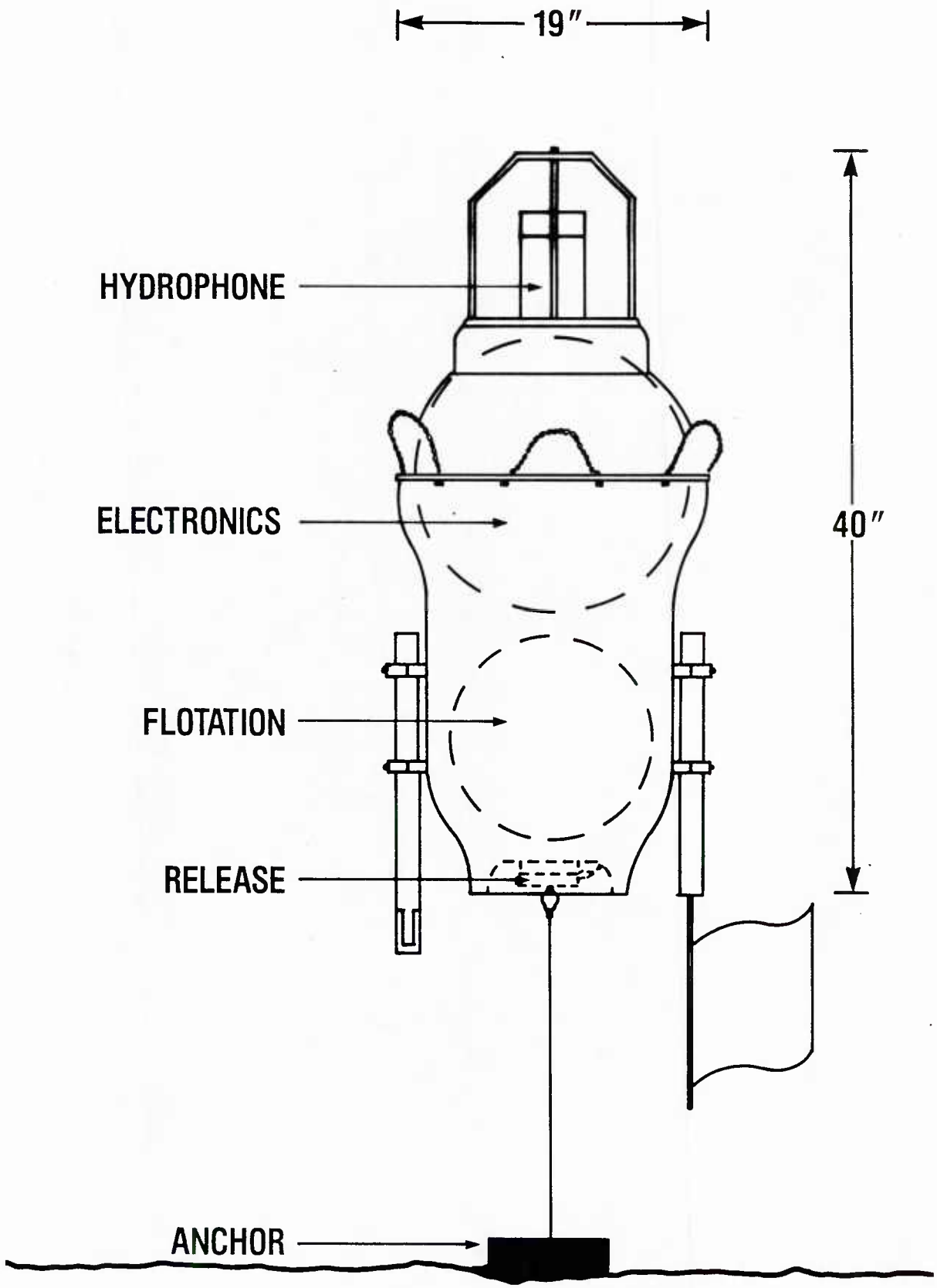

Figure 3. Sea Data Model 1665 Inverted Echo Sounder.

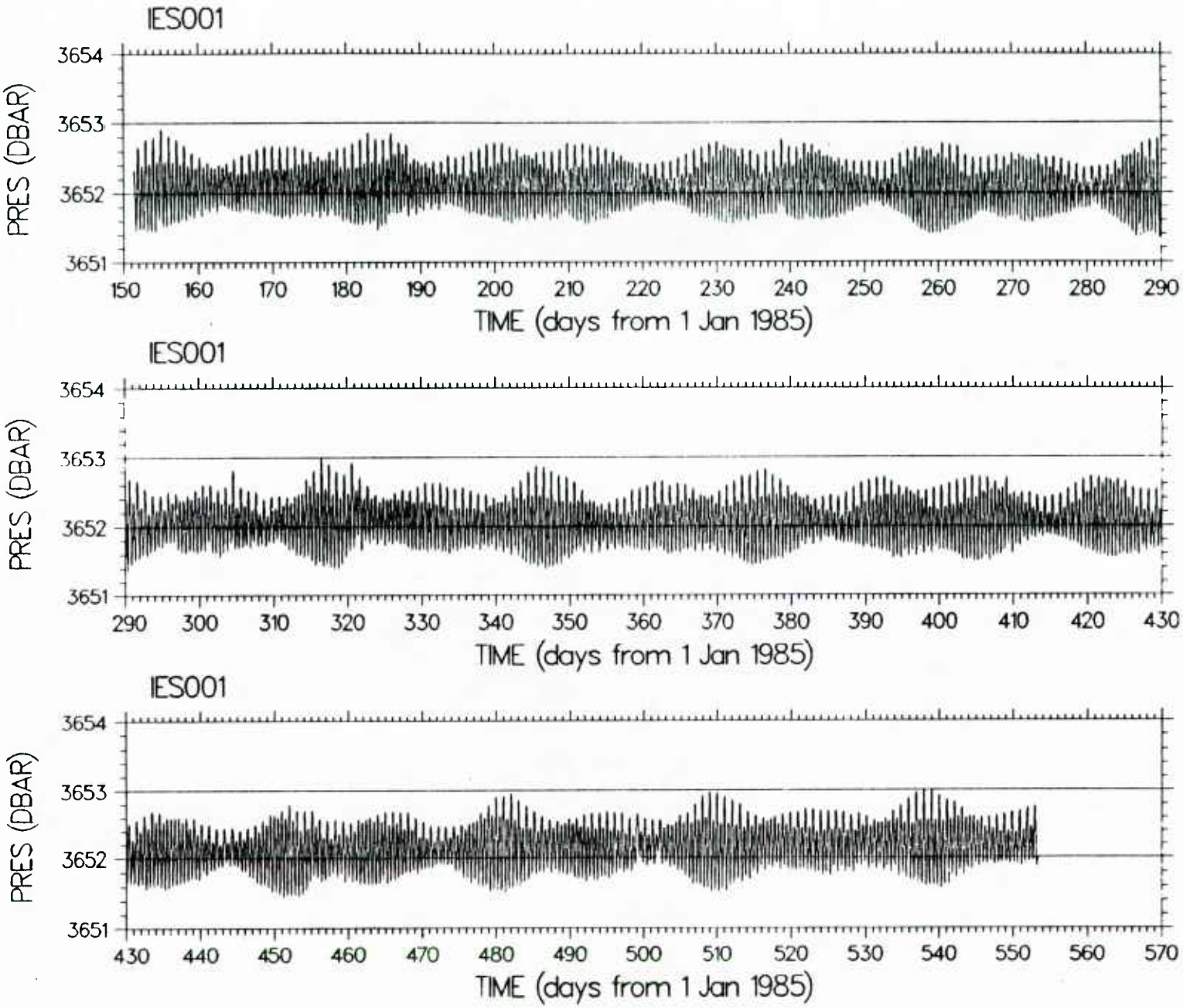

Figure 4. Unfiltered pressure record.

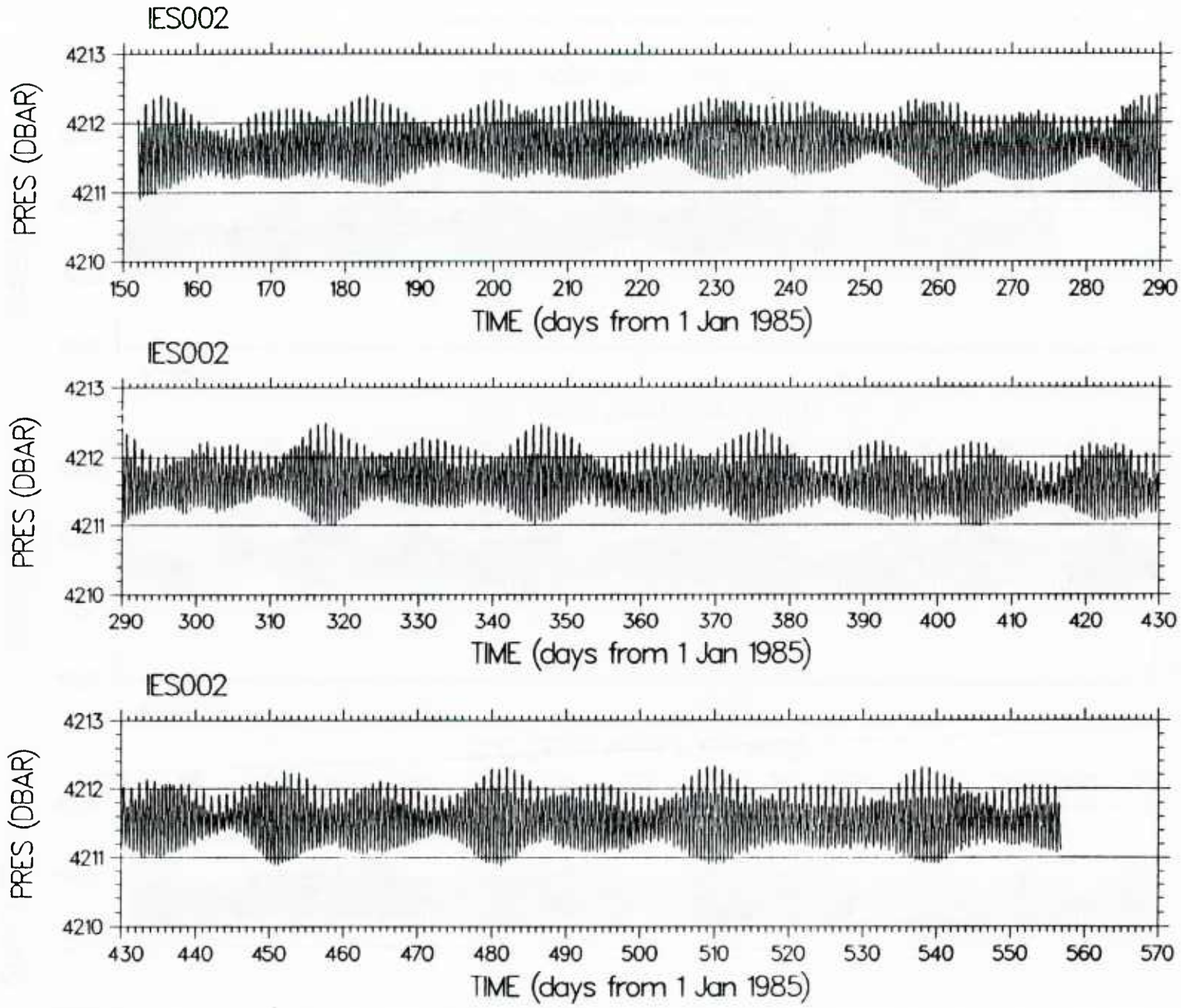

Figure 5. Unfiltered pressure record.

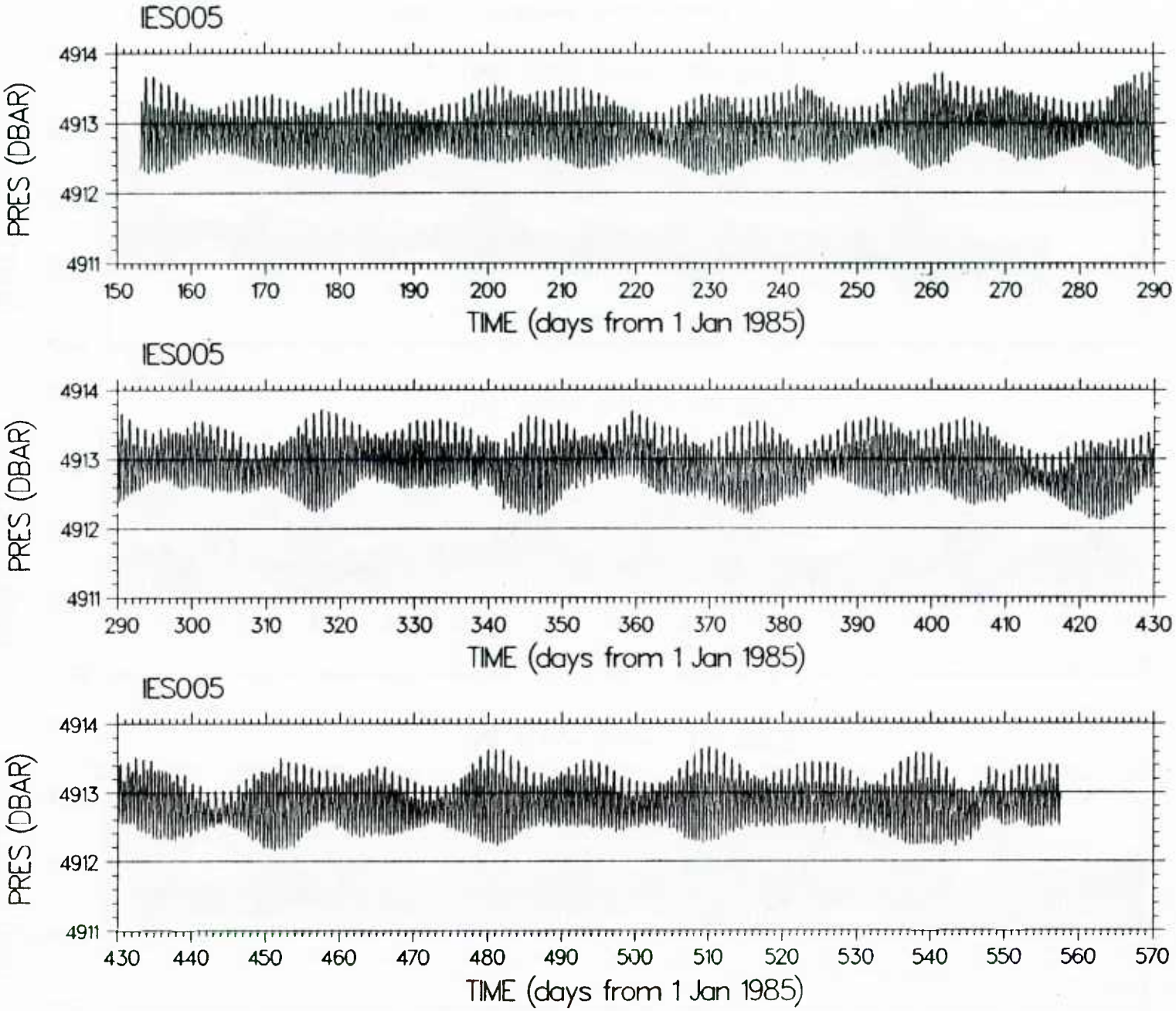

Figure 8. Unfiltered pressure record.

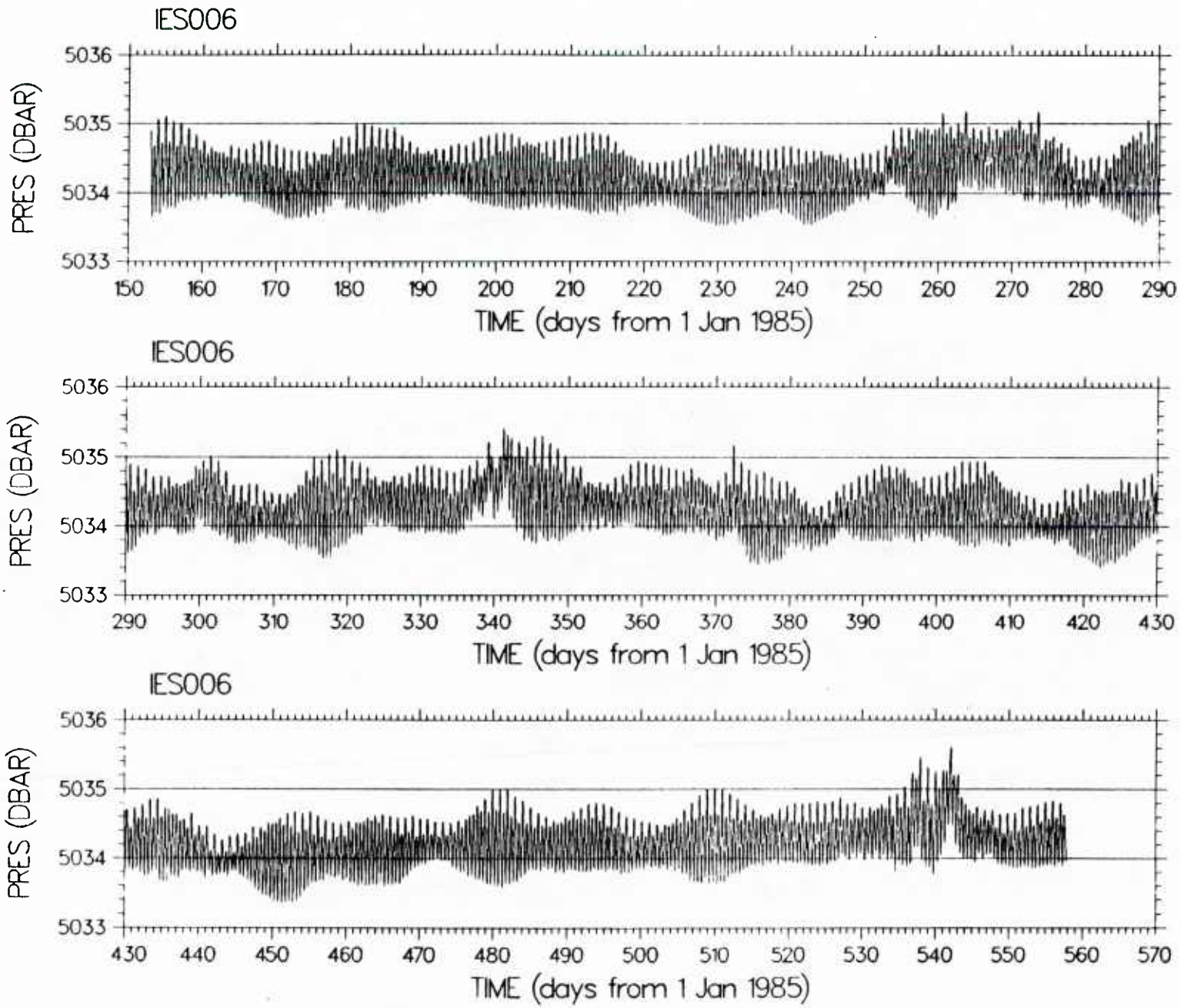

Figure 9. Unfiltered pressure record.

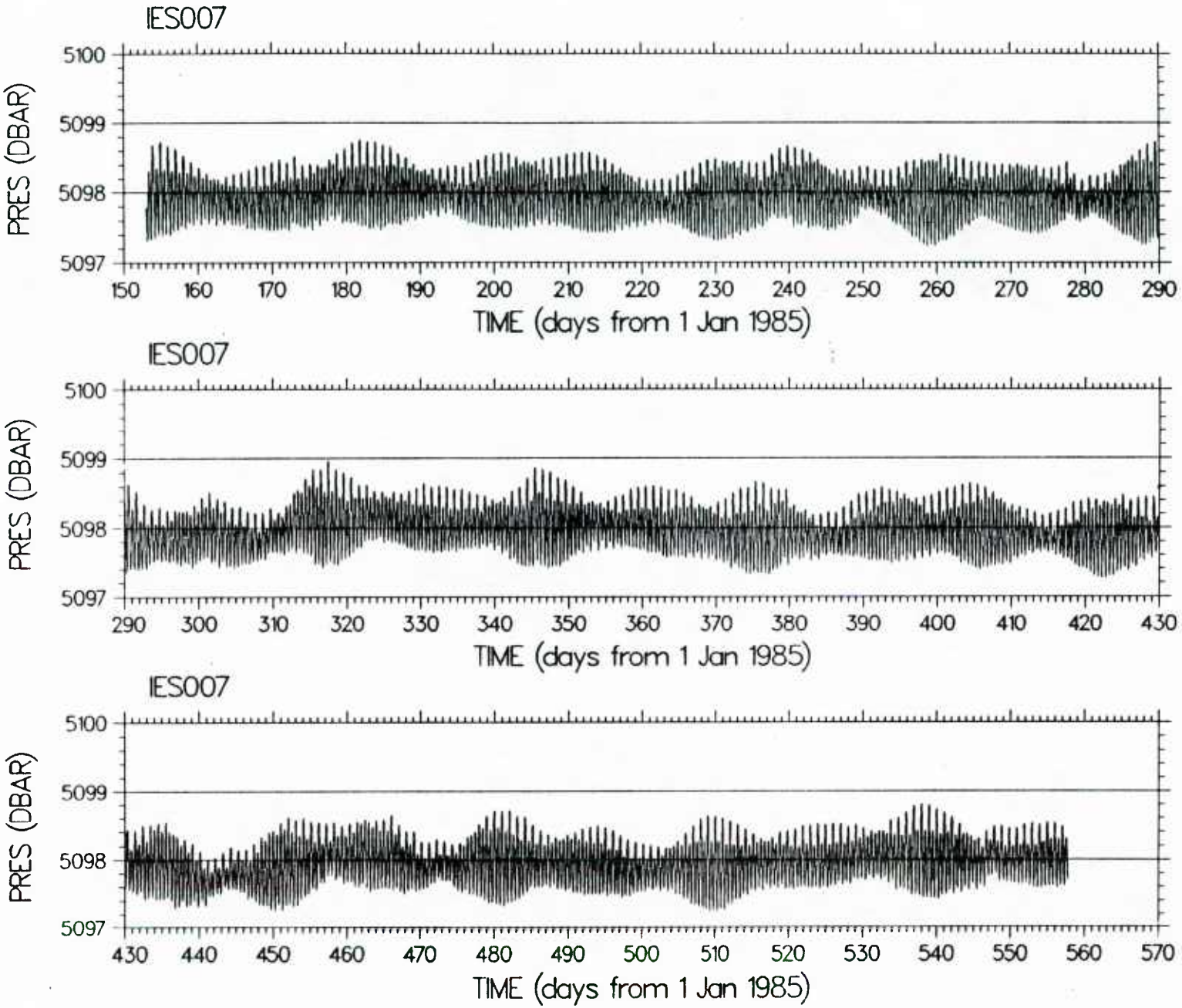

Figure 10. Unfiltered pressure record.

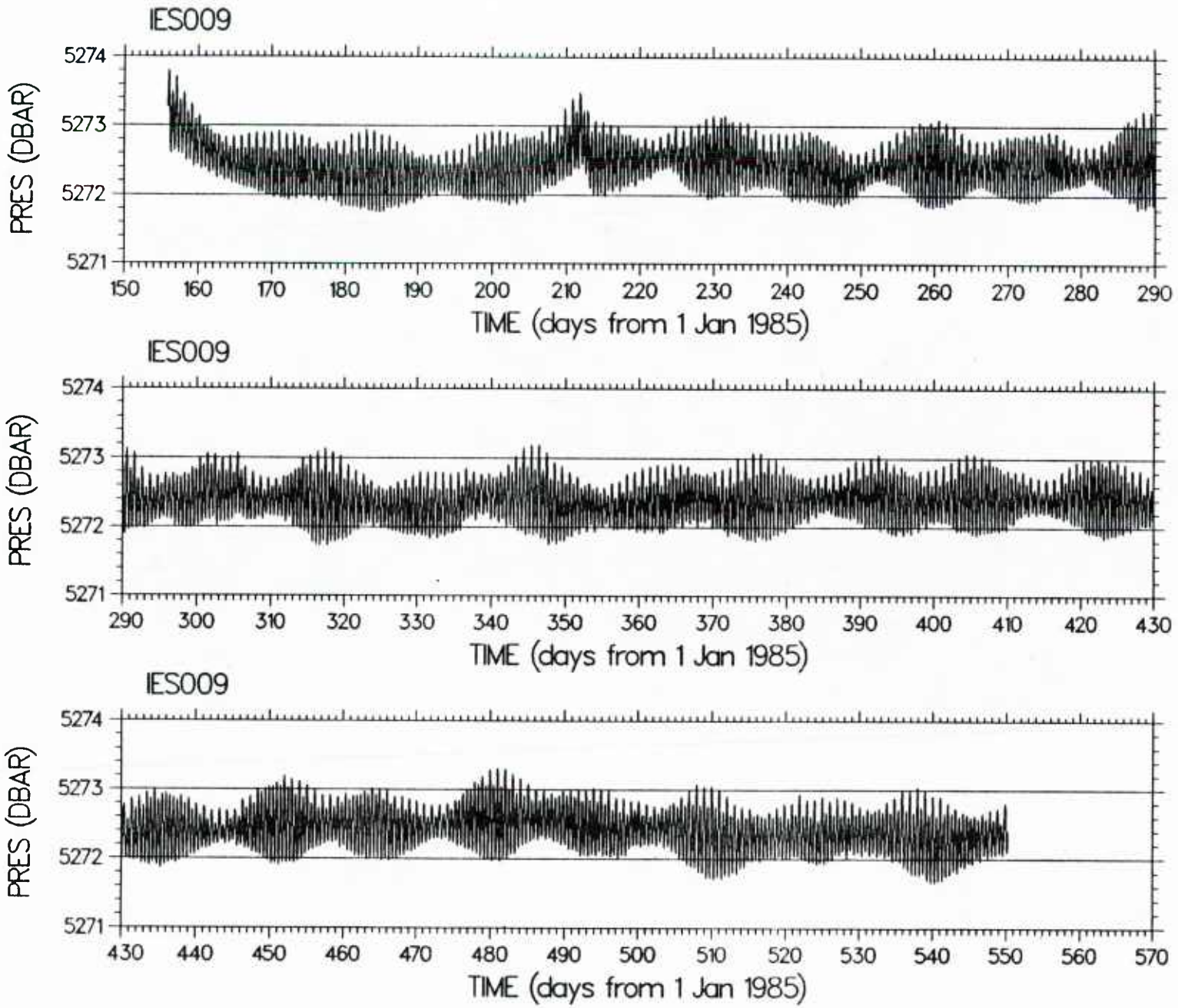

Figure 11. Unfiltered pressure record.

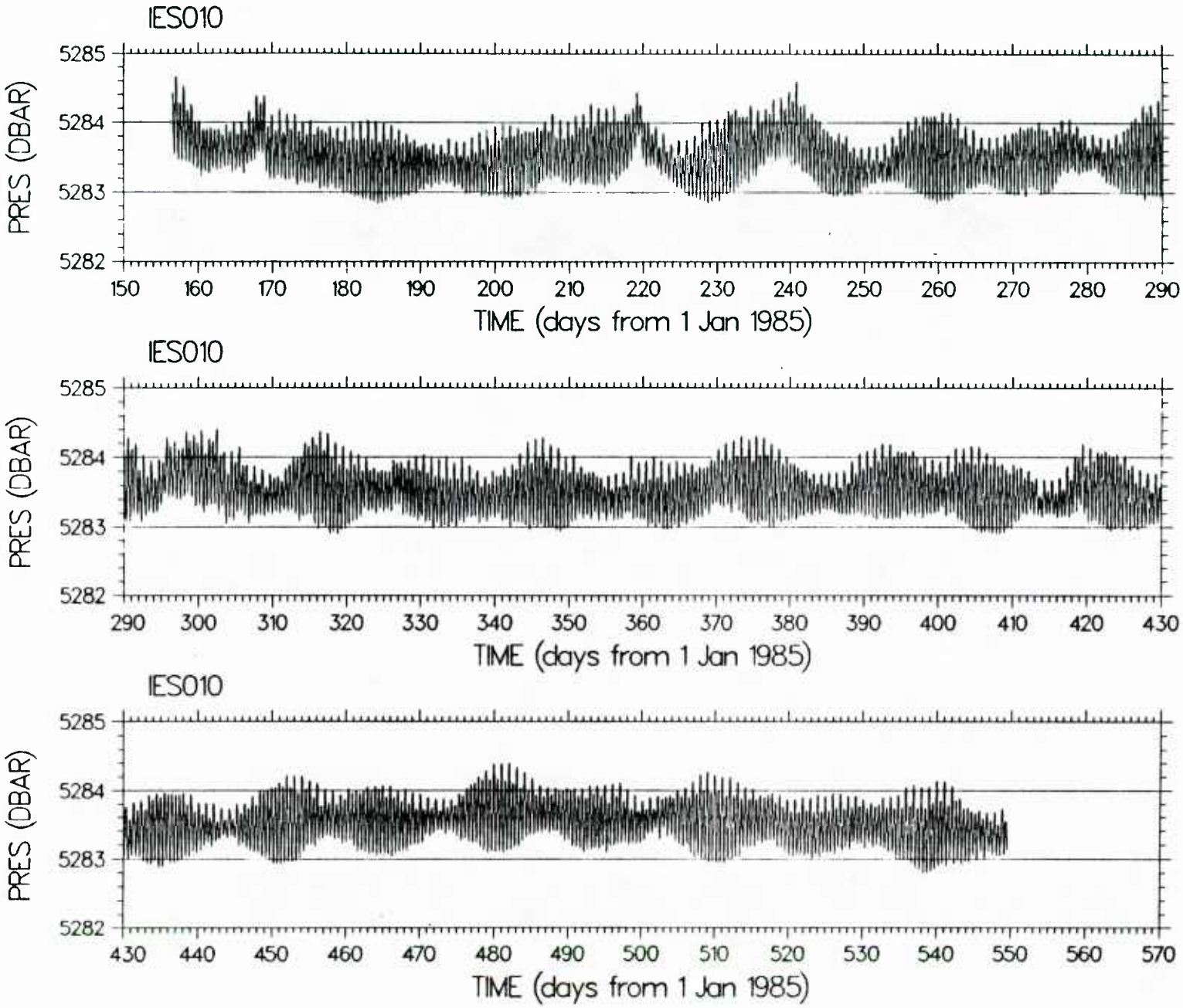

Figure 12. Unfiltered pressure record.

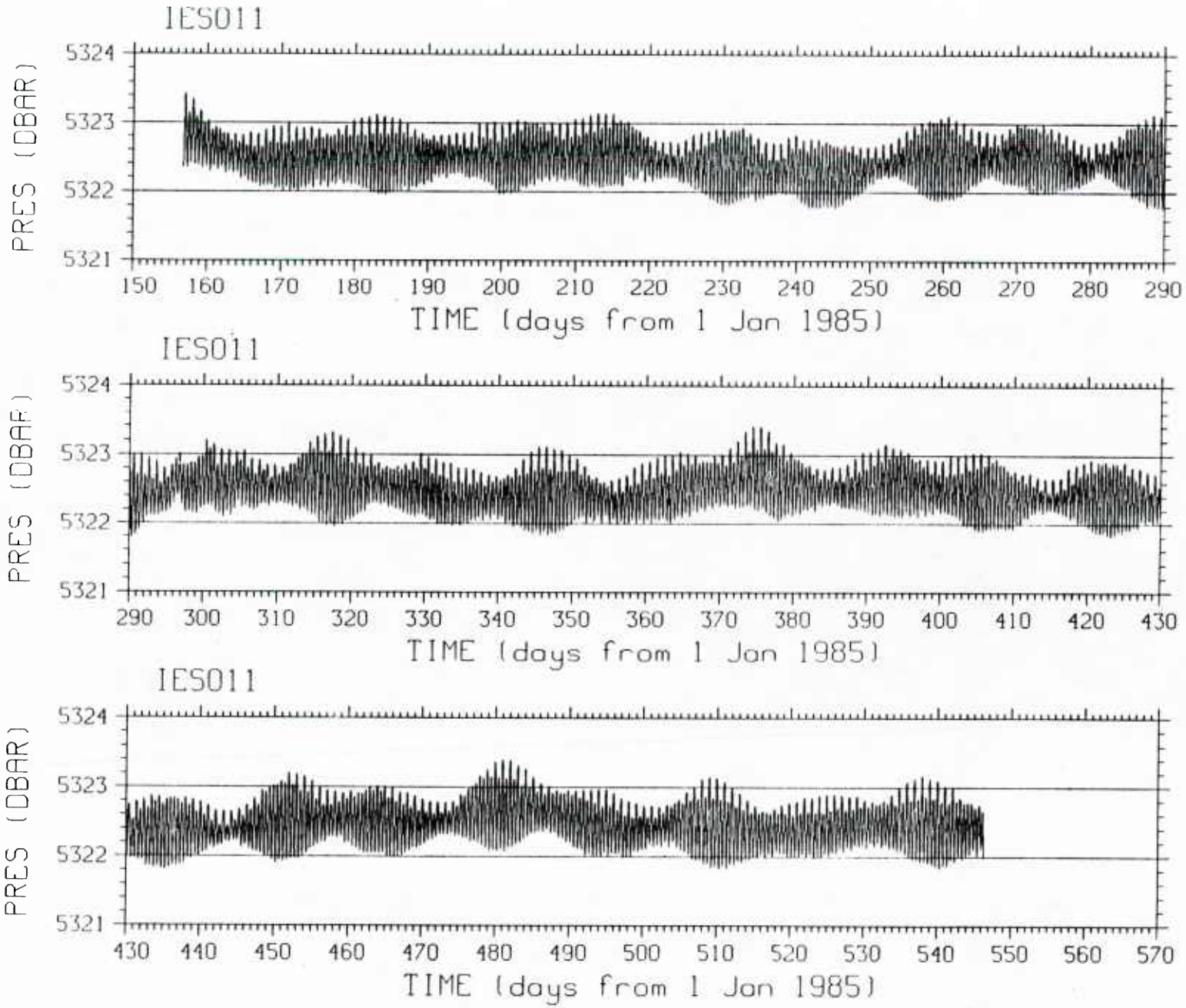

Figure 13. Unfiltered pressure record.

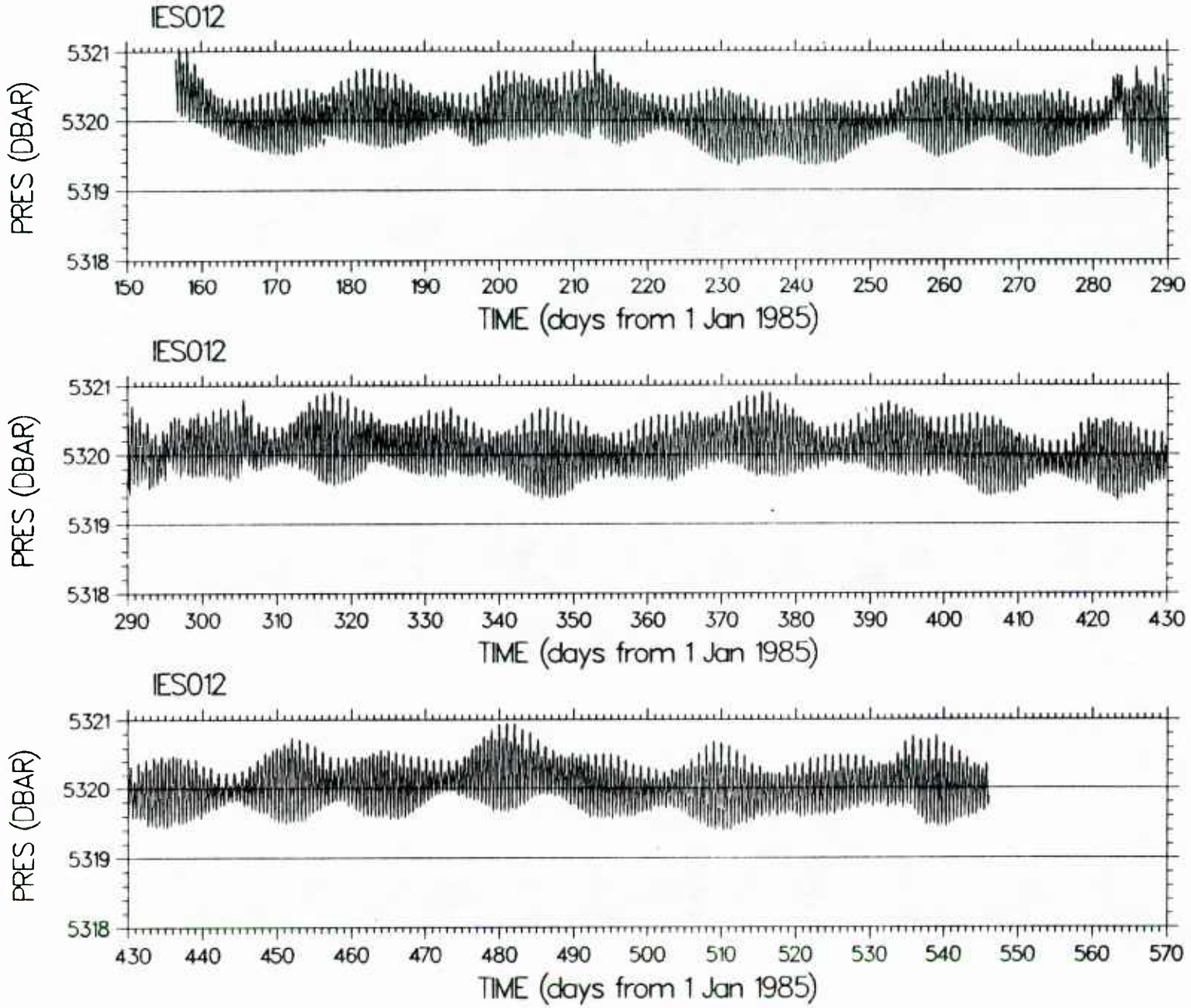

Figure 14. Unfiltered pressure record.

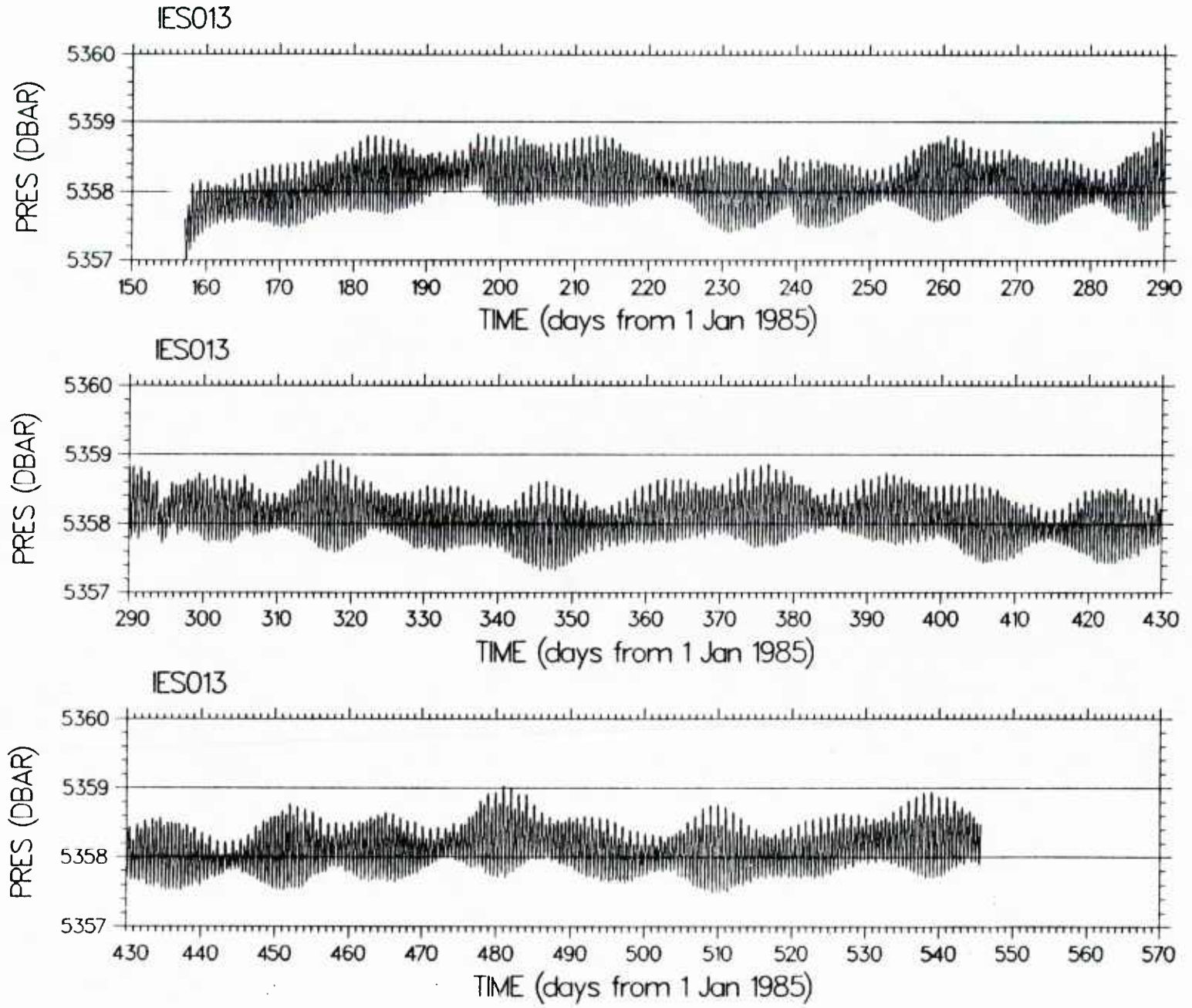

Figure 15. Unfiltered pressure record.

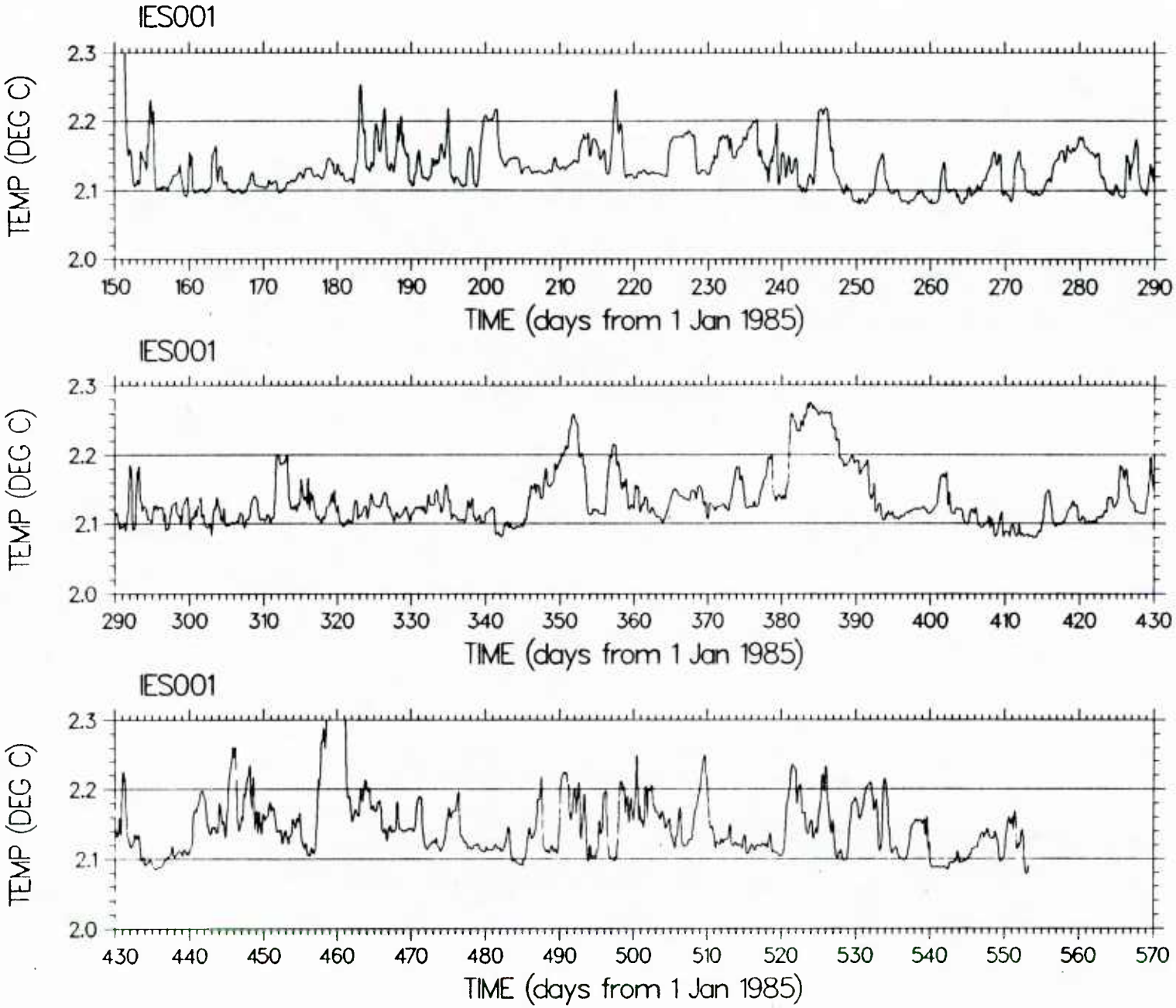

Figure 16. Unfiltered temperature record.

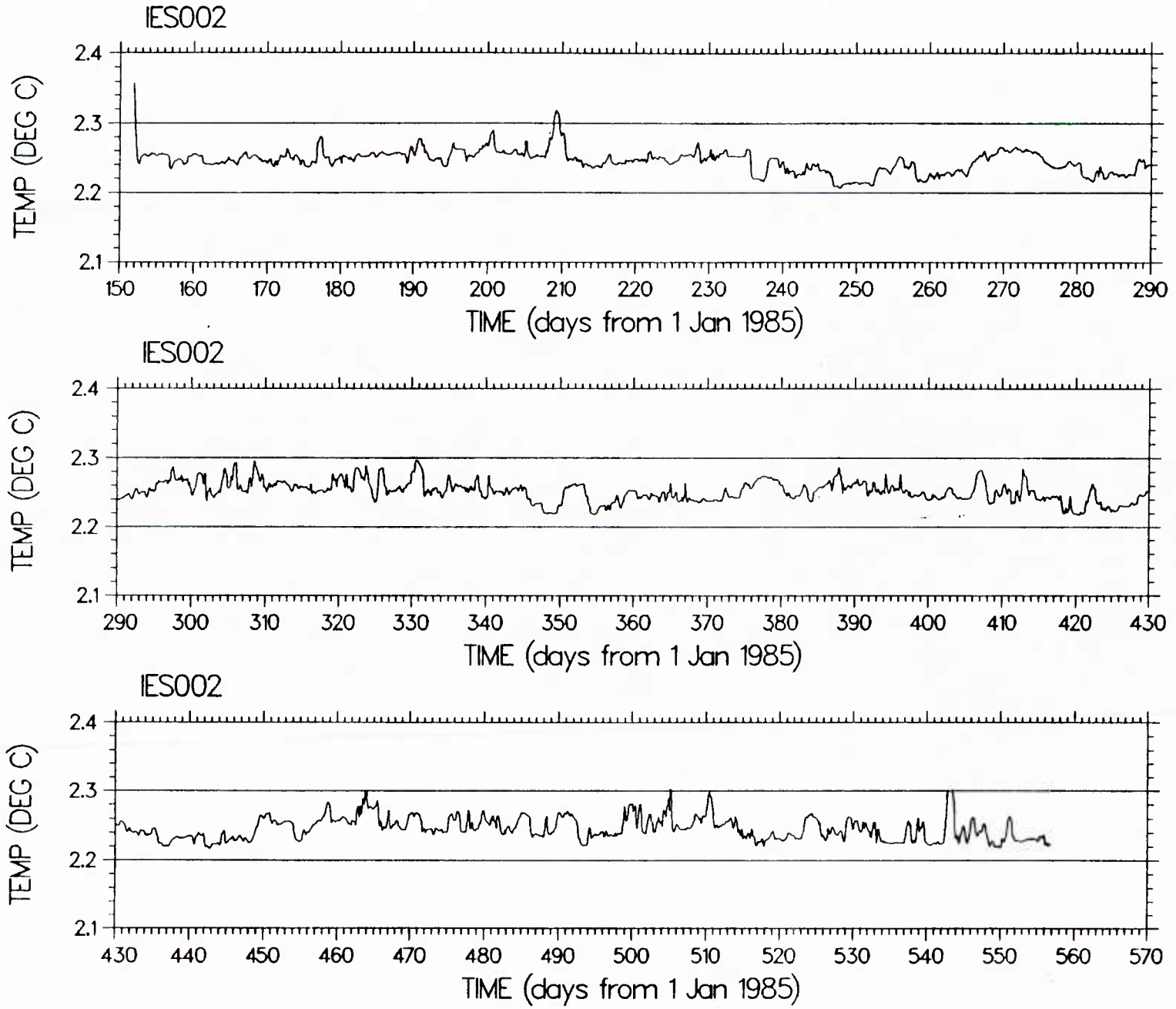

Figure 17. Unfiltered temperature record.

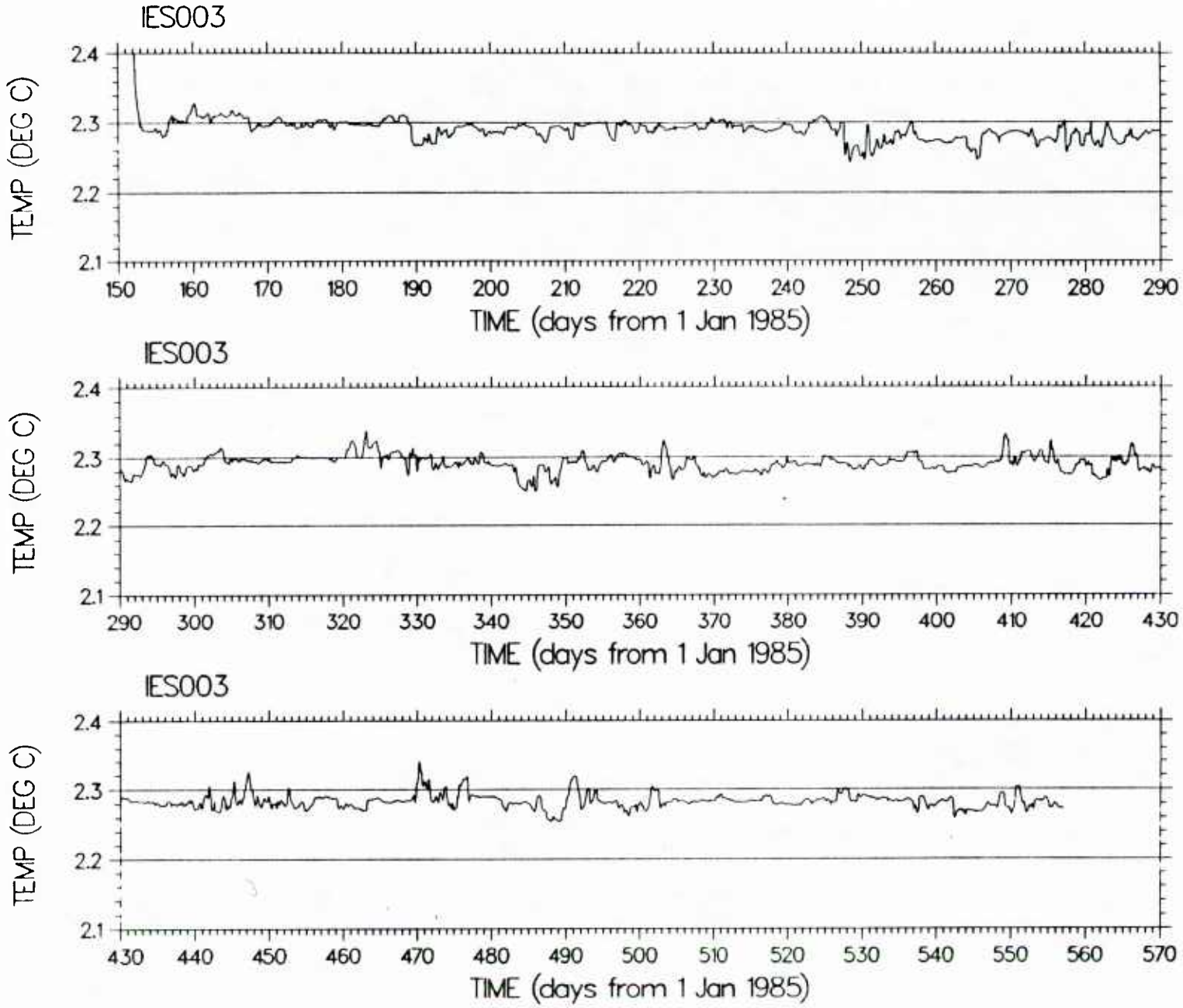

Figure 18. Unfiltered temperature record.

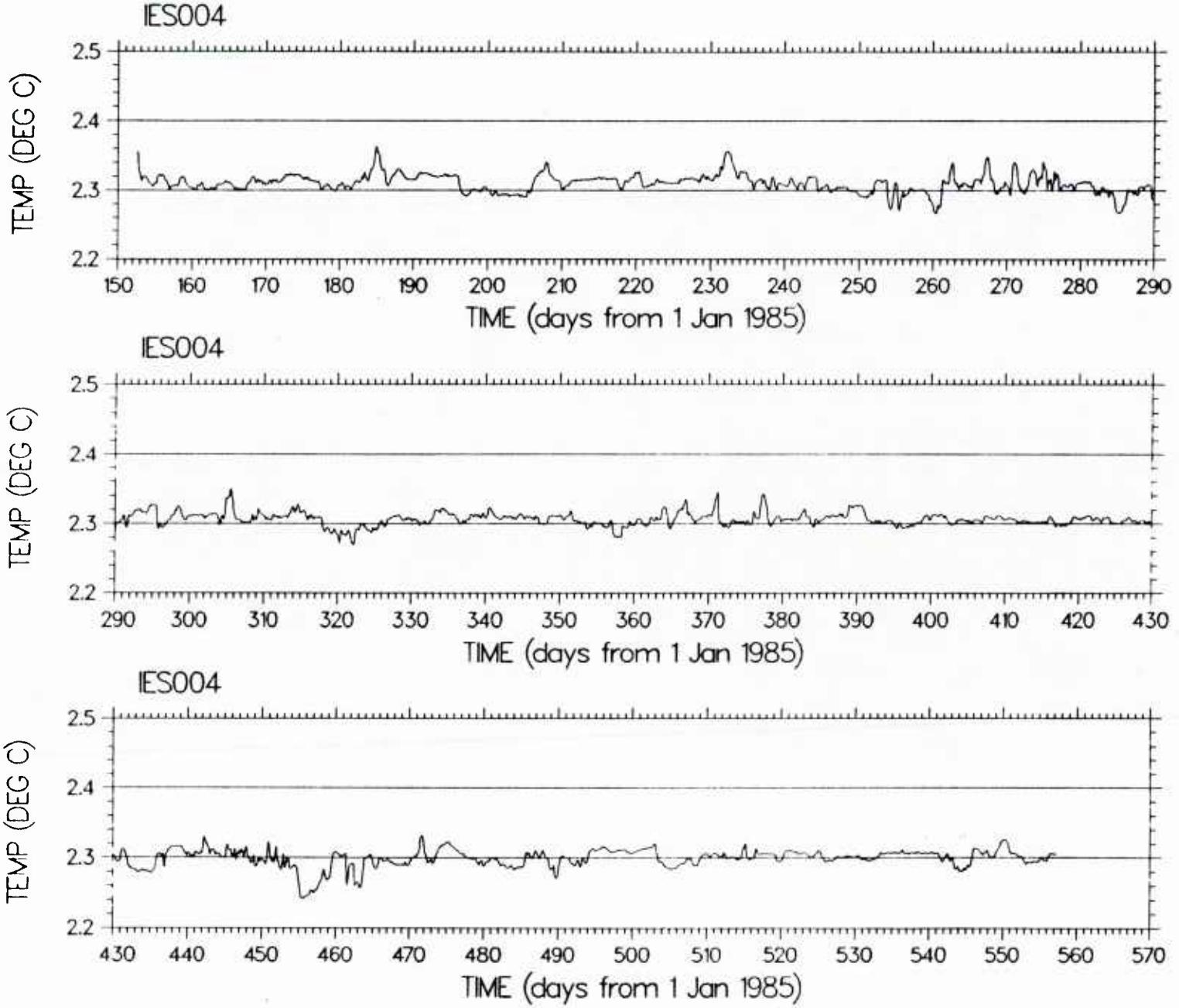

Figure 19. Unfiltered temperature record.

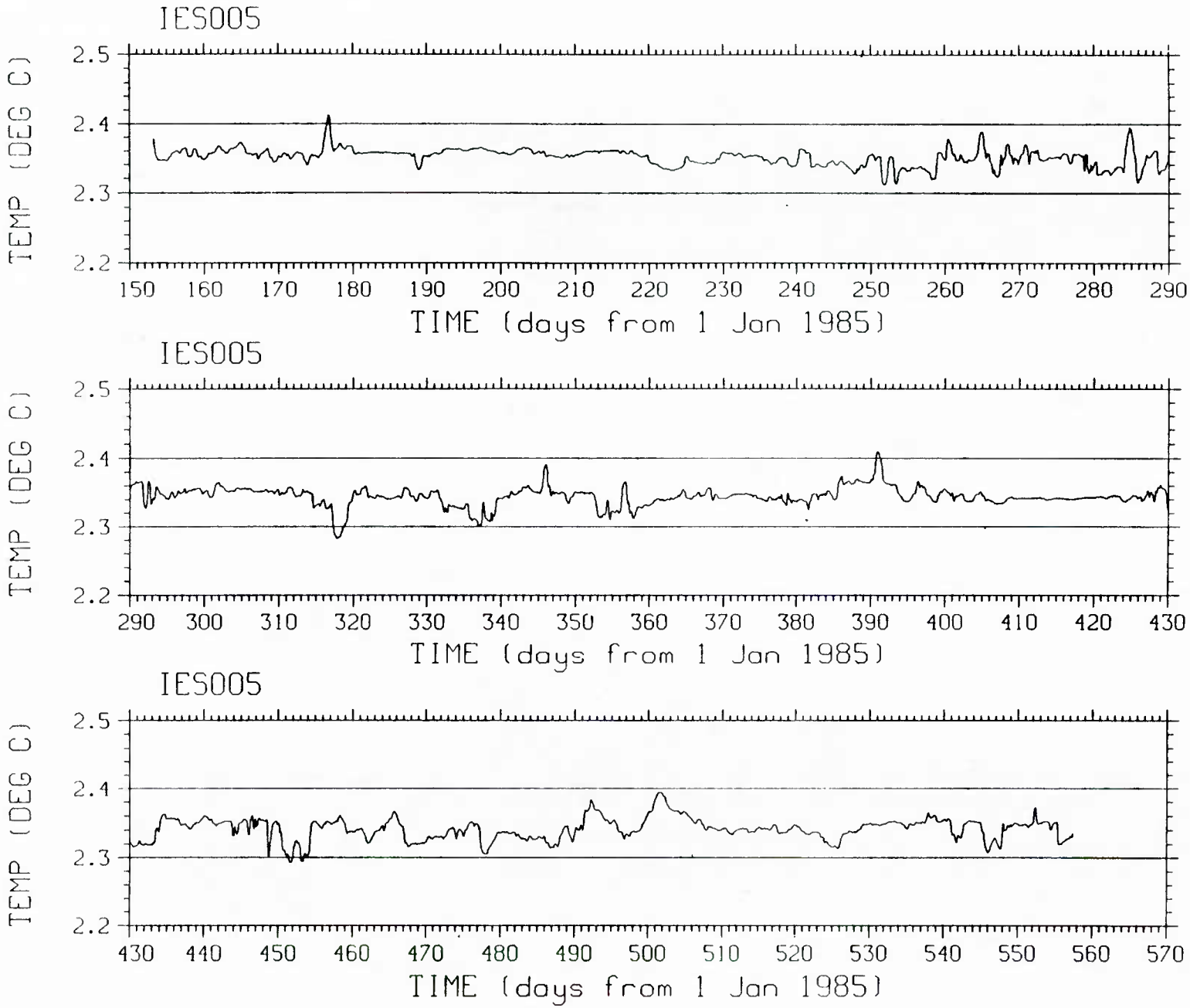

Figure 20. Unfiltered temperature record.

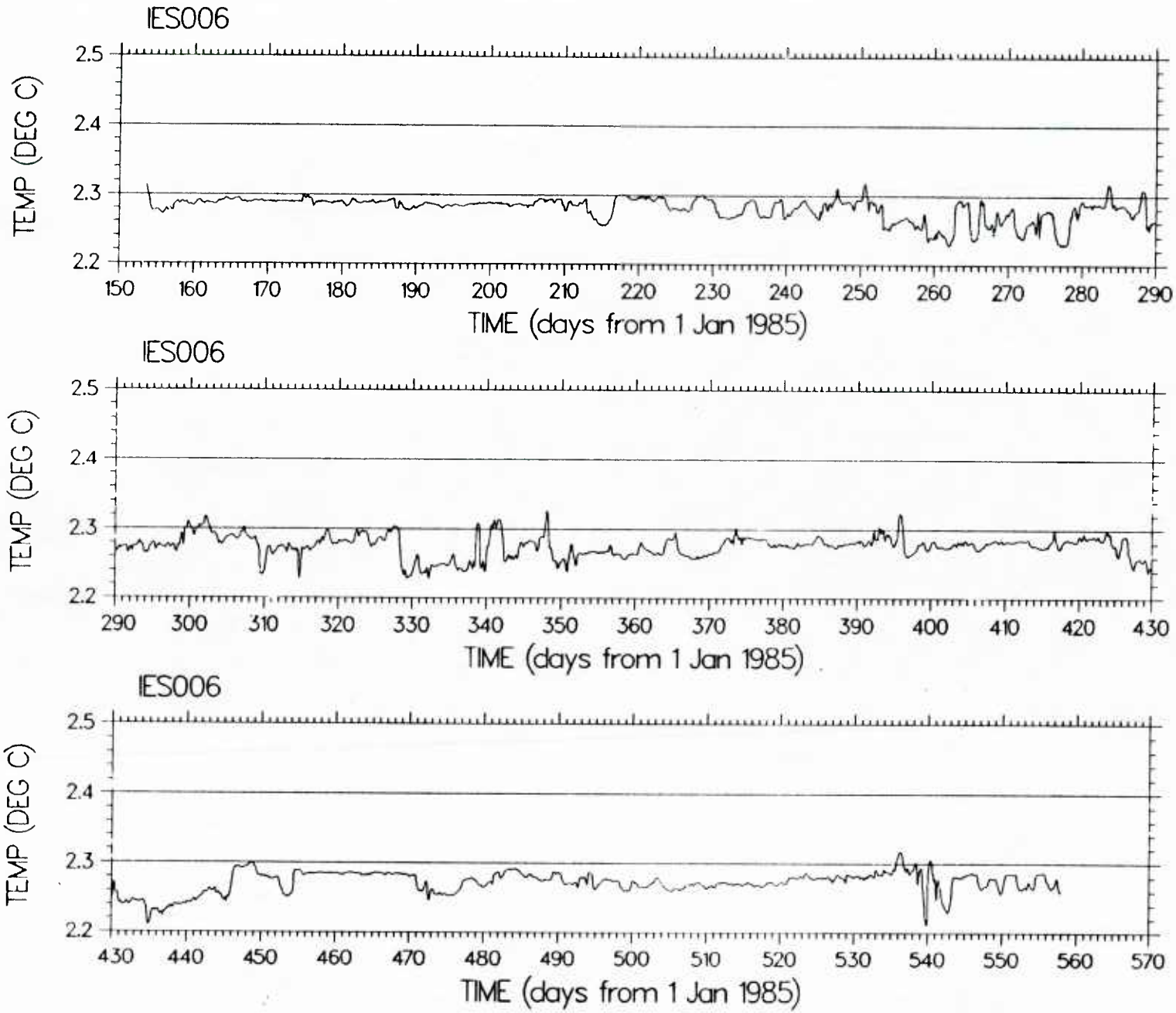

Figure 21. Unfiltered temperature record.

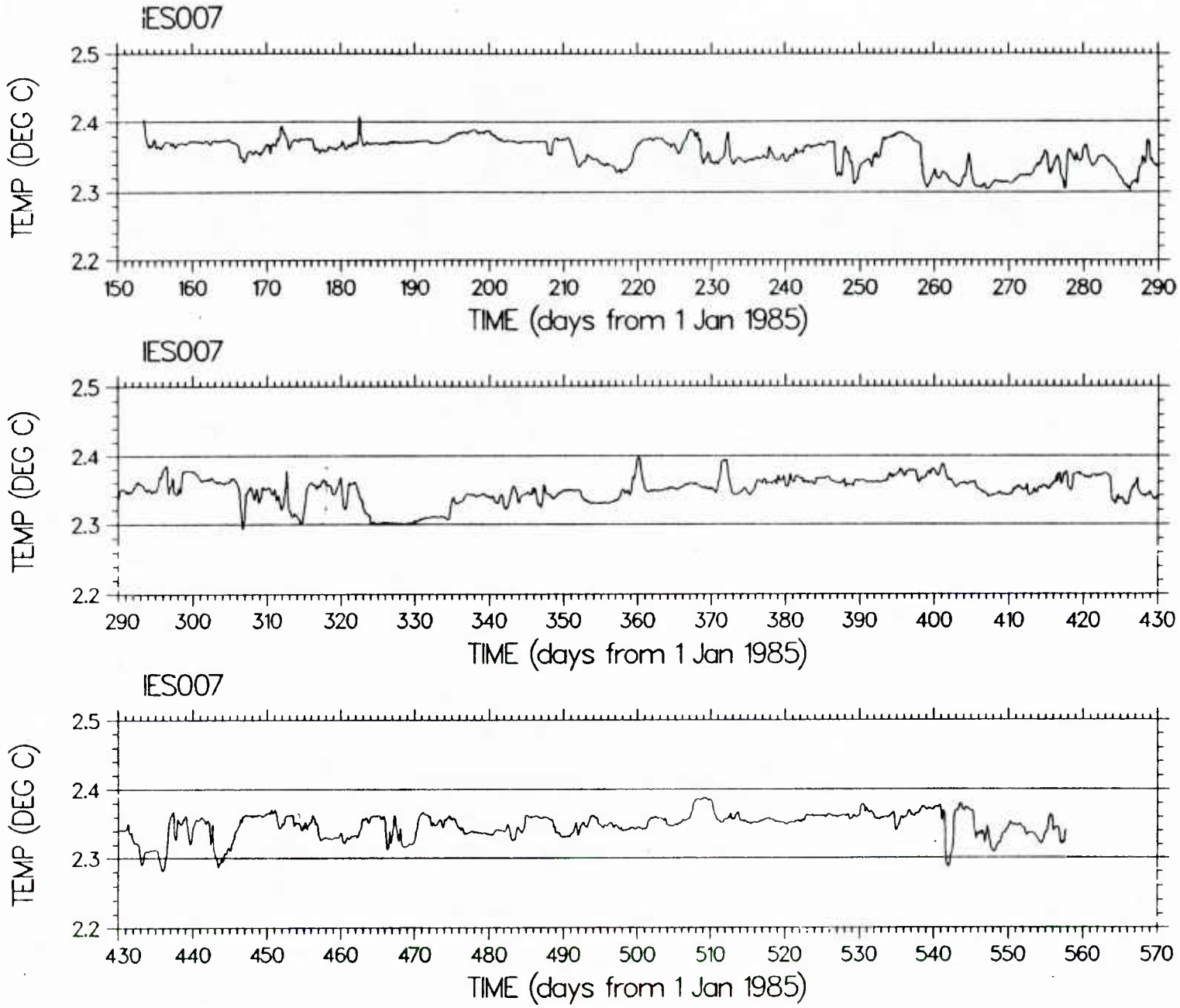

Figure 22. Unfiltered temperature record.

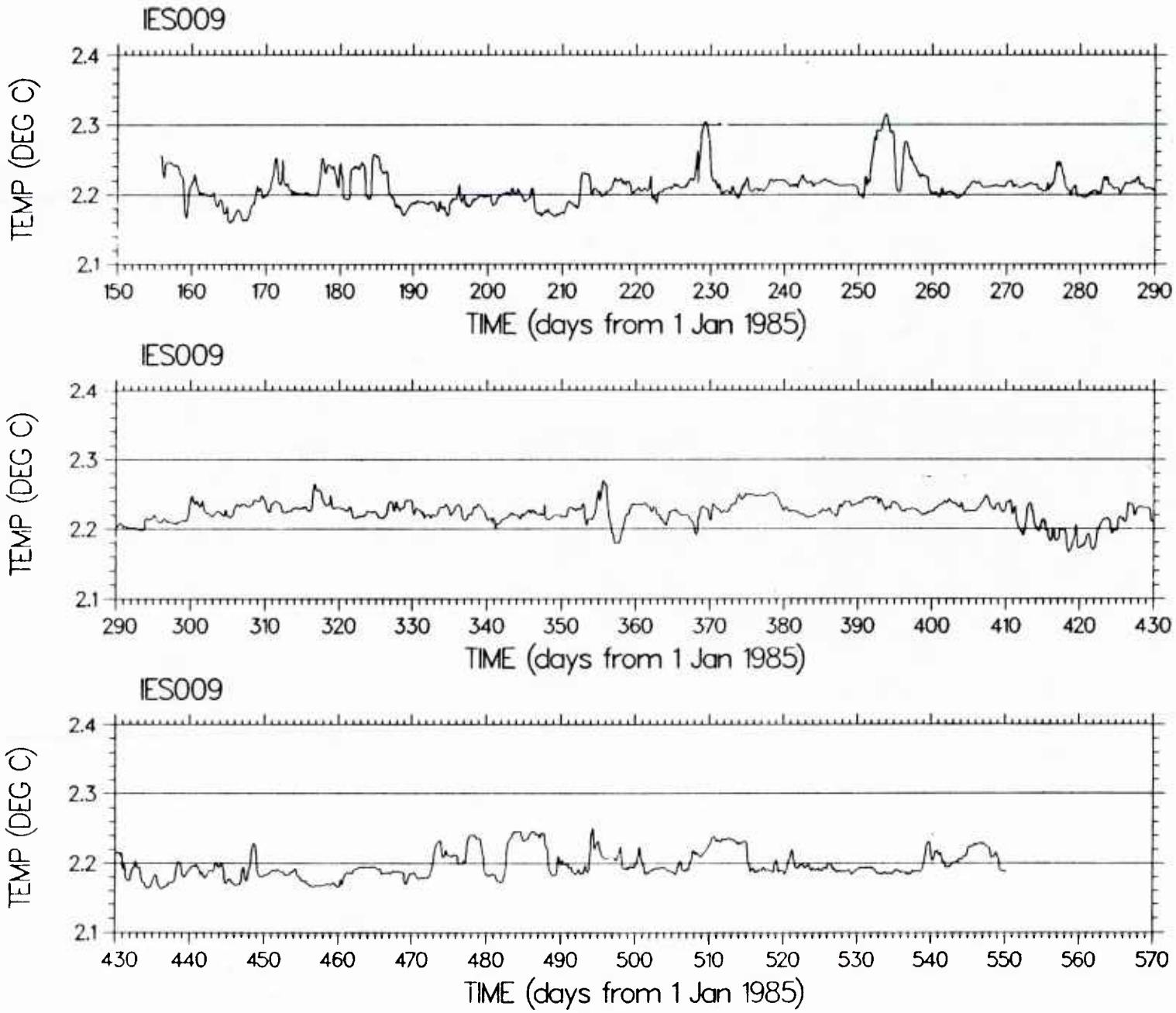

Figure 23. Unfiltered temperature recora.

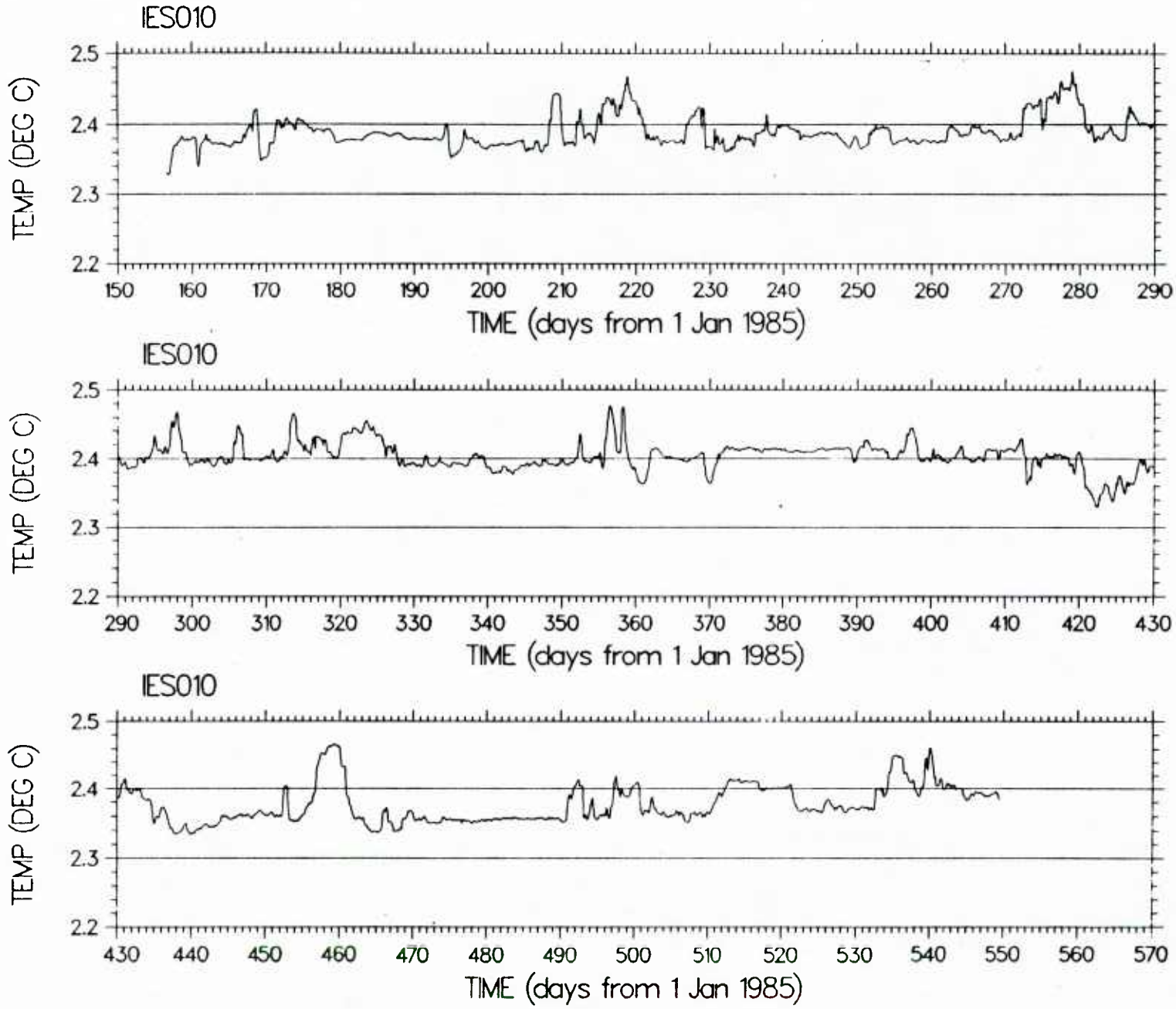

Figure 24. Unfiltered temperature record.

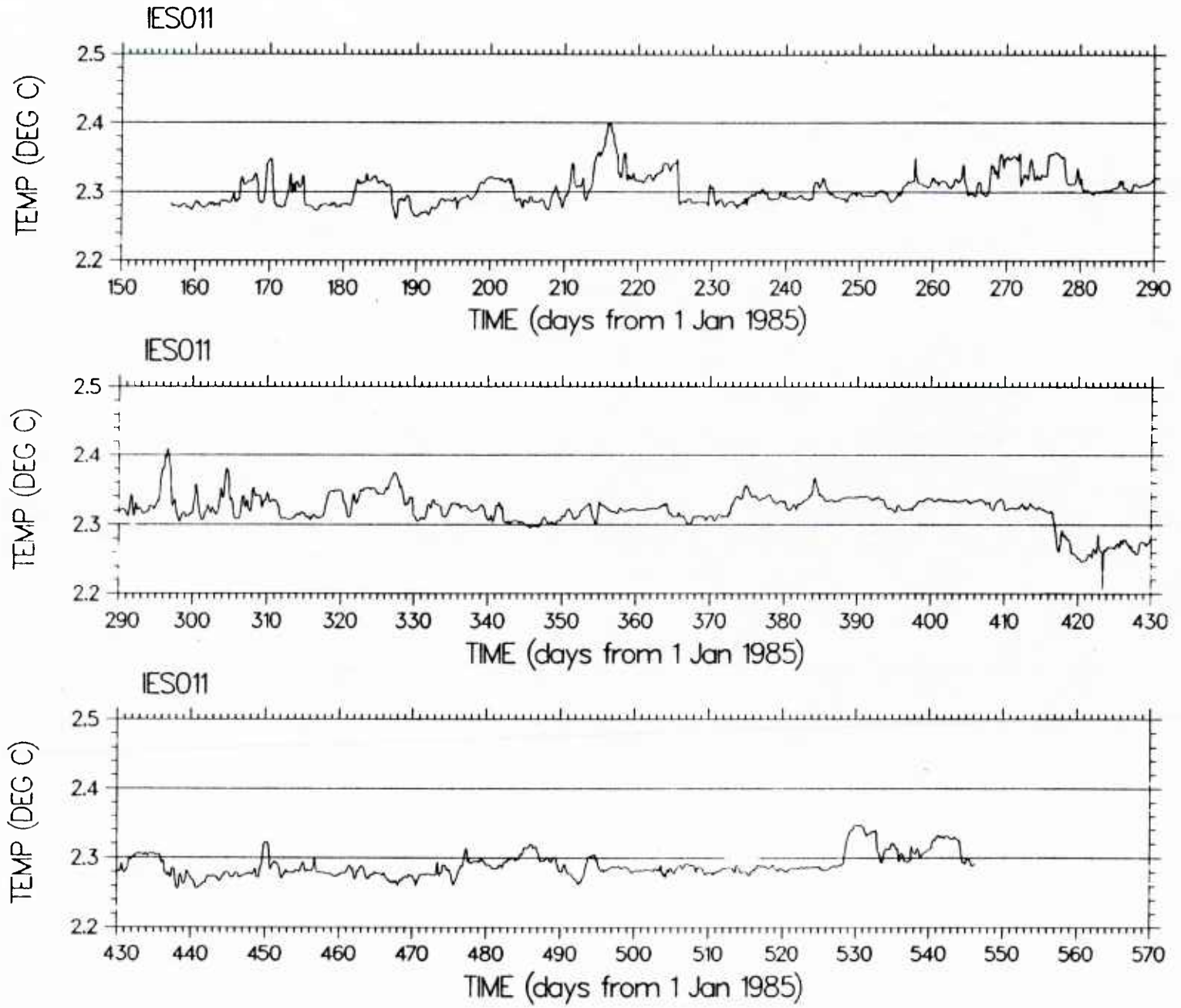

Figure 25. Unfiltered temperature record.

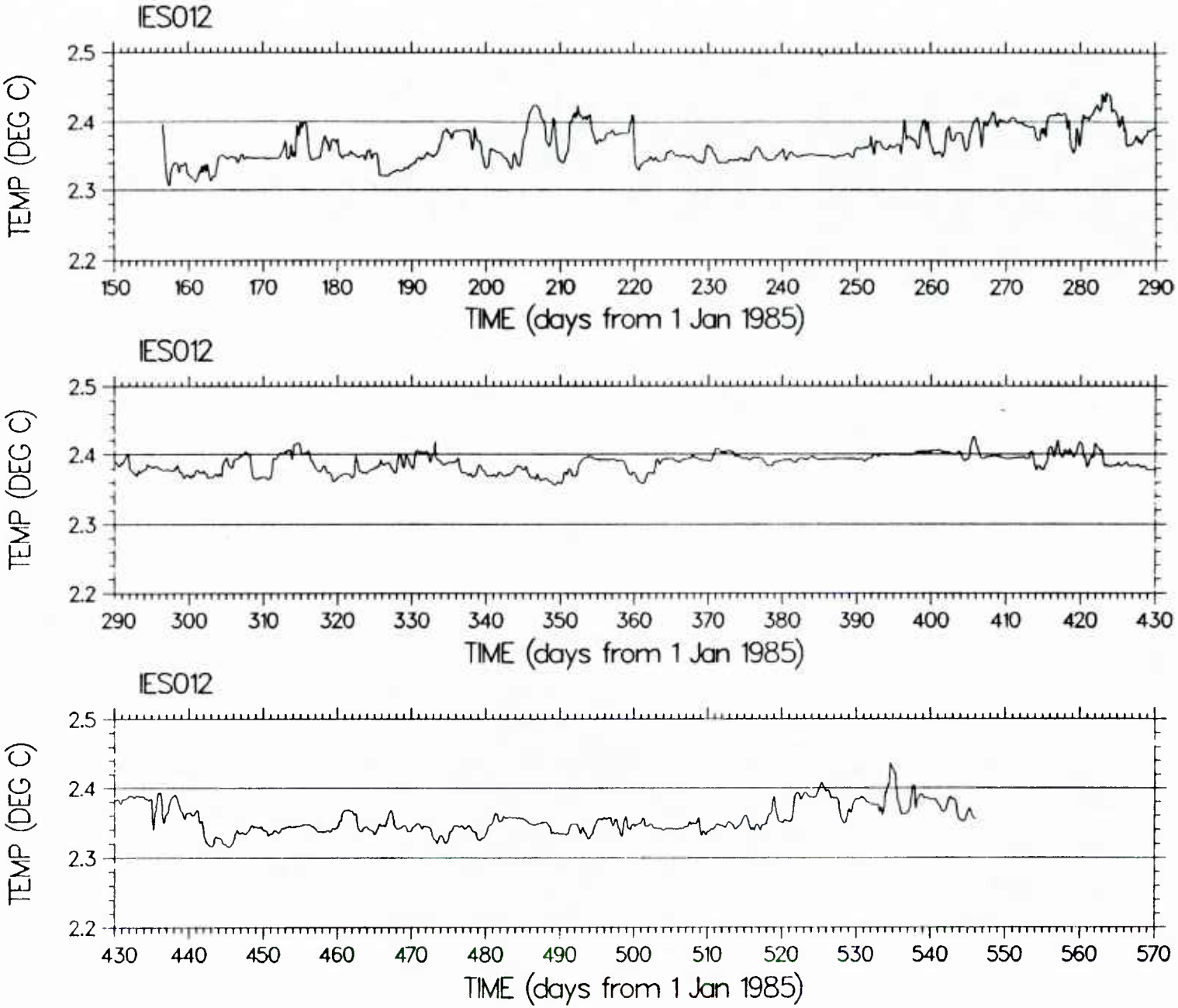

Figure 26. Unfiltered temperature record.

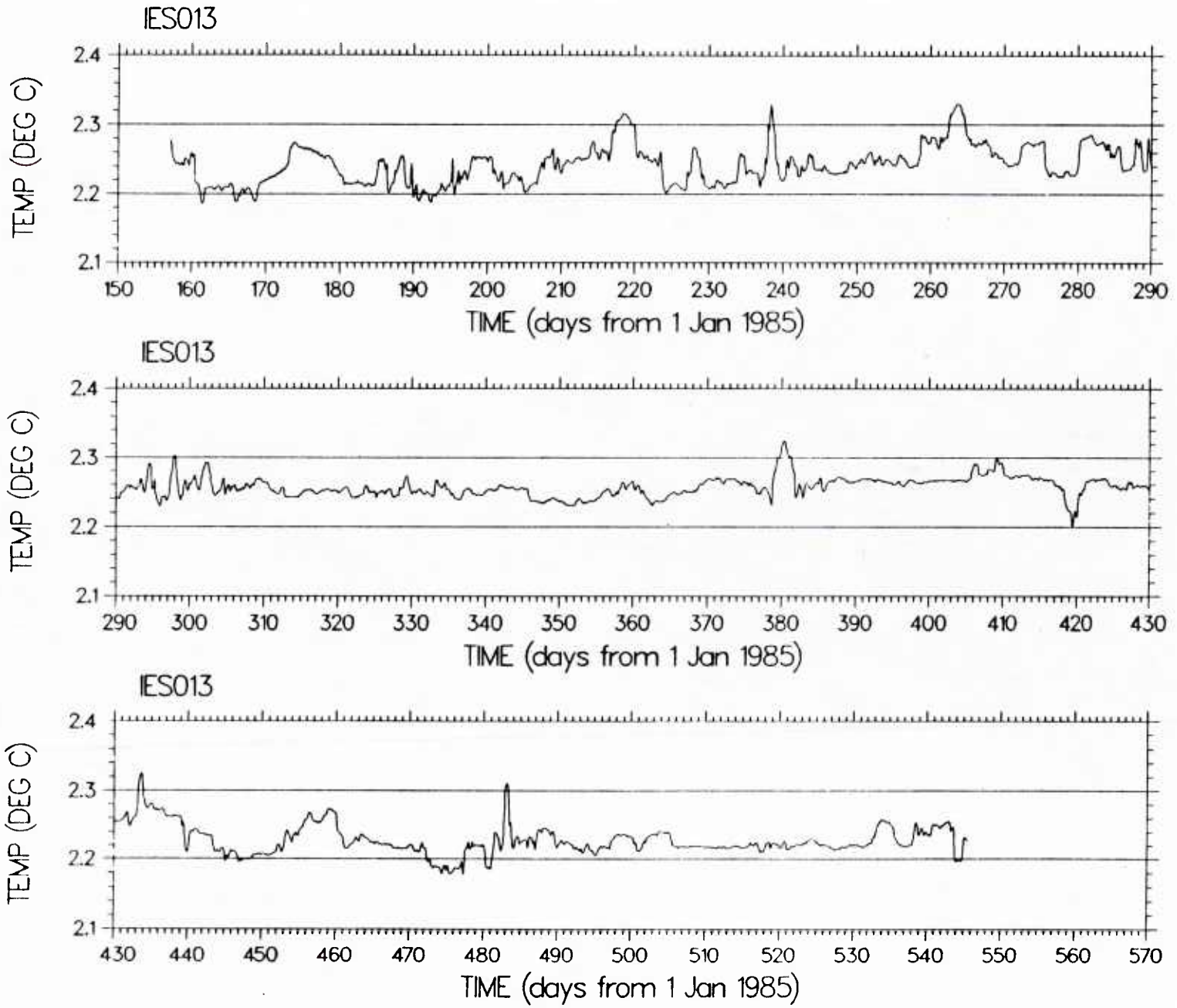

Figure 27. Unfiltered temperature record.

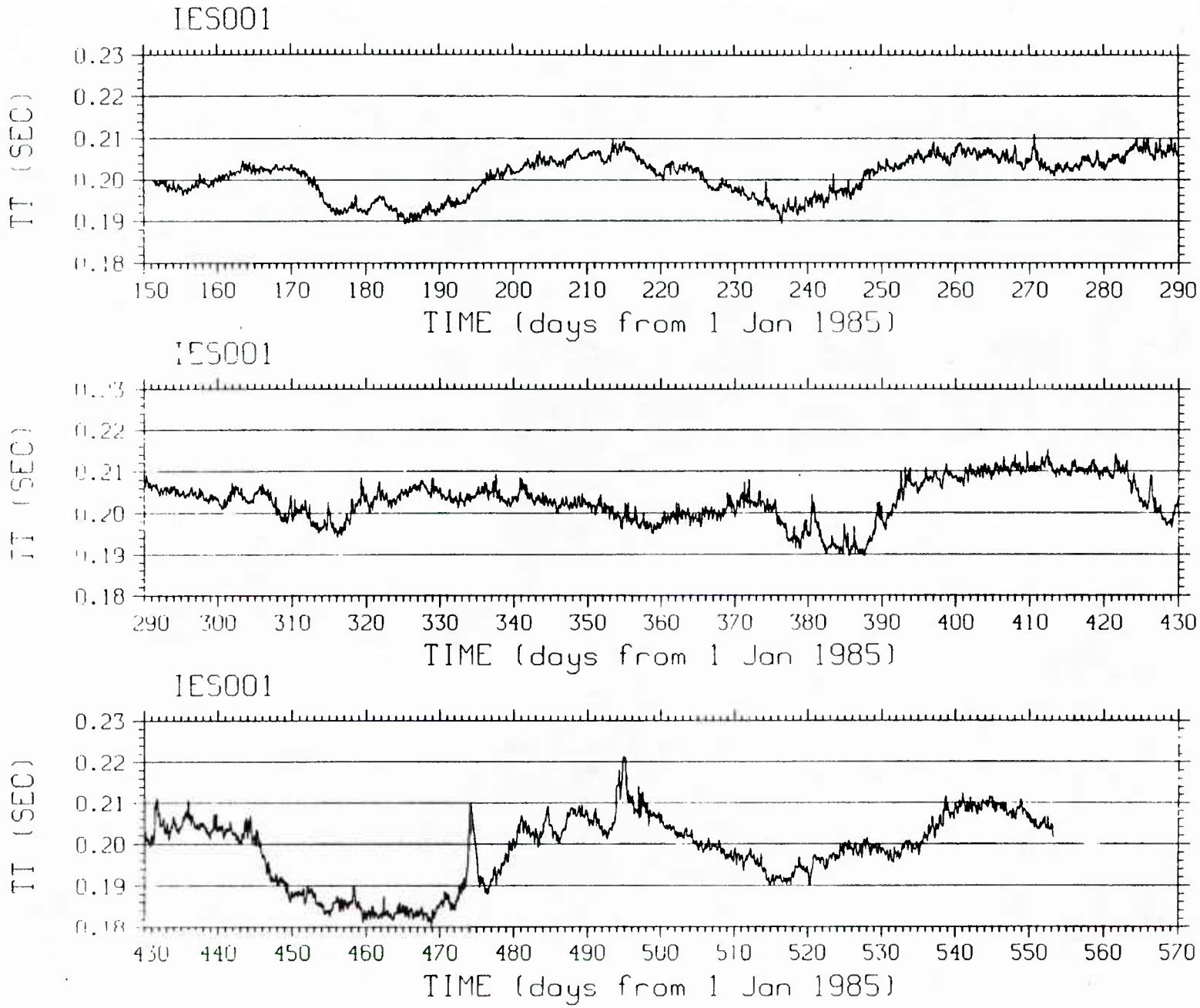

Figure 28. Unfiltered travel-time record.

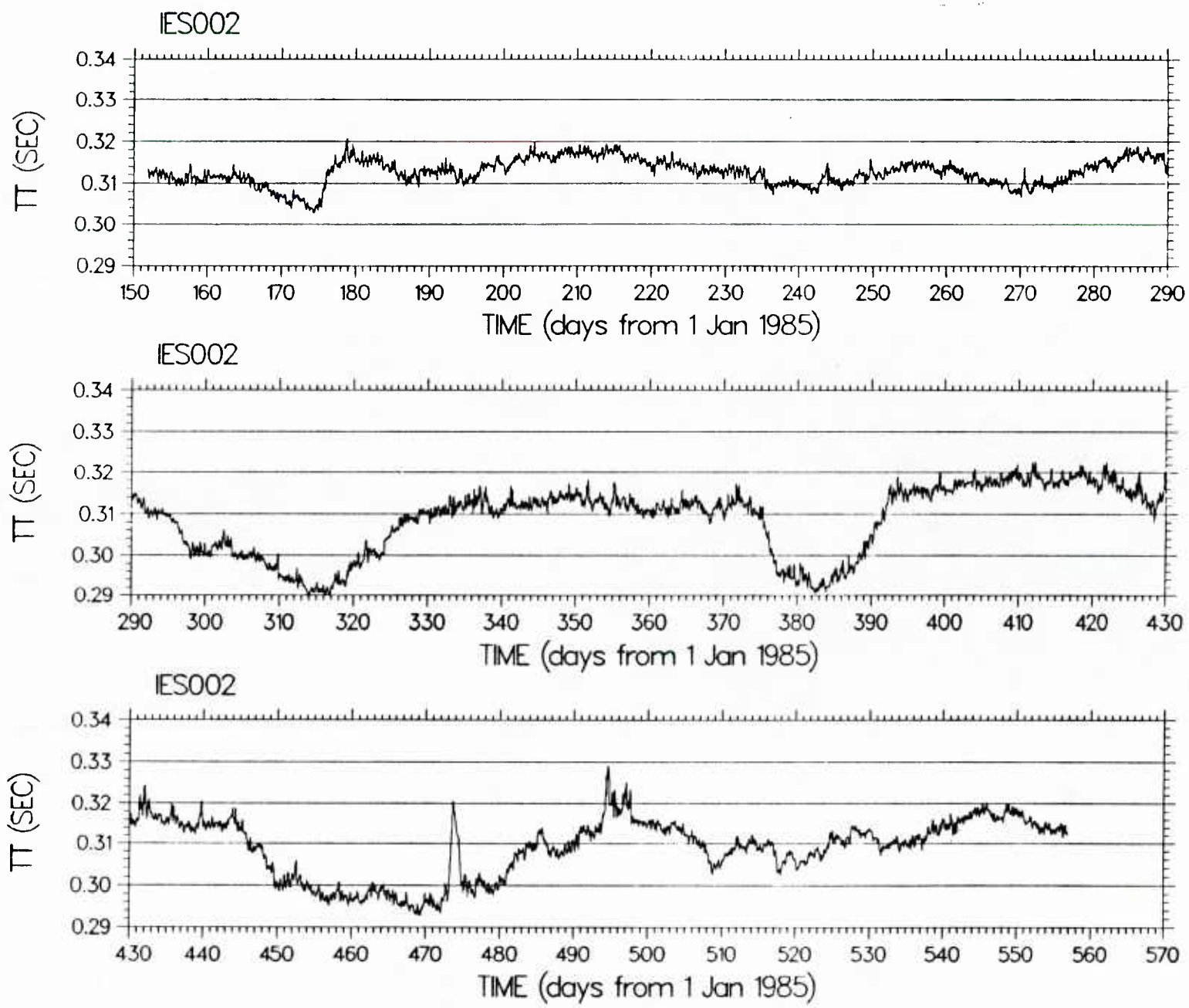

Figure 29. Unfiltered travel-time record.

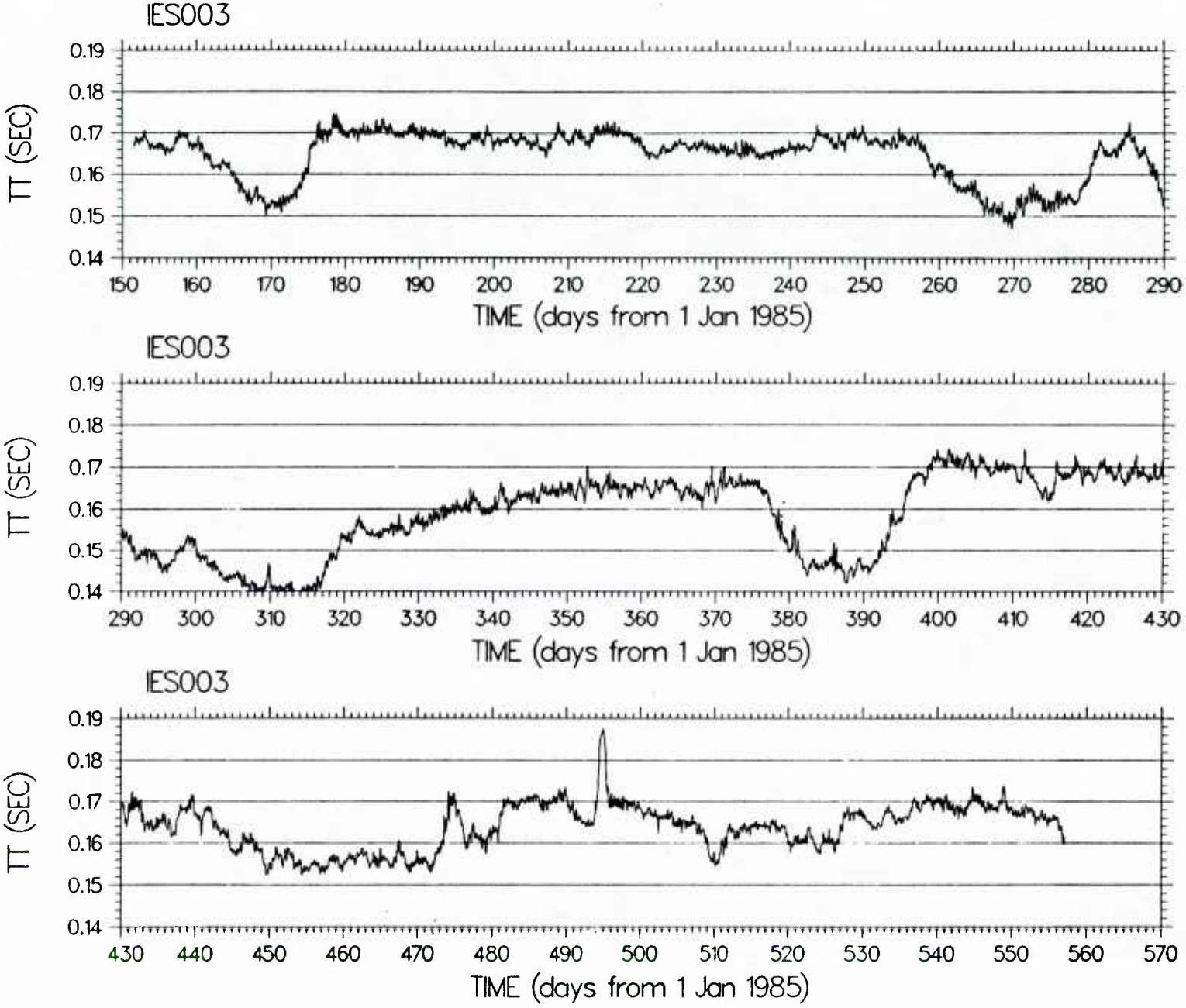

Figure 30. Unfiltered travel-time record.

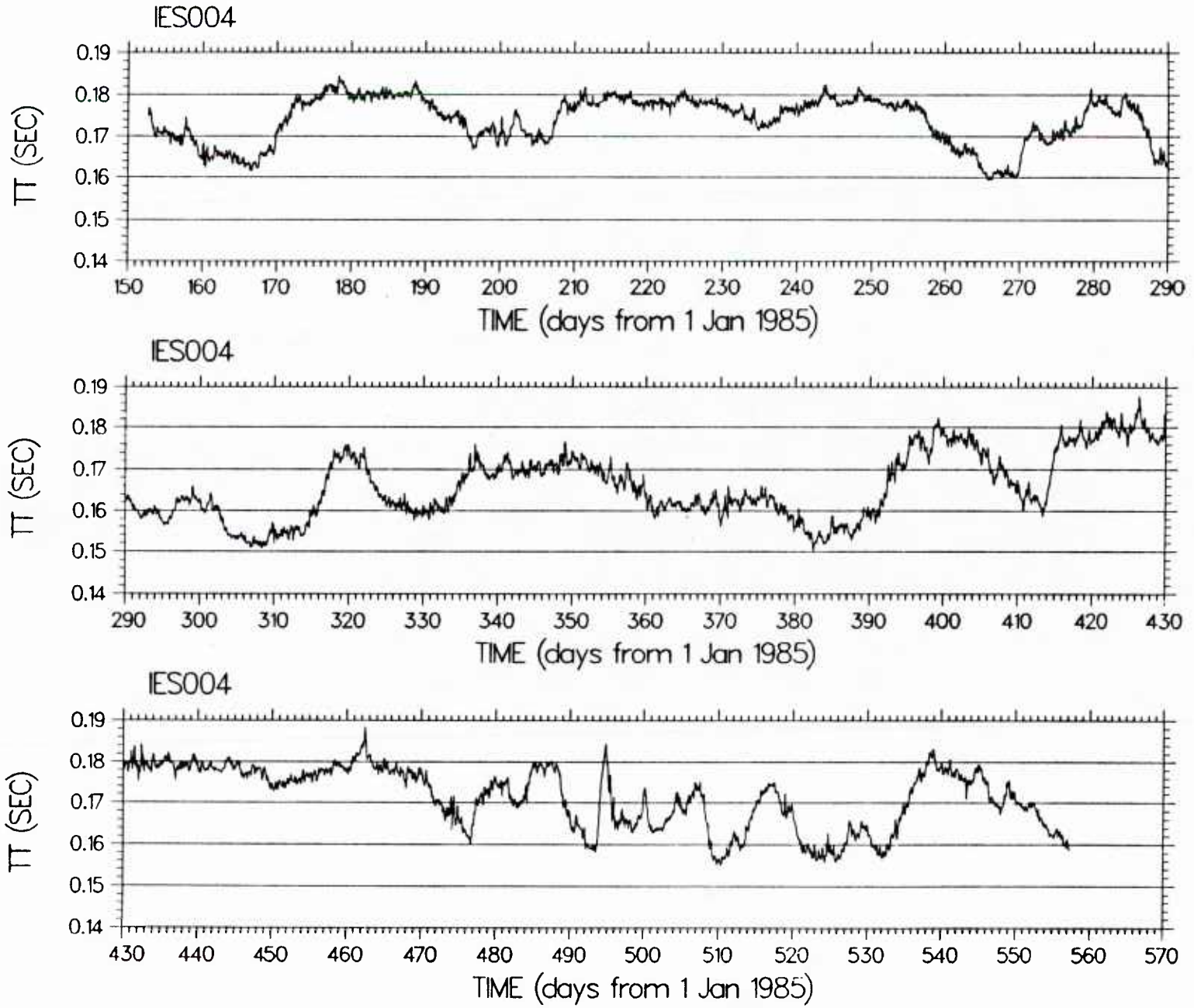

Figure 31. Unfiltered travel-time record.

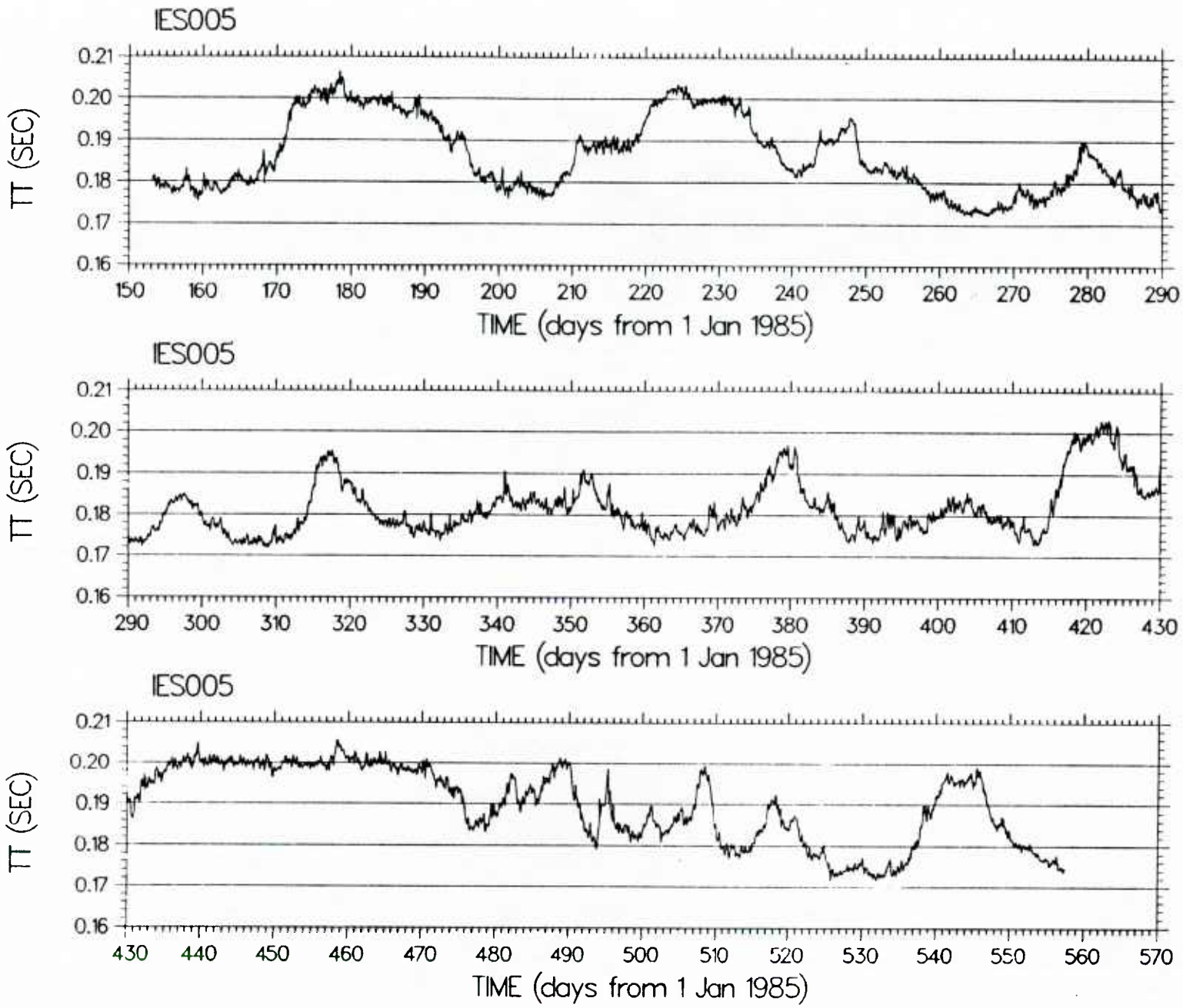

Figure 32. Unfiltered travel-time record.

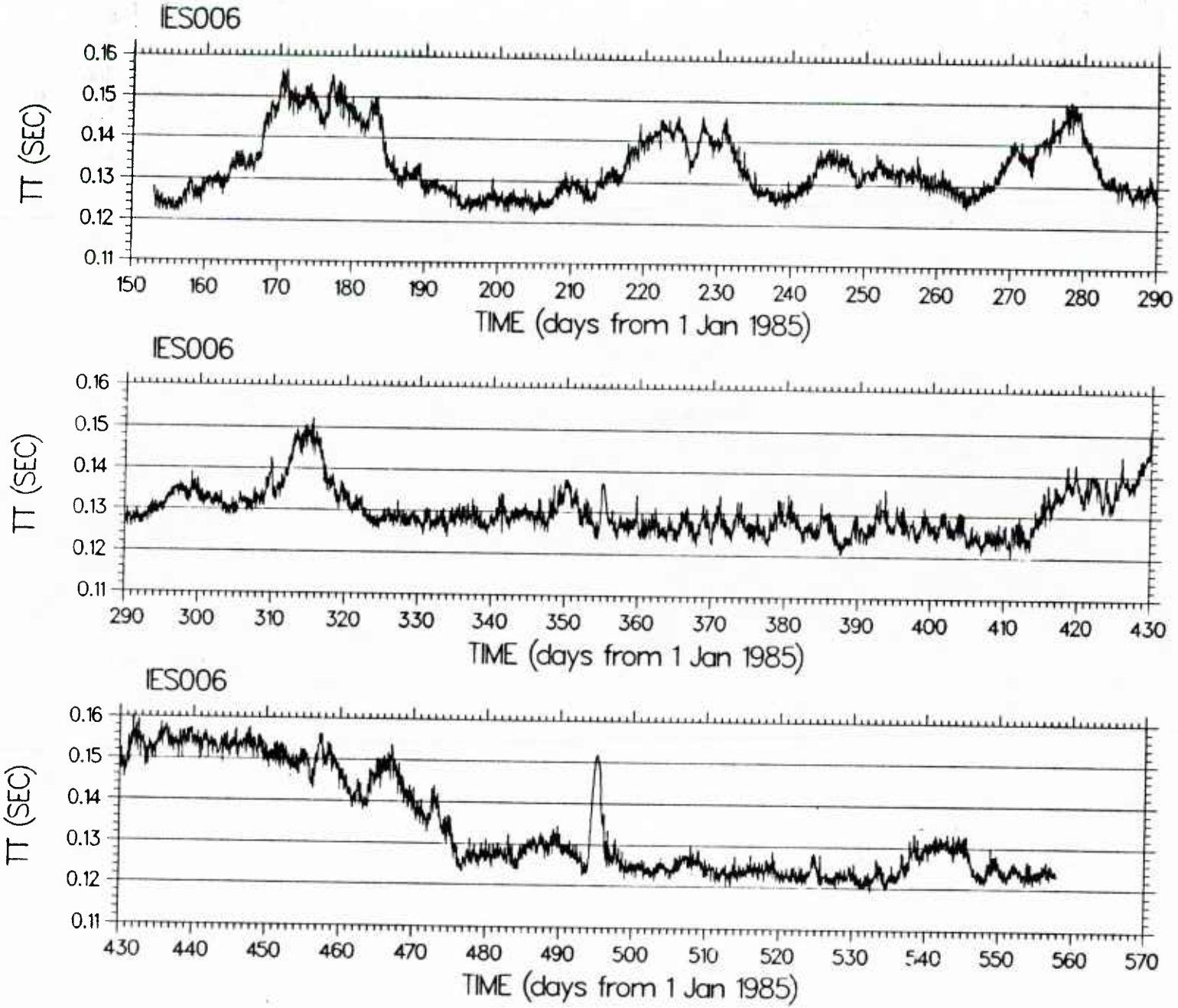

Figure 33. Unfiltered travel-time record.

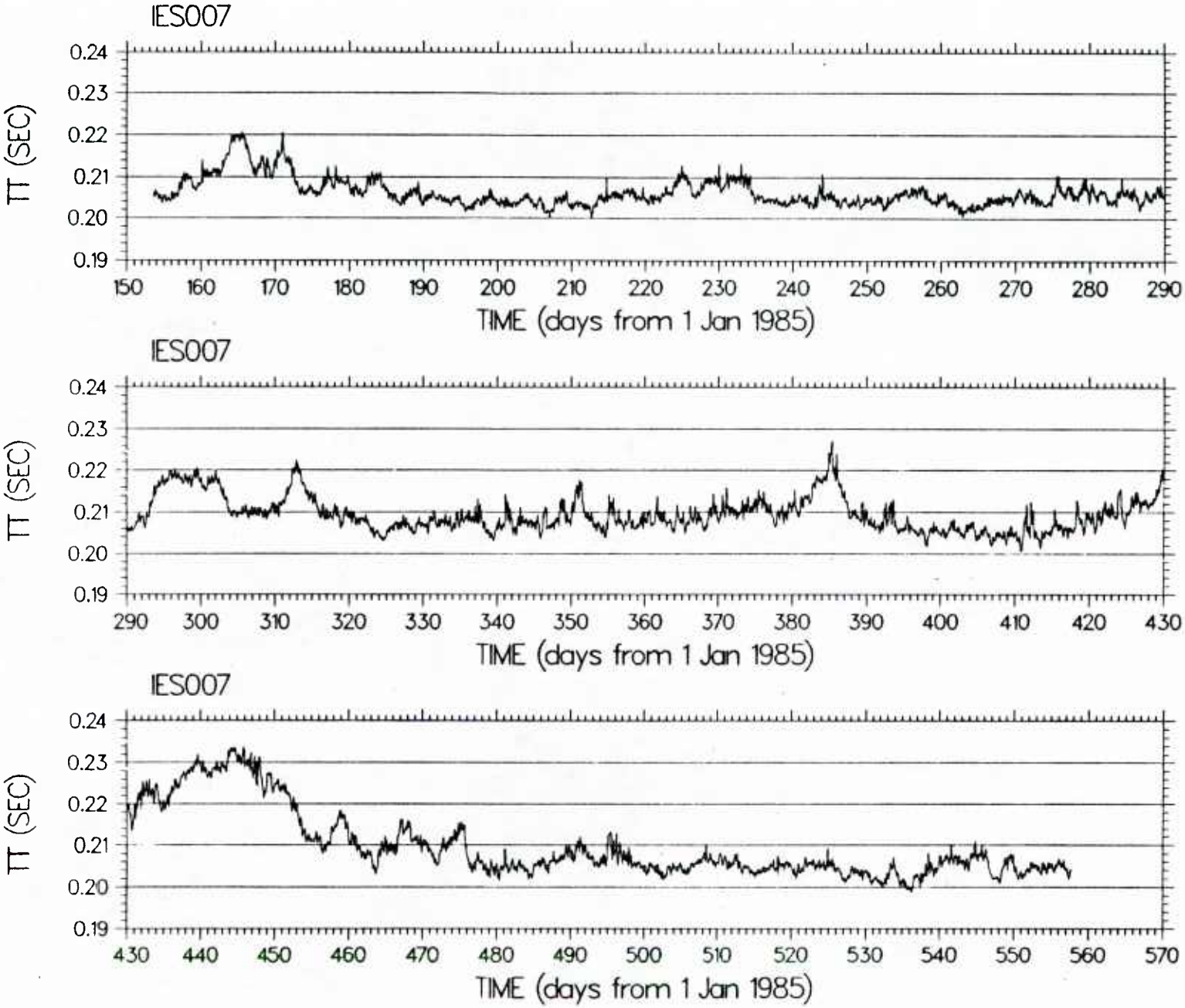

Figure 34. Unfiltered travel-time record.

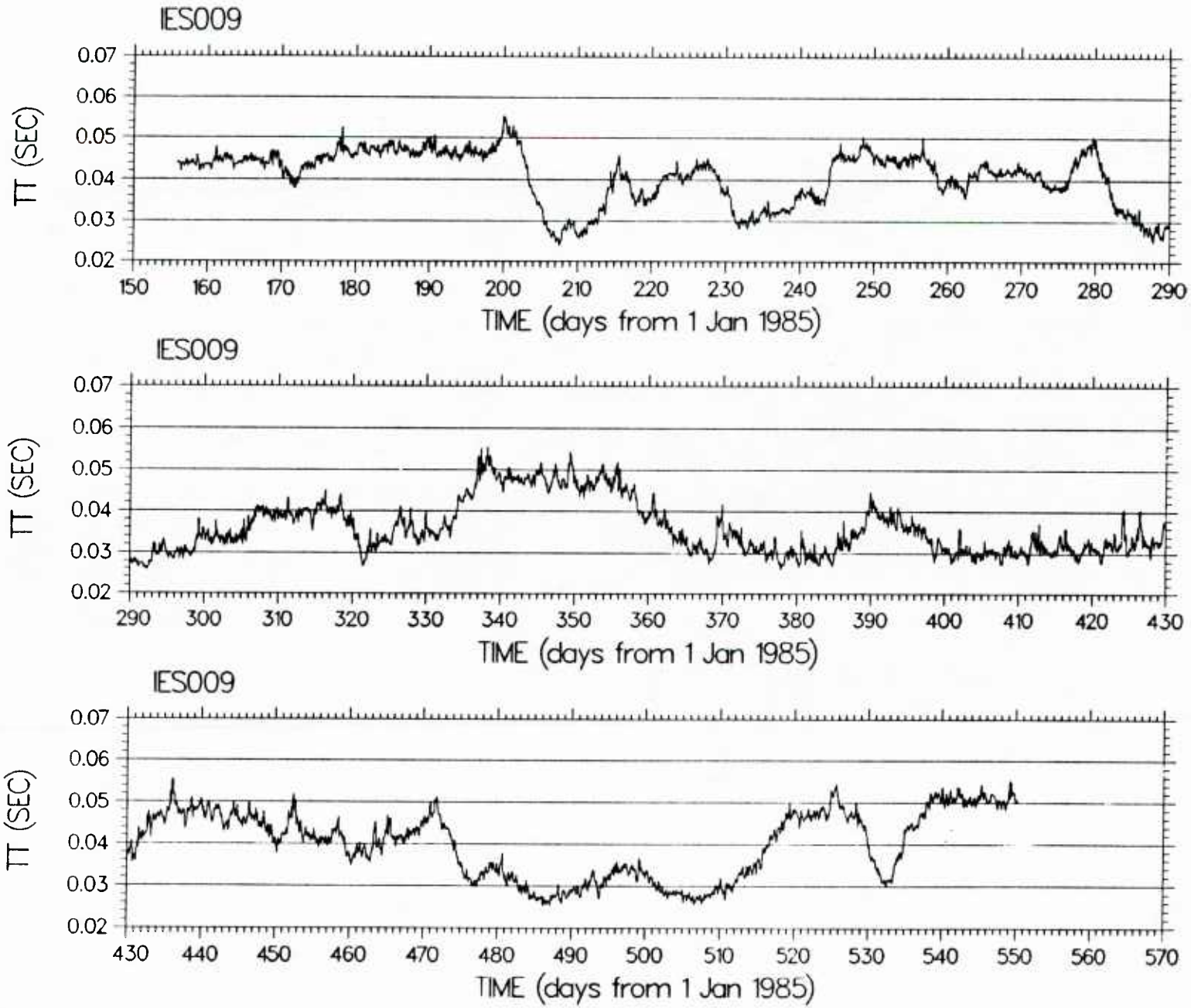

Figure 35. Unfiltered travel-time record.

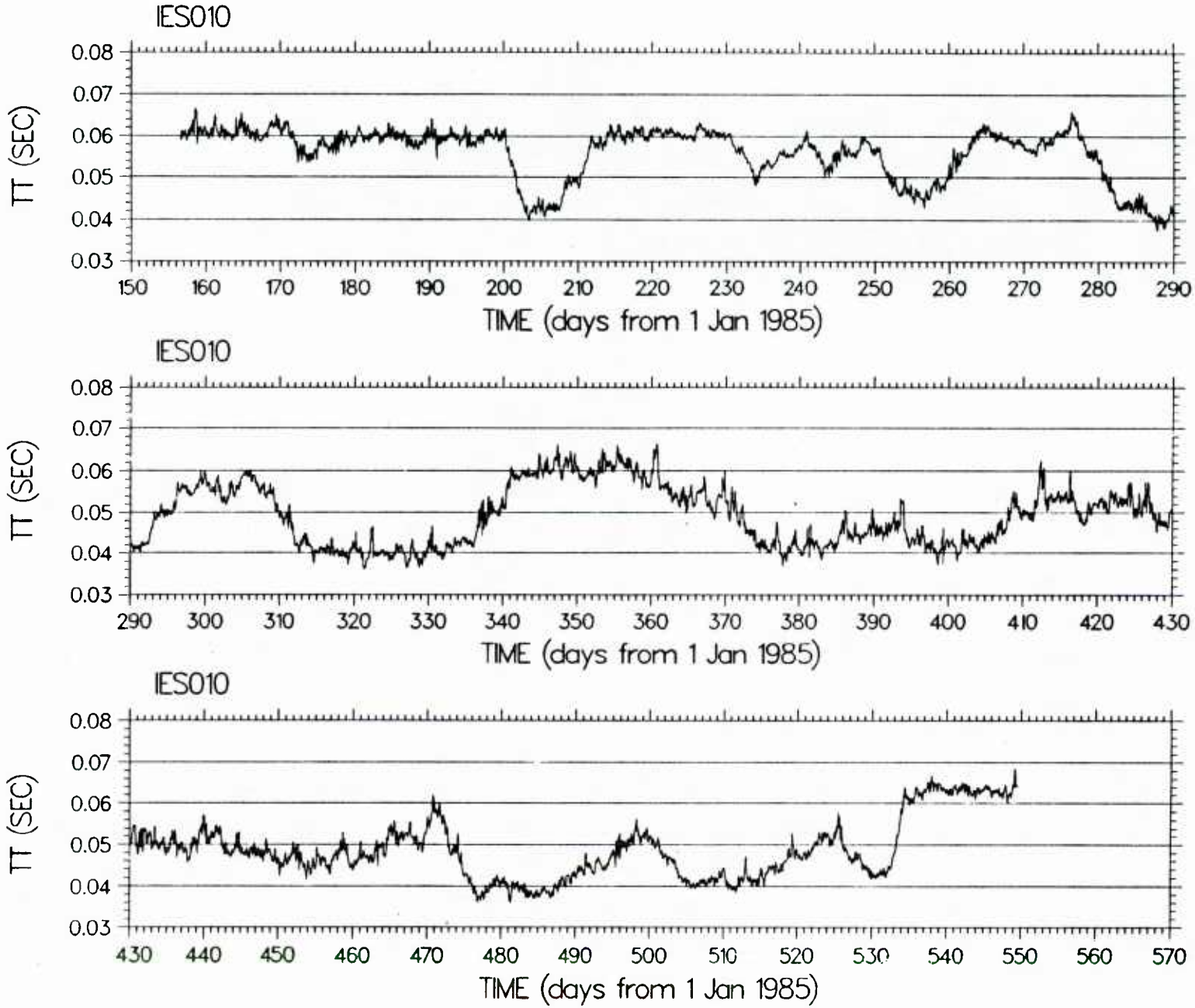

Figure 36. Unfiltered travel-time record.

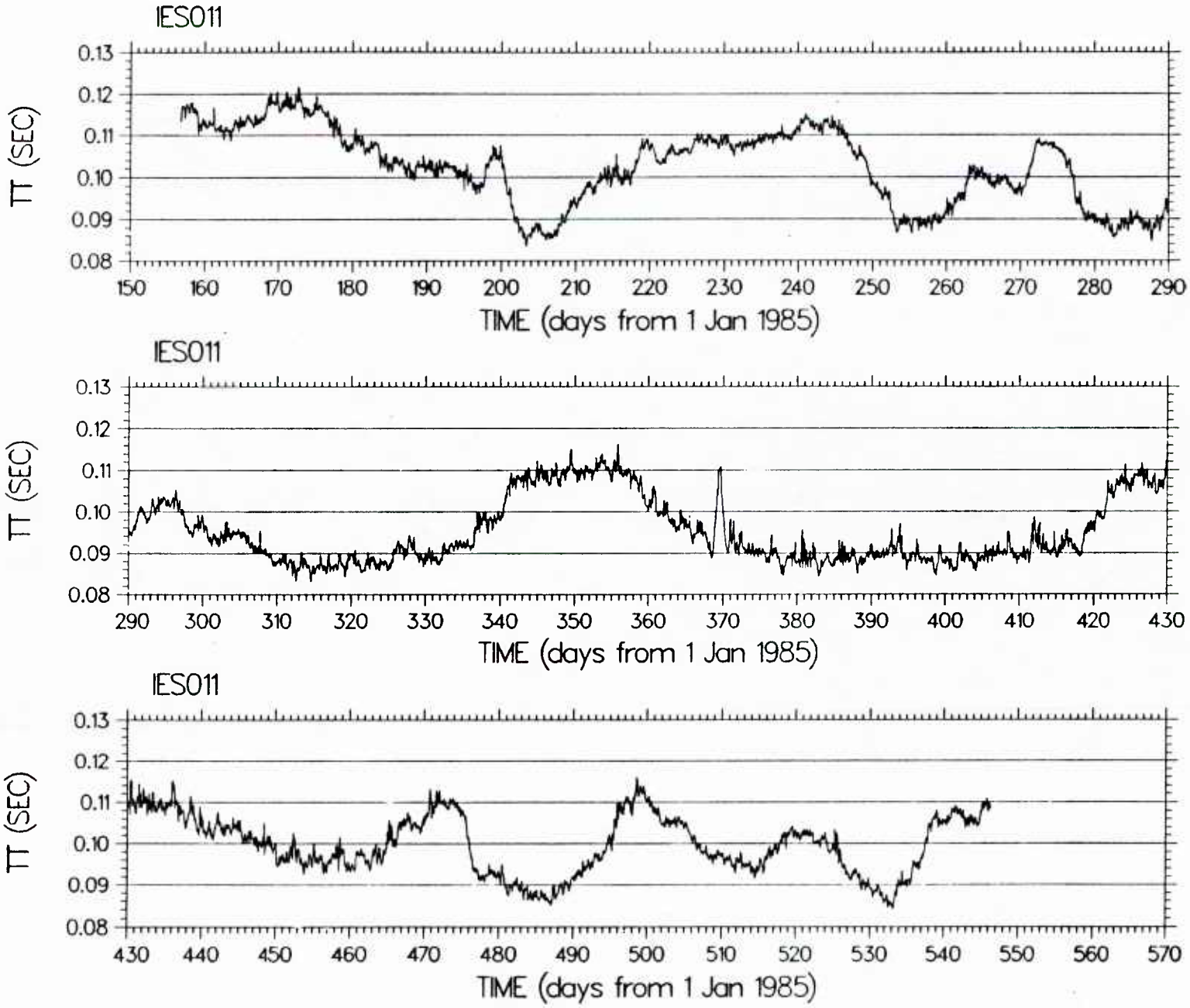

Figure 37. Unfiltered travel-time record.

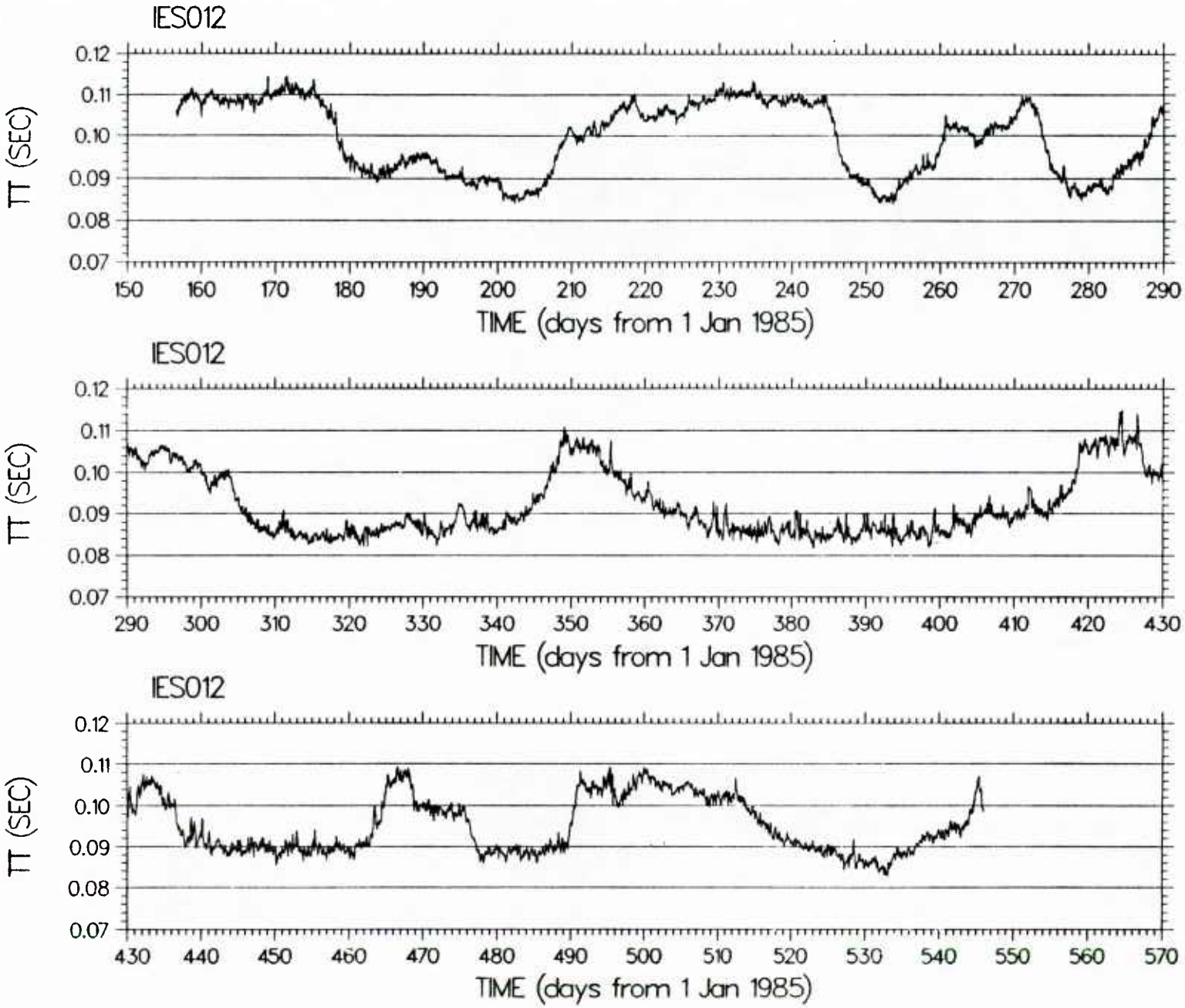

Figure 38. Unfiltered travel-time record.

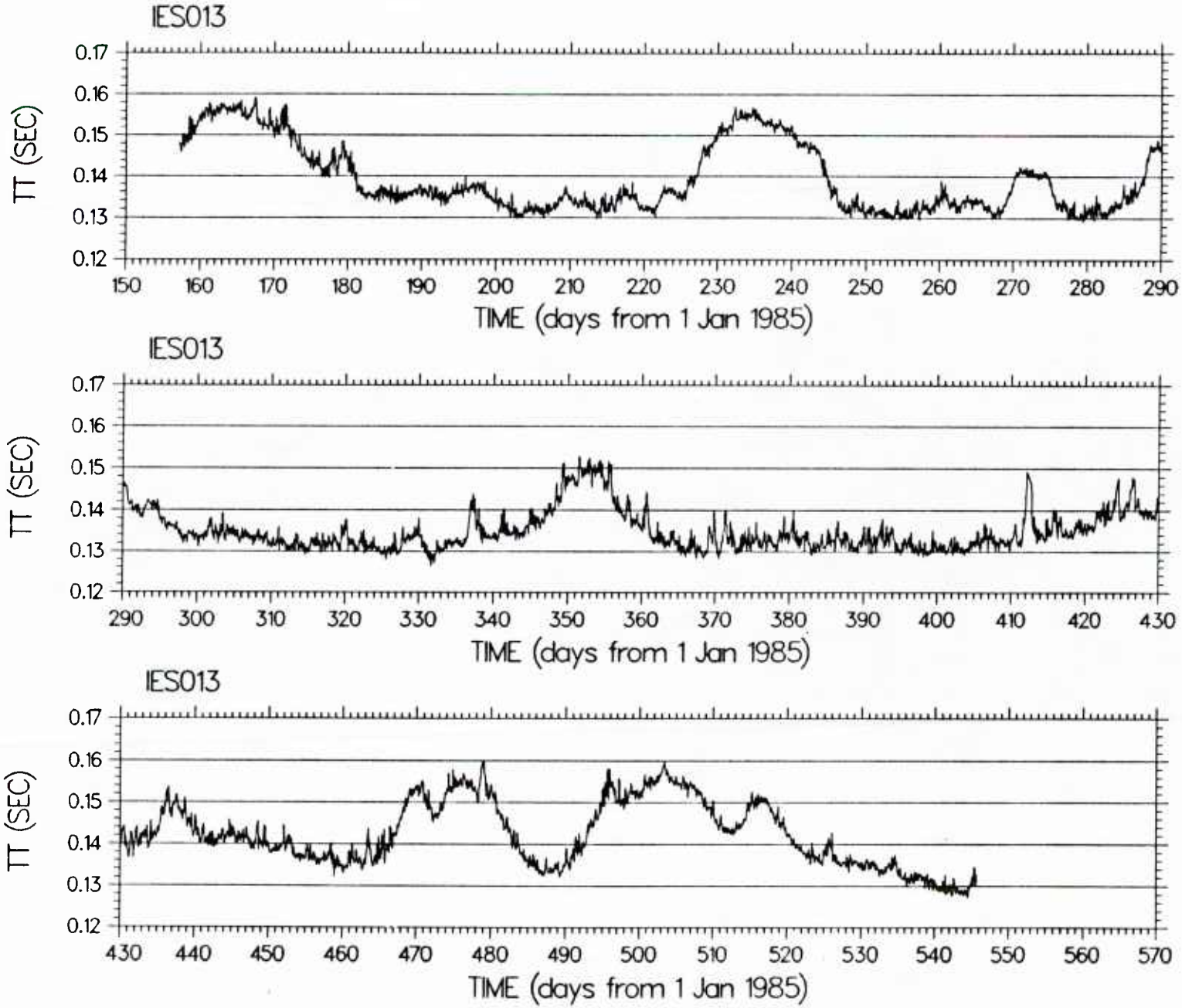

Figure 39. Unfiltered travel-time record.

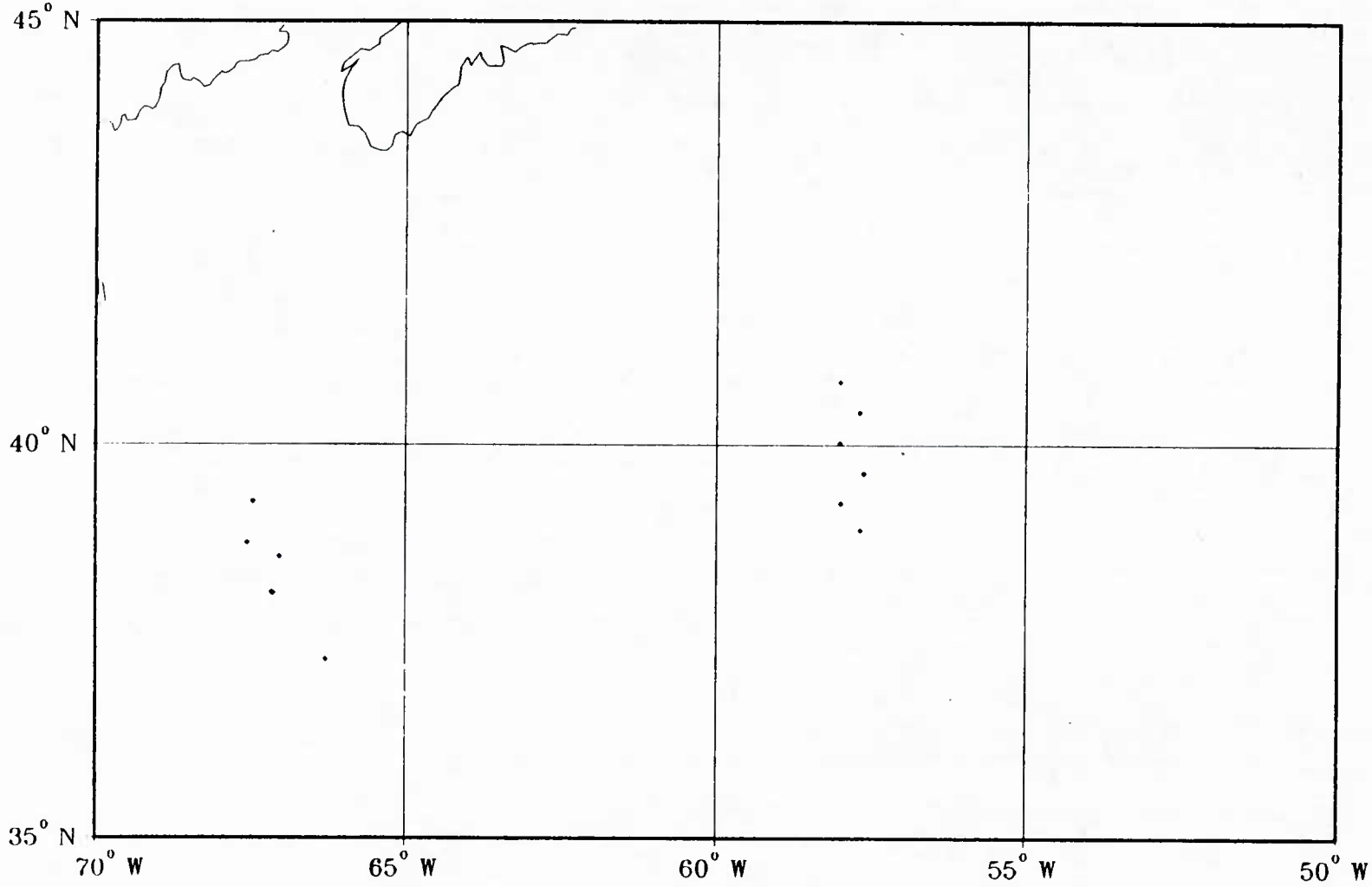

Figure 40. Locations of the CTD casts.

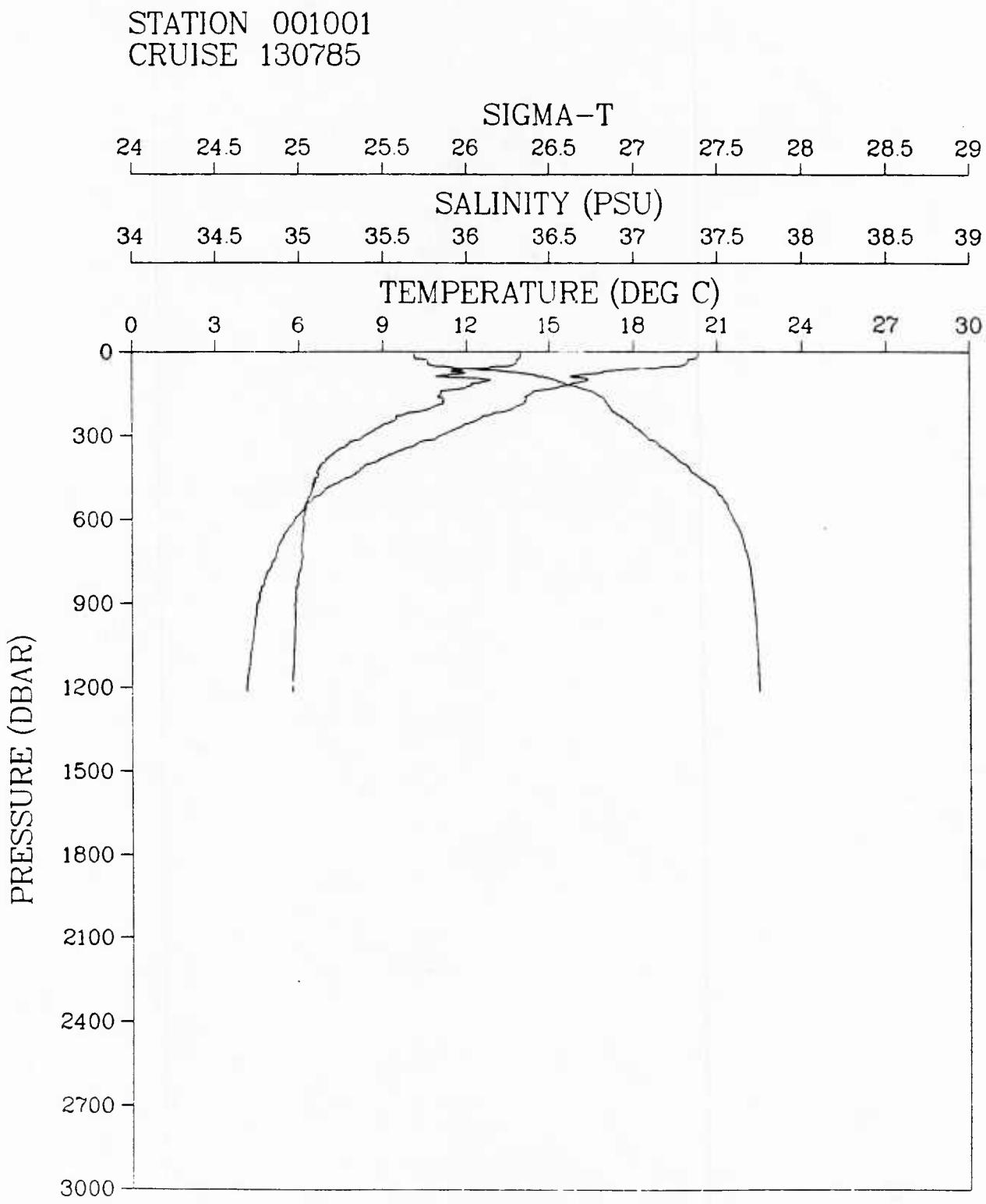

Figure 41. CTD profile plot.

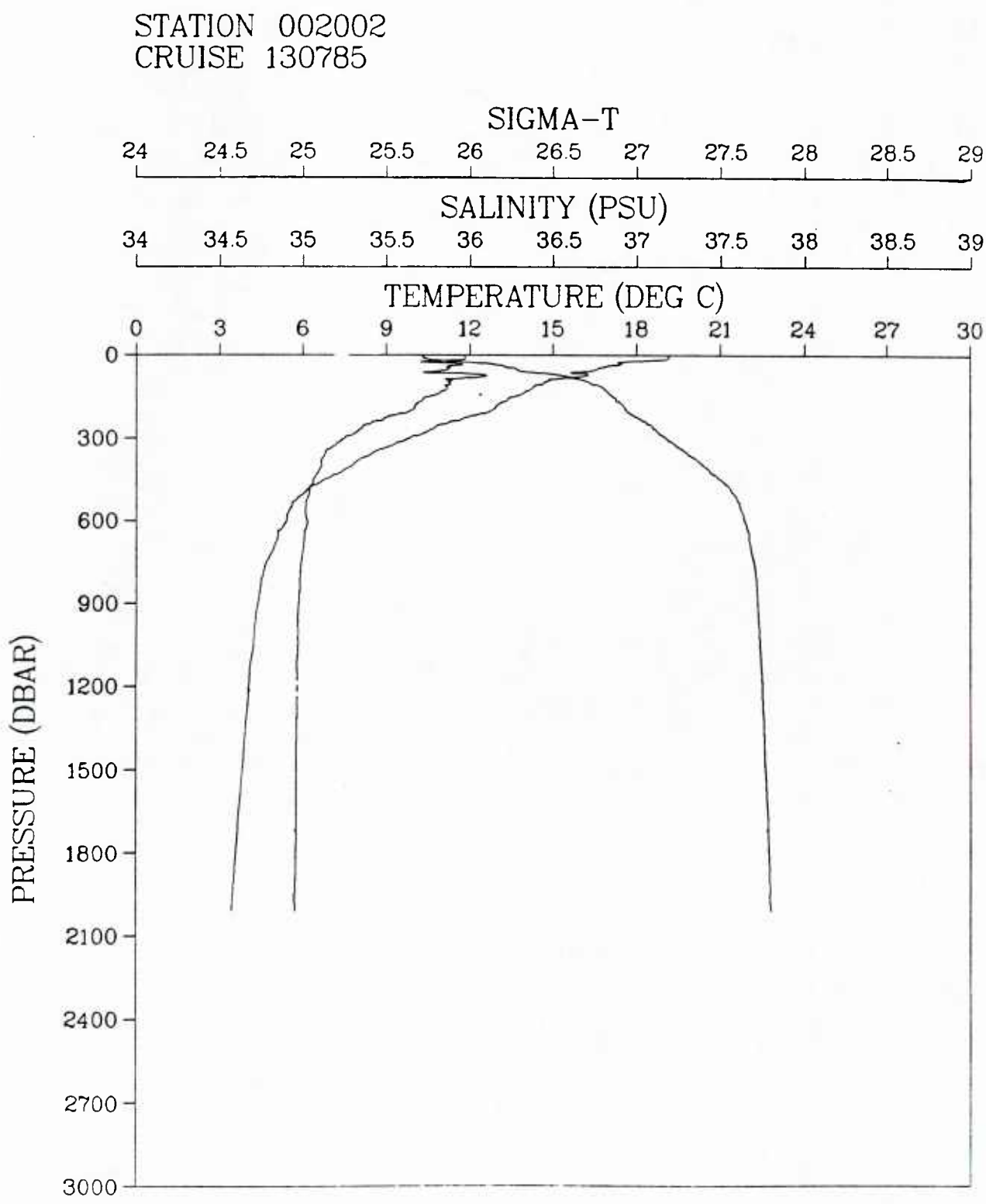

Figure 42. CTD profile plot.

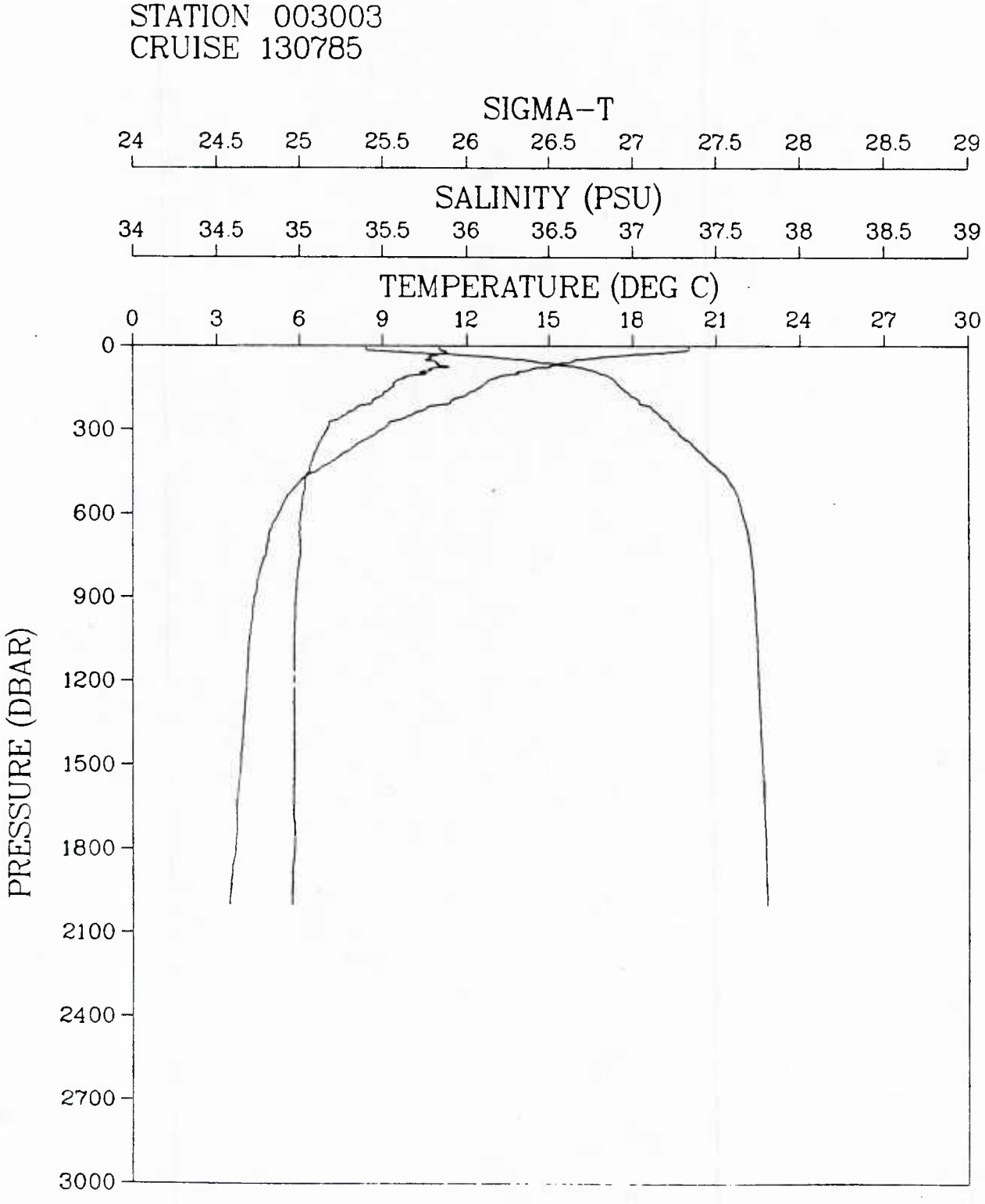

Figure 43. CTD profile plot.

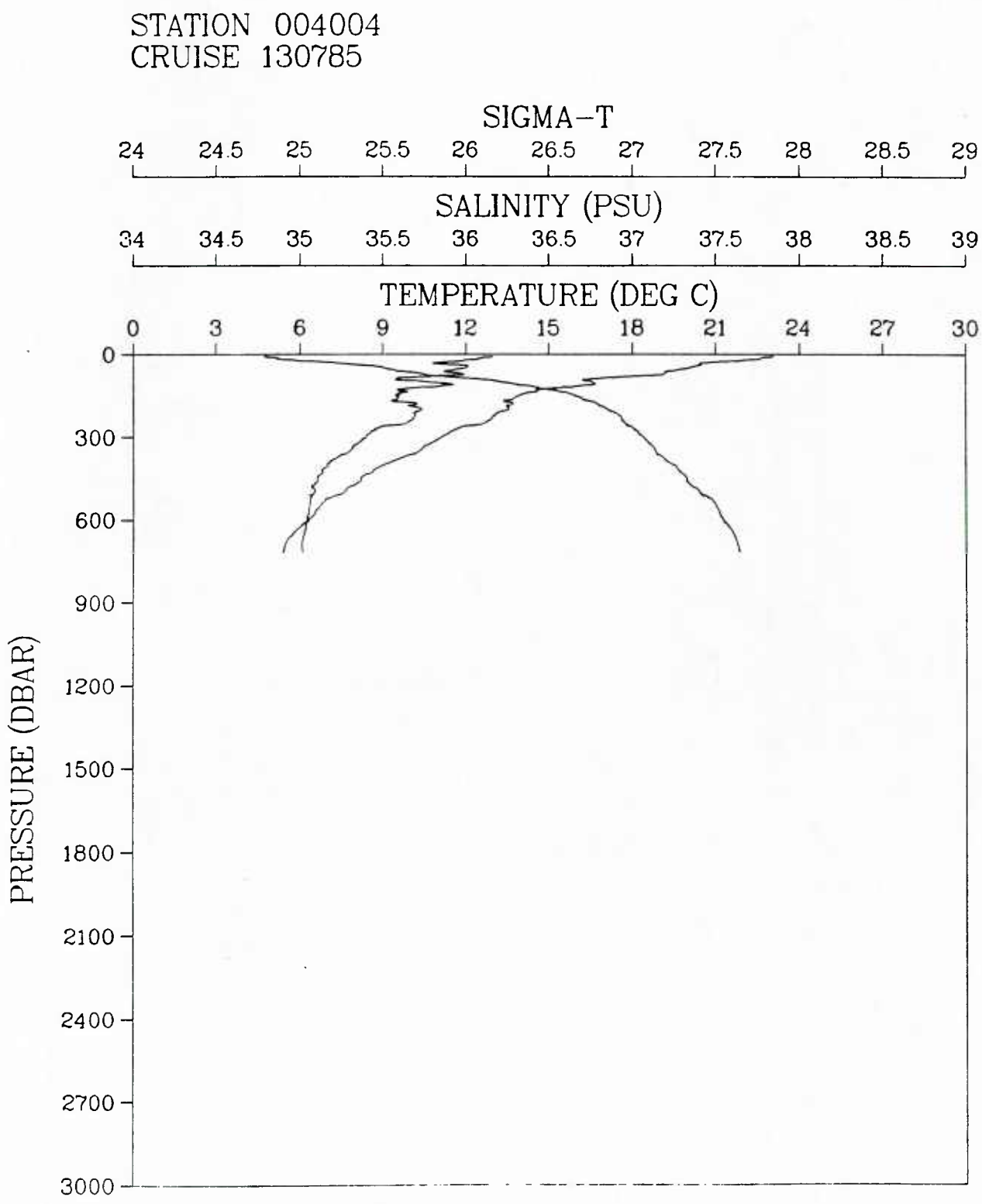

Figure 44. CTD profile plot.

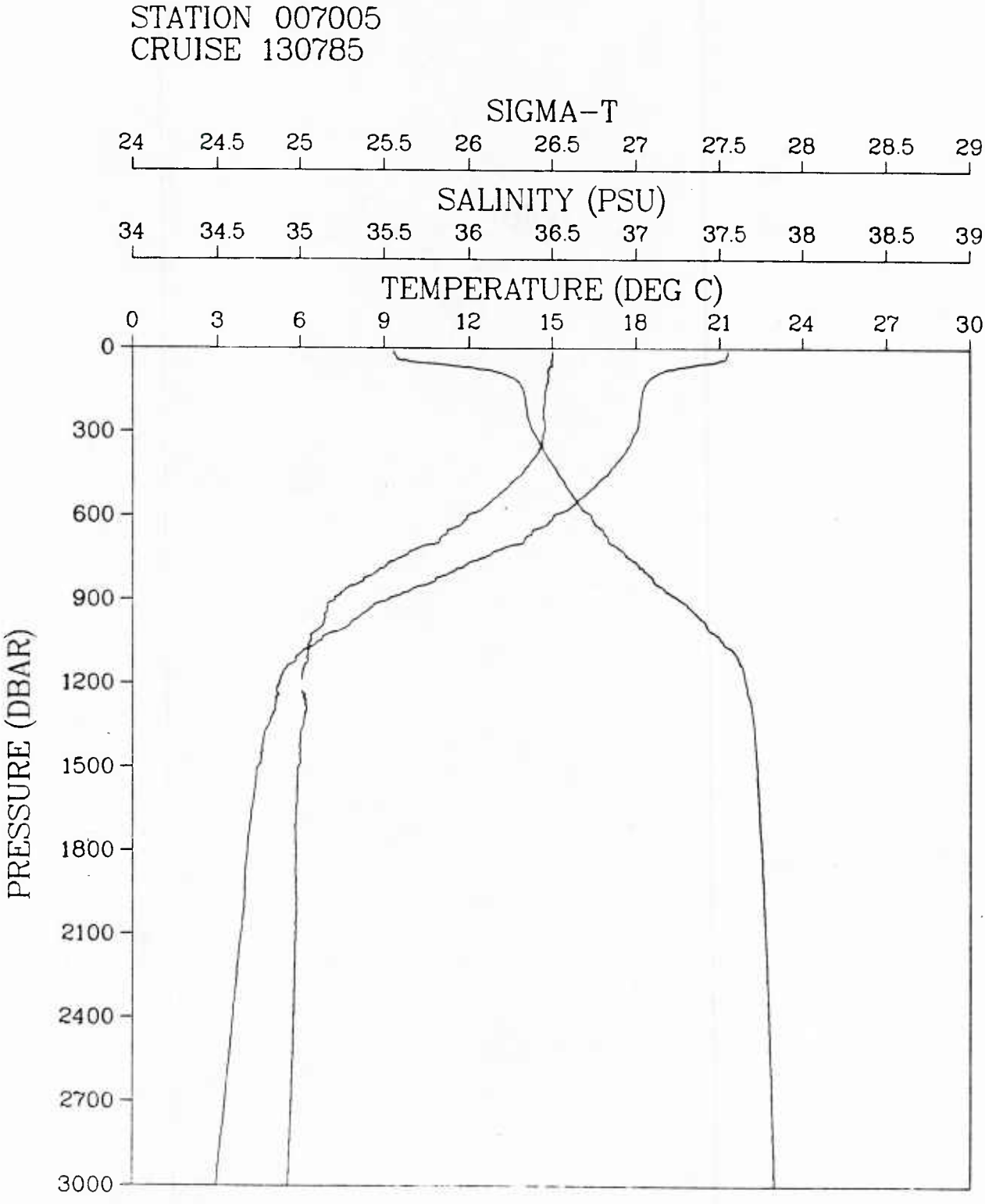

Figure 45. CTD profile plot.

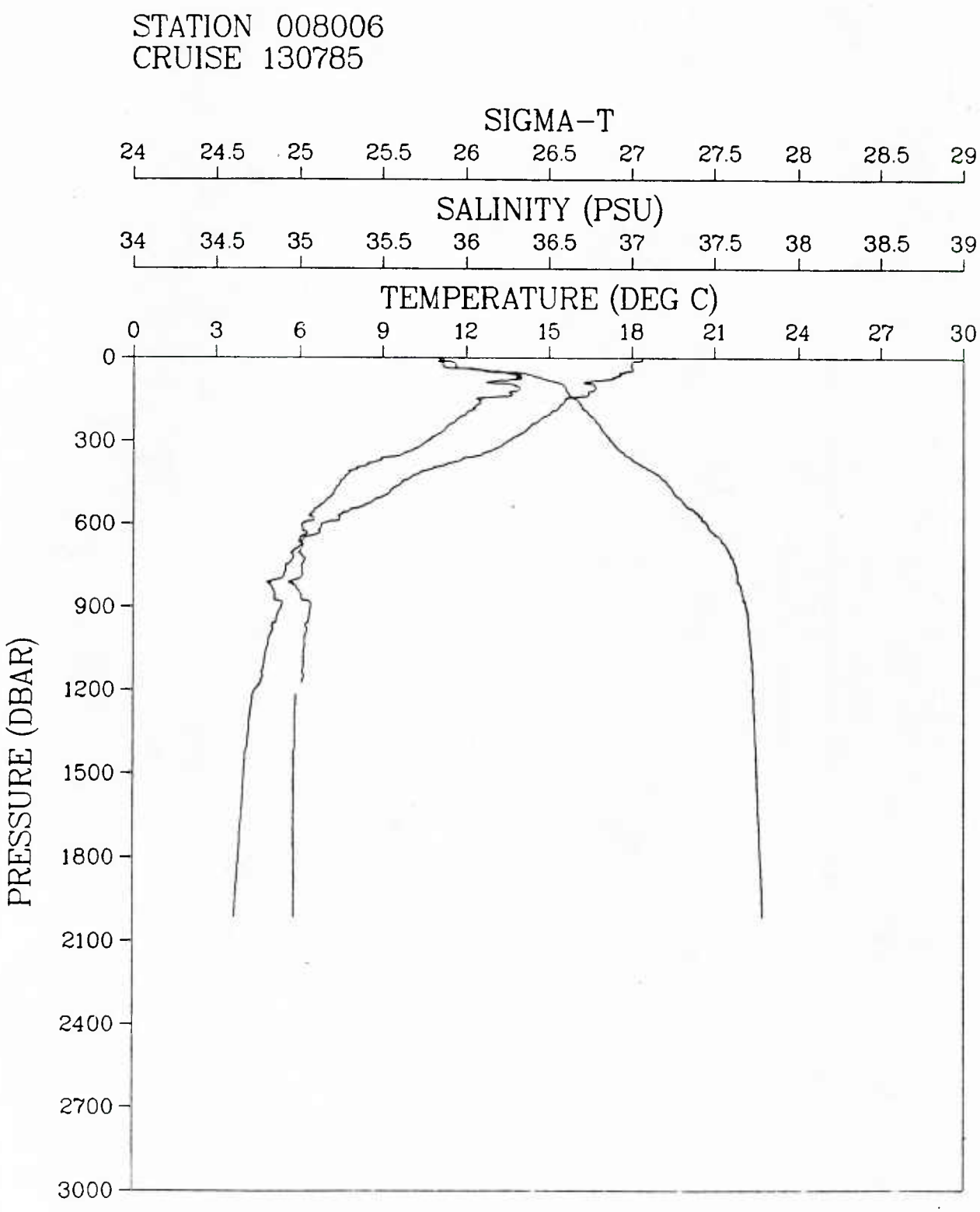

Figure 46. CTD profile plot.

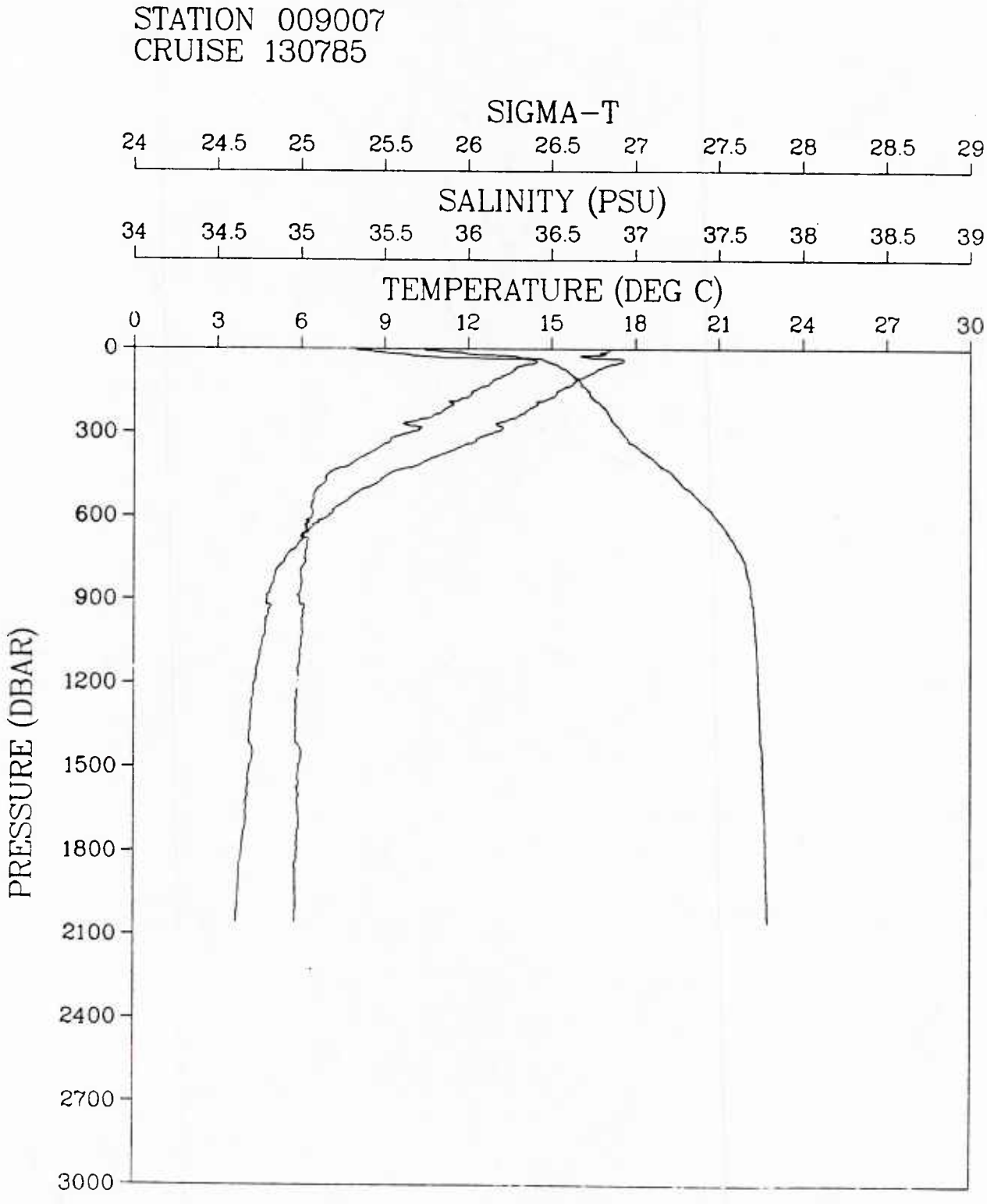

Figure 47. CTD profile plot.

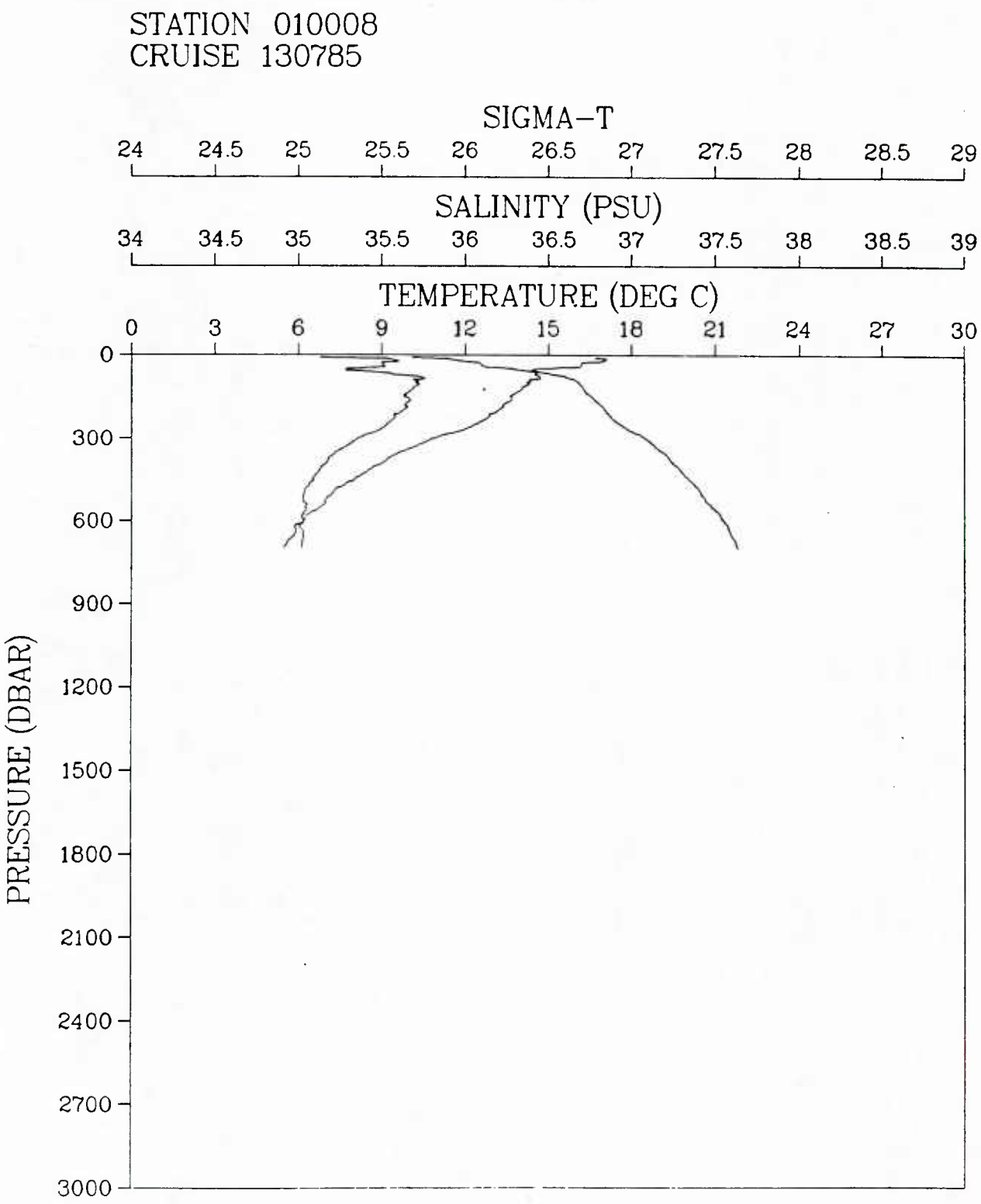

Figure 48. CTD profile plot.

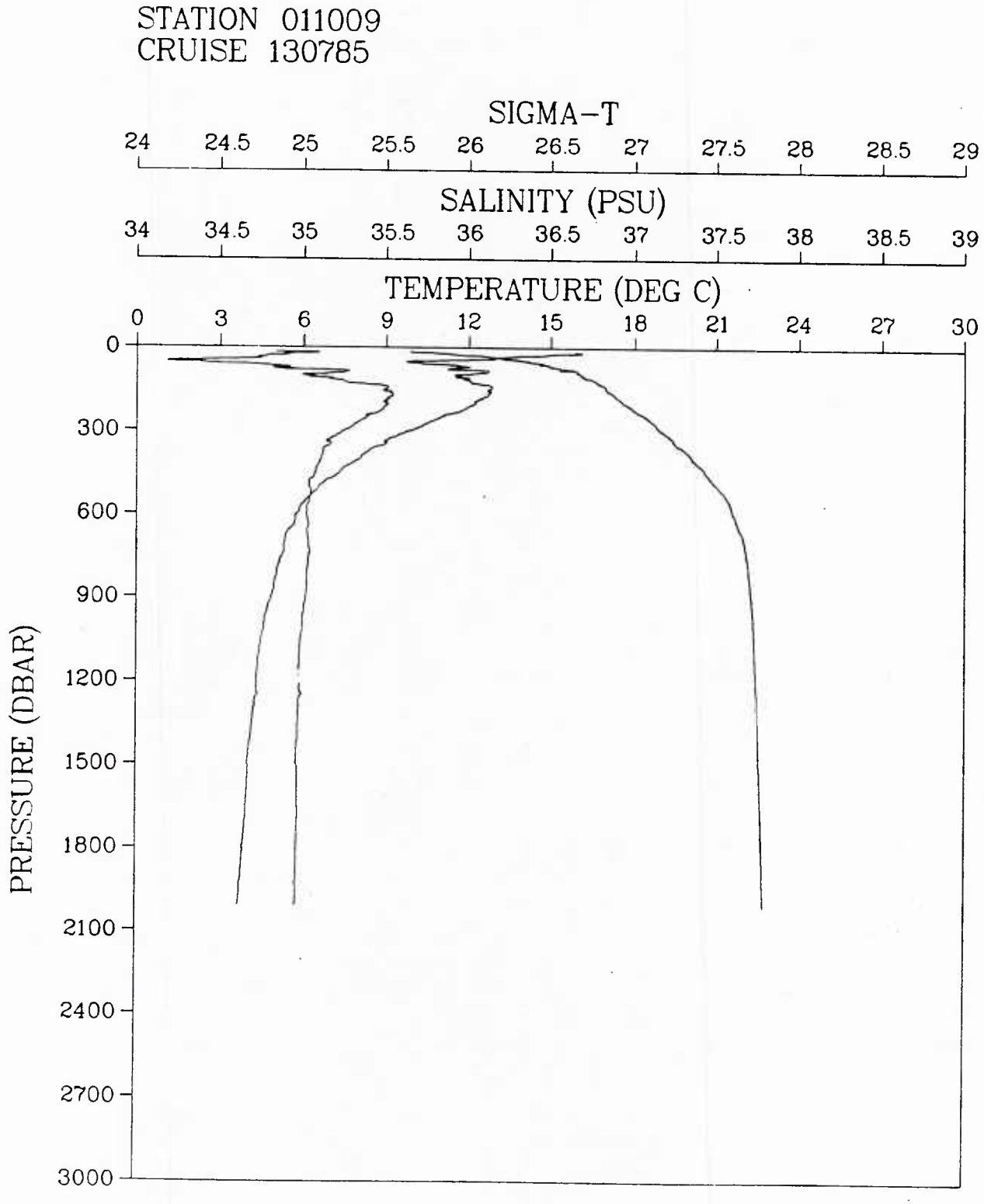

Figure 49. CTD profile plot.

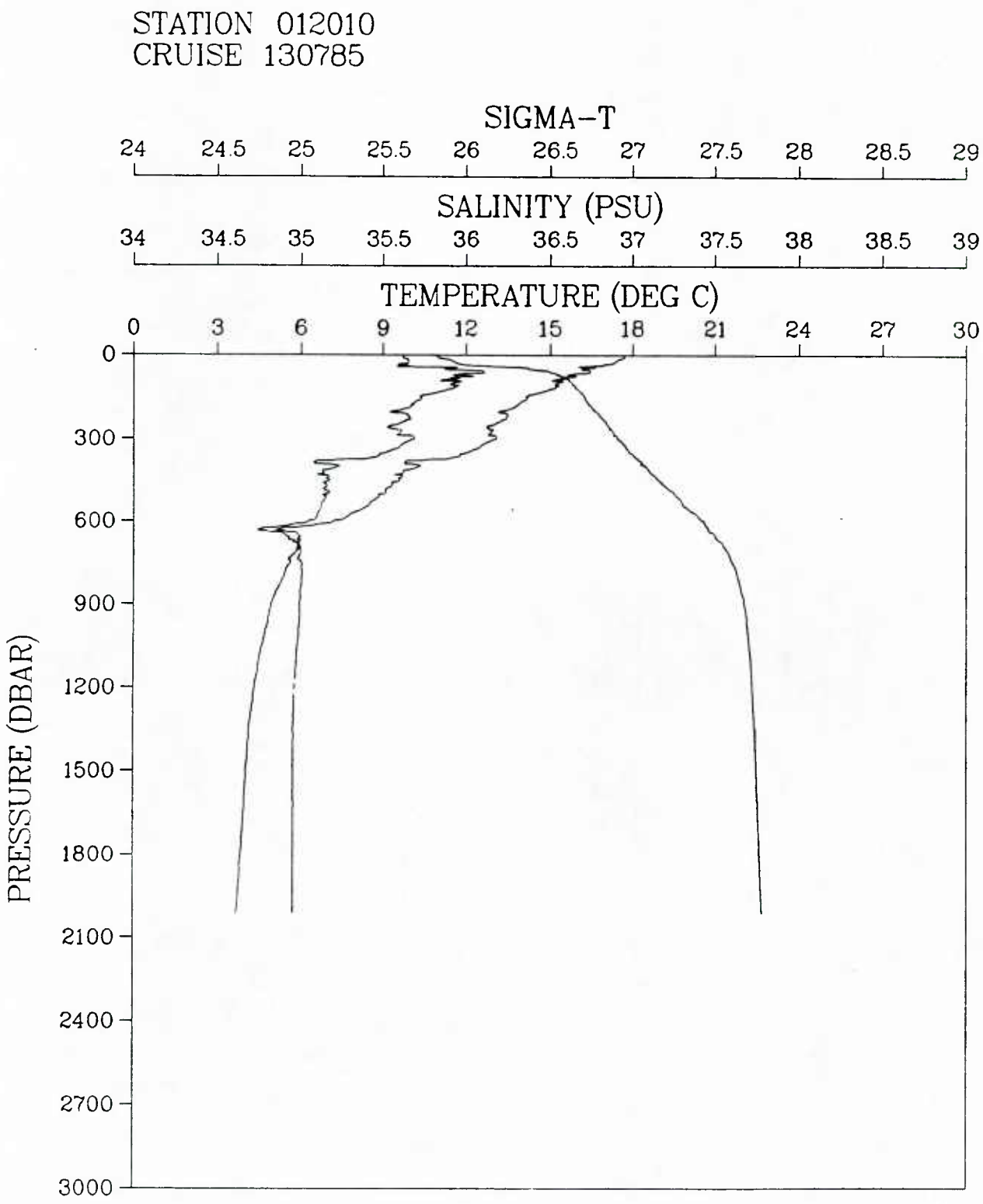

Figure 50. CTD profile plot.

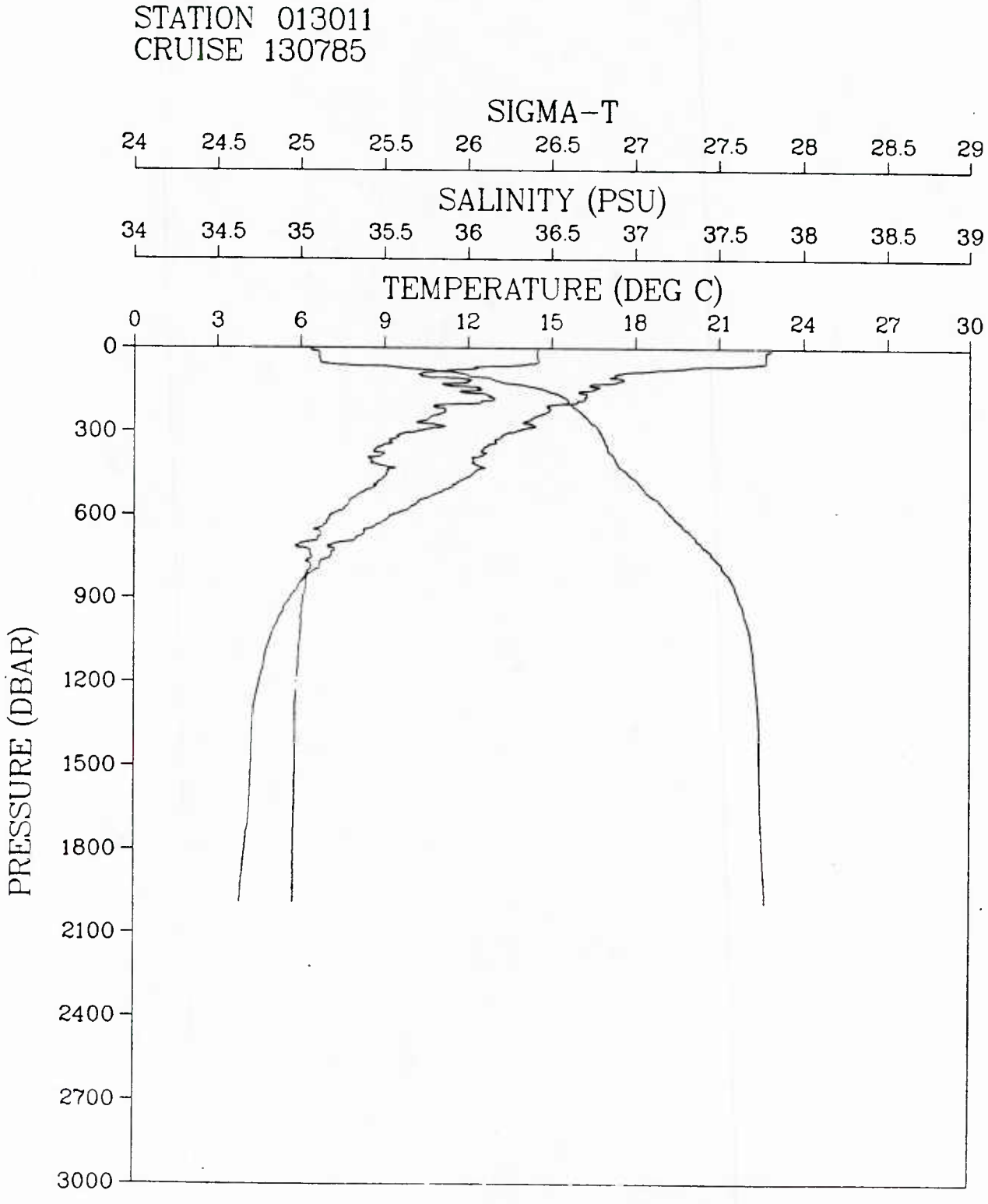

Figure 51. CTD profile plot.

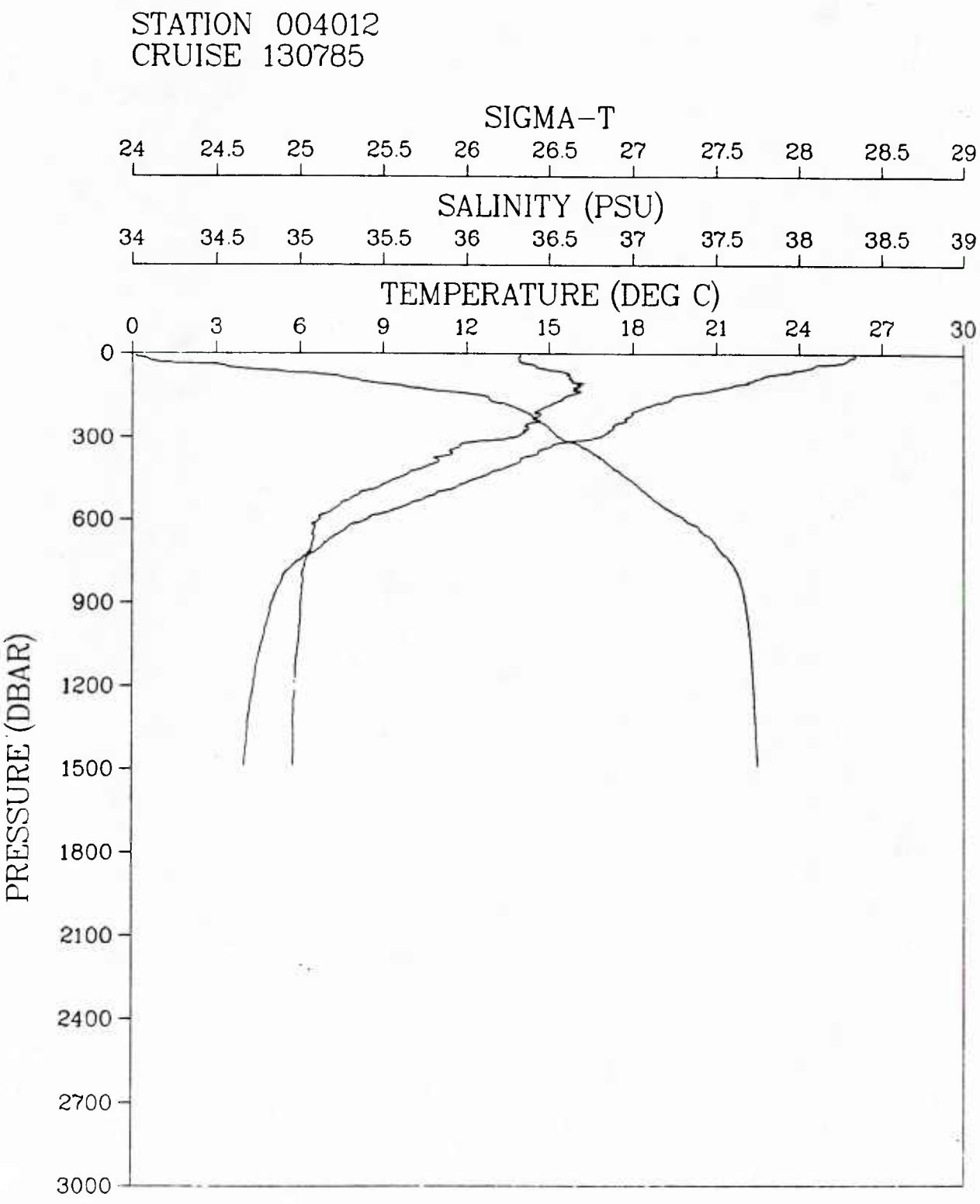

Figure 52. CTD profile plot.

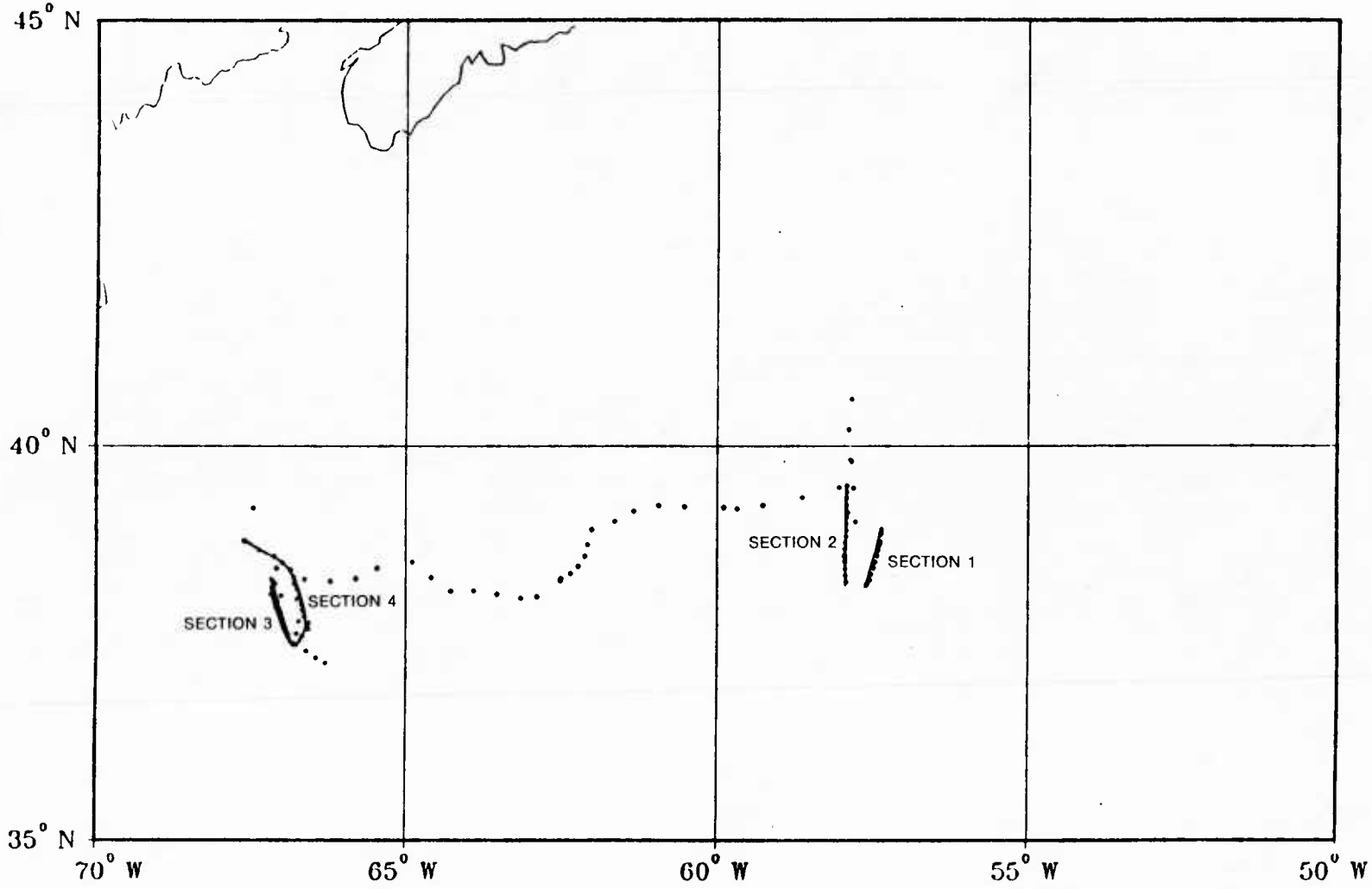

Figure 53. Locations of the XBT drops during the IES deployment cruise.

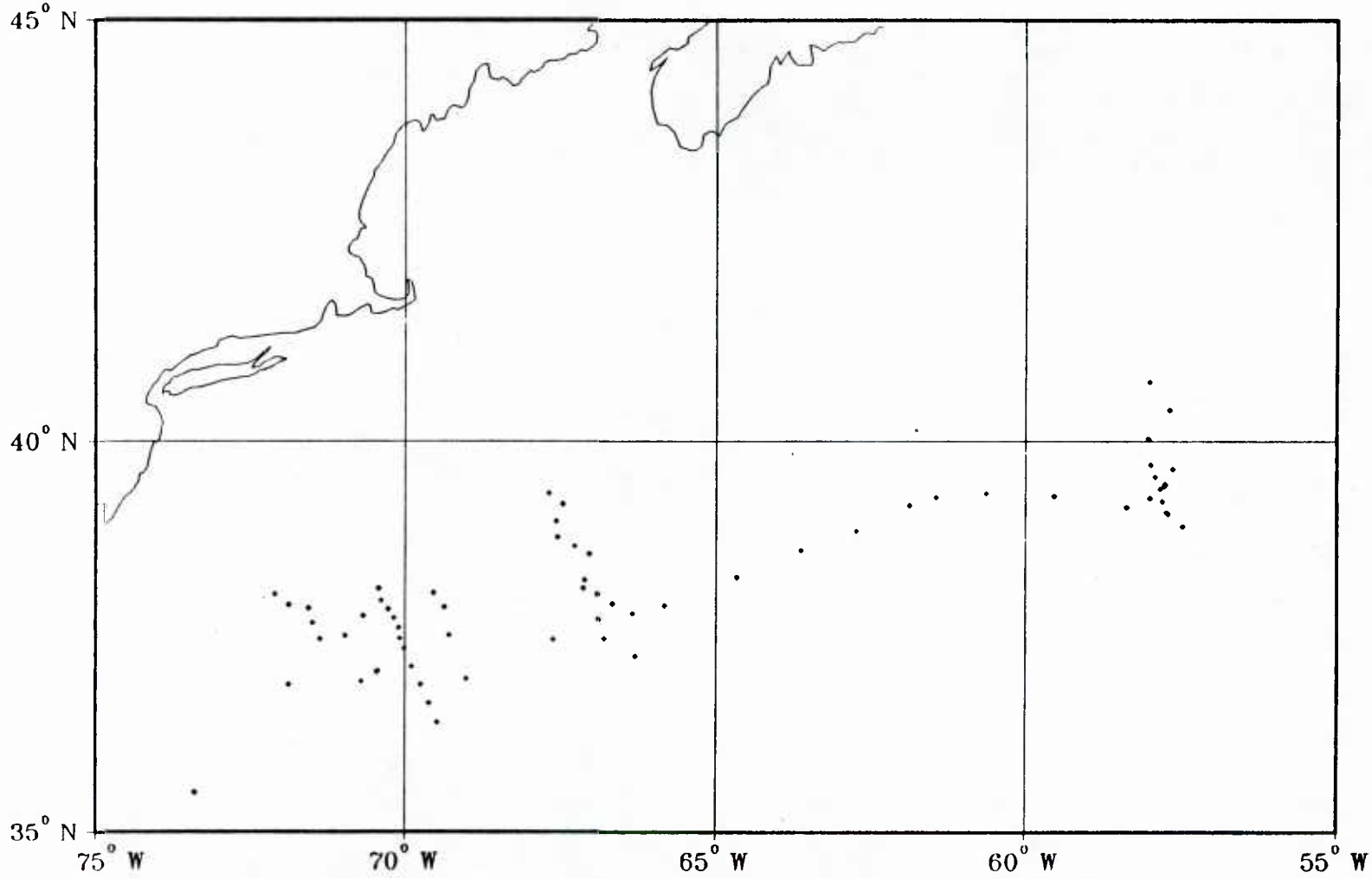

Figure 54. Locations of the XBT drops during the IES recovery cruise.

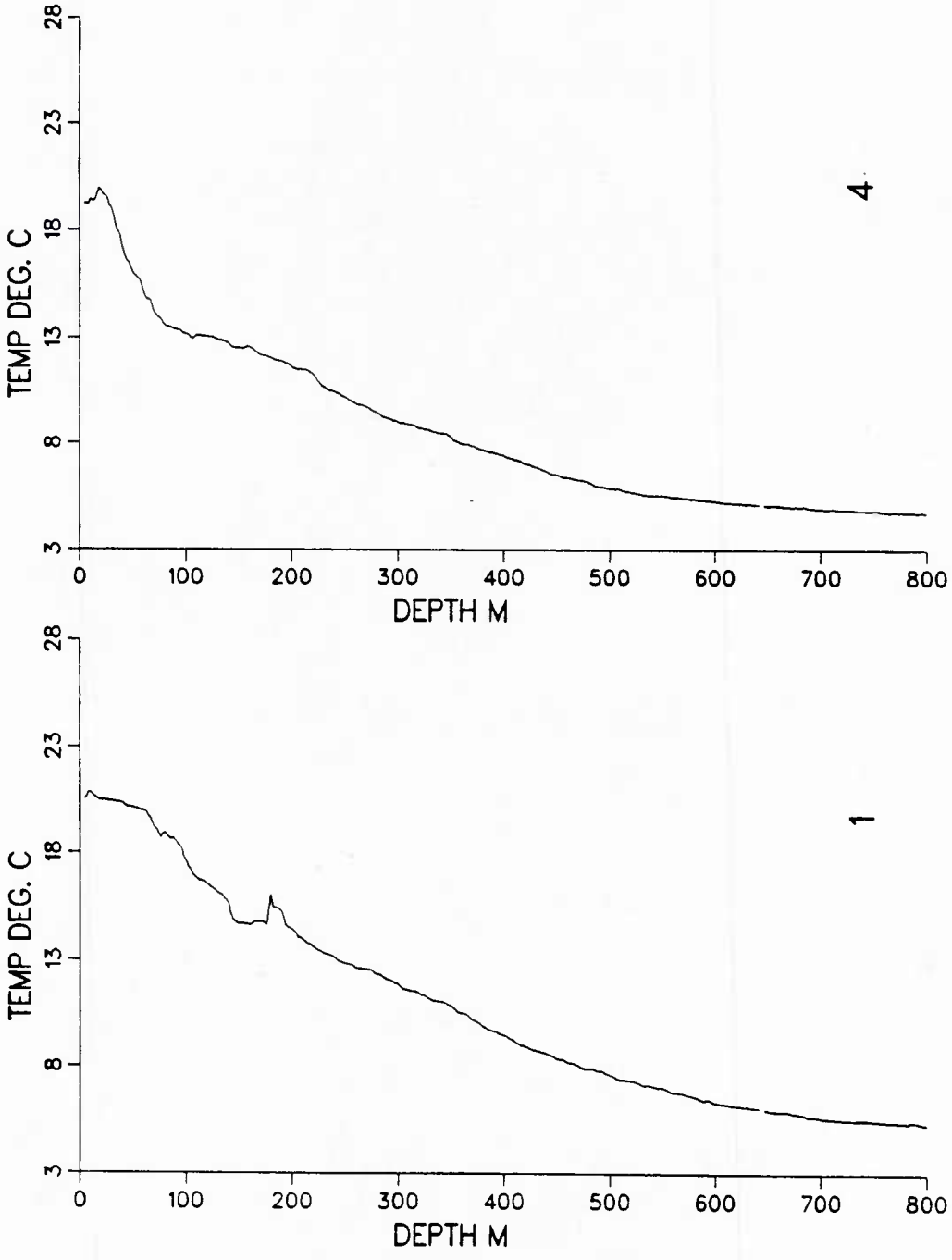

Figure 55. XBT profiles from IES deployment cruise.

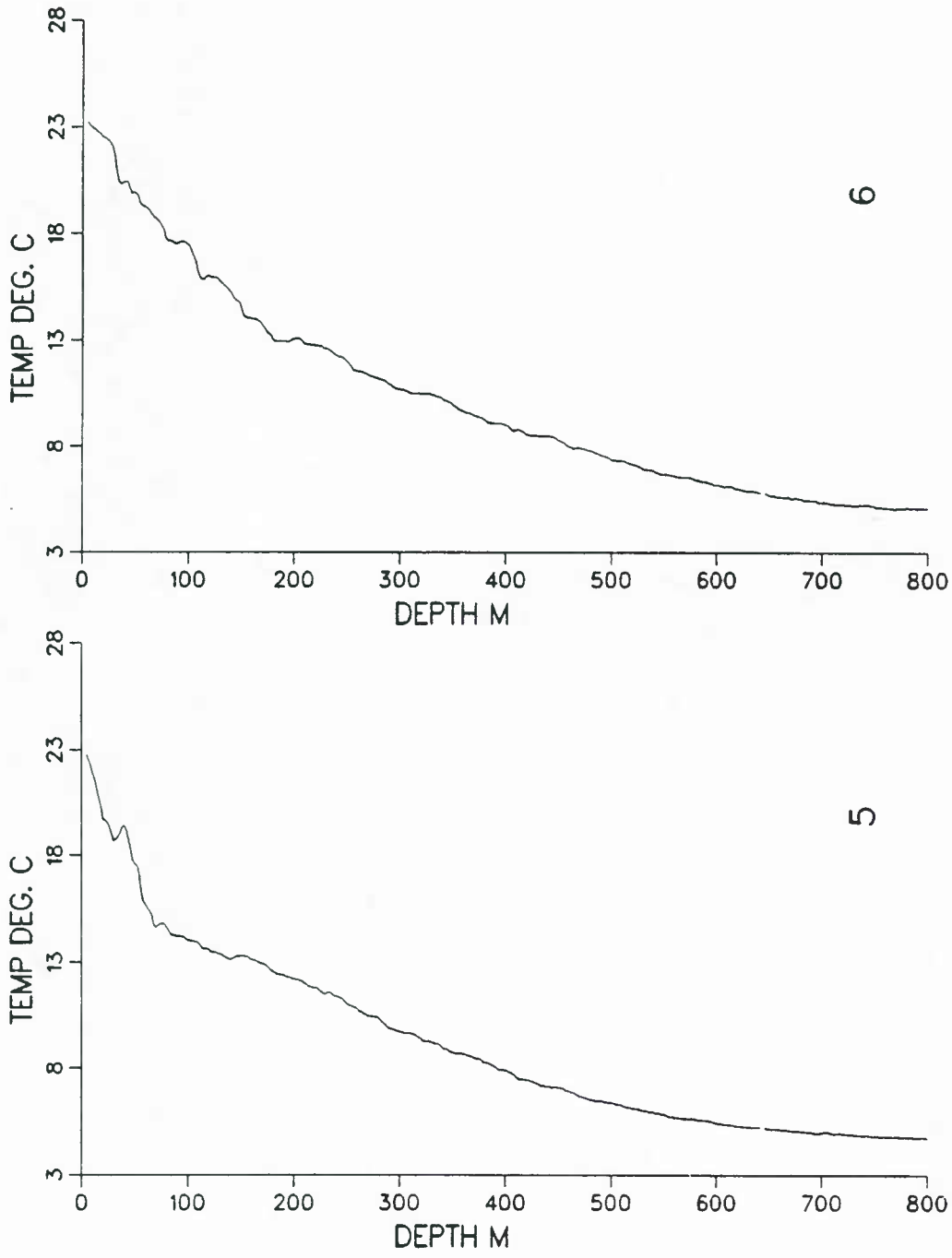

Figure 56. XBT profiles from IES deployment cruise.

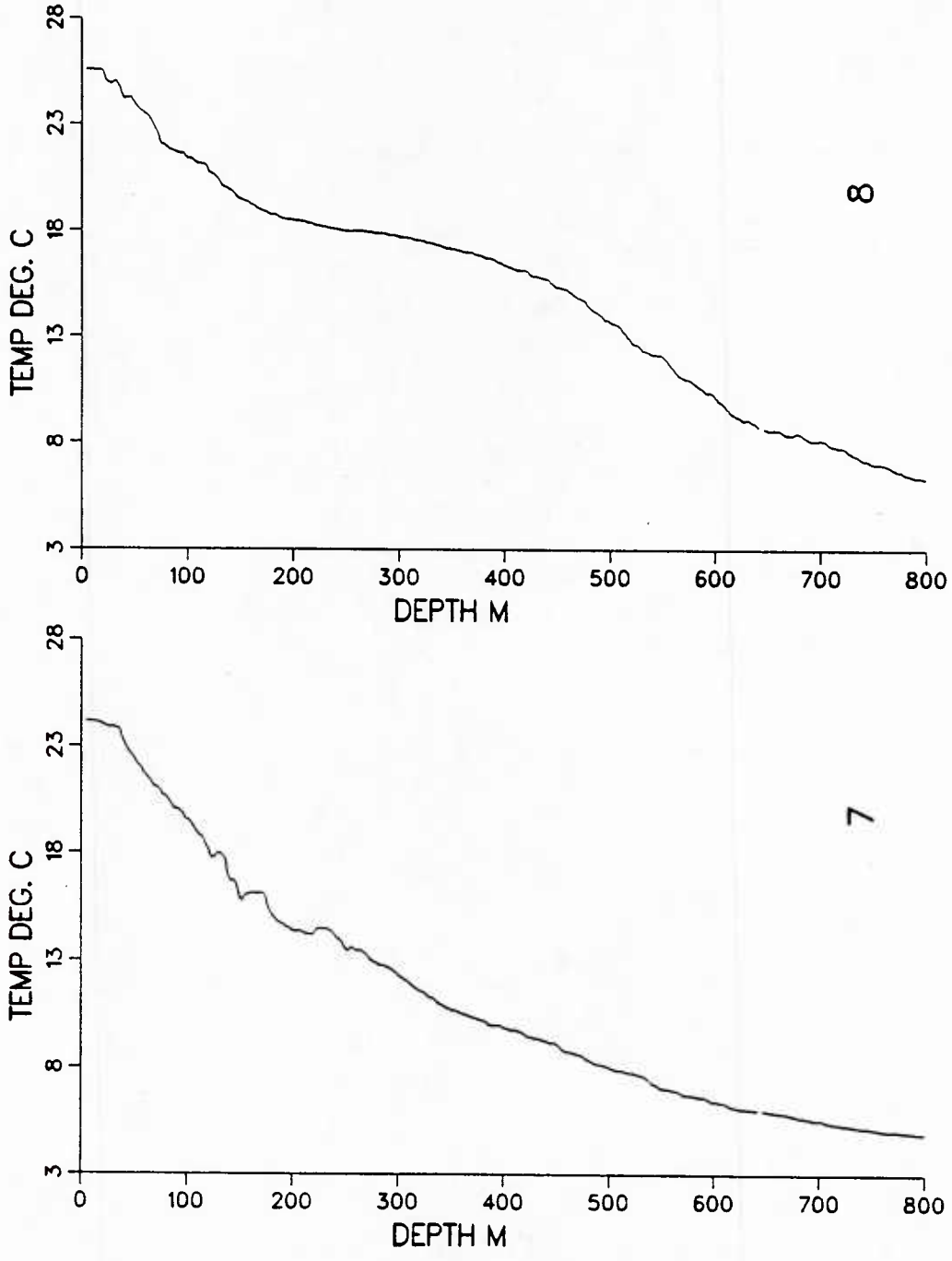

Figure 57. XBT profiles from IES deployment cruise.

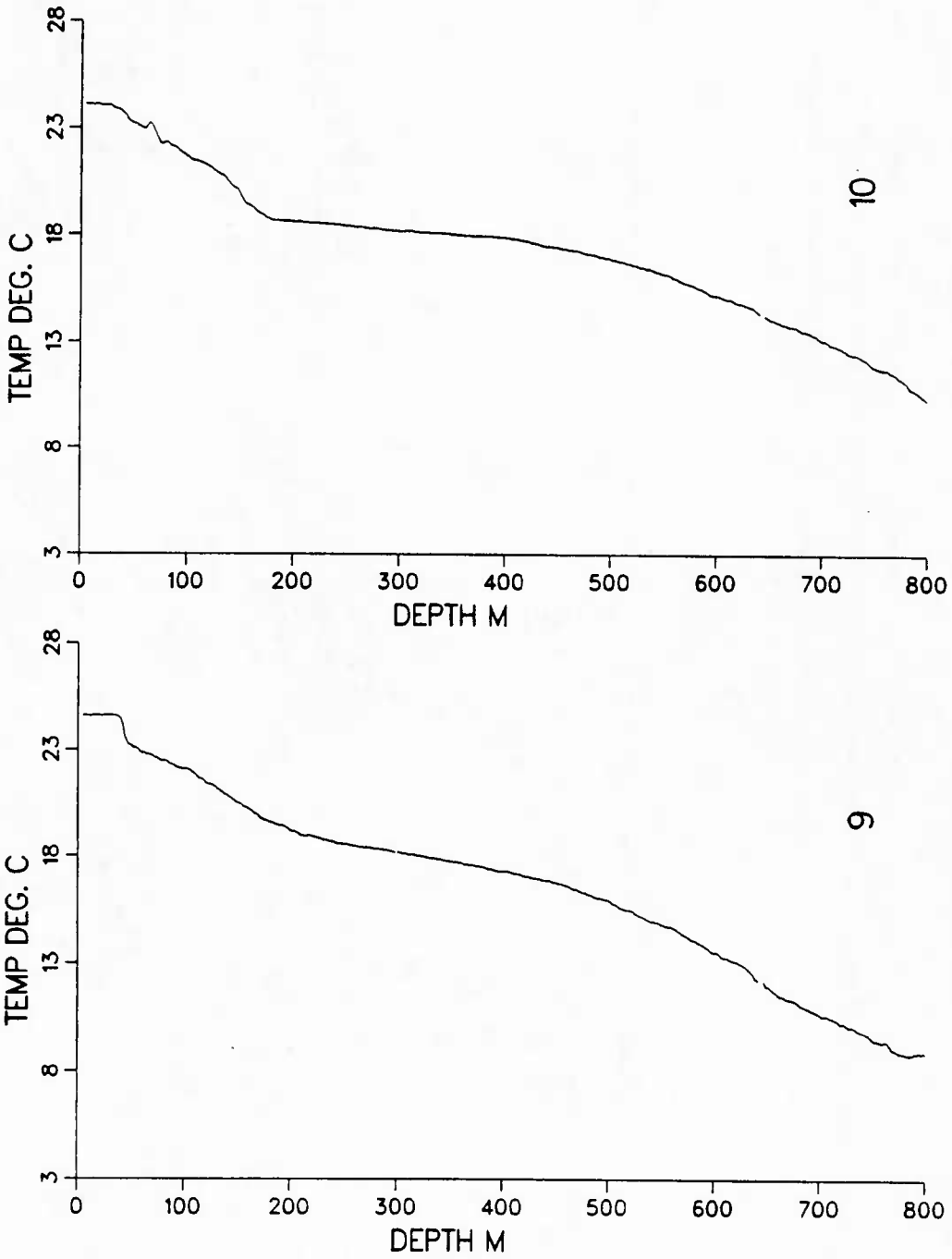

Figure 58. XBT profiles from IES deployment cruise.

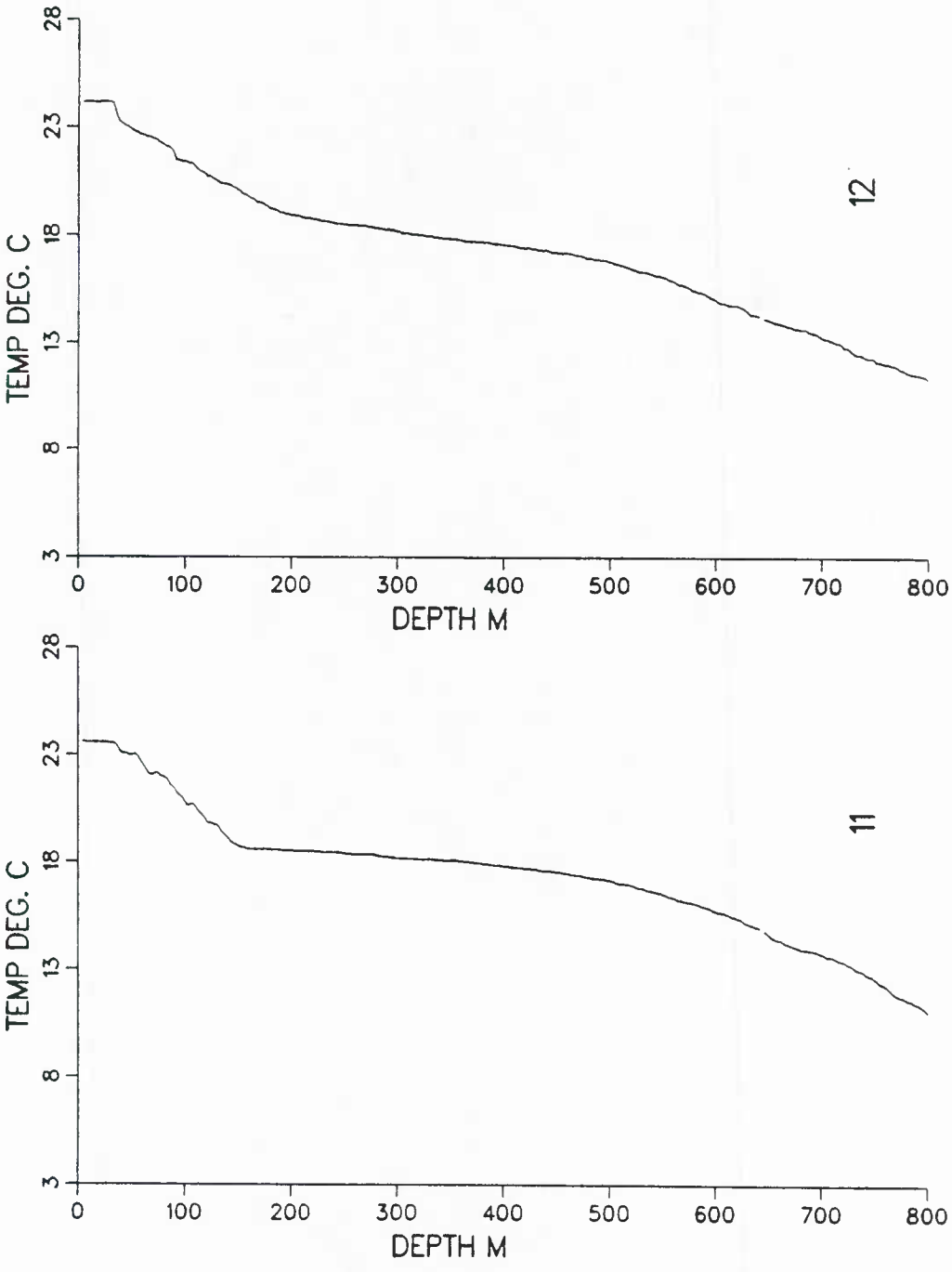

Figure 59. XBT profiles from IES deployment cruise.

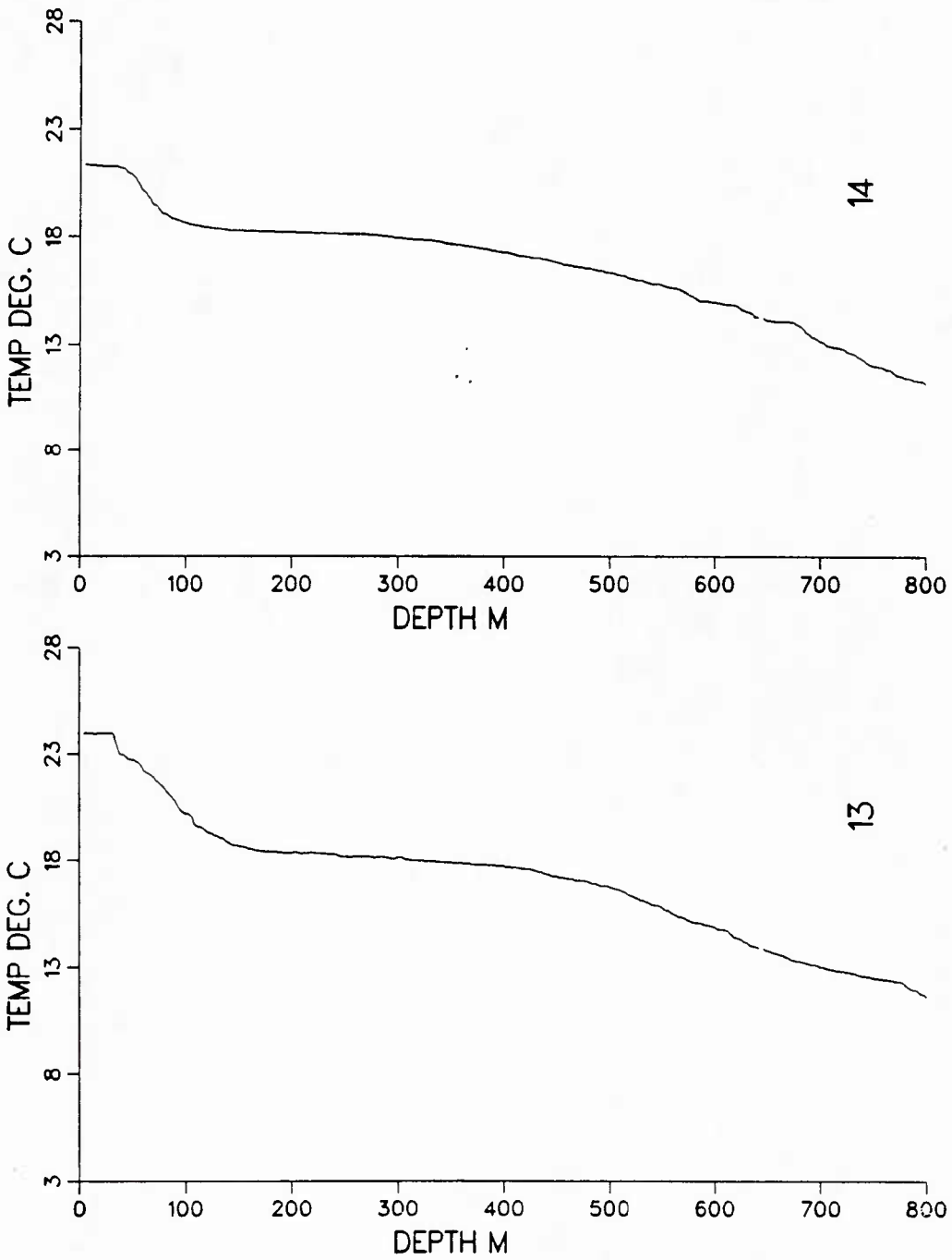

Figure 60. XBT profiles from IES deployment cruise.

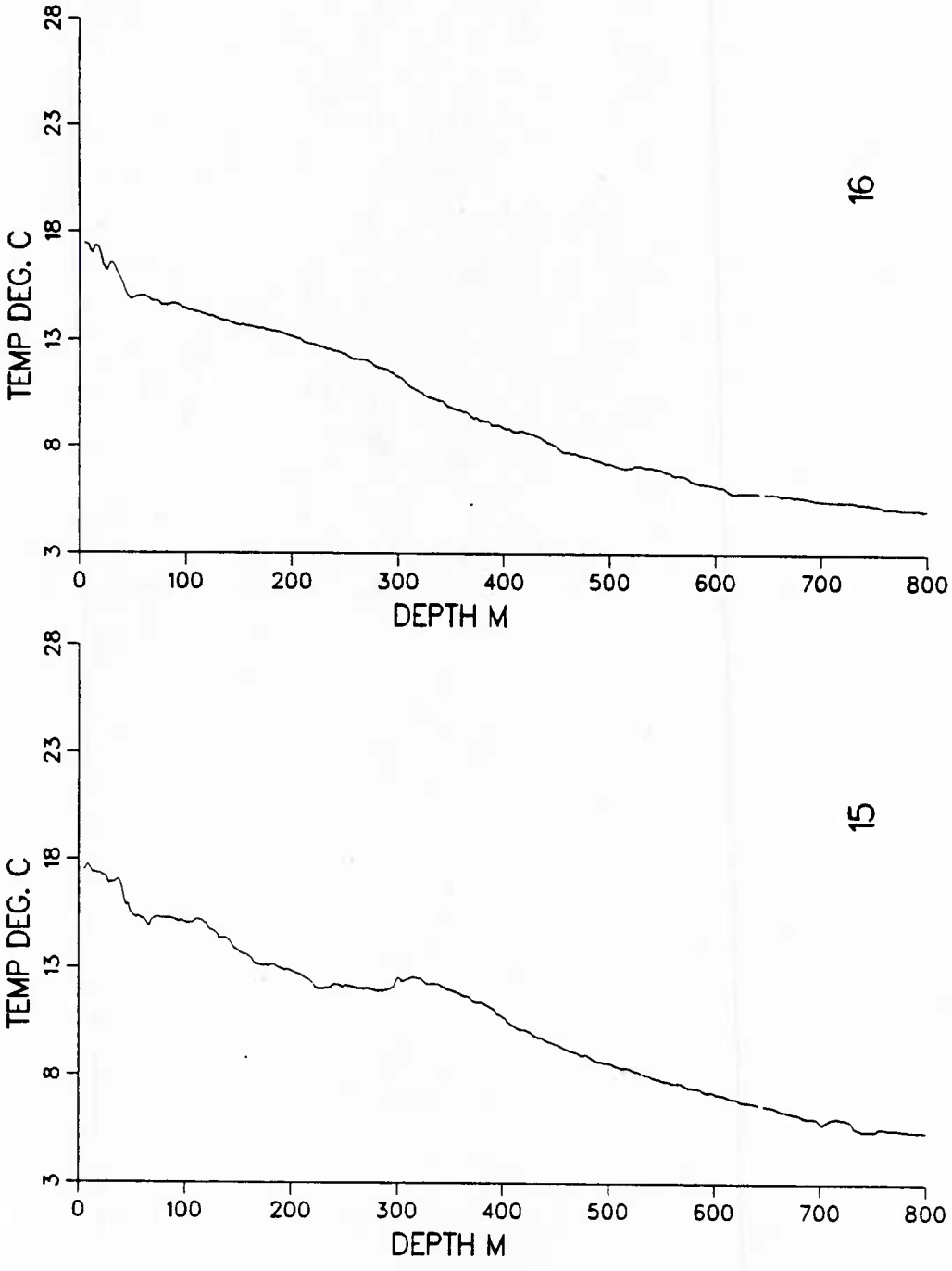

Figure 61. XBT profiles from IES deployment cruise.

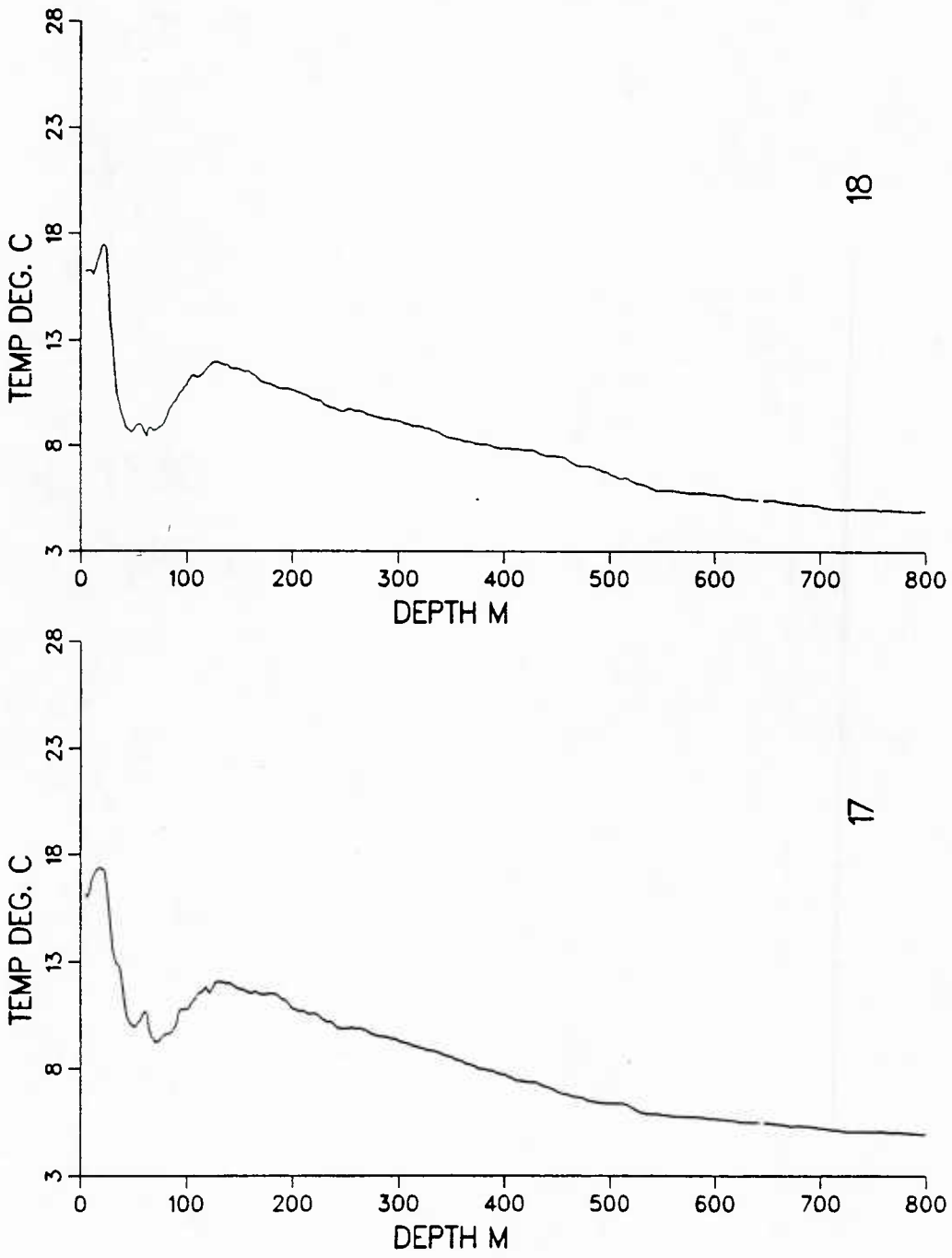

Figure 62. XBT profiles from IES deployment cruise.

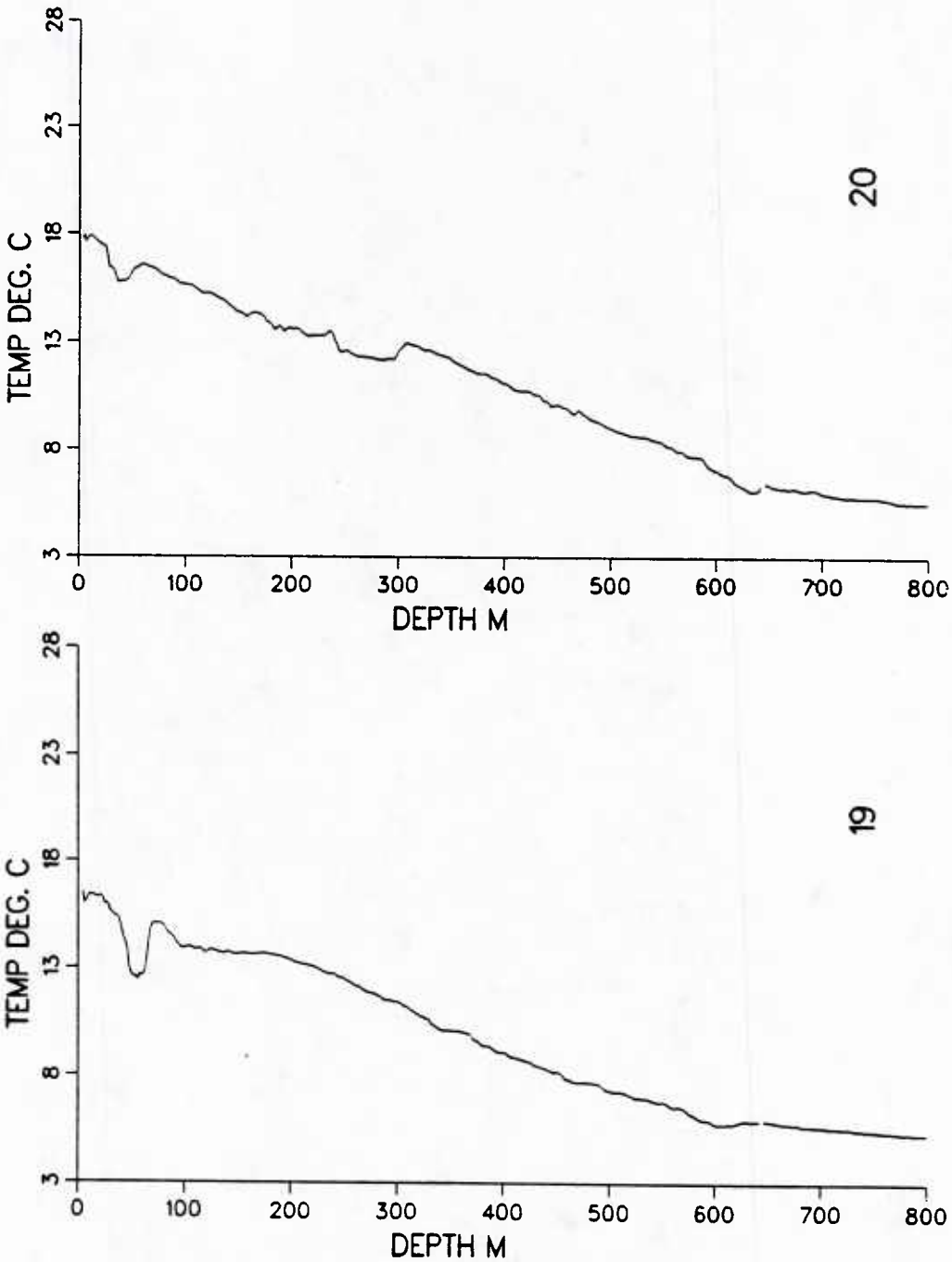

Figure 63. XBT profiles from IES deployment cruise.

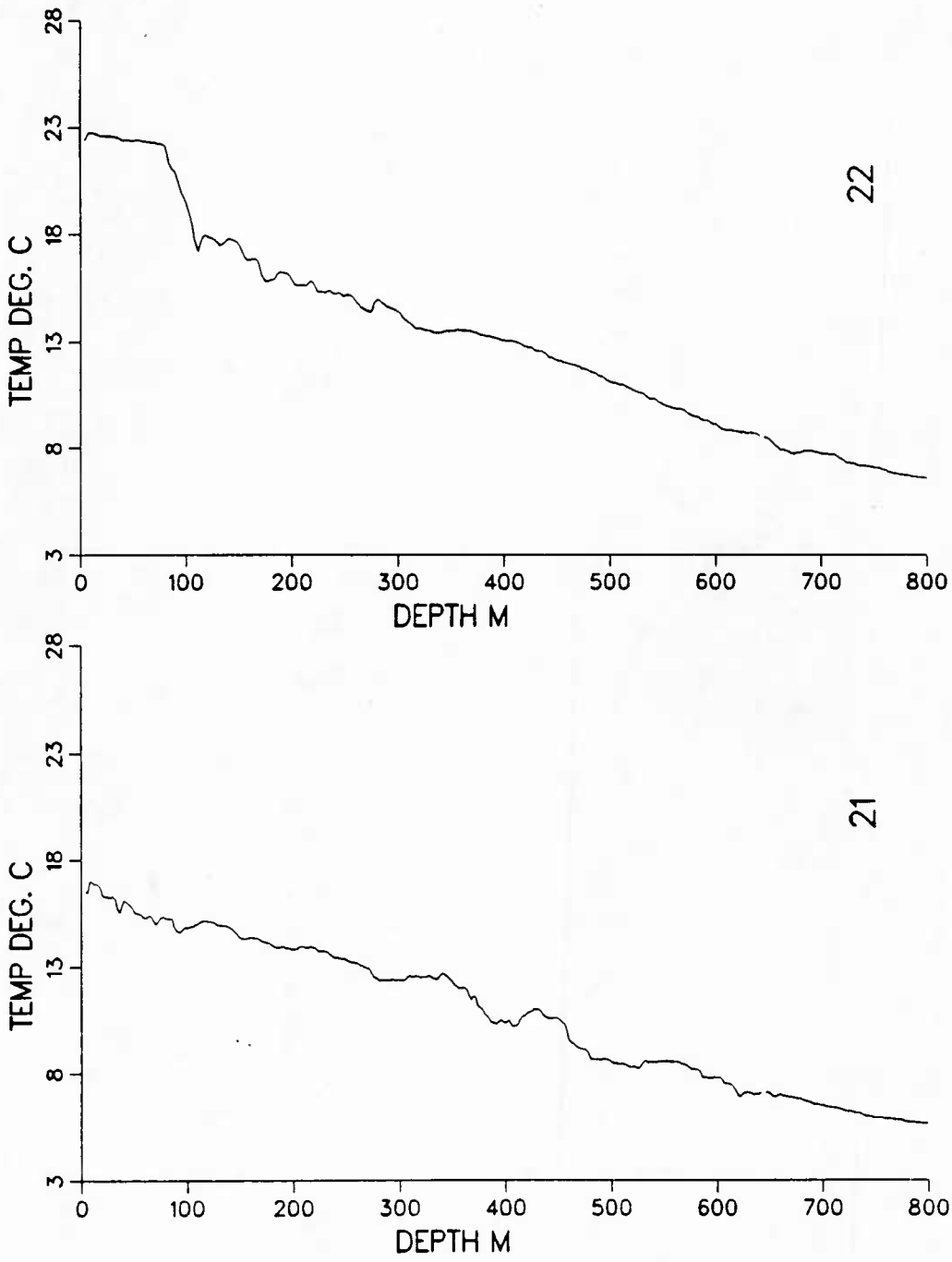

Figure 64. XBT profiles from IES deployment cruise.

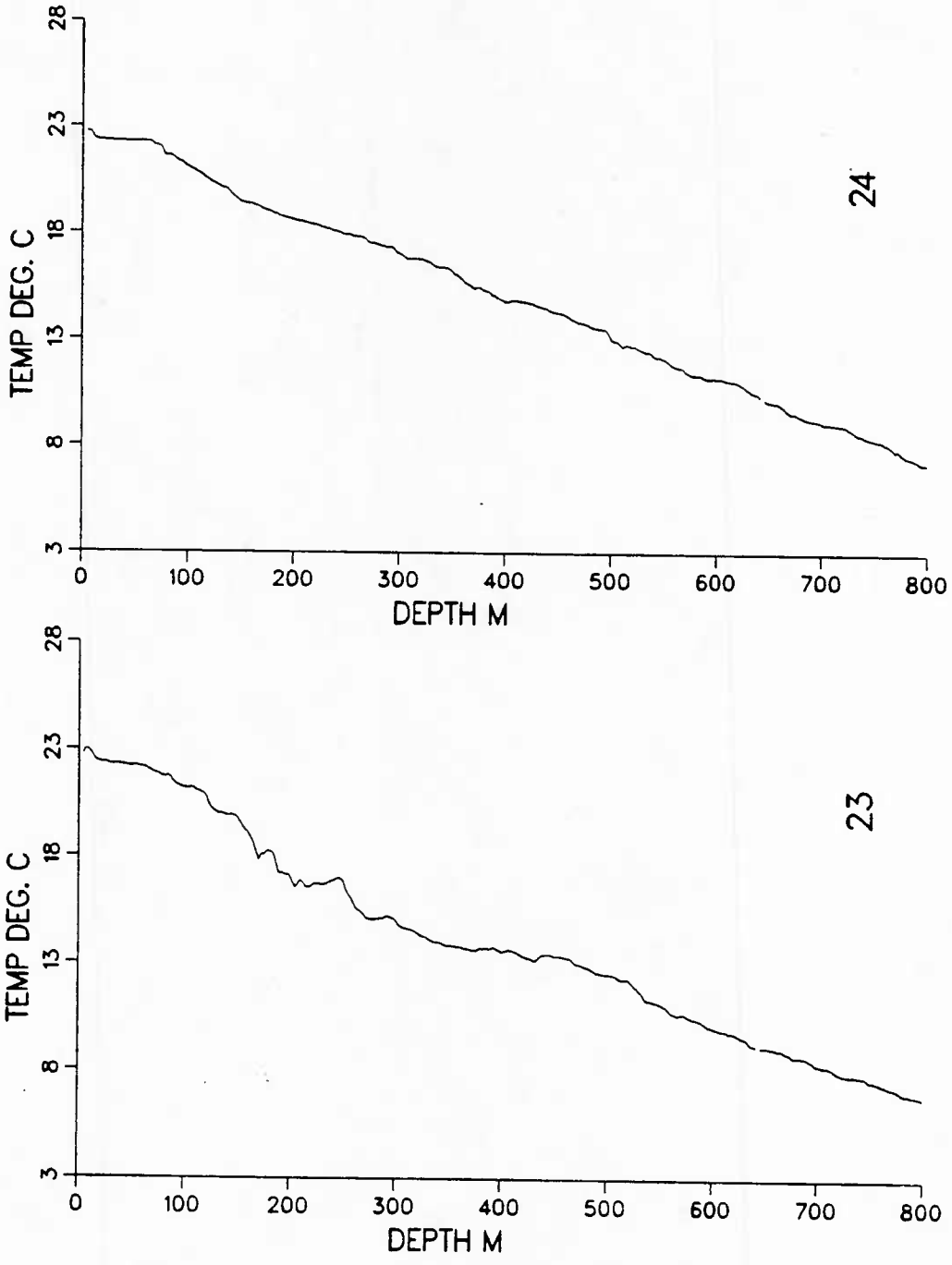

Figure 65. XBT profiles from IES deployment cruise.

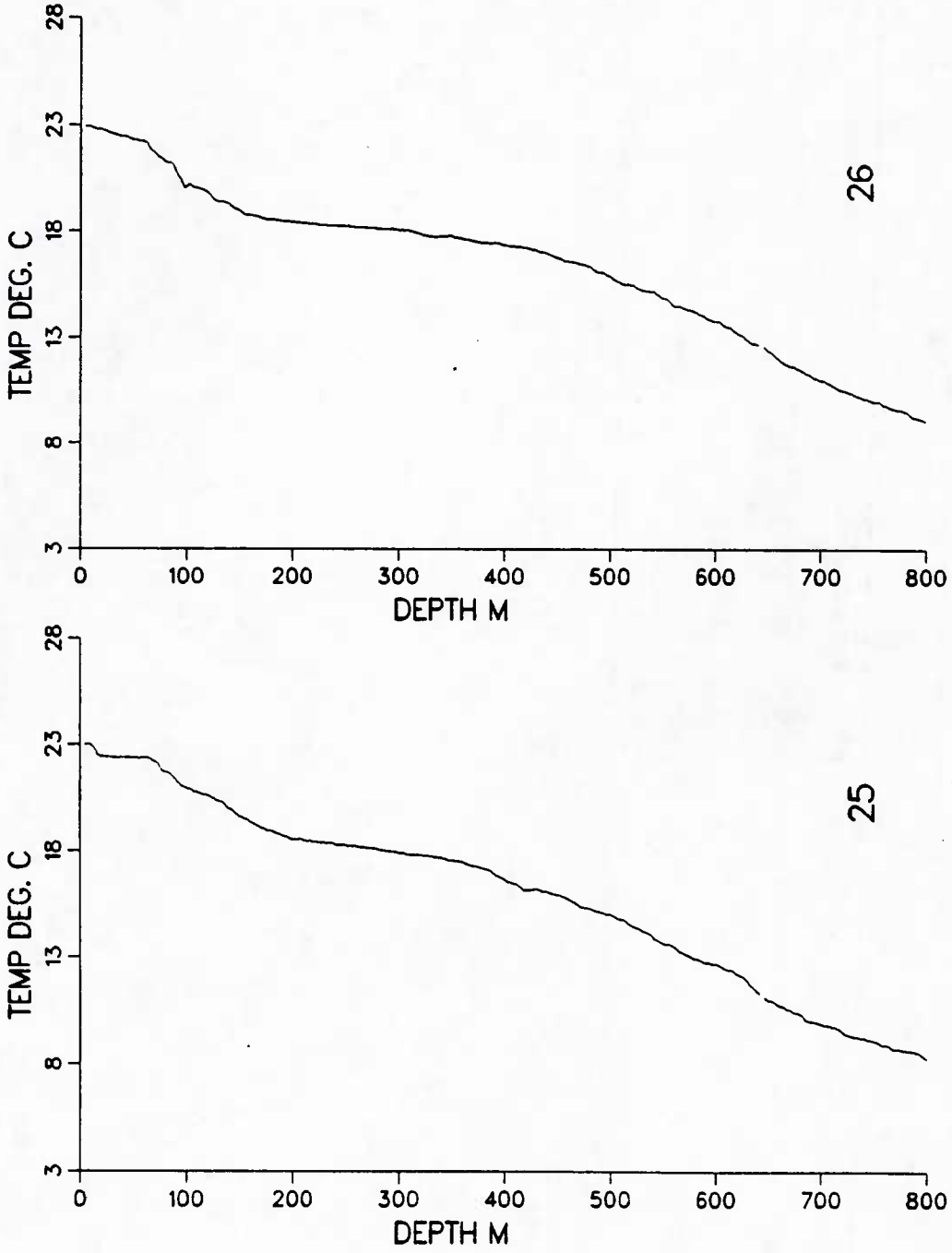

Figure 66. XBT profiles from IES deployment cruise.

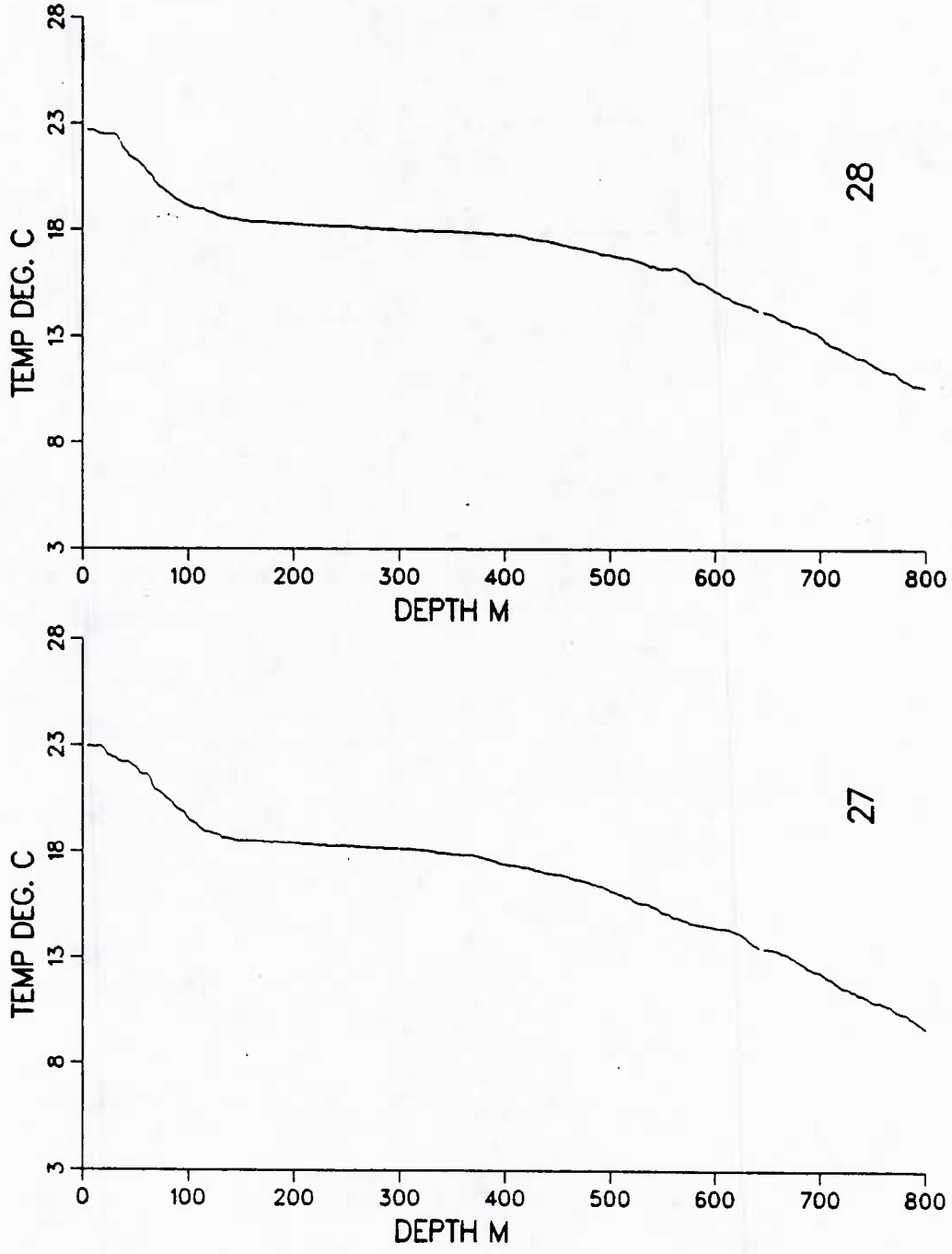

Figure 67. XBT profiles from IES deployment cruise.

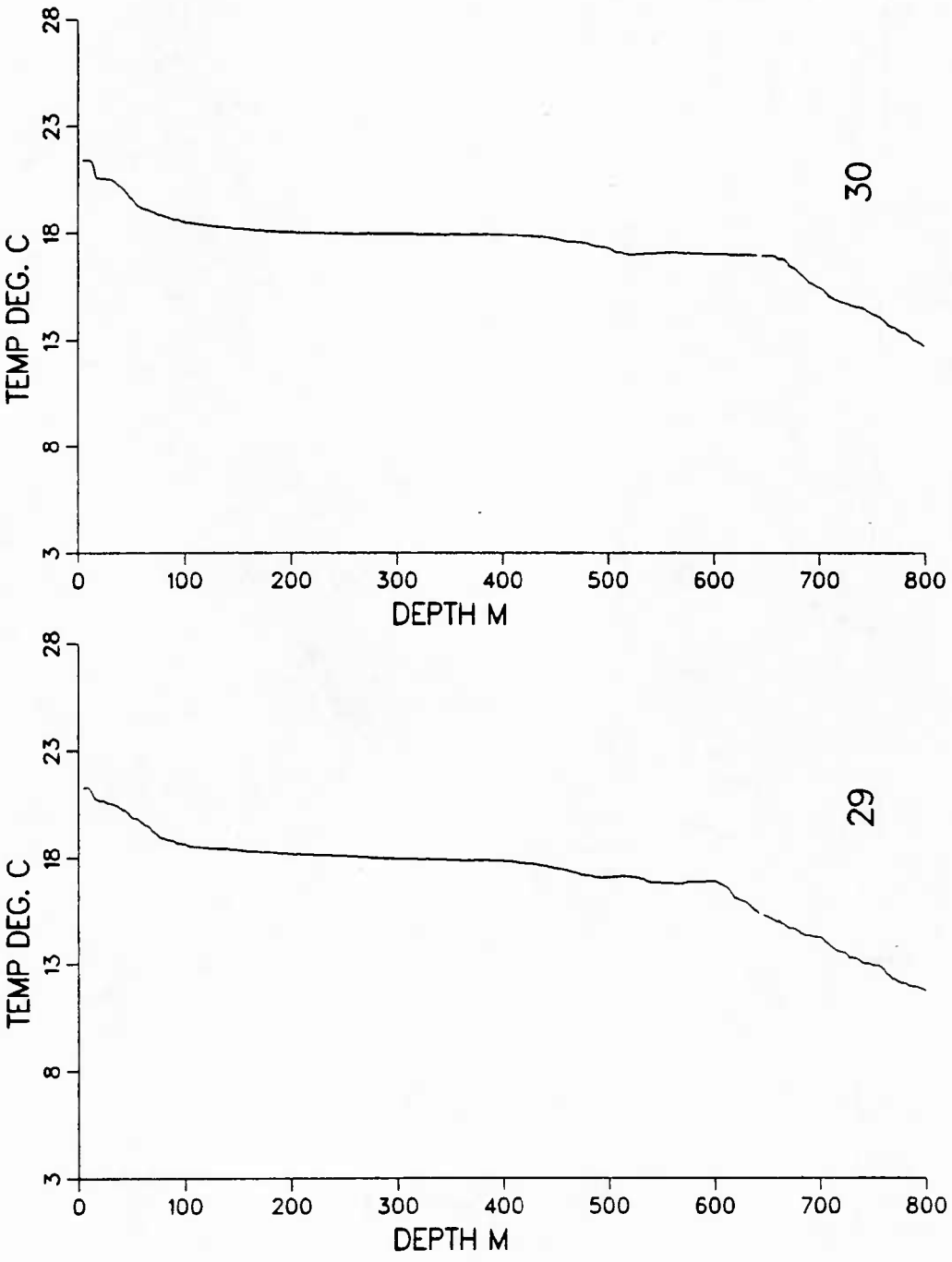

Figure 68. XBT profiles from IES deployment cruise.

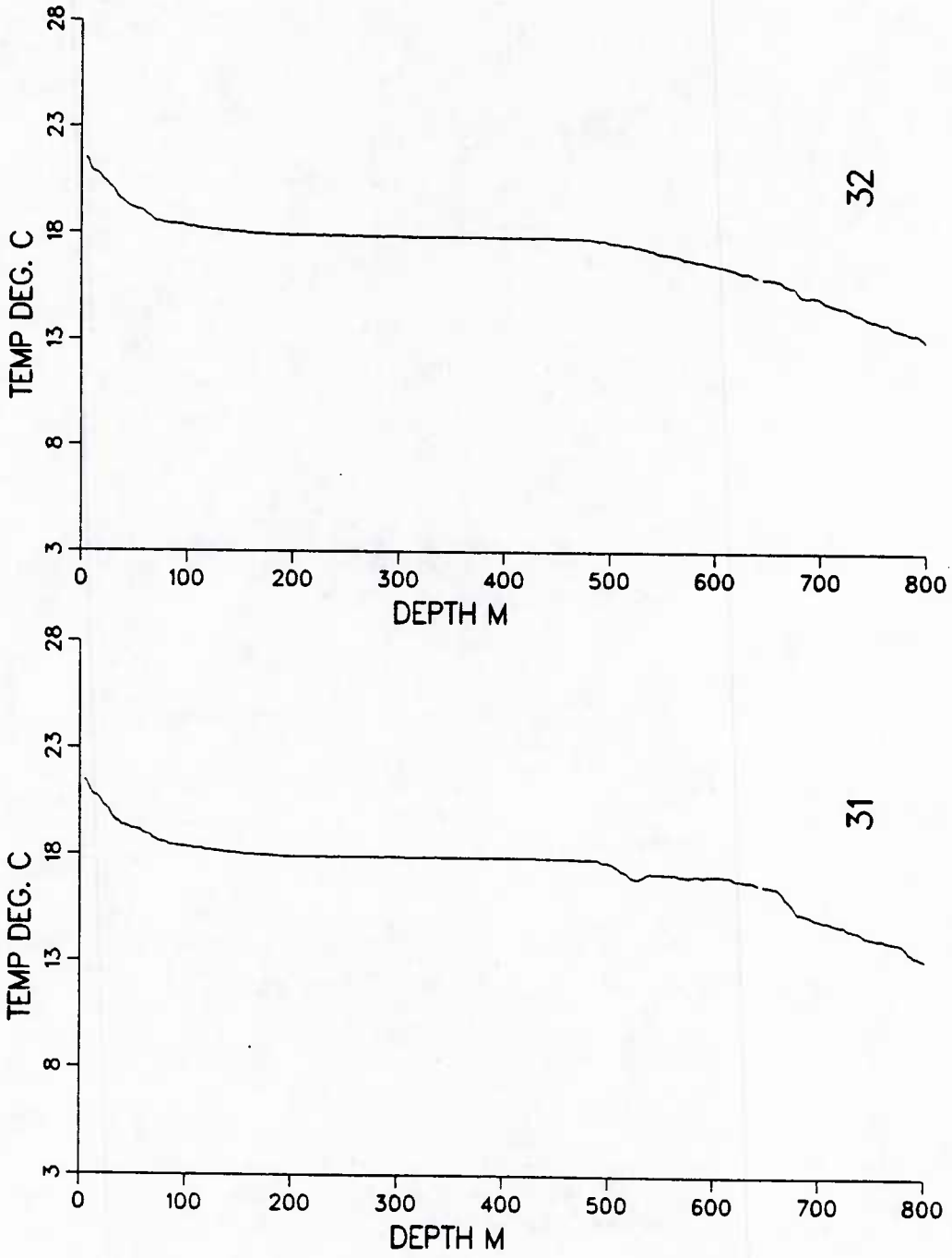

Figure 69. XBT profiles from IES deployment cruise.

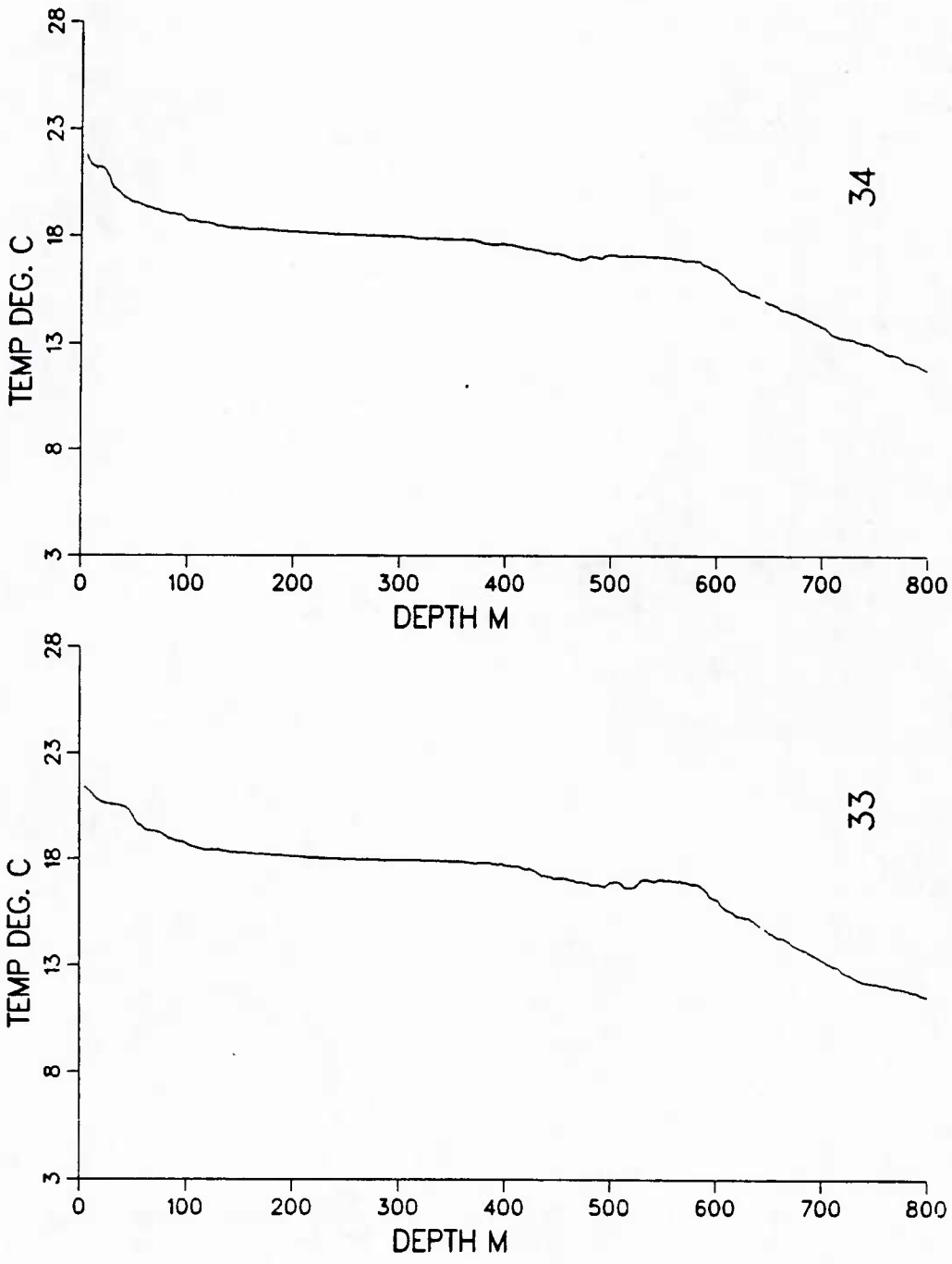

Figure 70. XBT profiles from IES deployment cruise.

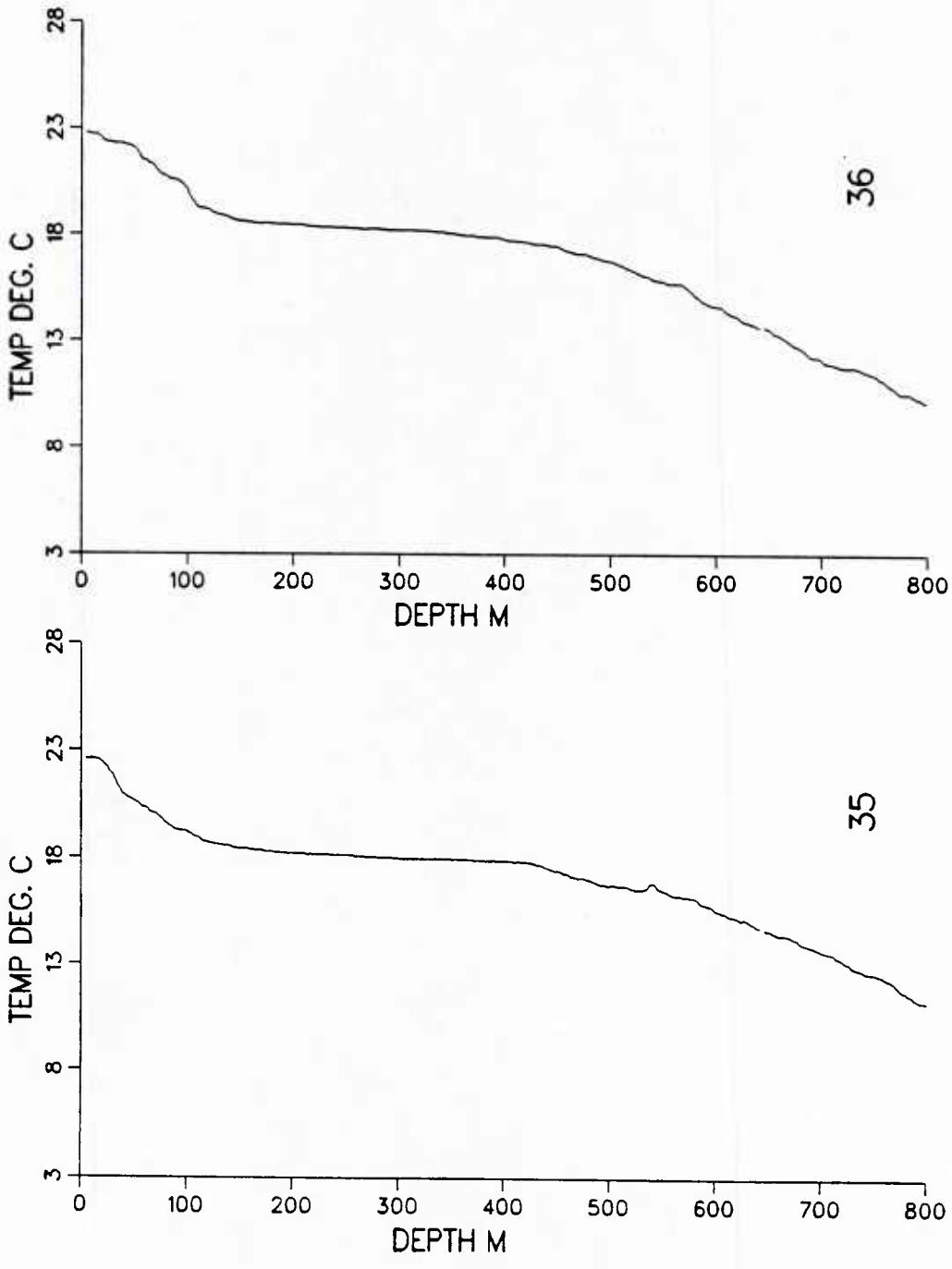

Figure 71. XBT profiles from IES deployment cruise.

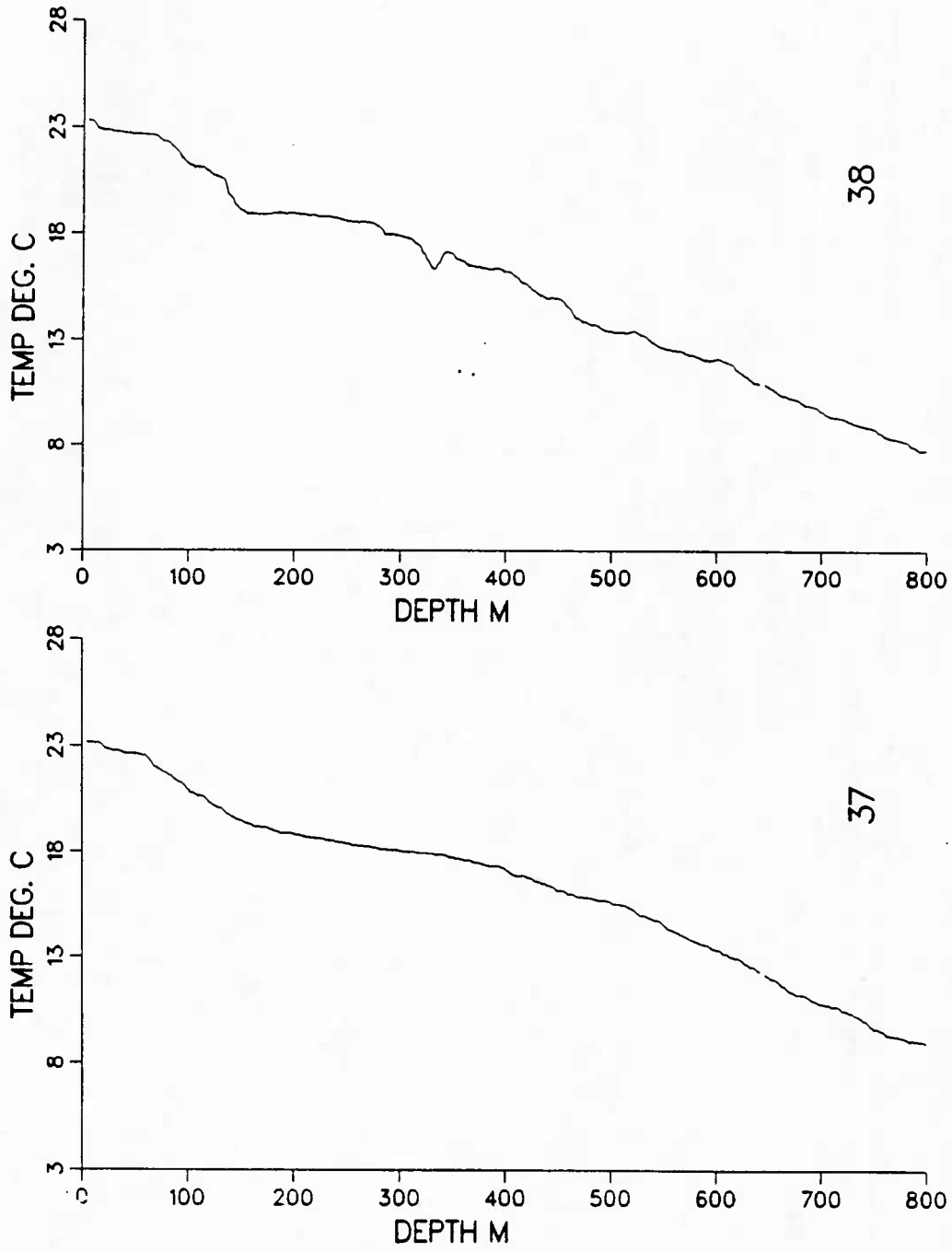

Figure 72. XBT profiles from IES deployment cruise.

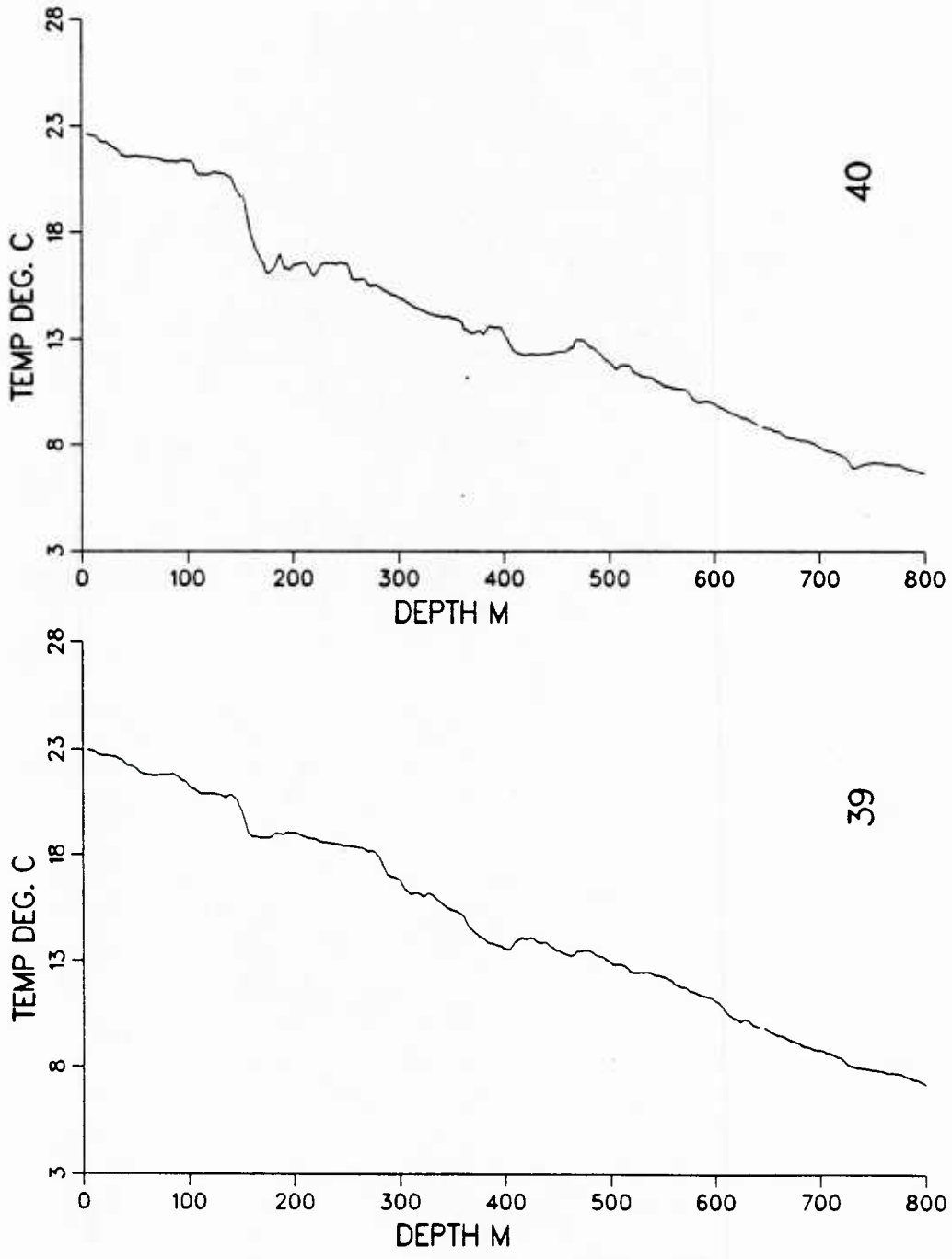

Figure 73. XBT profiles from IES deployment cruise.

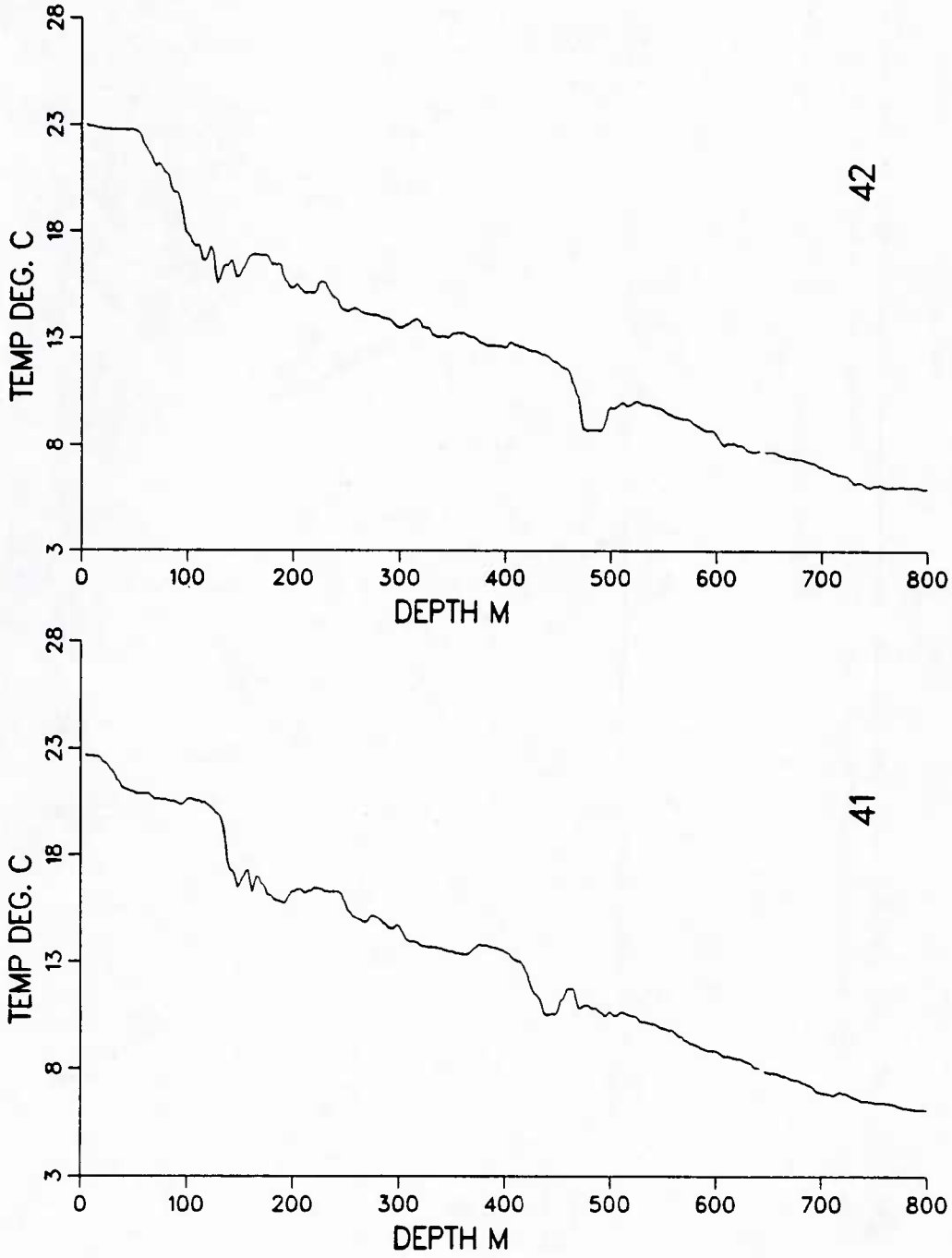

Figure 74. XBT profiles from IES deployment cruise.

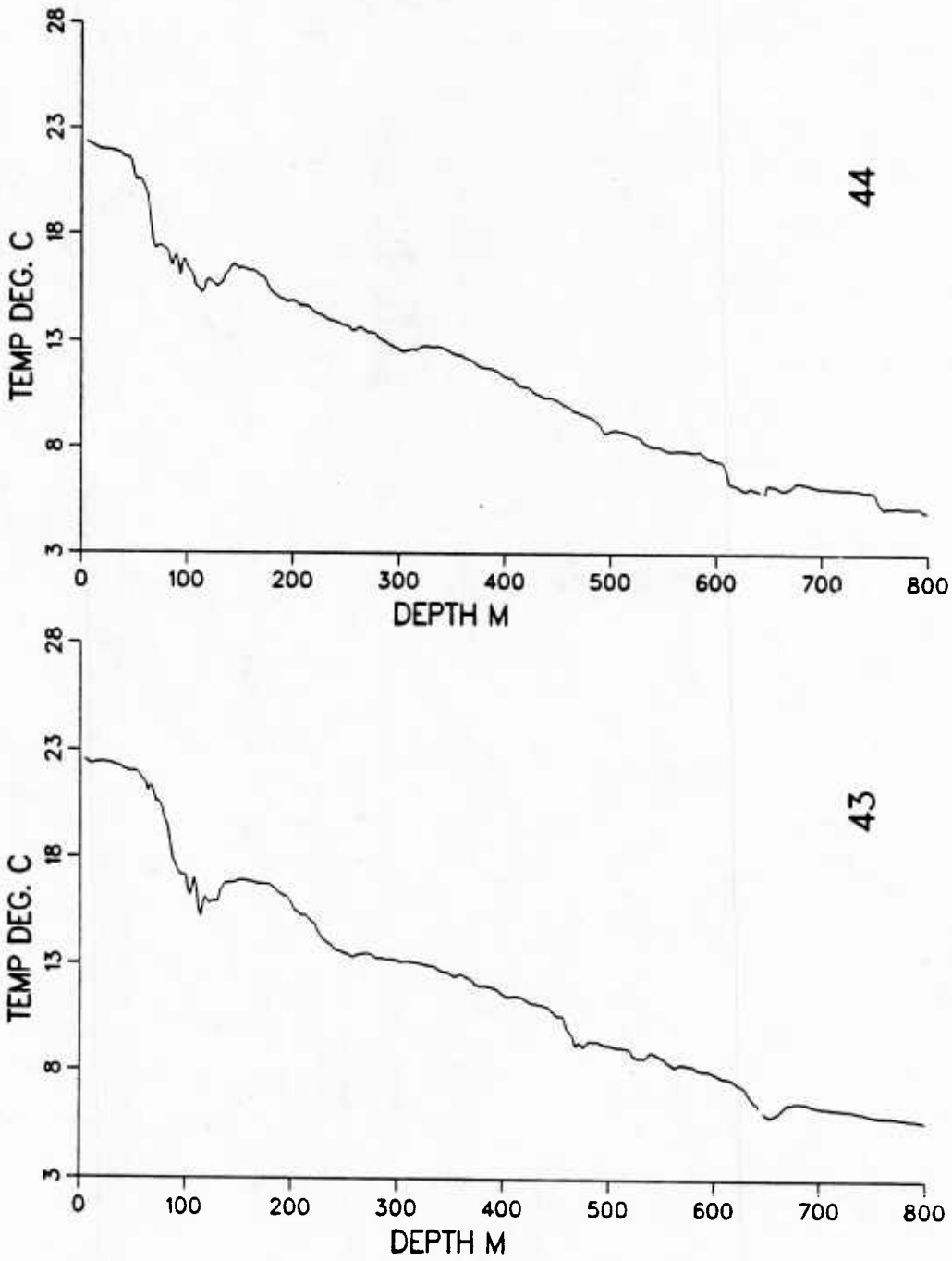

Figure 75. XBT profiles from IES deployment cruise.

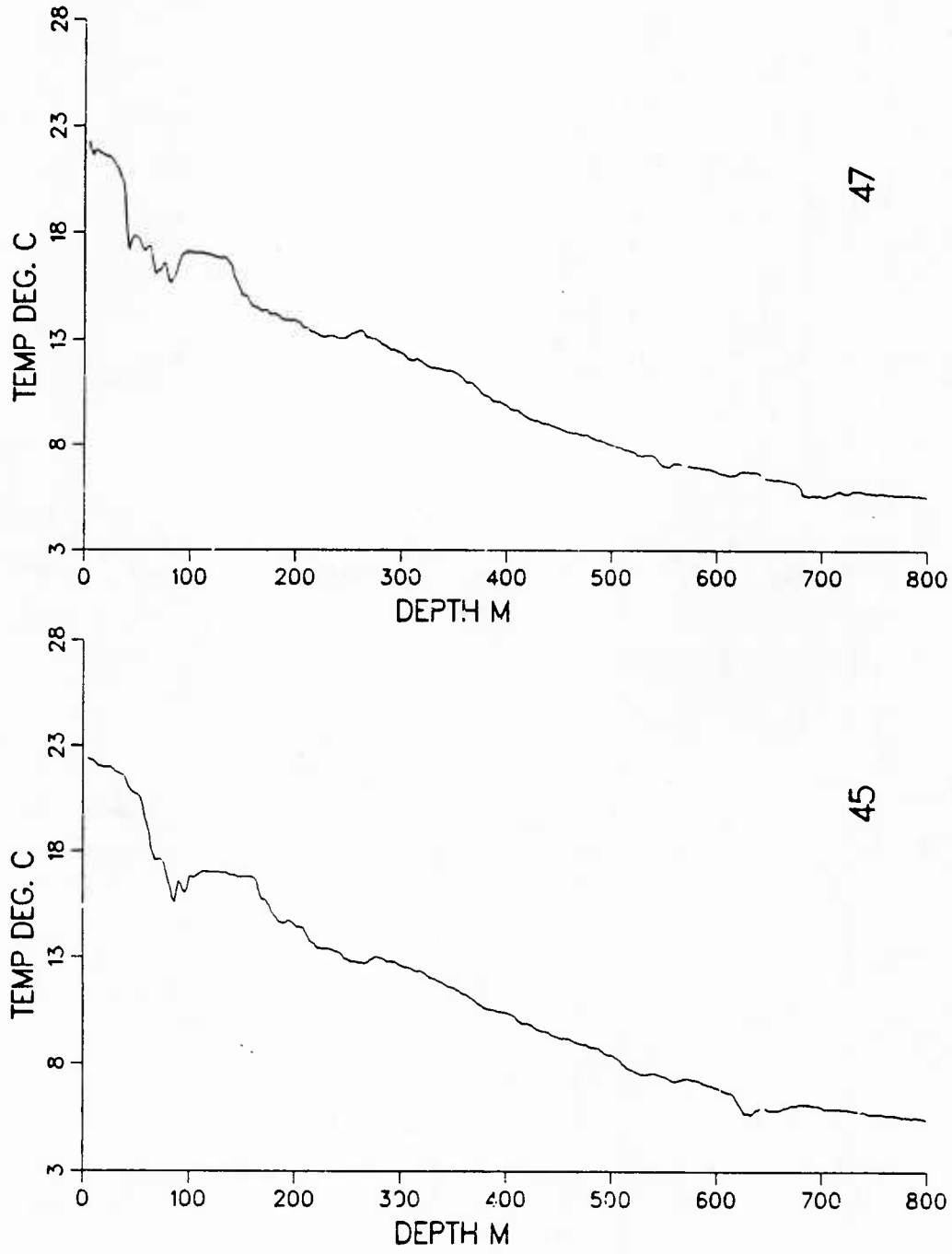

Figure 76. XBT profiles from IES deployment cruise.

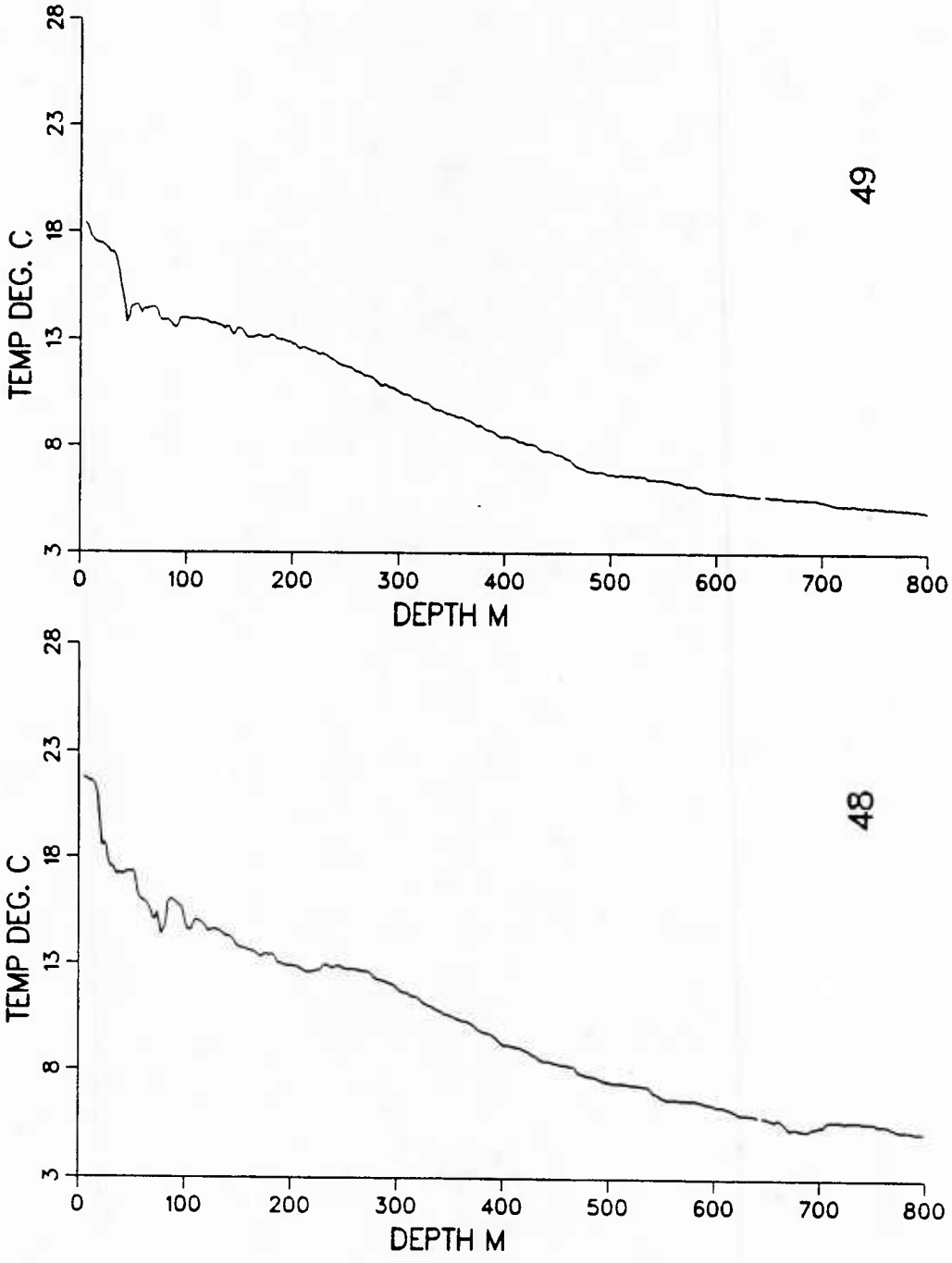

Figure 77. XBT profiles from IES deployment cruise.

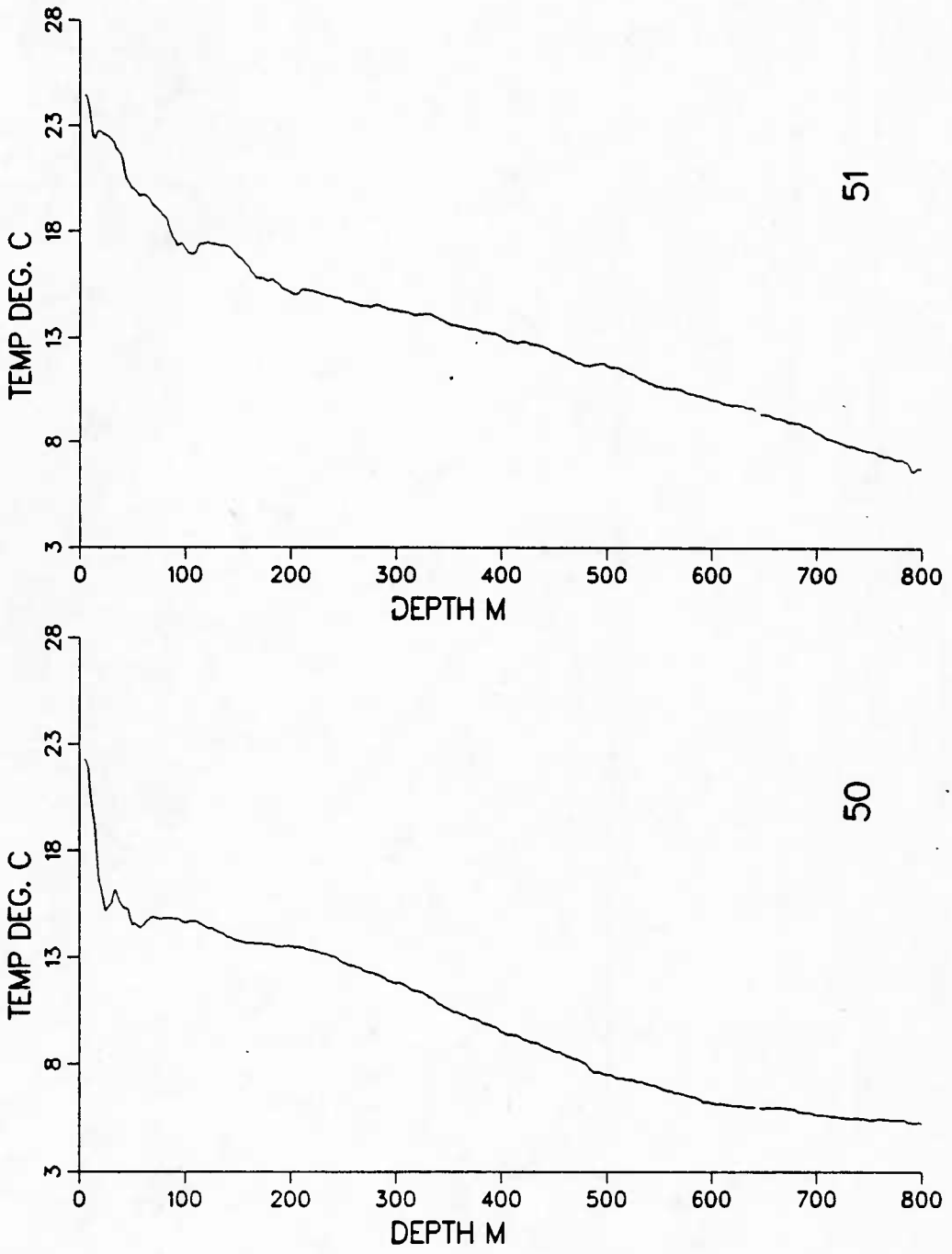

Figure 78. XBT profiles from IES deployment cruise.

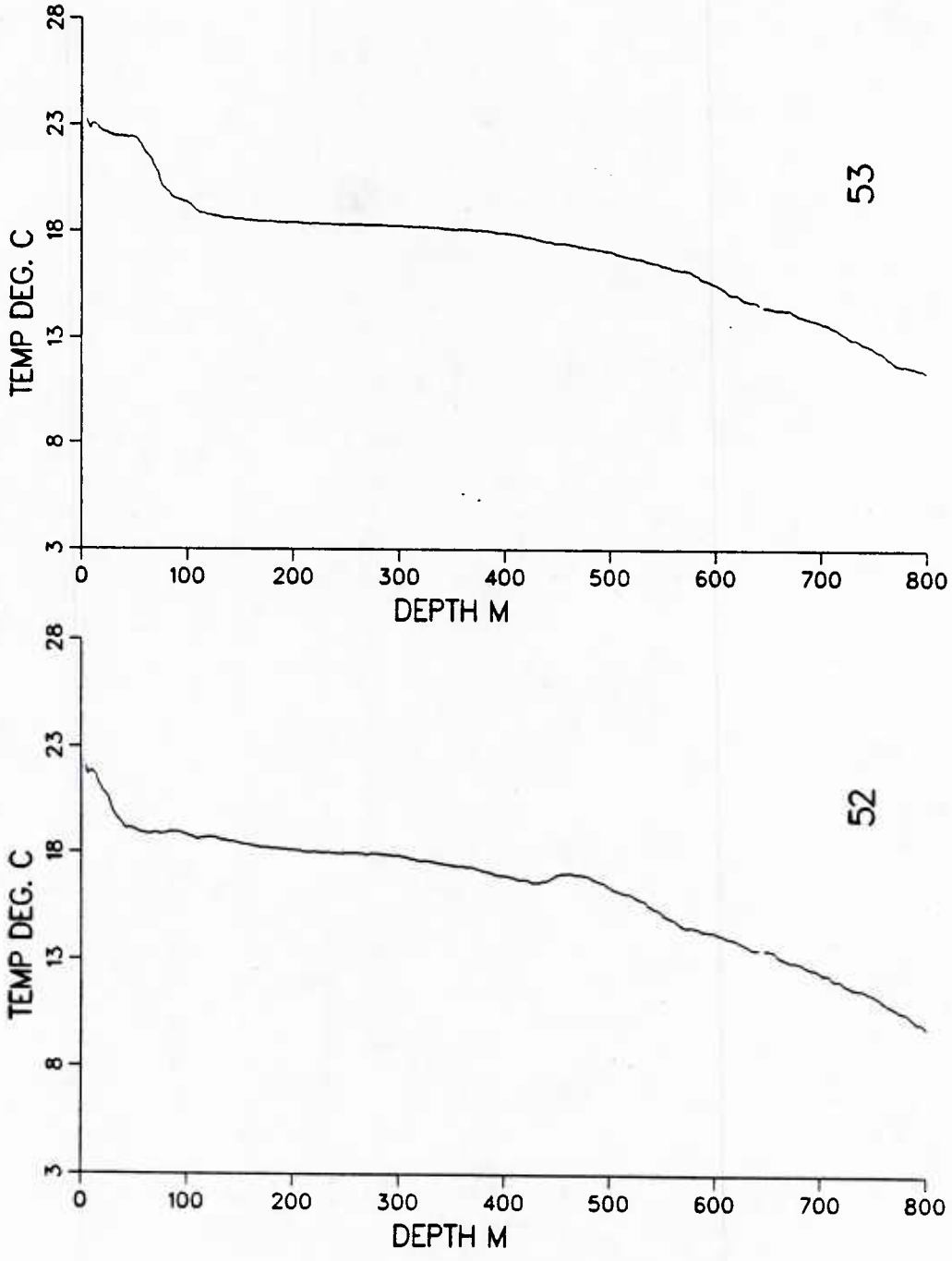

Figure 79. XBT profiles from IES deployment cruise.

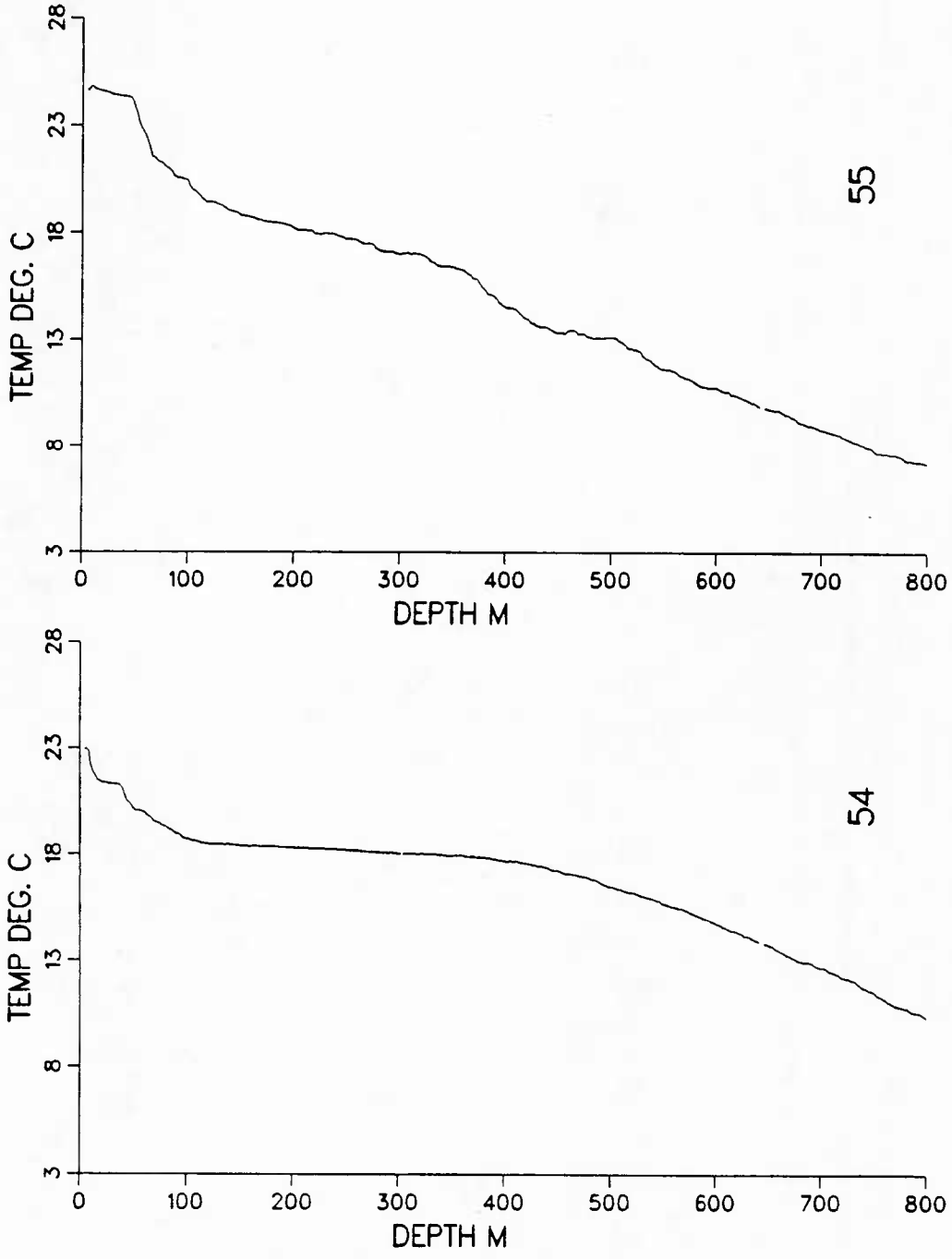

Figure 80. XBT profiles from IES deployment cruise.

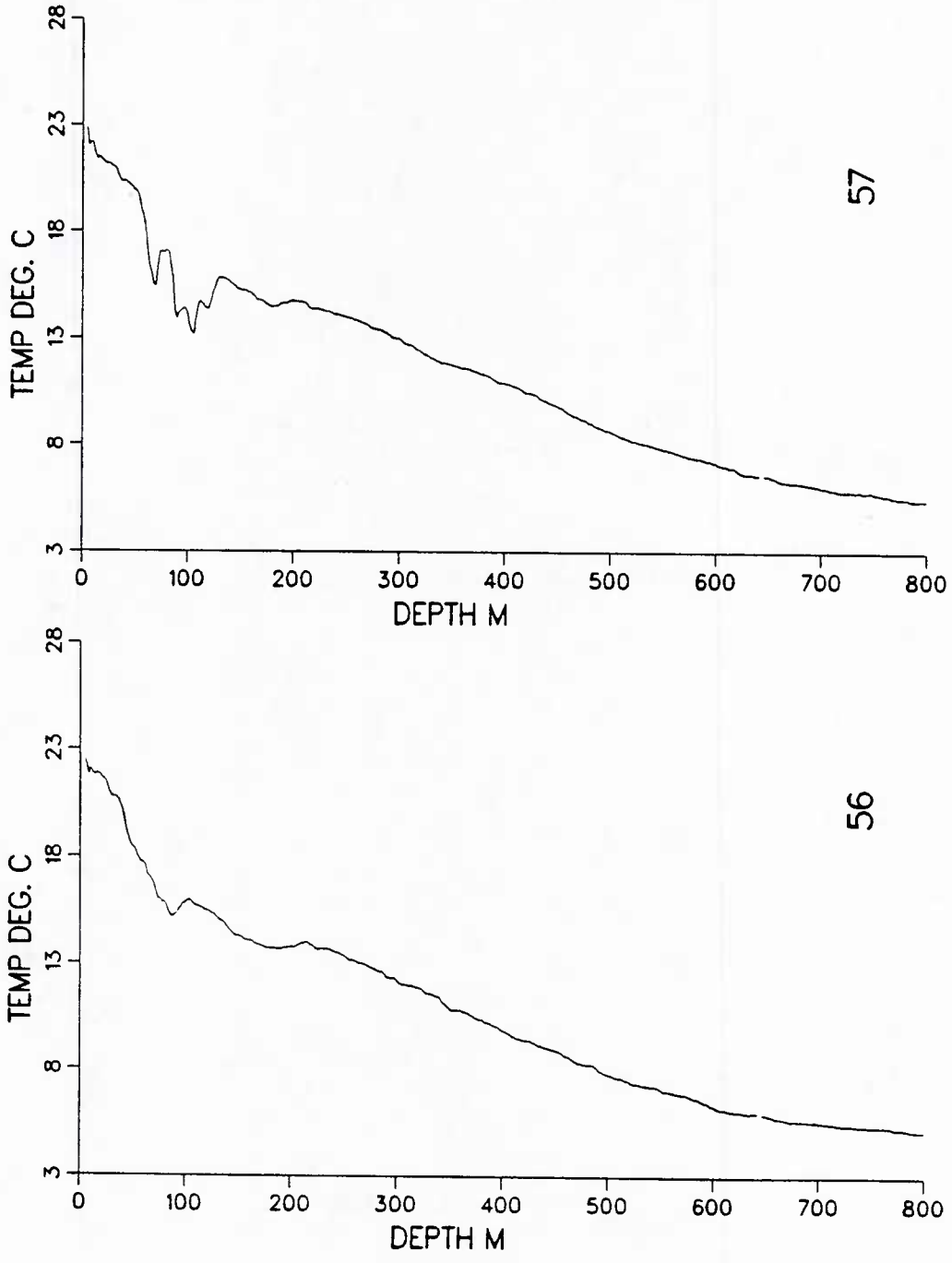

Figure 81. XBT profiles from IES deployment cruise.

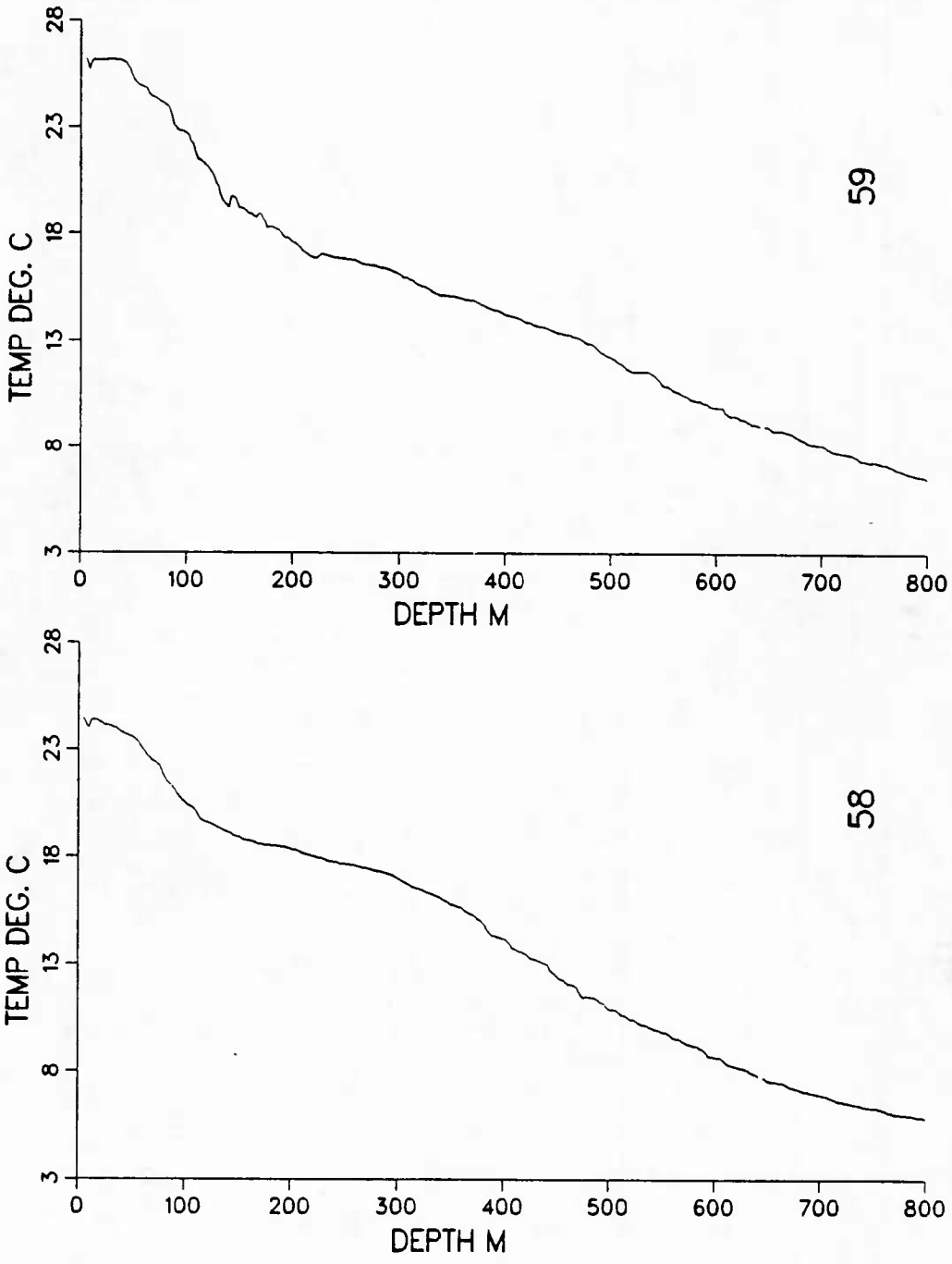

Figure 82. XBT profiles from IES deployment cruise.

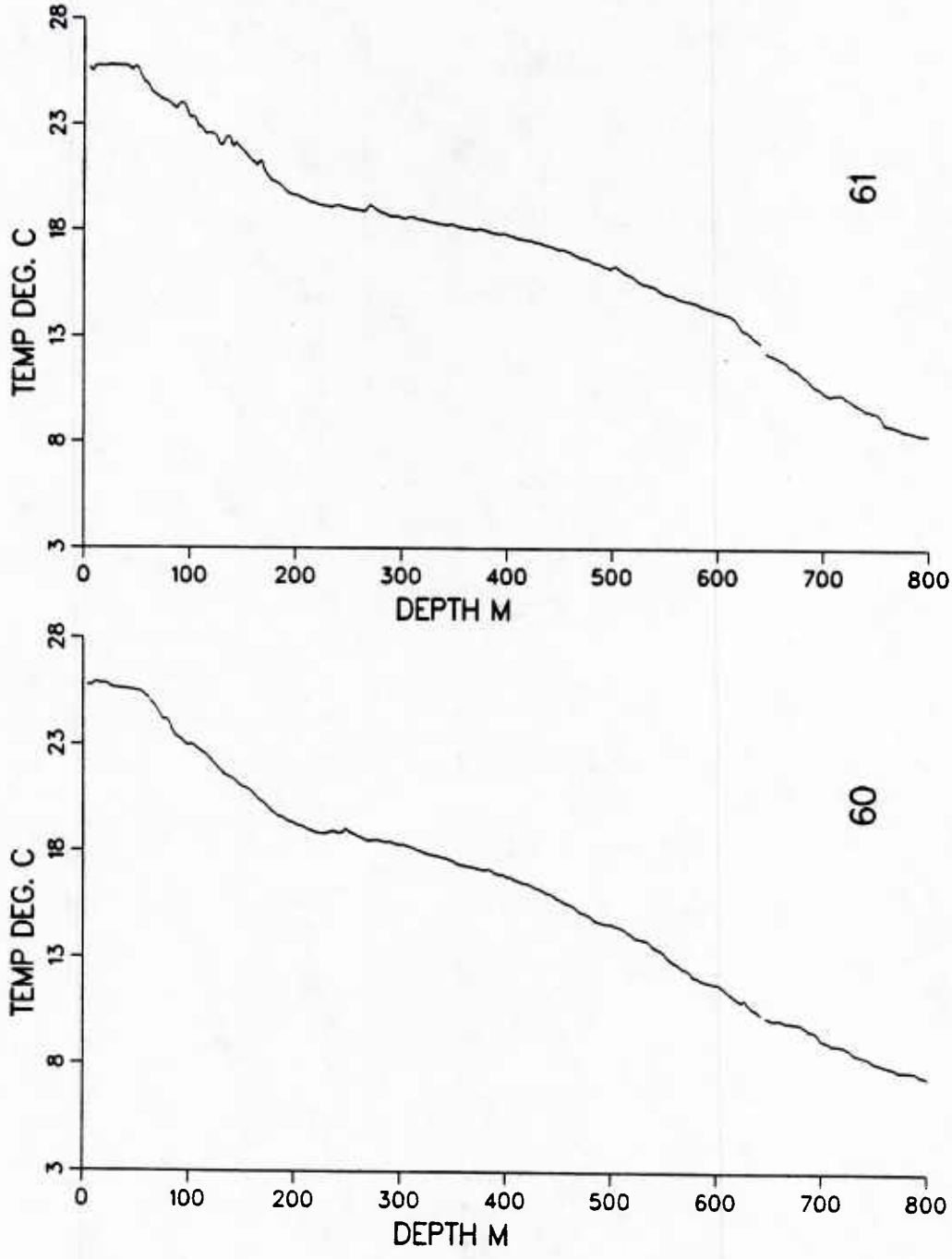

Figure 83. XBT profiles from IES deployment cruise.

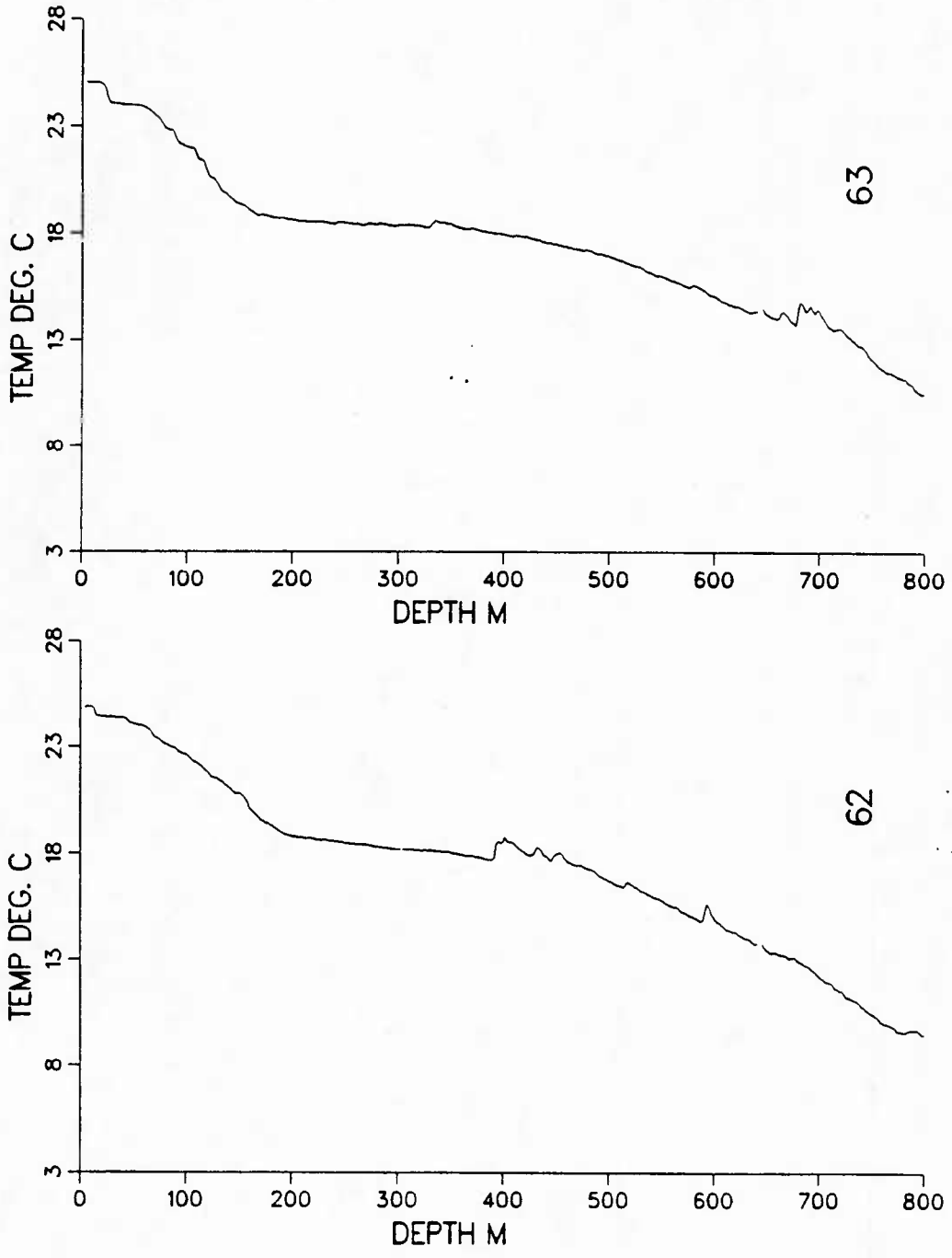

Figure 84. XBT profiles from IES deployment cruise.

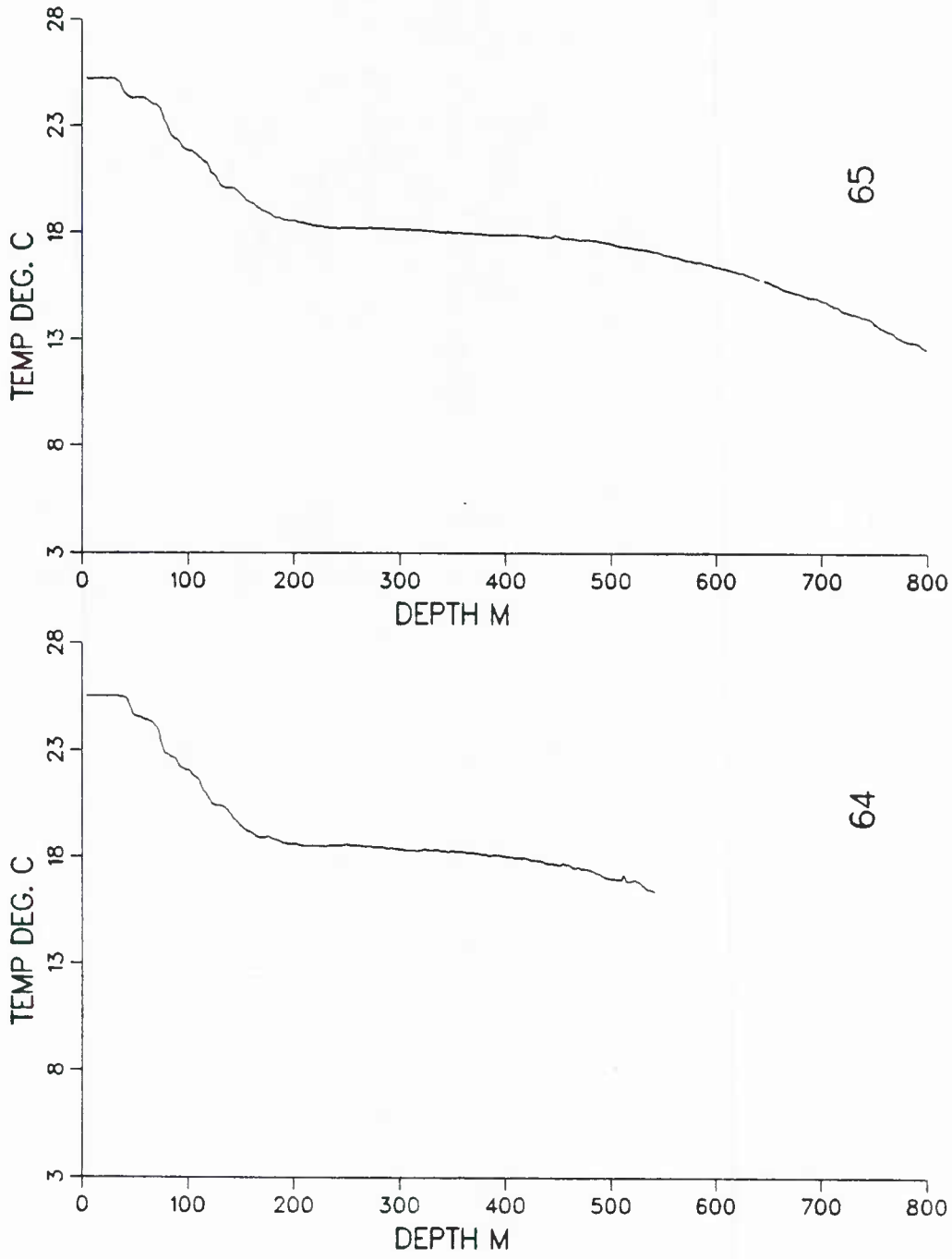

Figure 85. XBT profiles from IES deployment cruise.

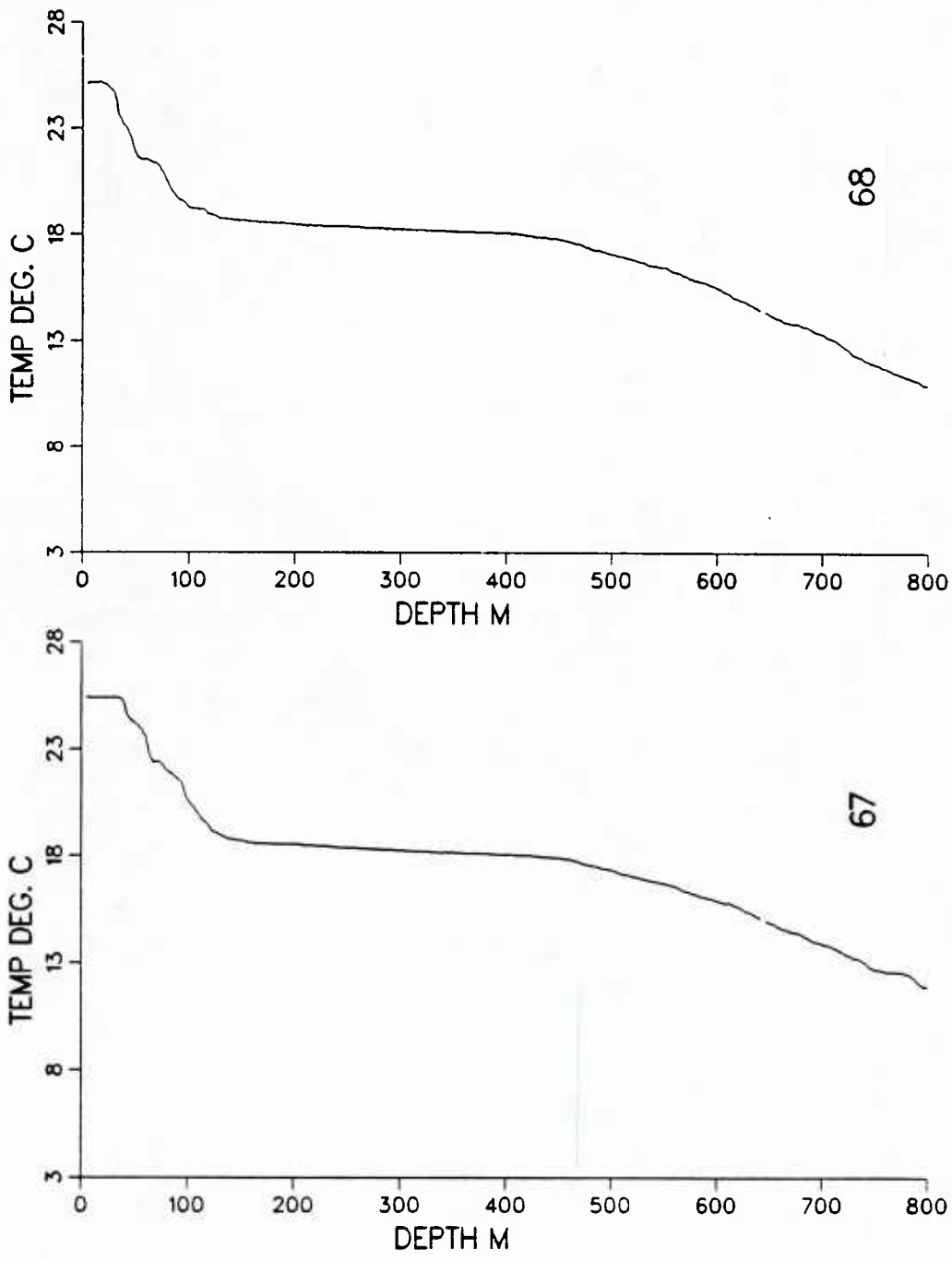

Figure 86. XBT profiles from IES deployment cruise.

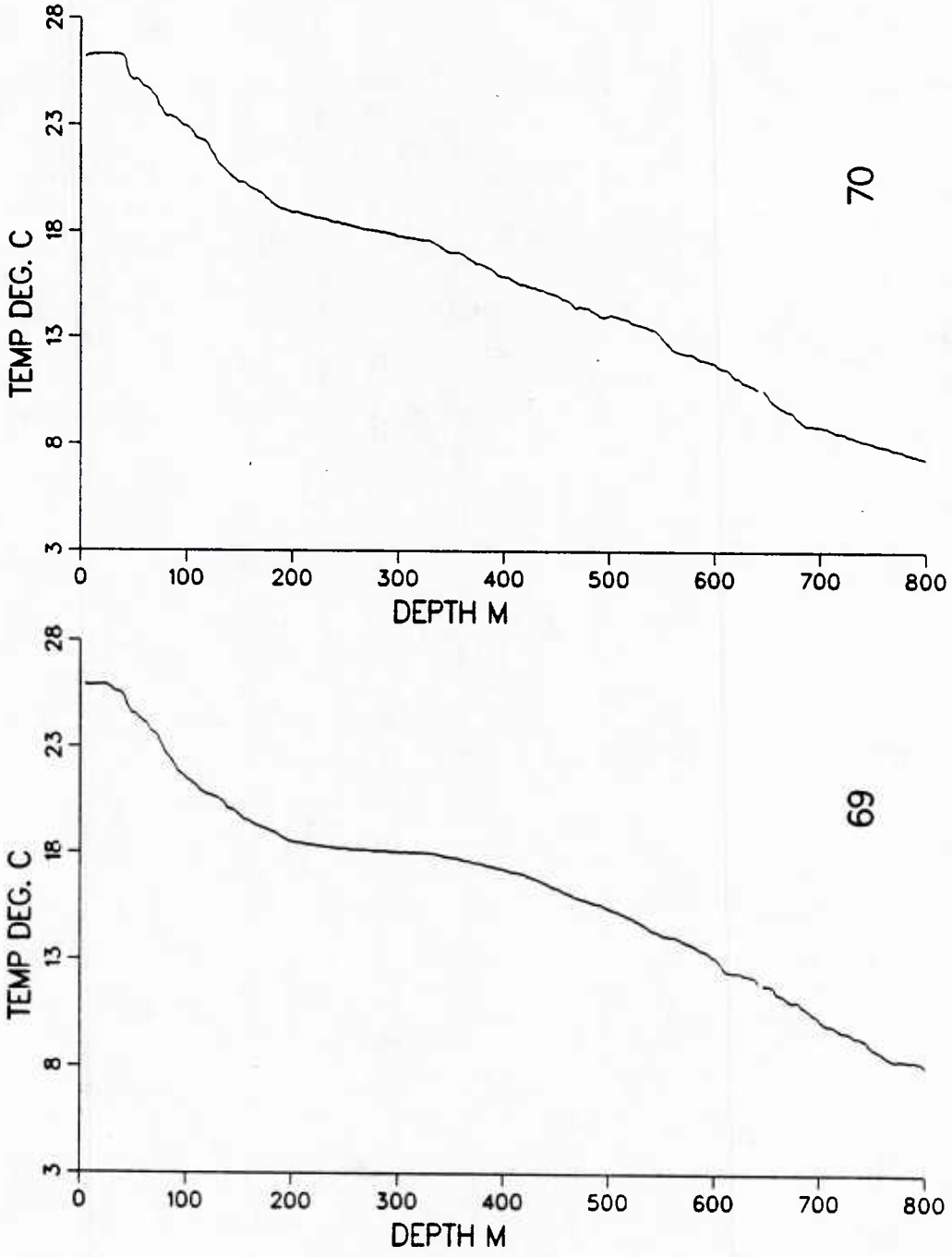

Figure 87. XBT profiles from IES deployment cruise.

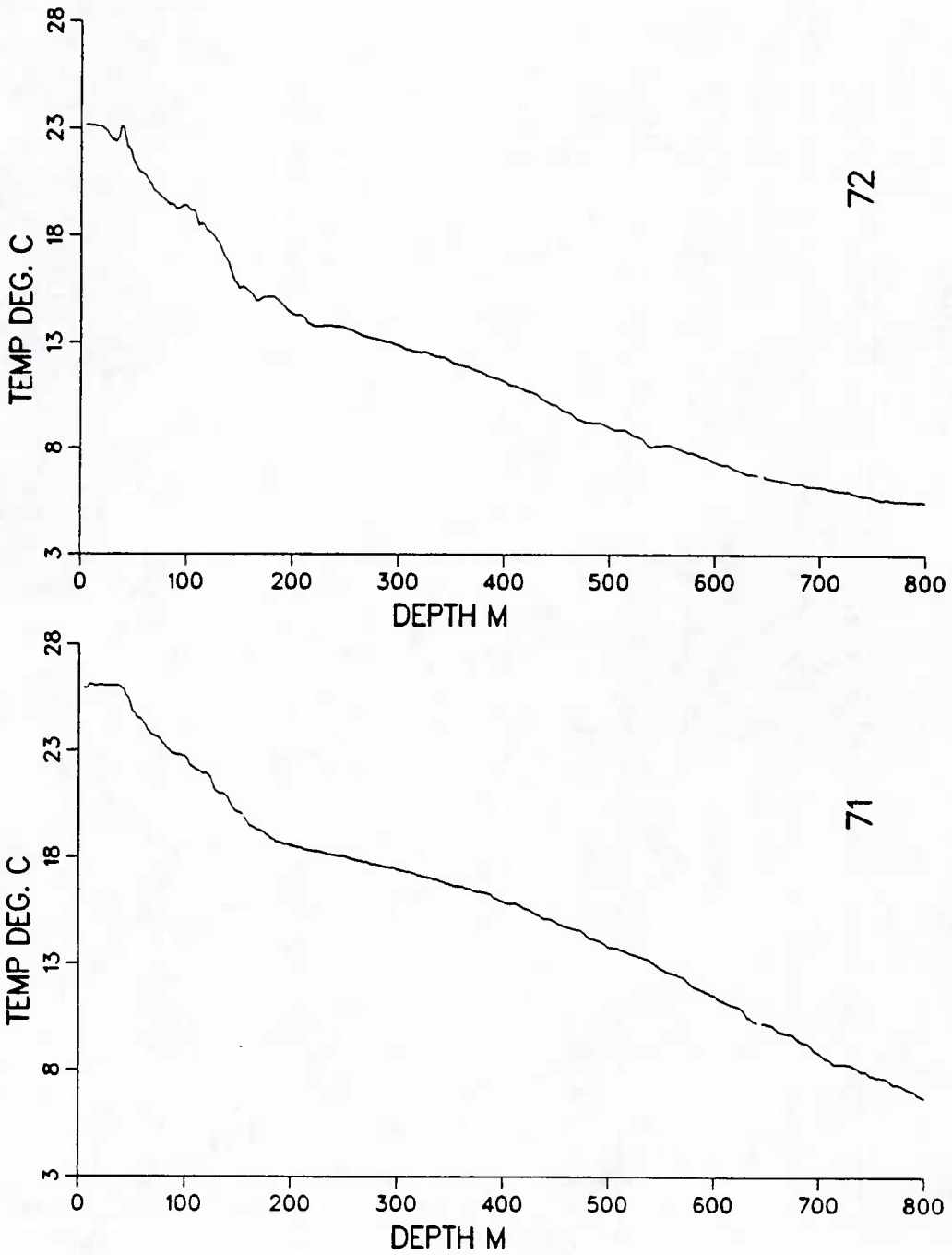

Figure 88. XBT profiles from IES deployment cruise.

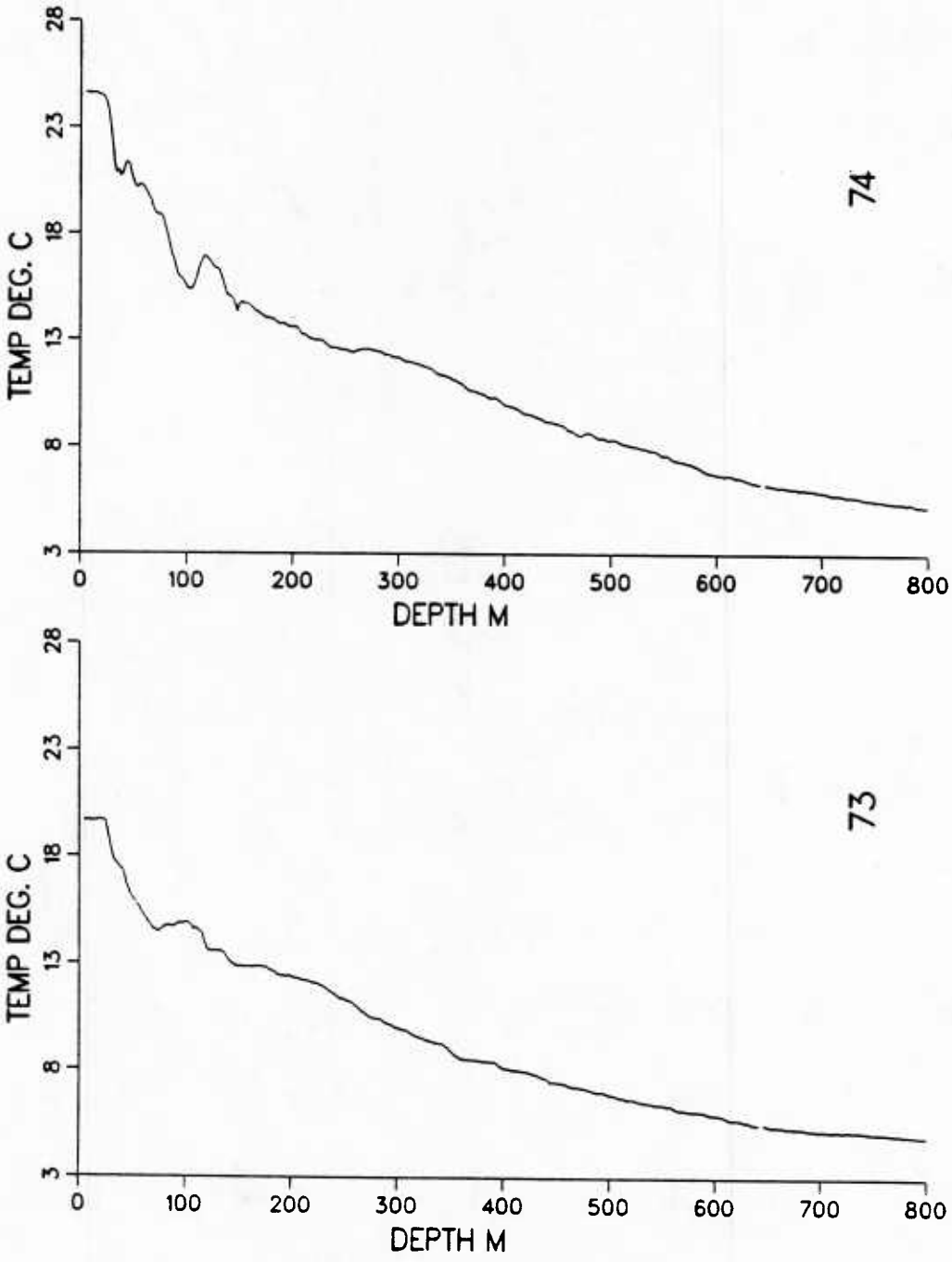

Figure 89. XBT profiles from IES deployment cruise.

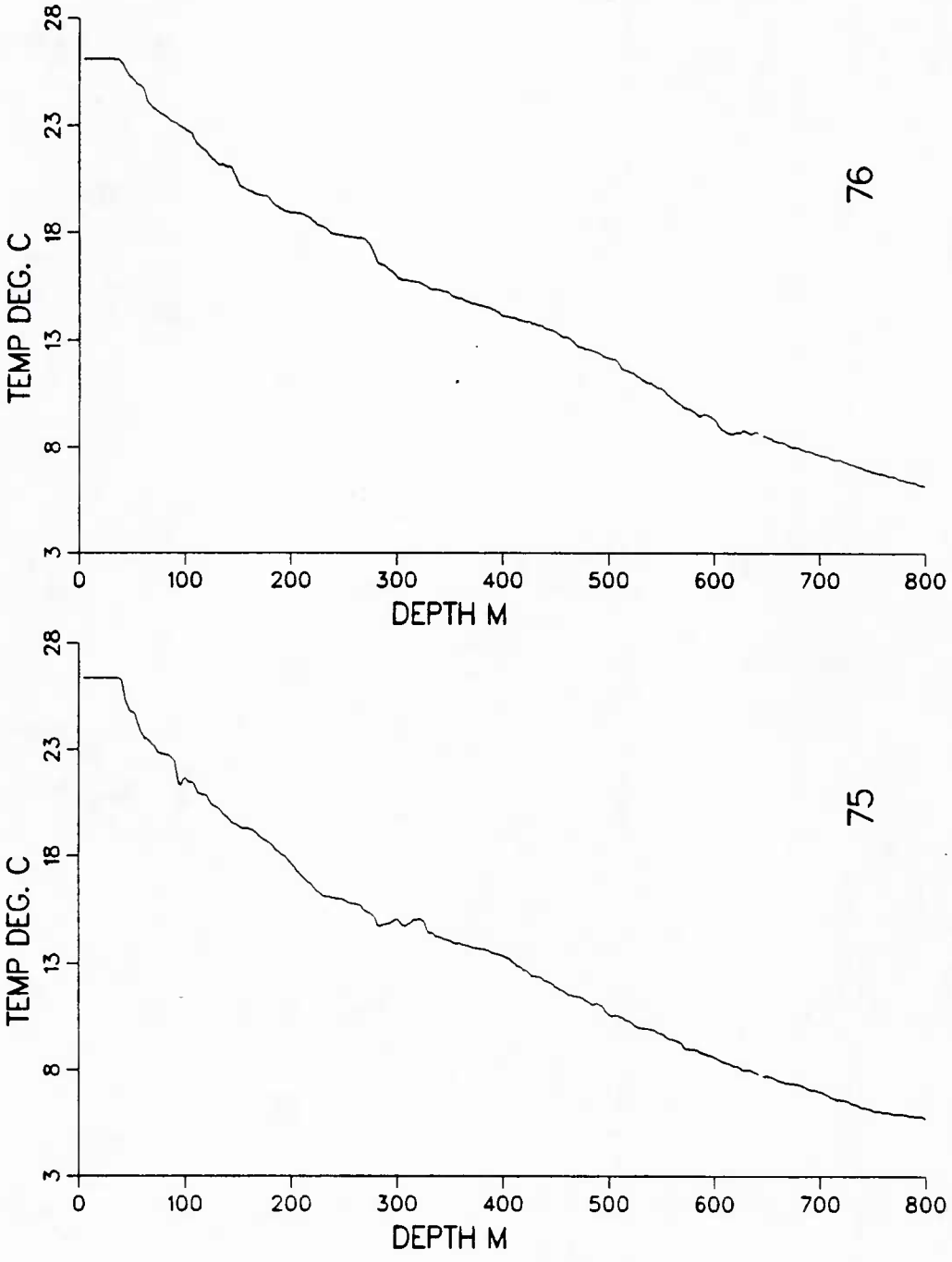

Figure 90. XBT profiles from IES deployment cruise.

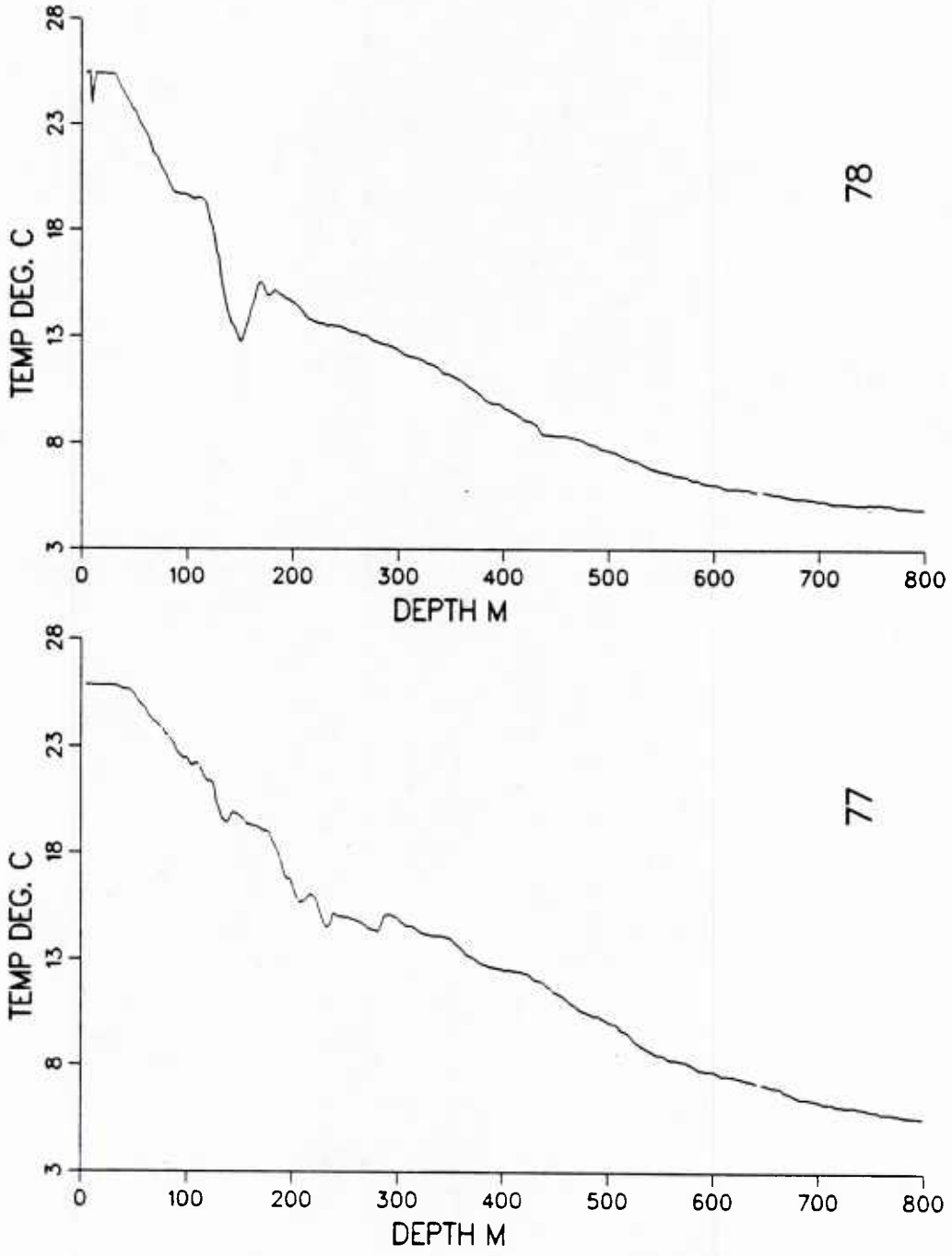

Figure 91. XBT profiles from IES deployment cruise.

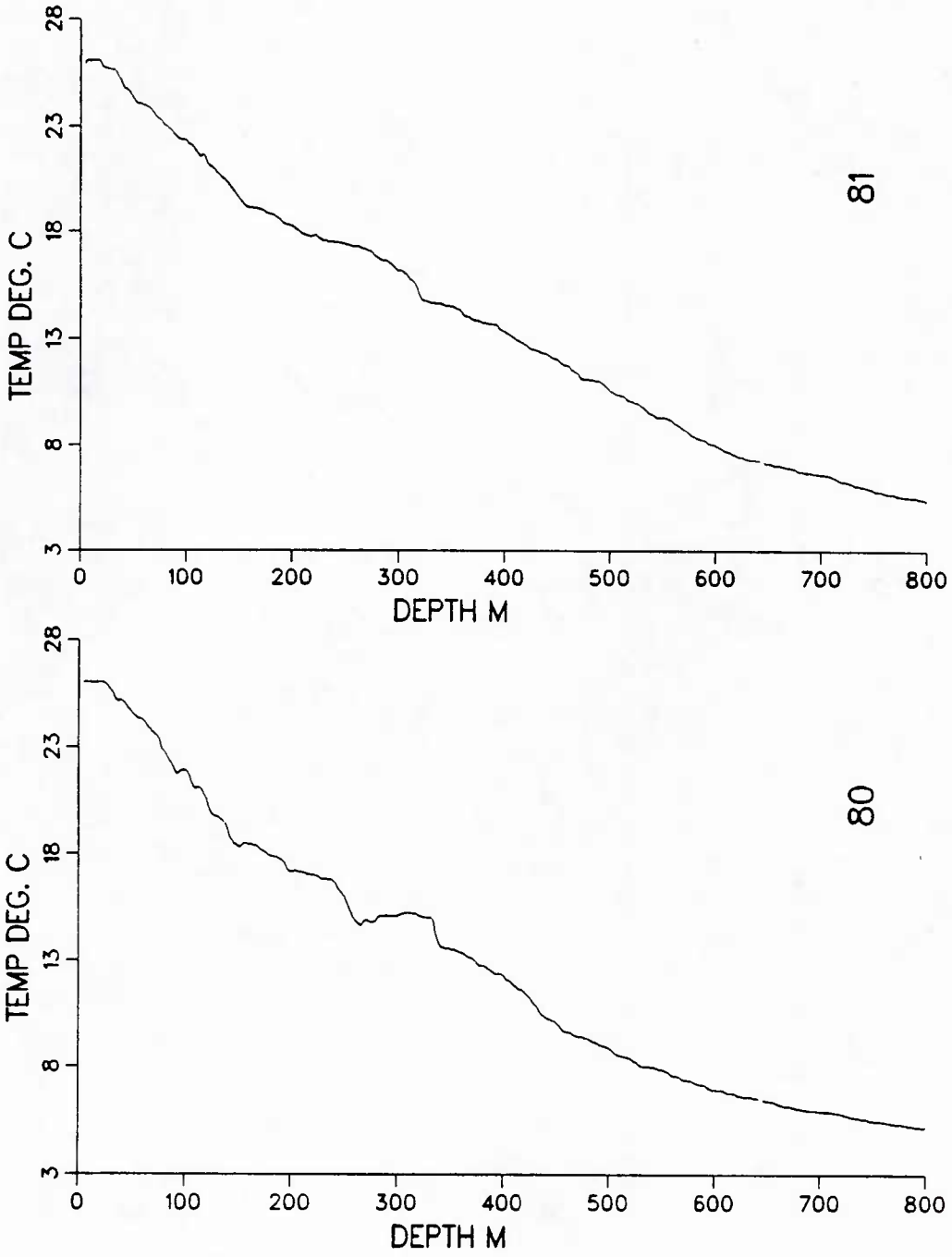

Figure 92. XBT profiles from IES deployment cruise.

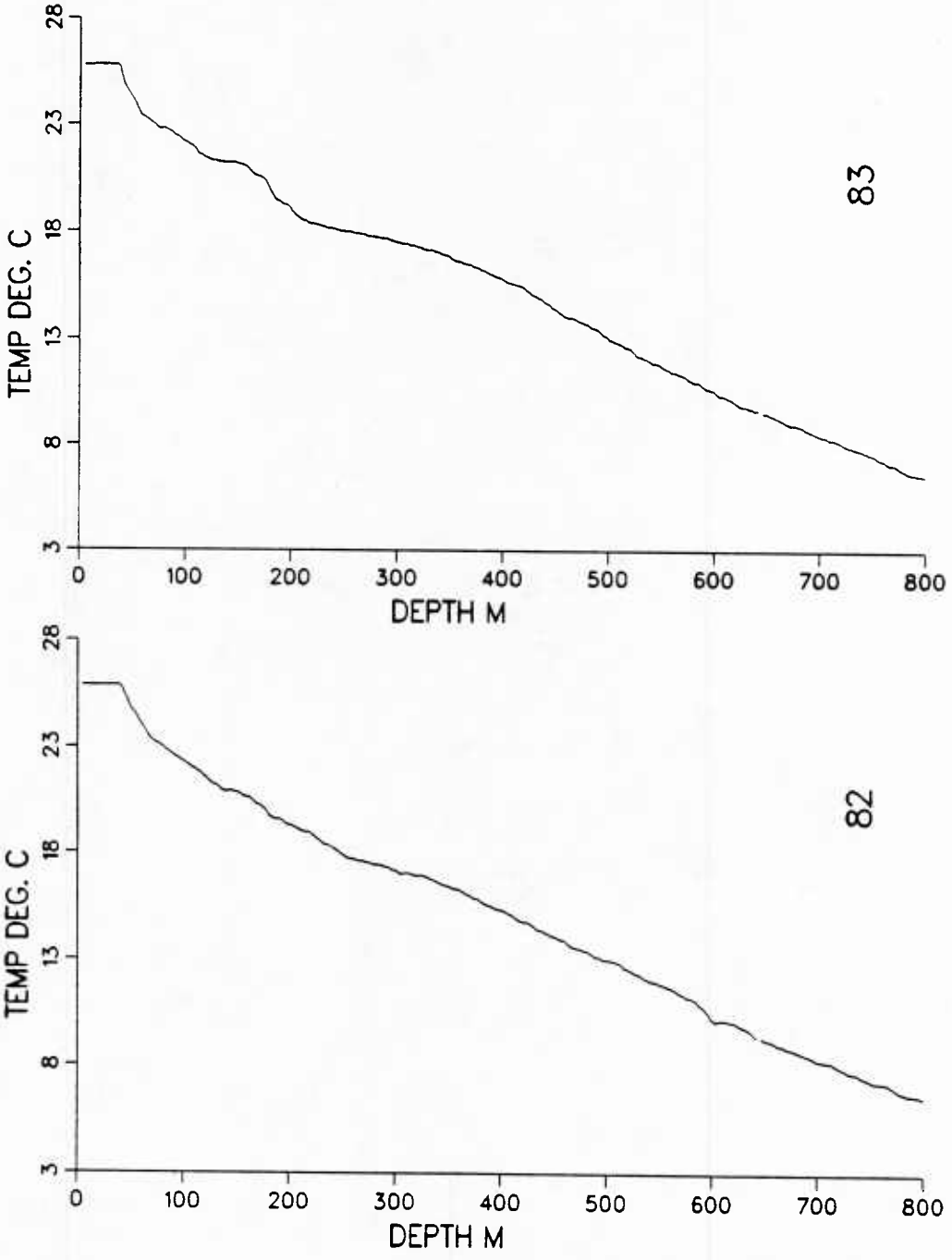

Figure 93. XBT profiles from IES deployment cruise.

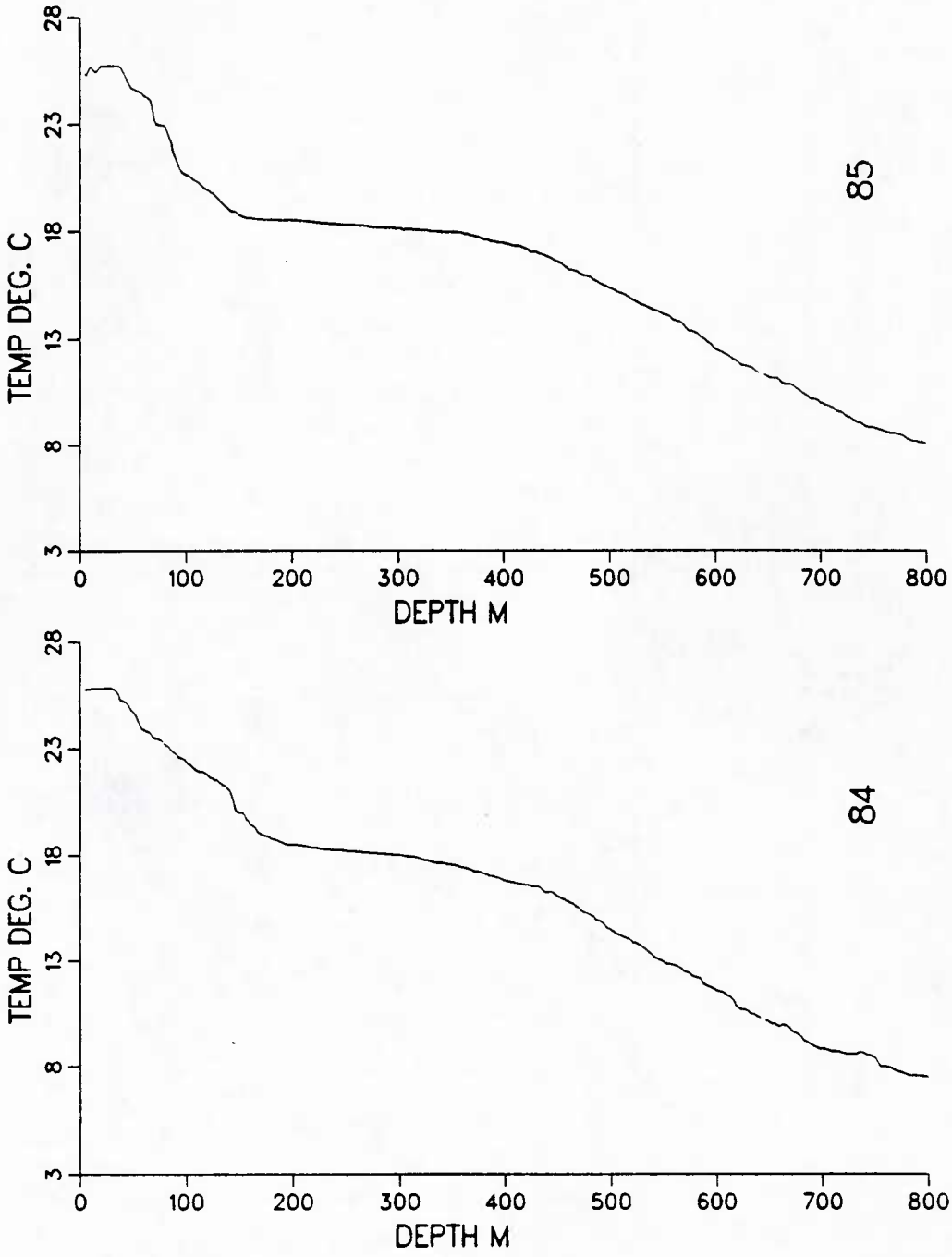

Figure 94. XBT profiles from IES deployment cruise.

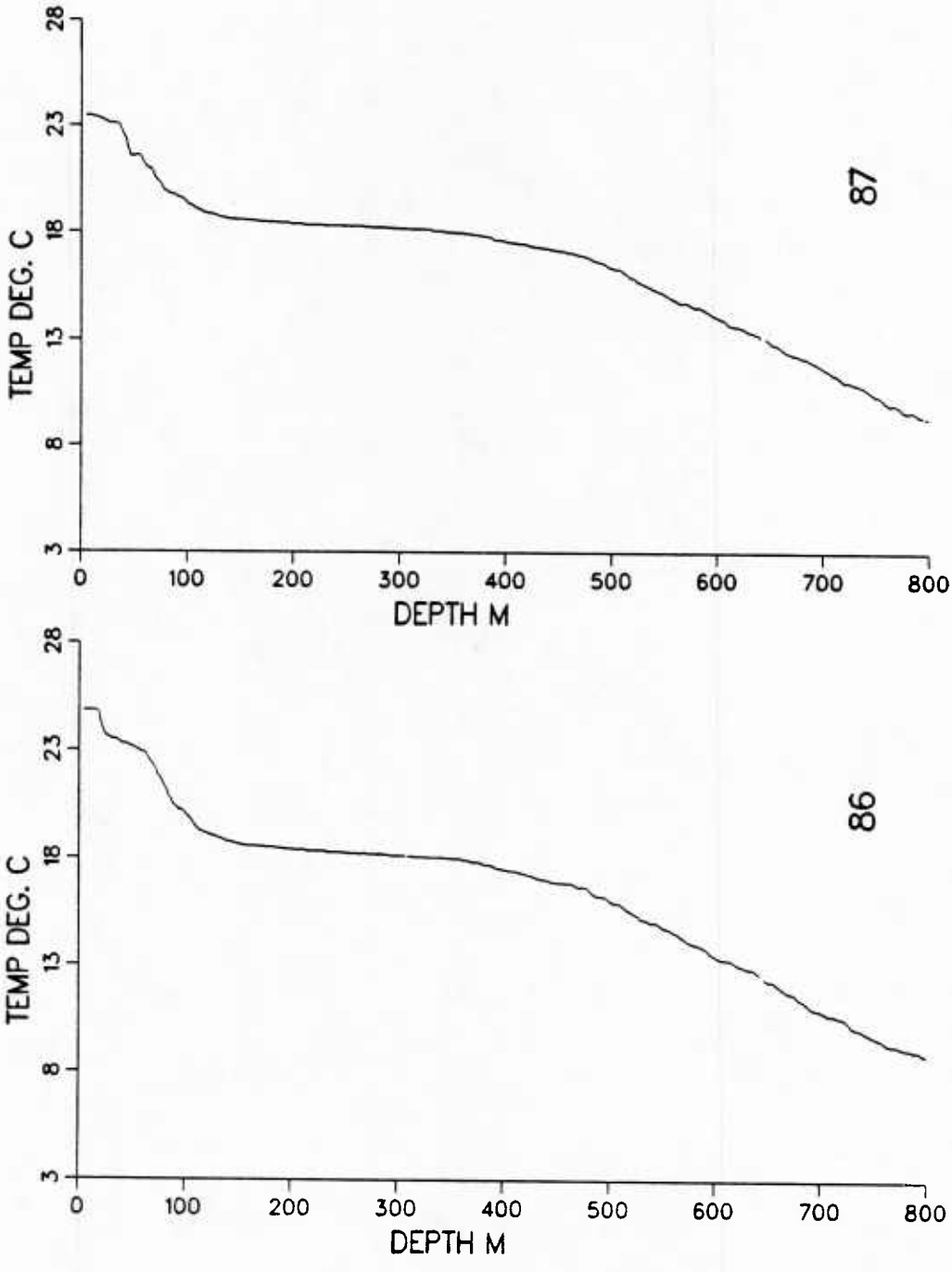

Figure 95. XBT profiles from IES deployment cruise.

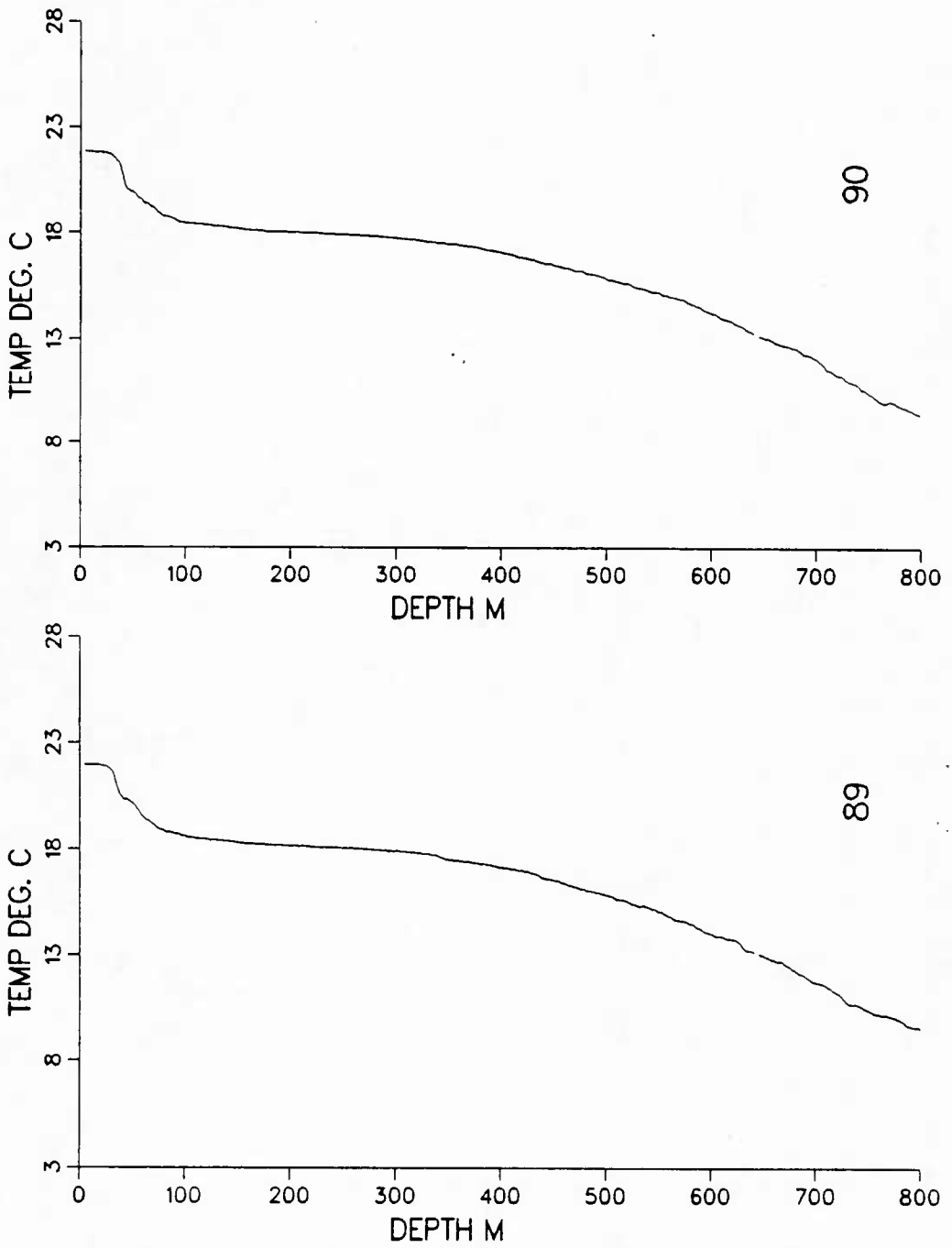

Figure 96. XBT profiles from IES deployment cruise.

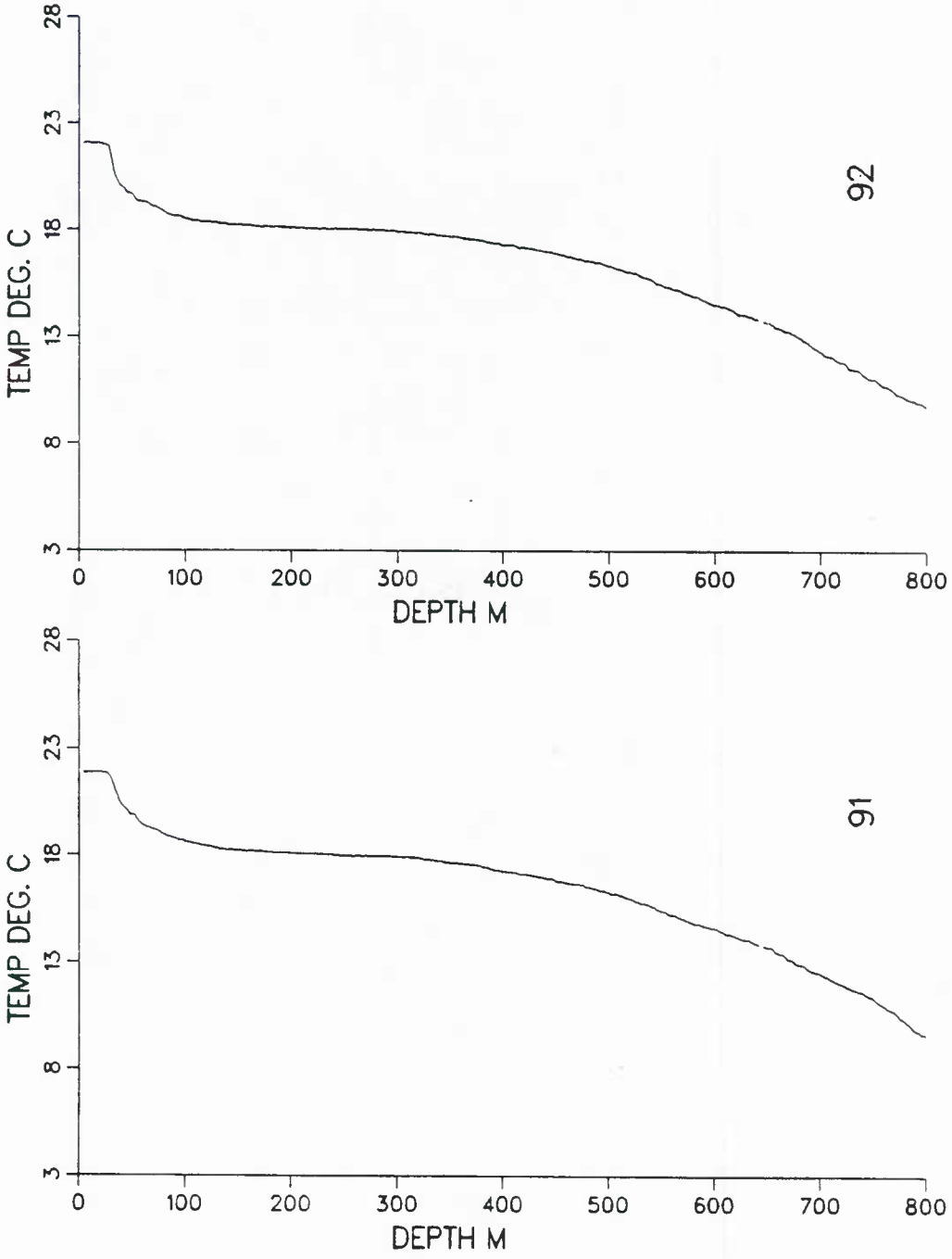

Figure 97. XBT profiles from IES deployment cruise.

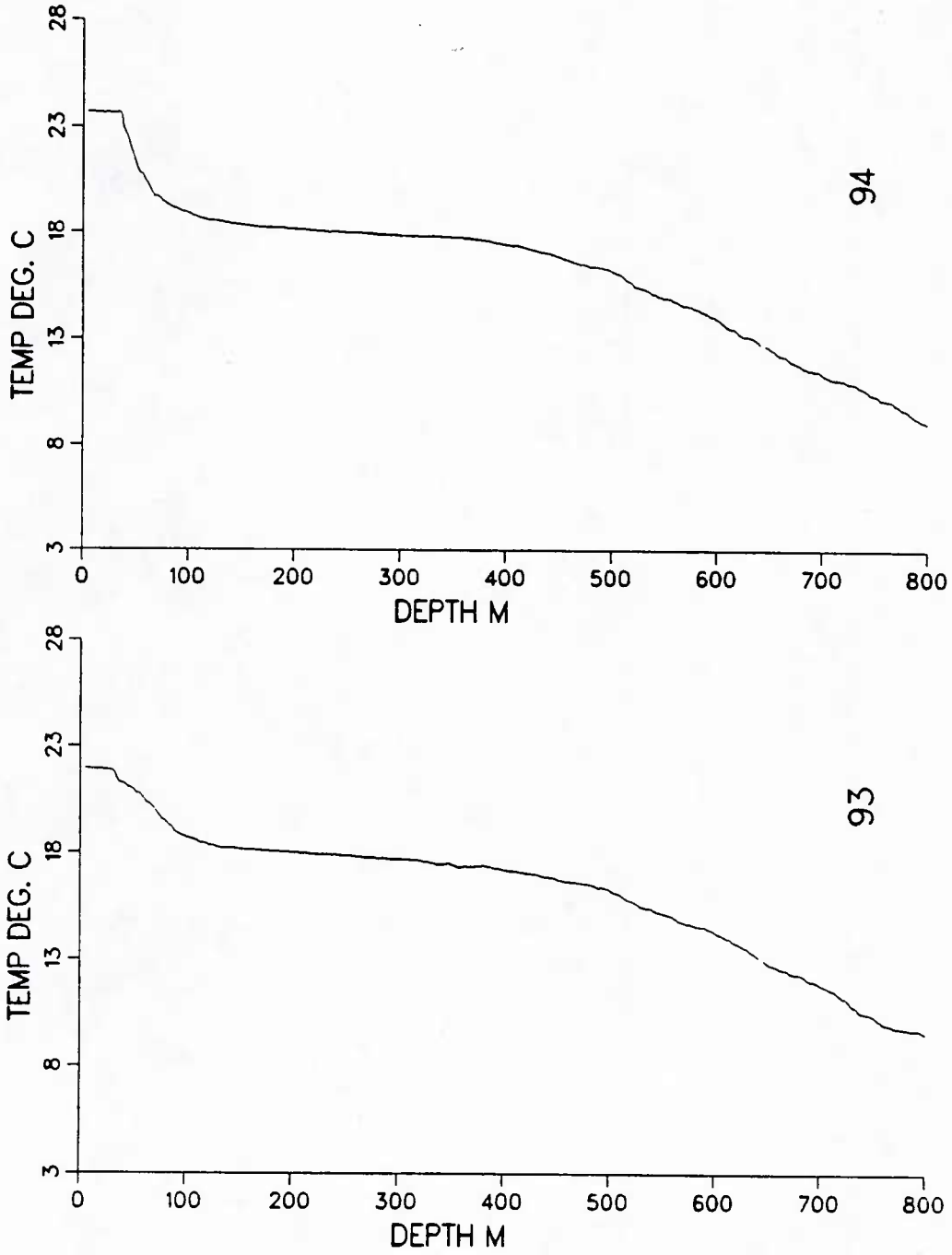

Figure 98. XBT profiles from IES deployment cruise.

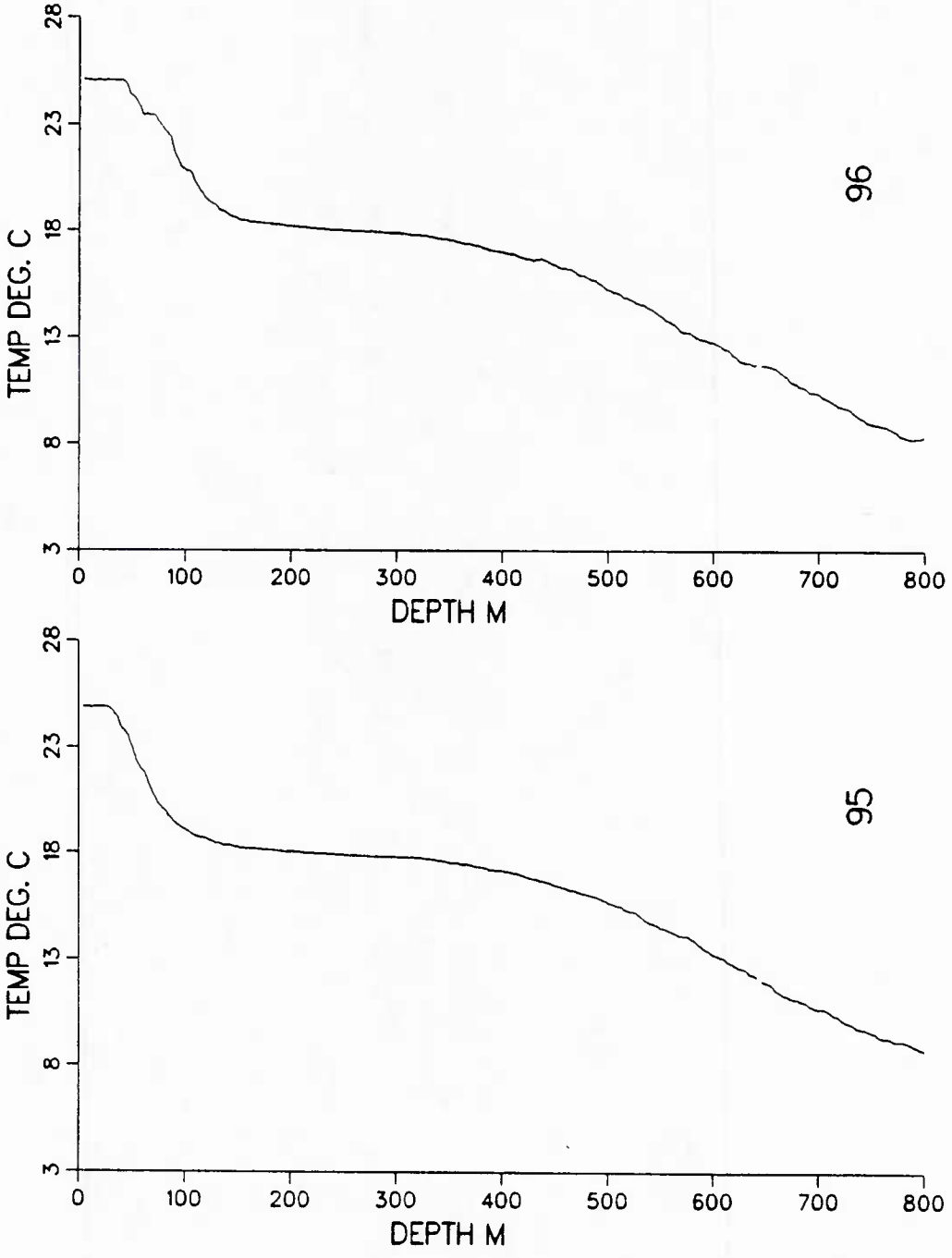

Figure 99. XBT profiles from IES deployment cruise.

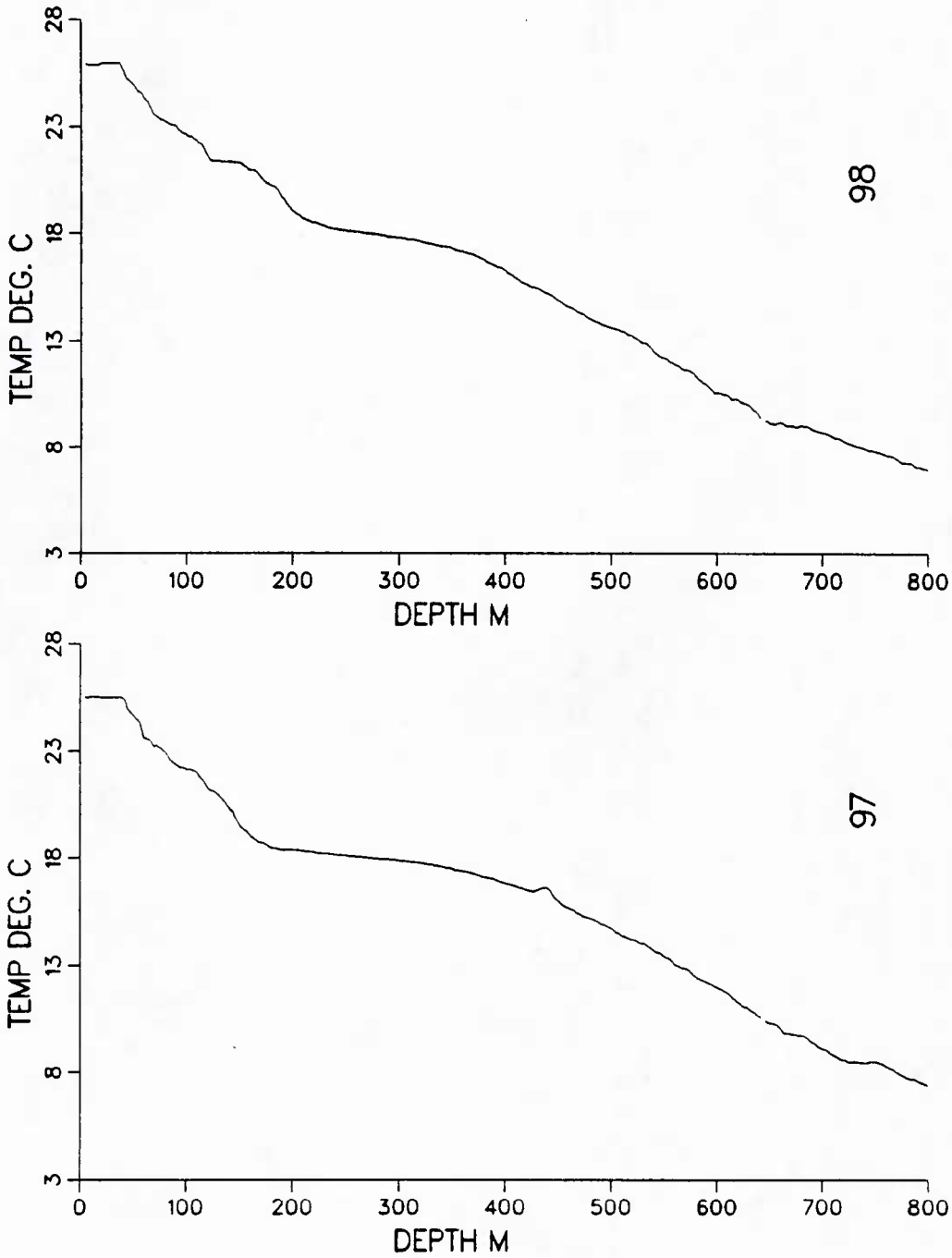

Figure 100. XBT profiles from IES deployment cruise.

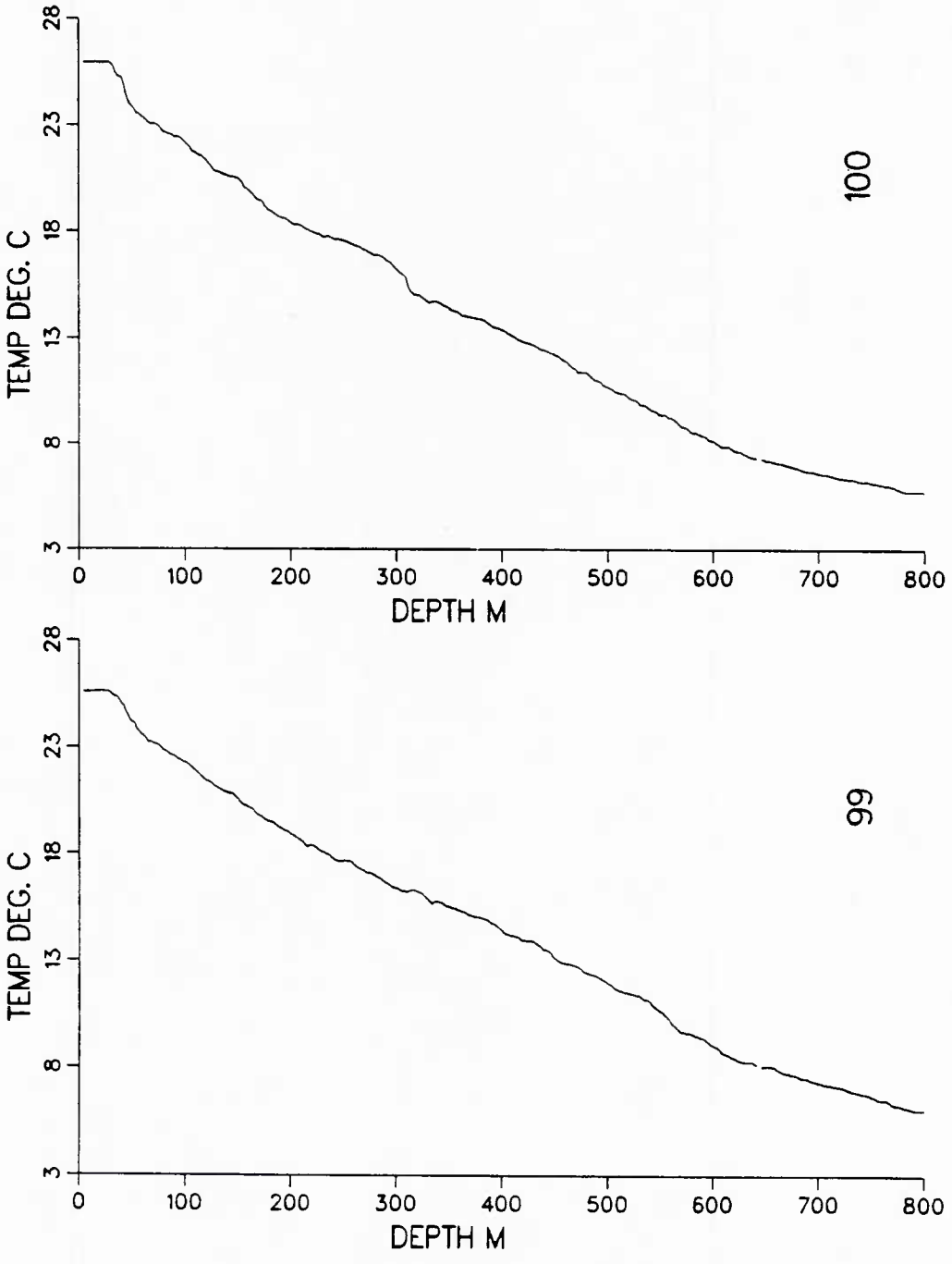

Figure 101. XBT profiles from IES deployment cruise.

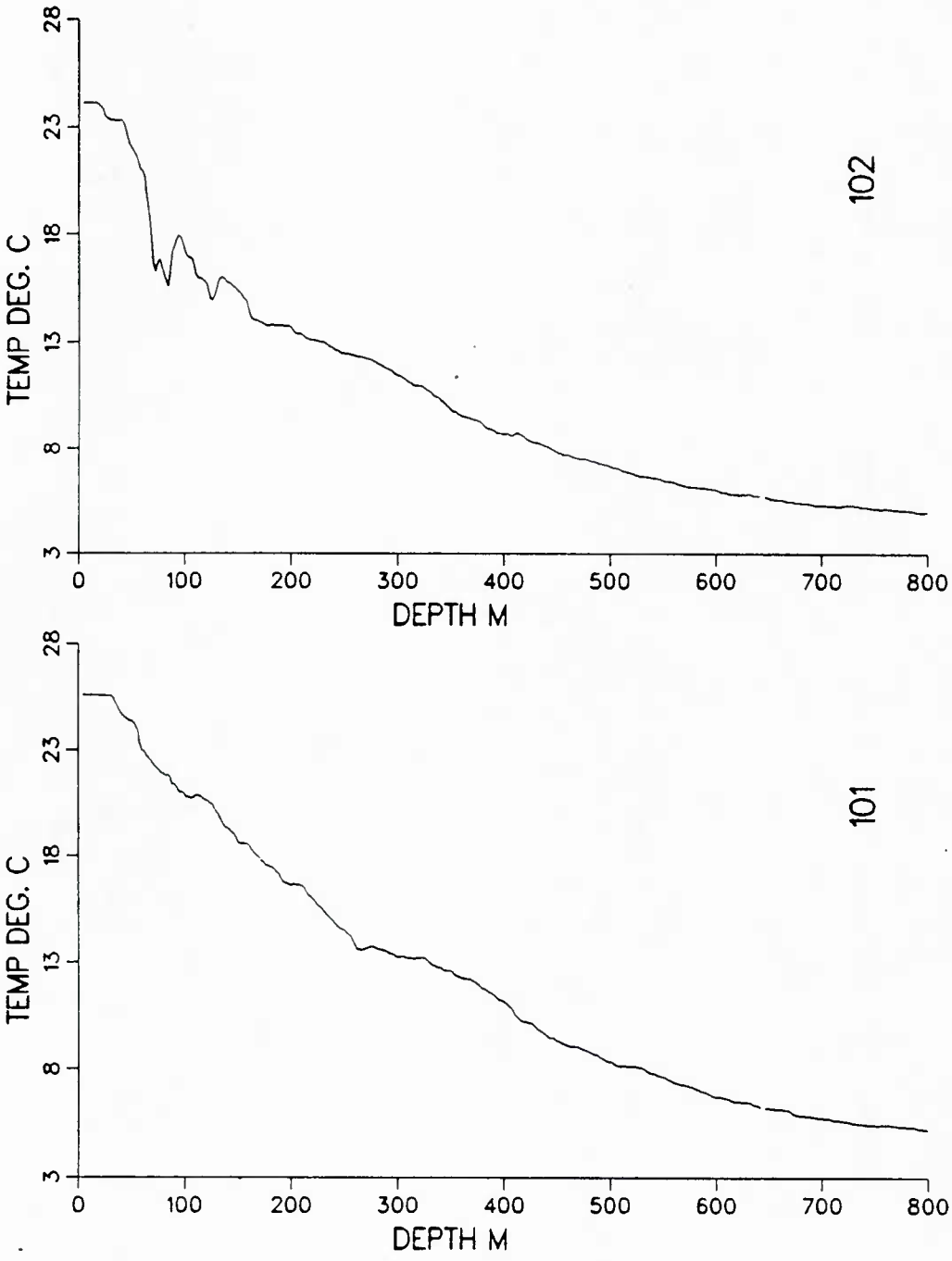

Figure 102. XBT profiles from IES deployment cruise.

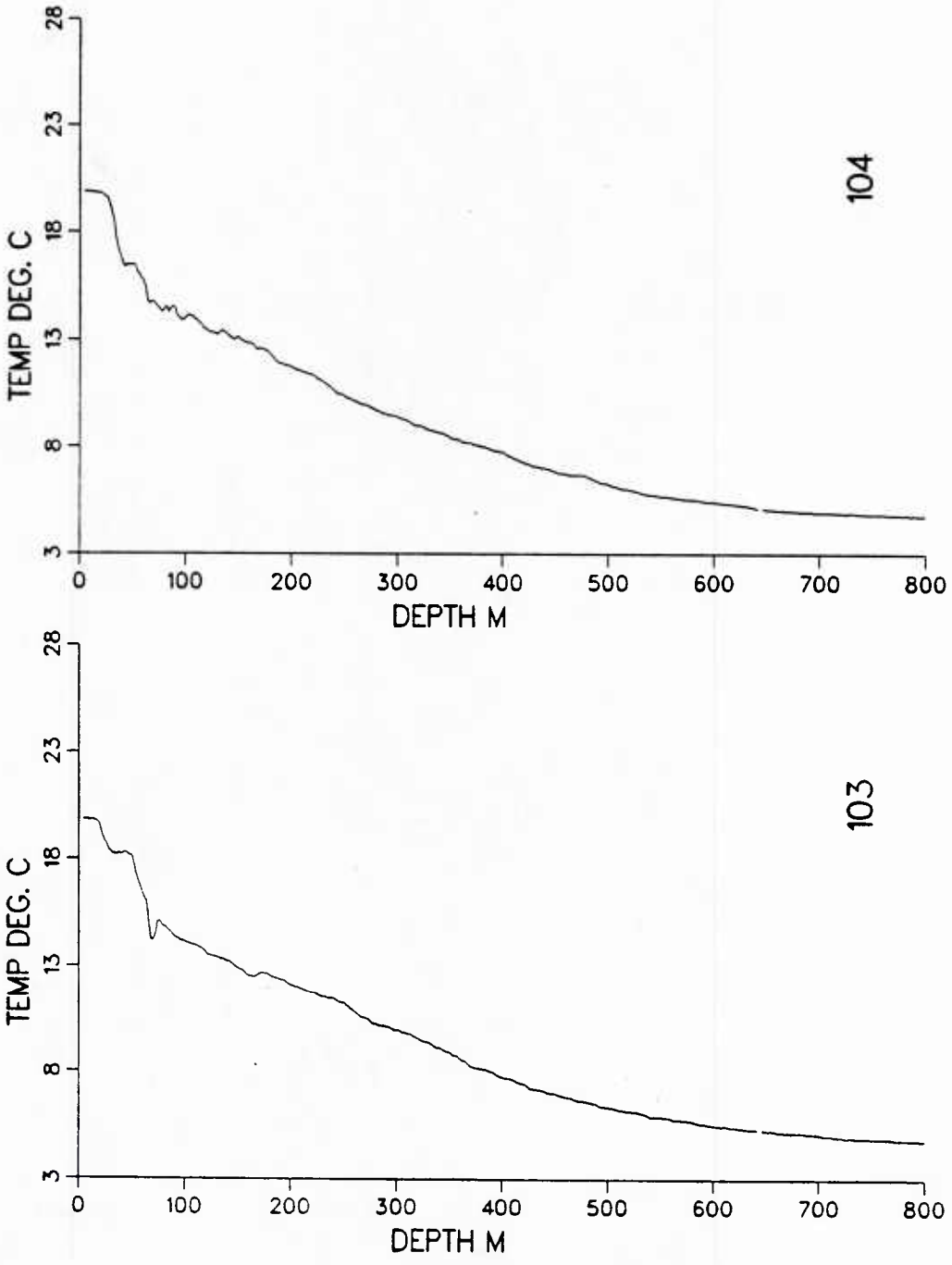

Figure 103. XBT profiles from IES deployment cruise.

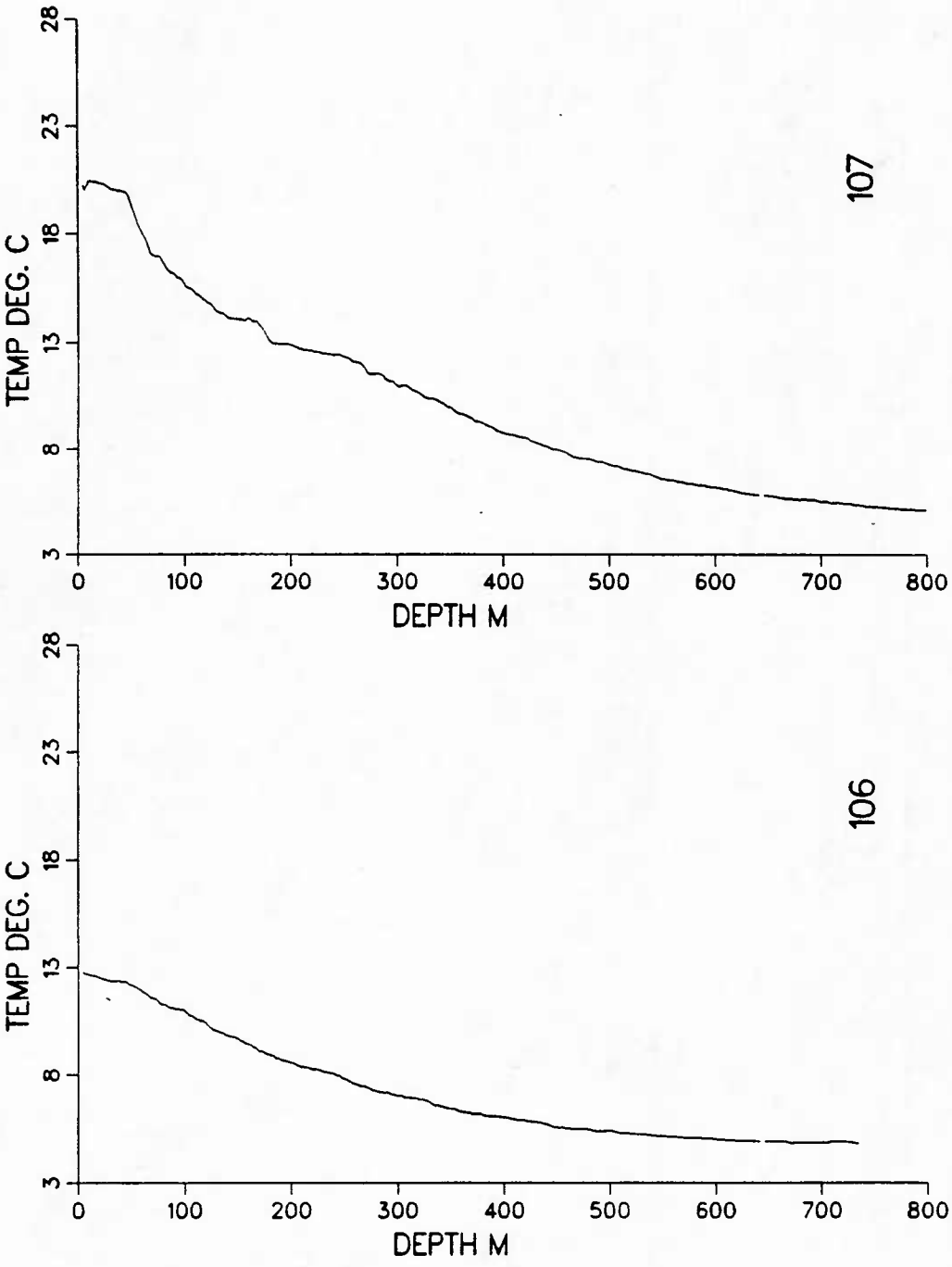

Figure 104. XBT profiles from IES deployment cruise.

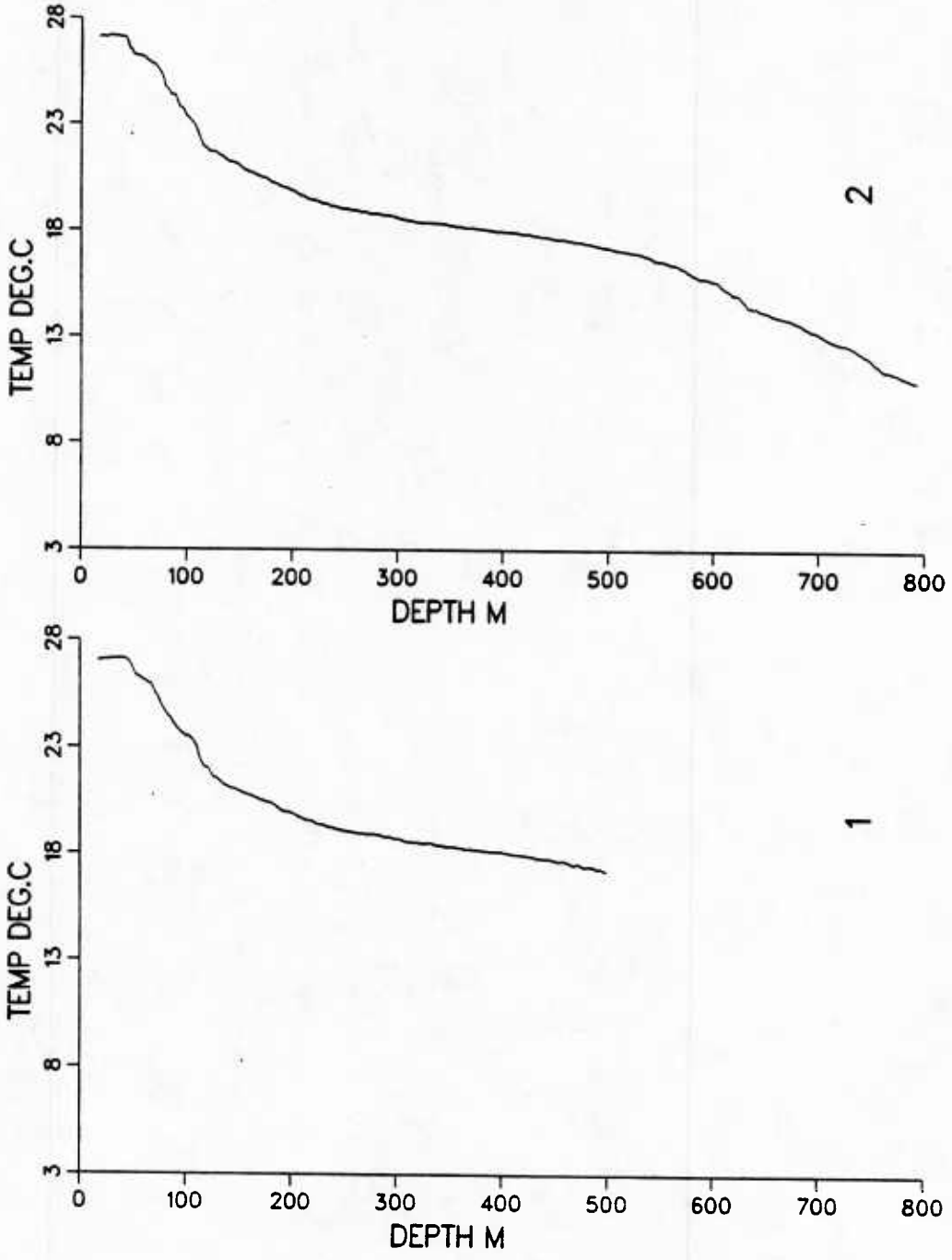

Figure 105. XBT profiles from IES recovery cruise.

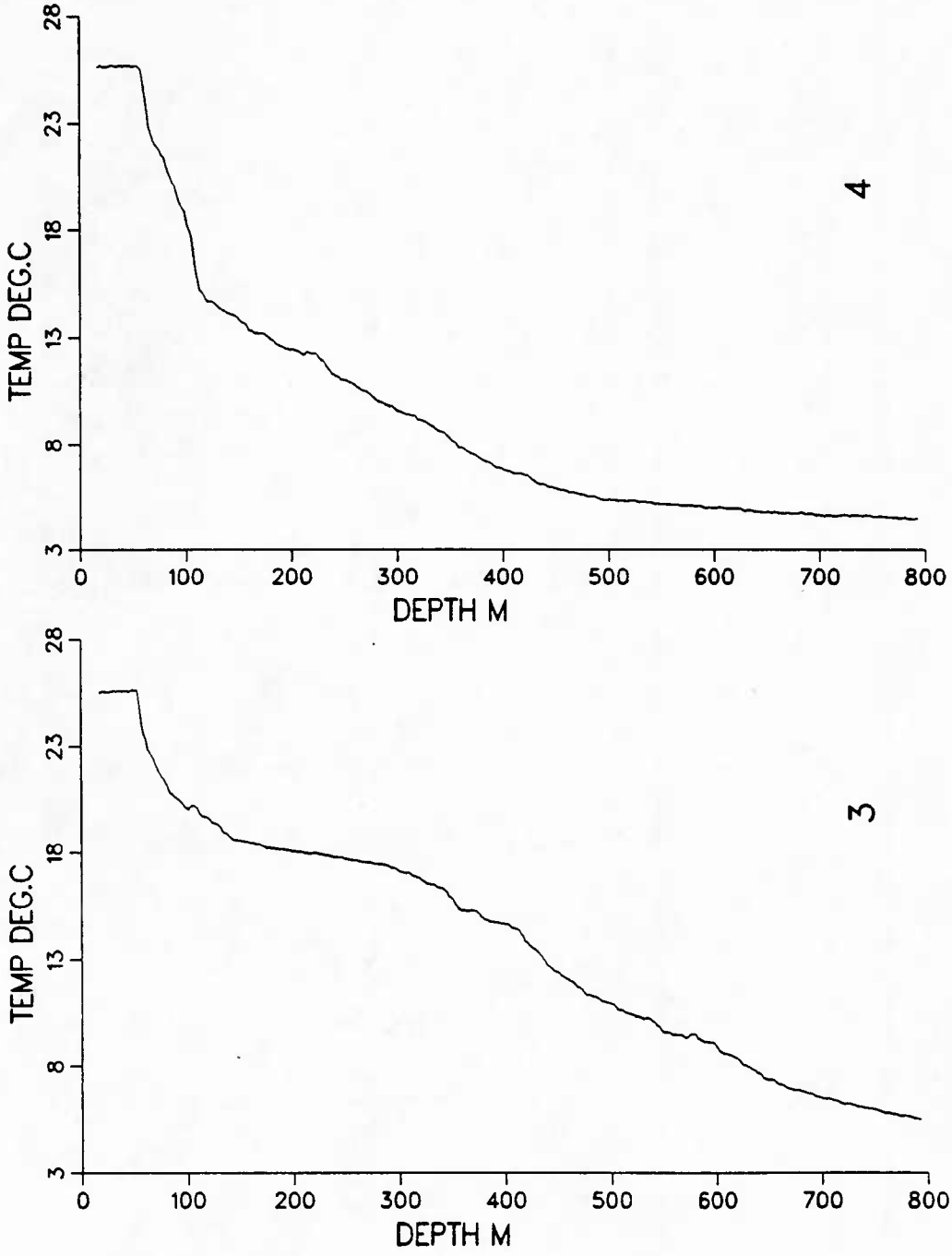

Figure 106. XBT profiles from IES recovery cruise.

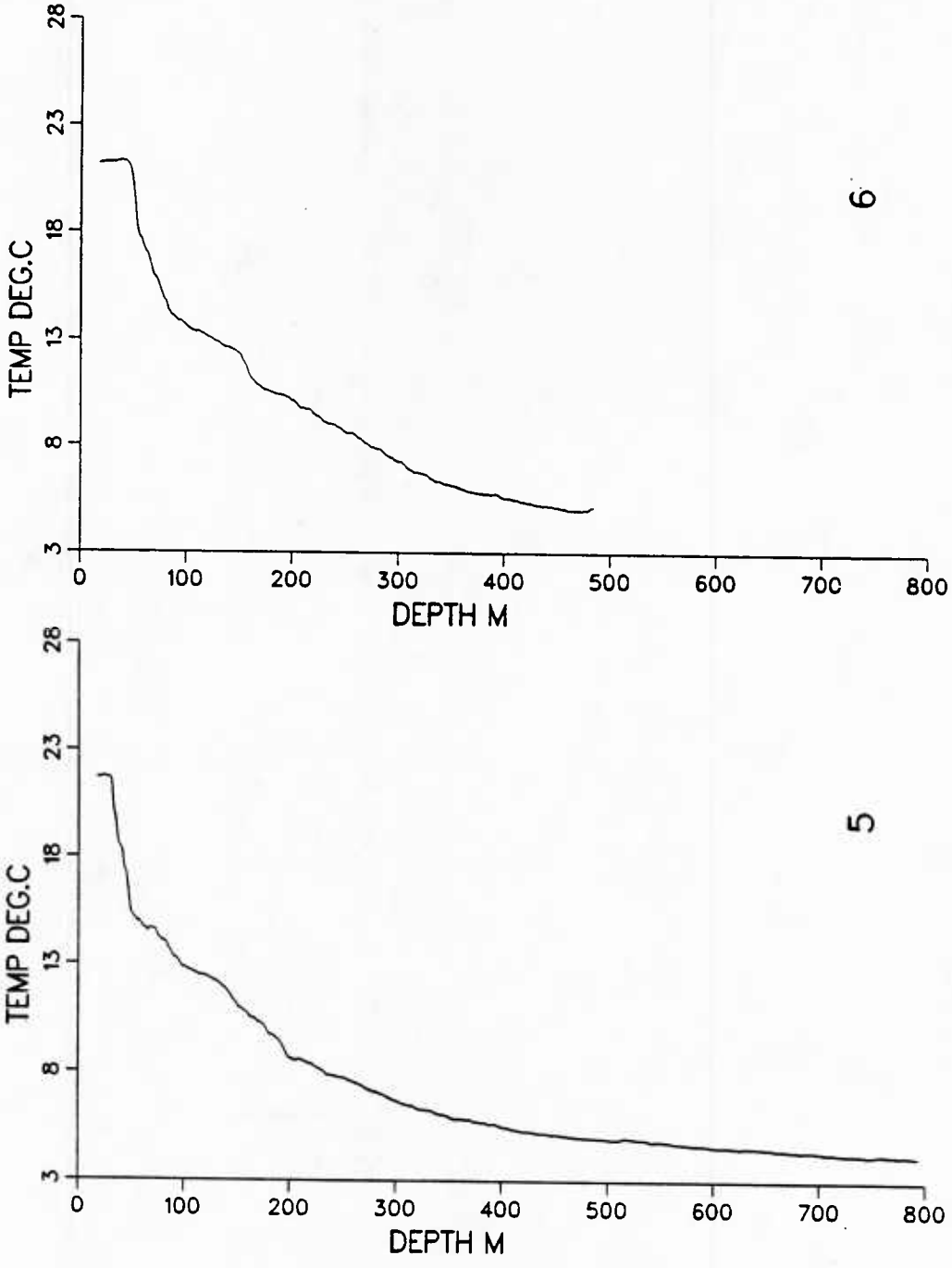

Figure 107. XBT profiles from IES recovery cruise.

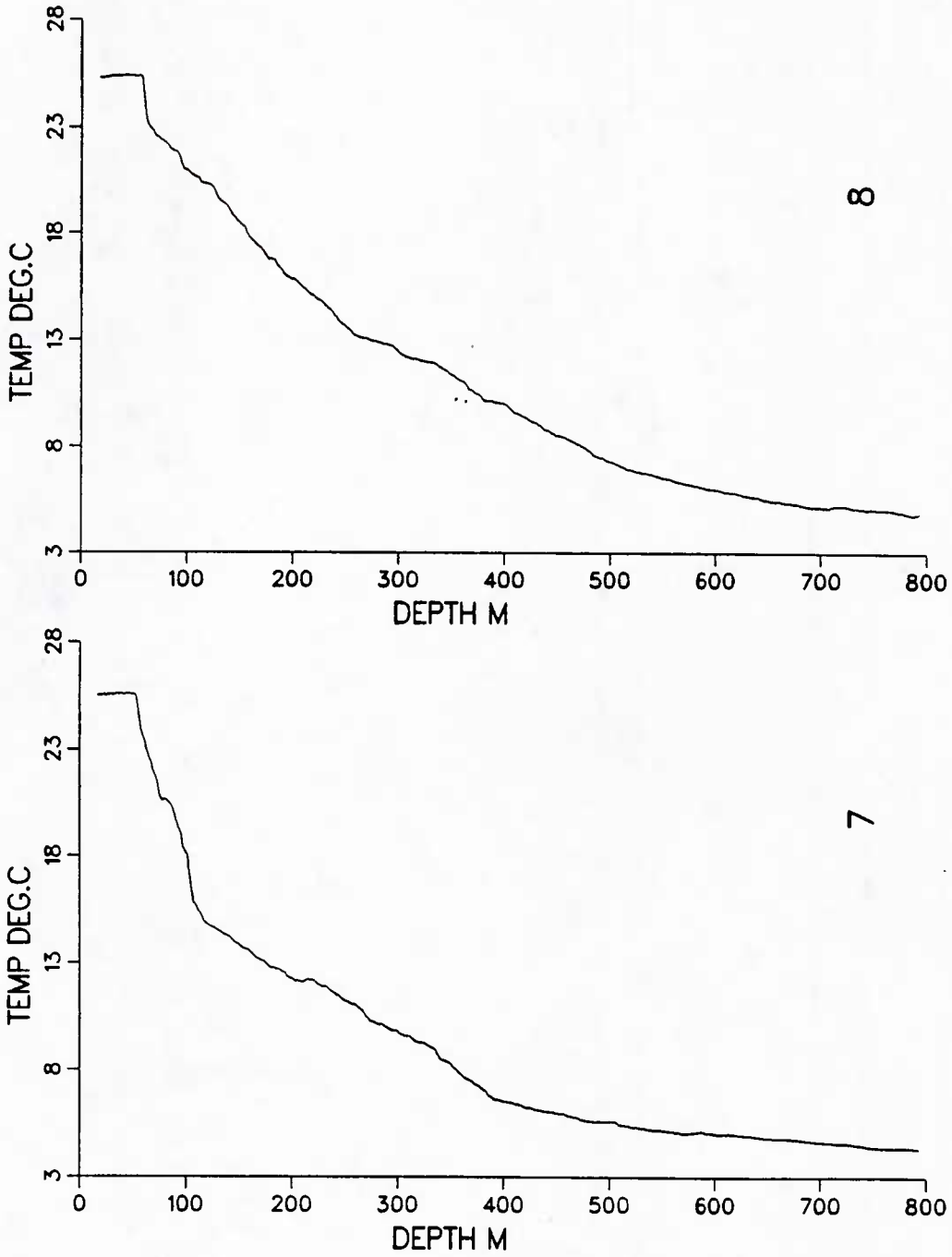

Figure 108. XBT profiles from IES recovery cruise.

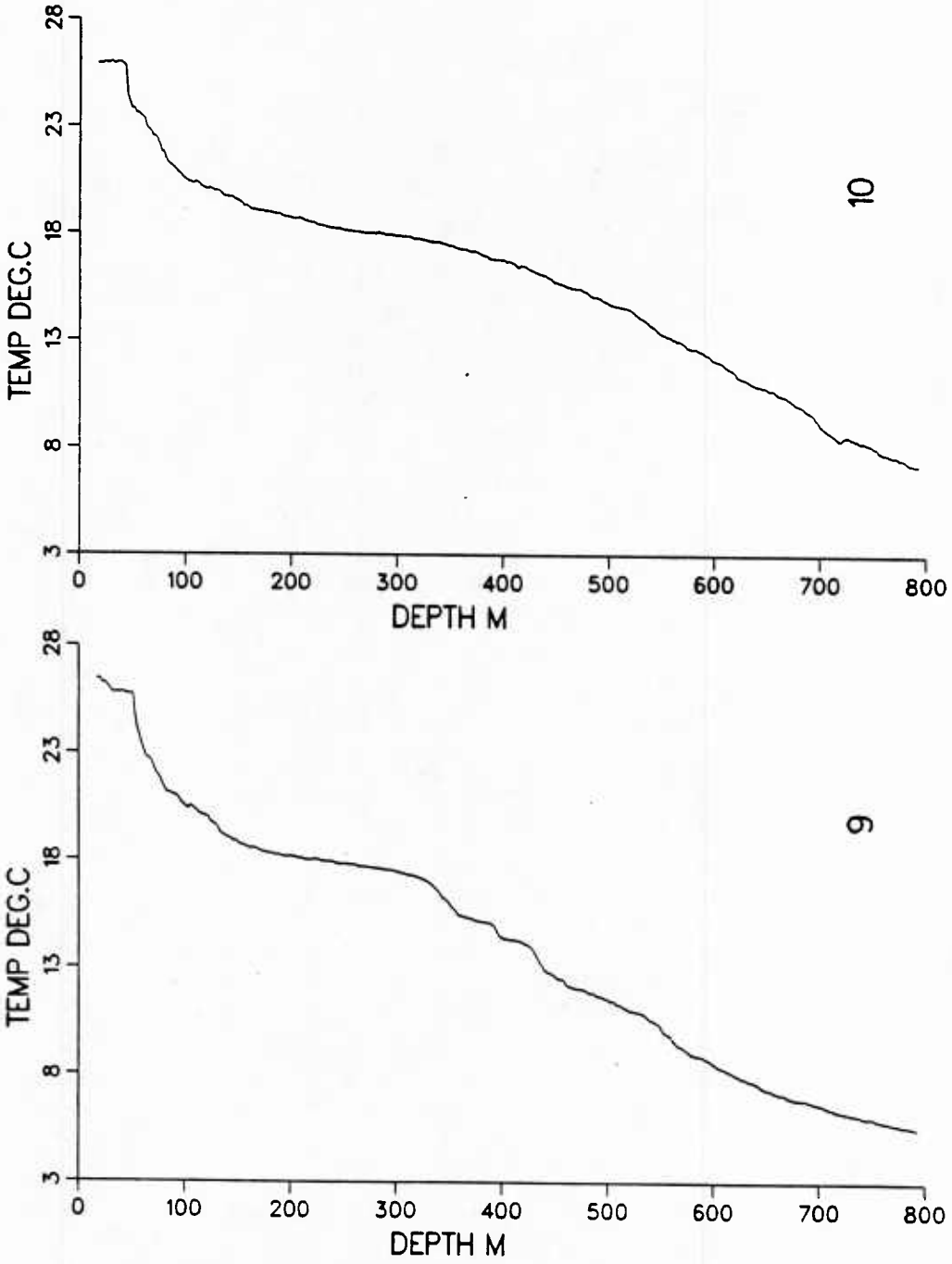

Figure 109. XBT profiles from IES recovery cruise.

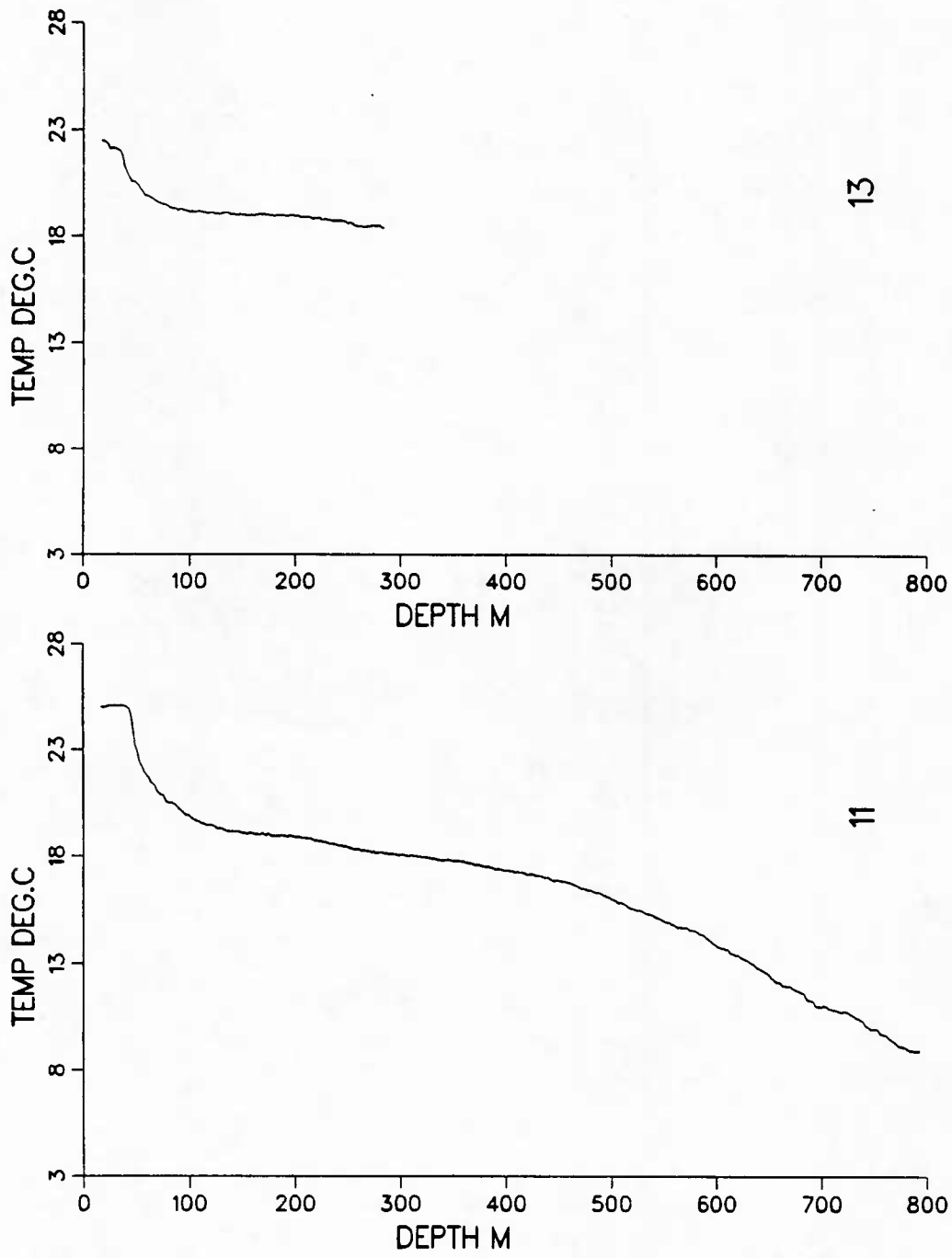

Figure 110. XBT profiles from IES recovery cruise.

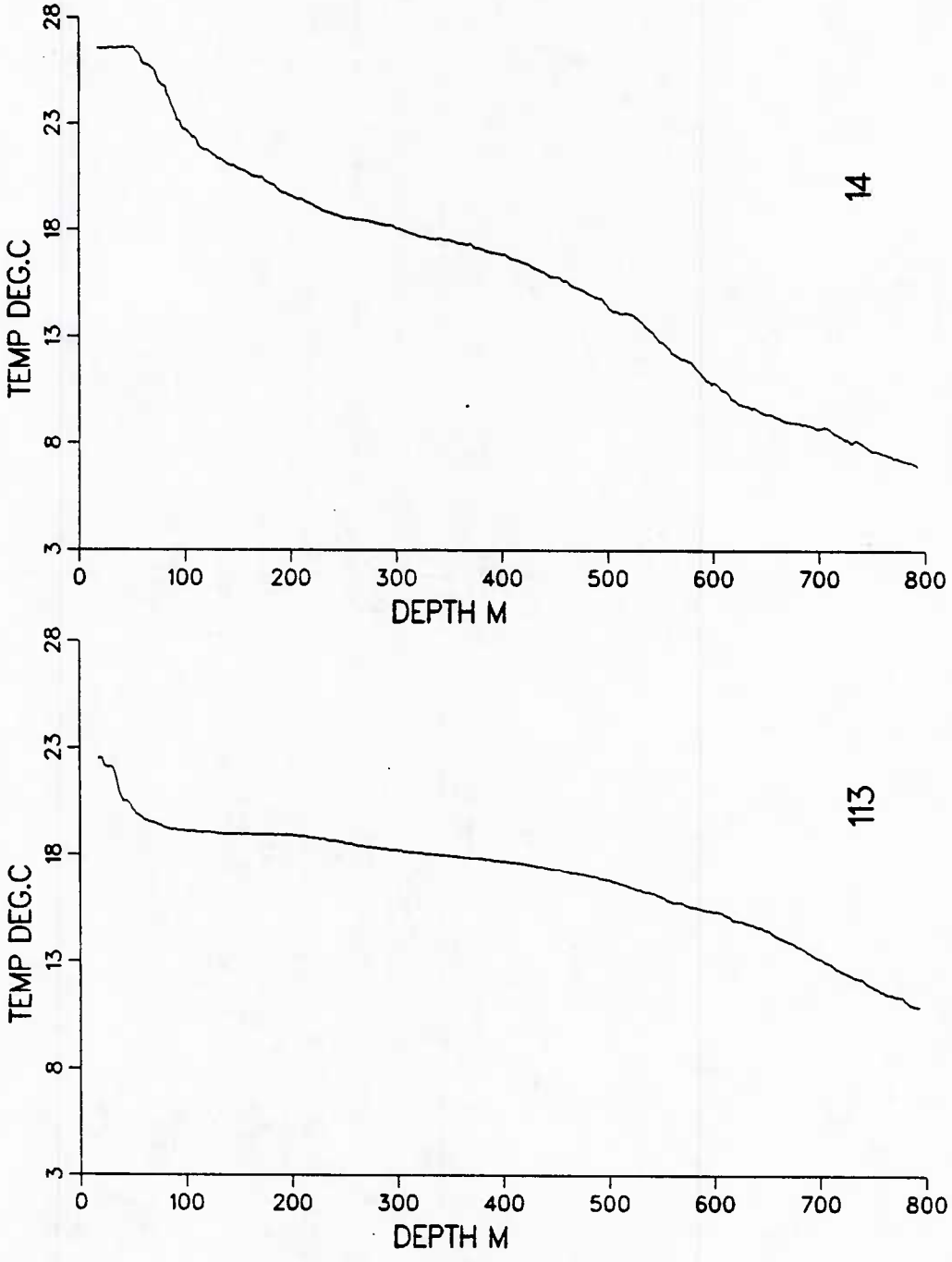

Figure 111. XBT profiles from IES recovery cruise.

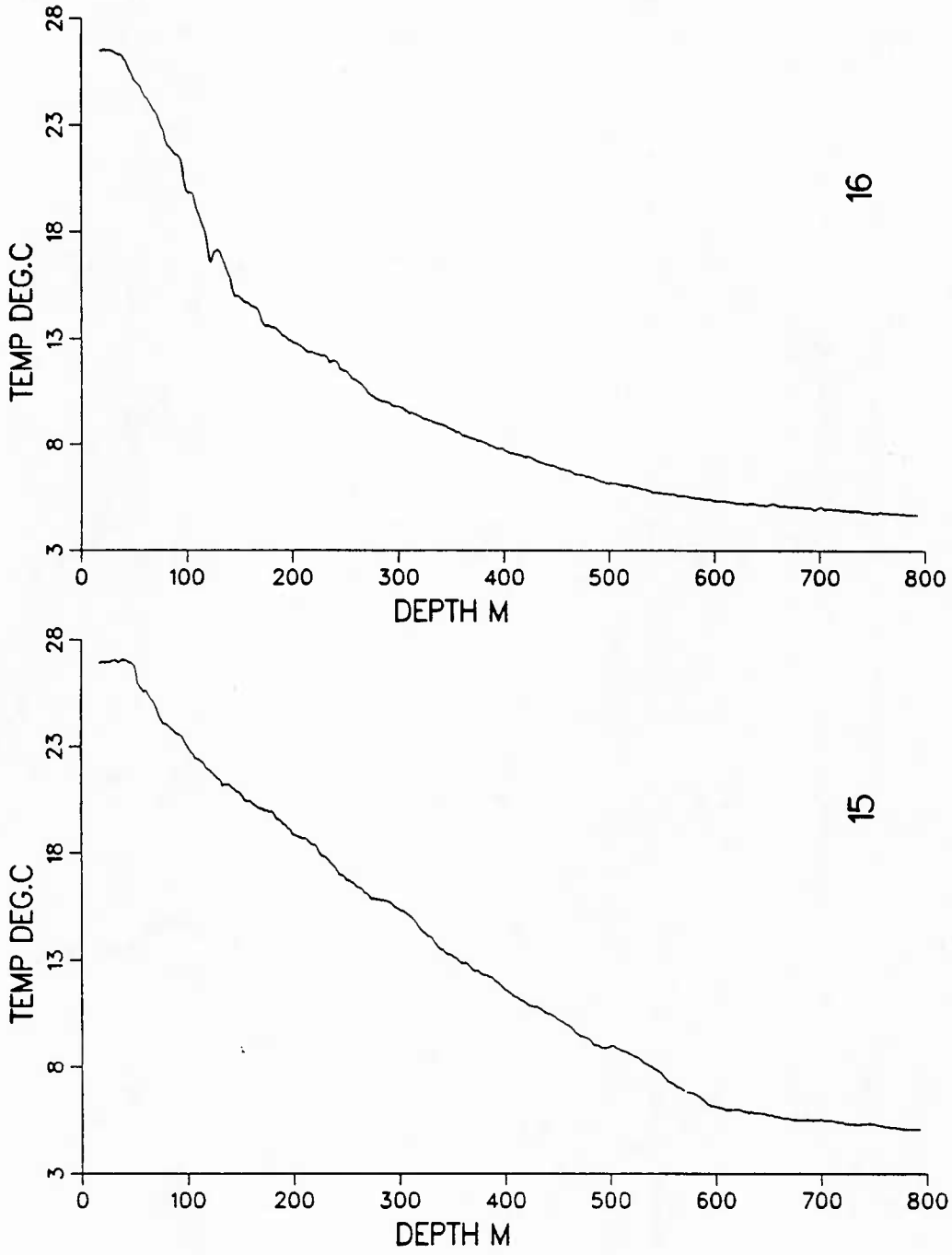

Figure 112. XBT profiles from IES recovery cruise.

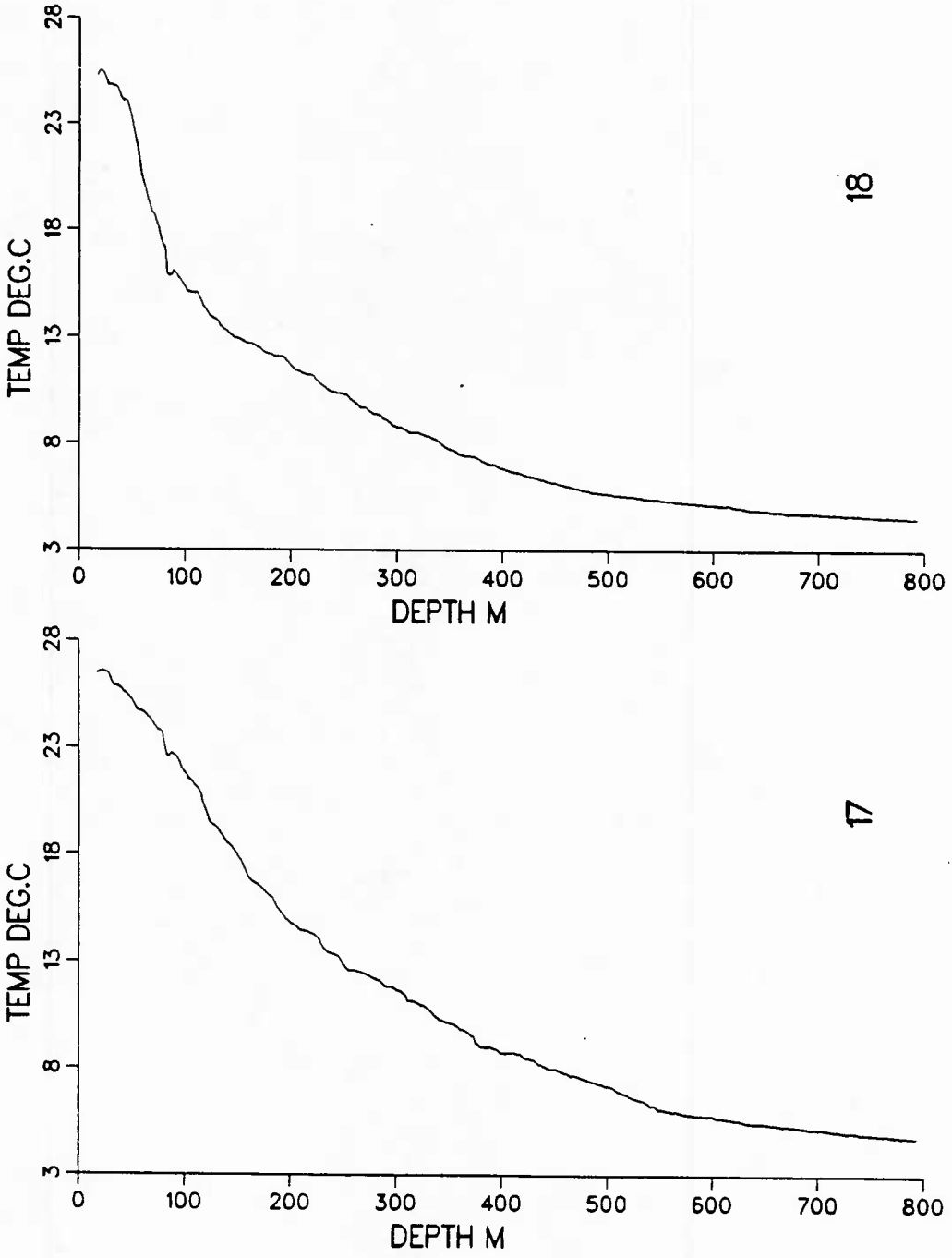

Figure 113. XBT profiles from IES recovery cruise.

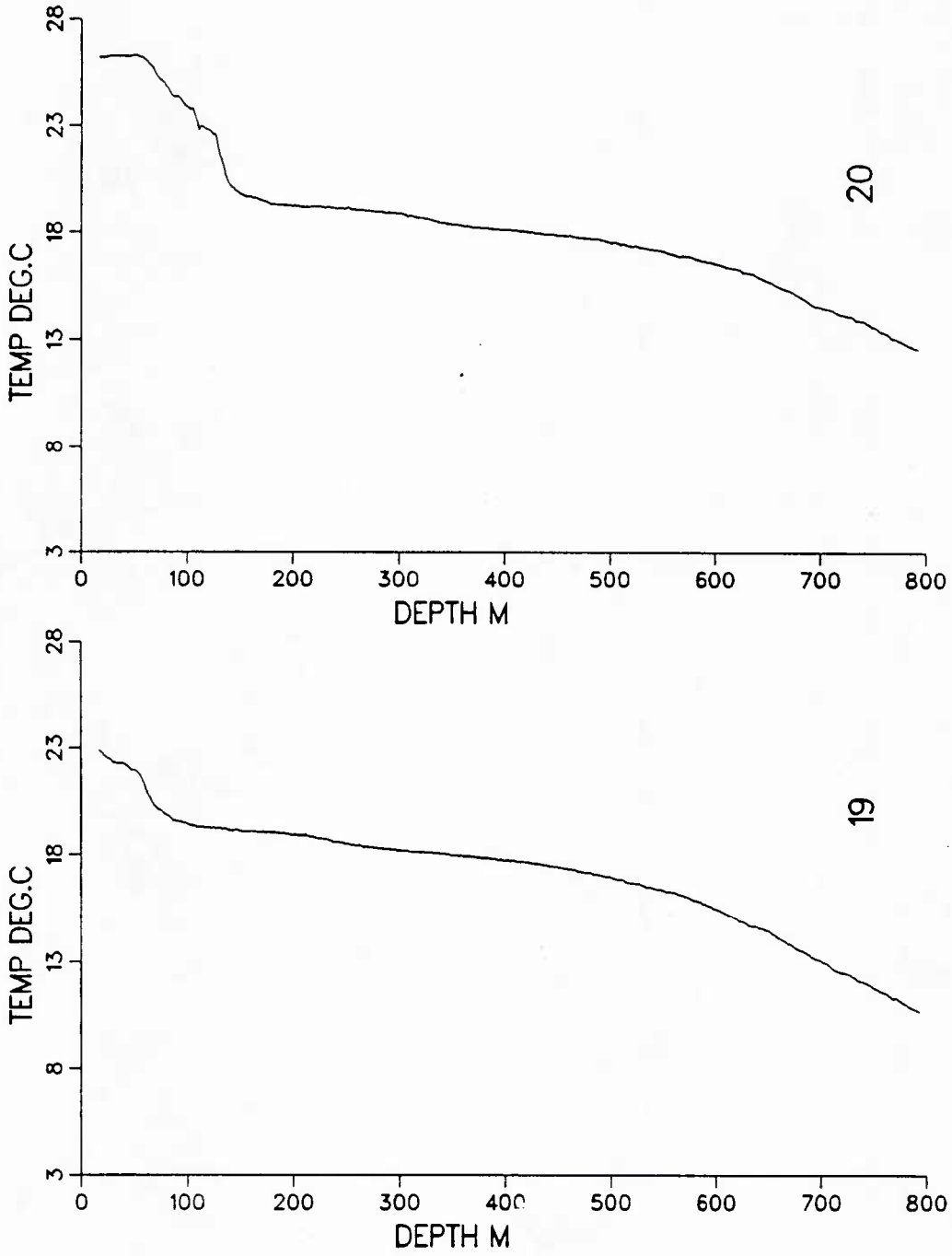

Figure 114. XBT profiles from IES recovery cruise.

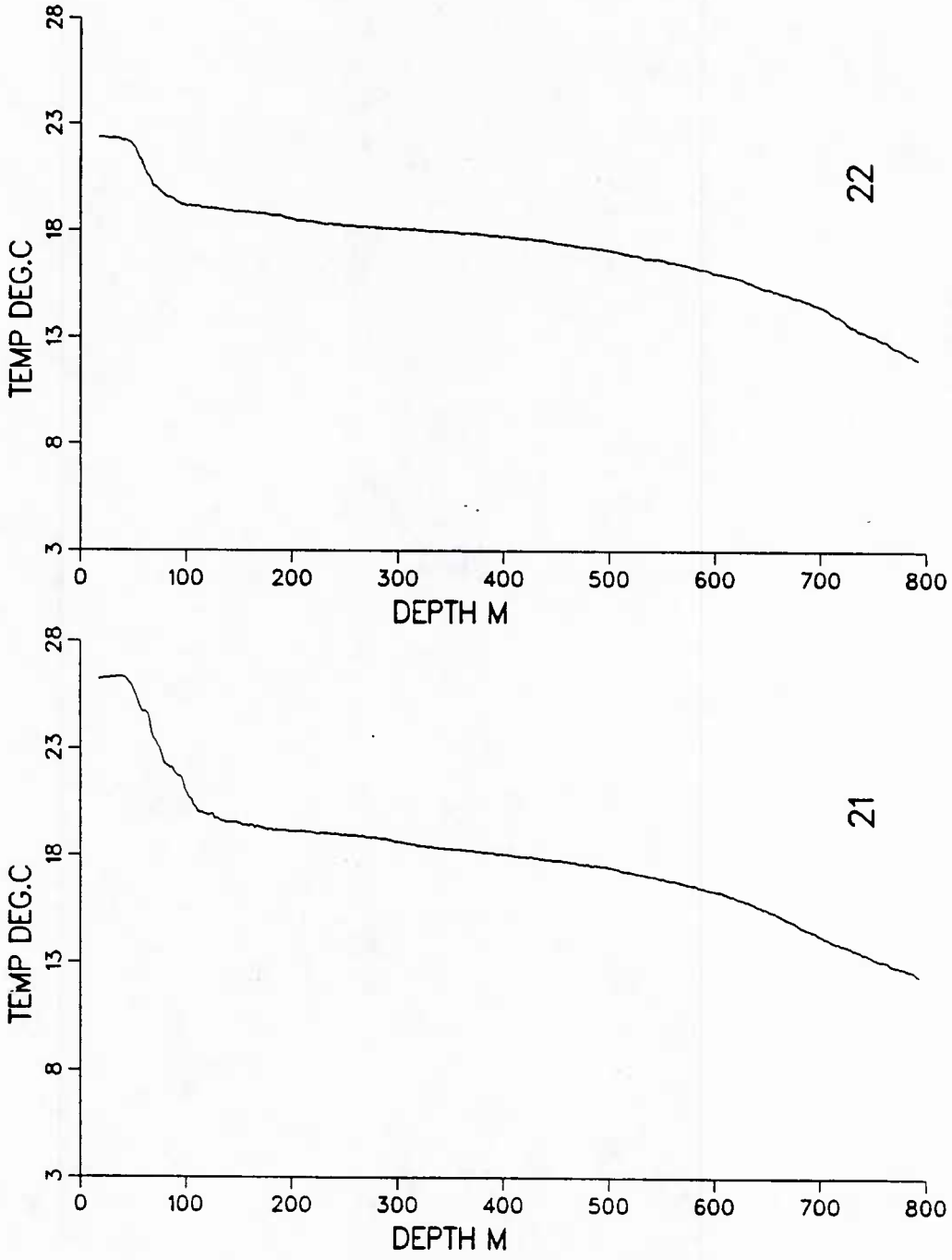

Figure 115. XBT profiles from IES recovery cruise.

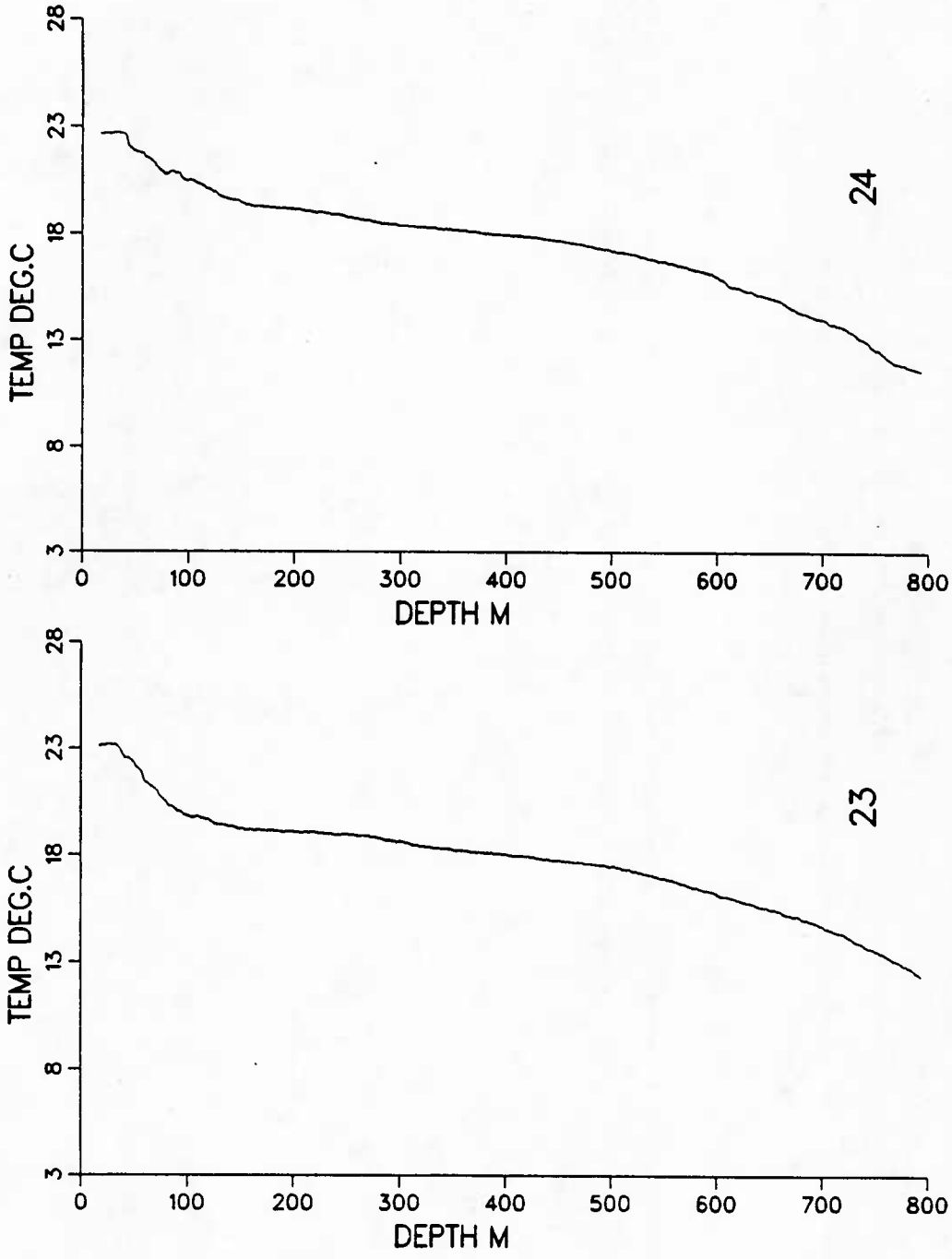

Figure 116. XBT profiles from IES recovery cruise.

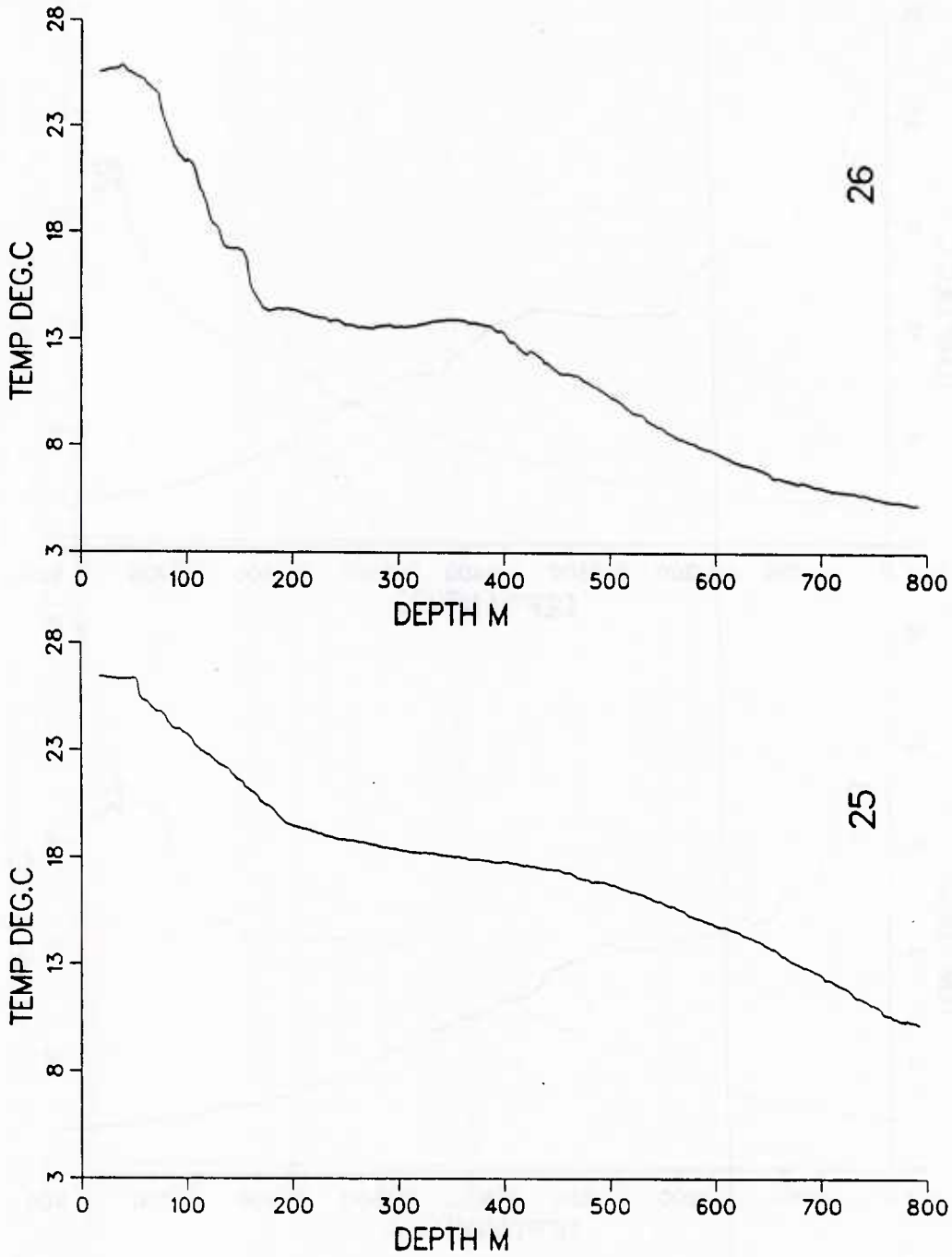

Figure 117. XBT profiles from IES recovery cruise.

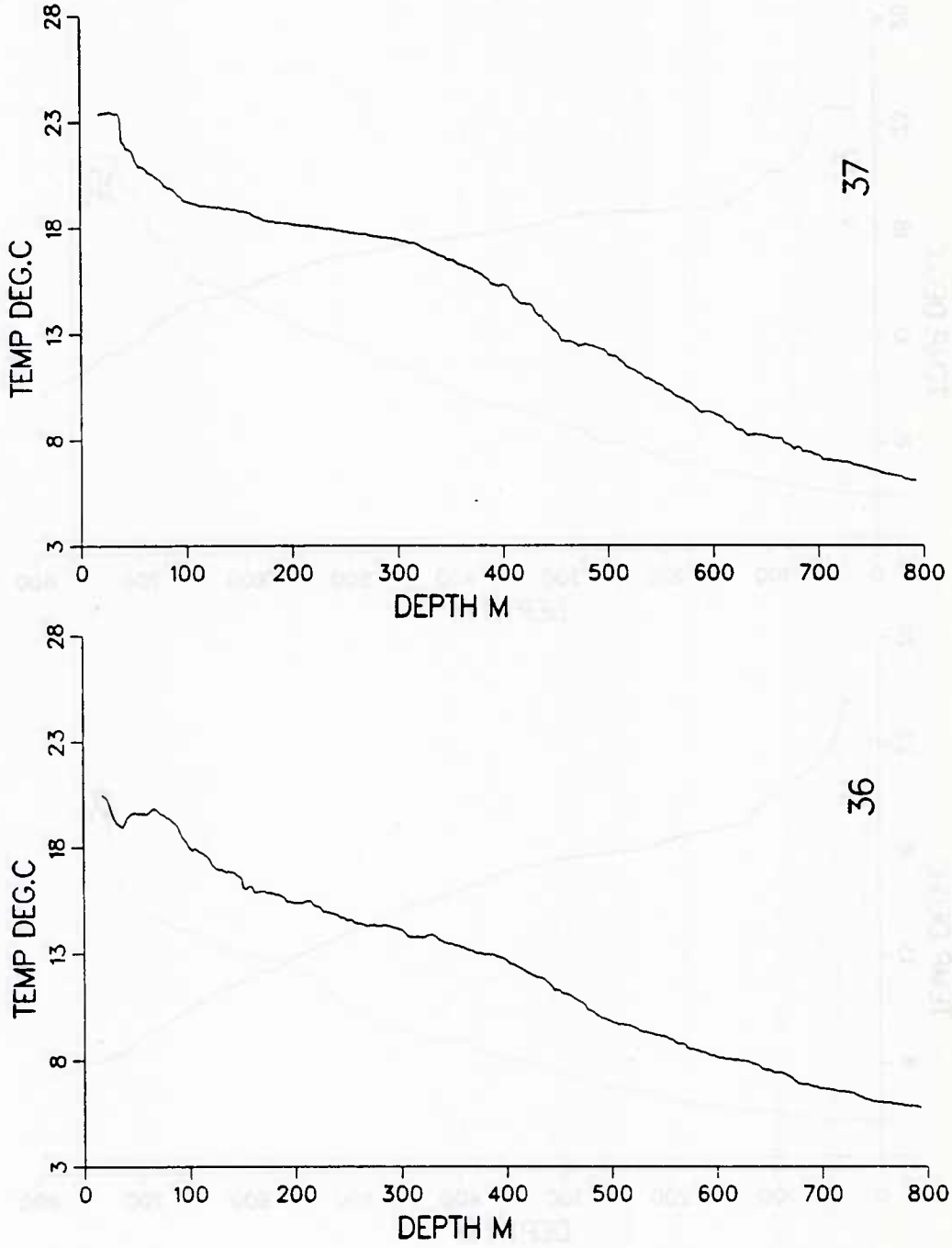

Figure 122. XBT profiles from IES recovery cruise.

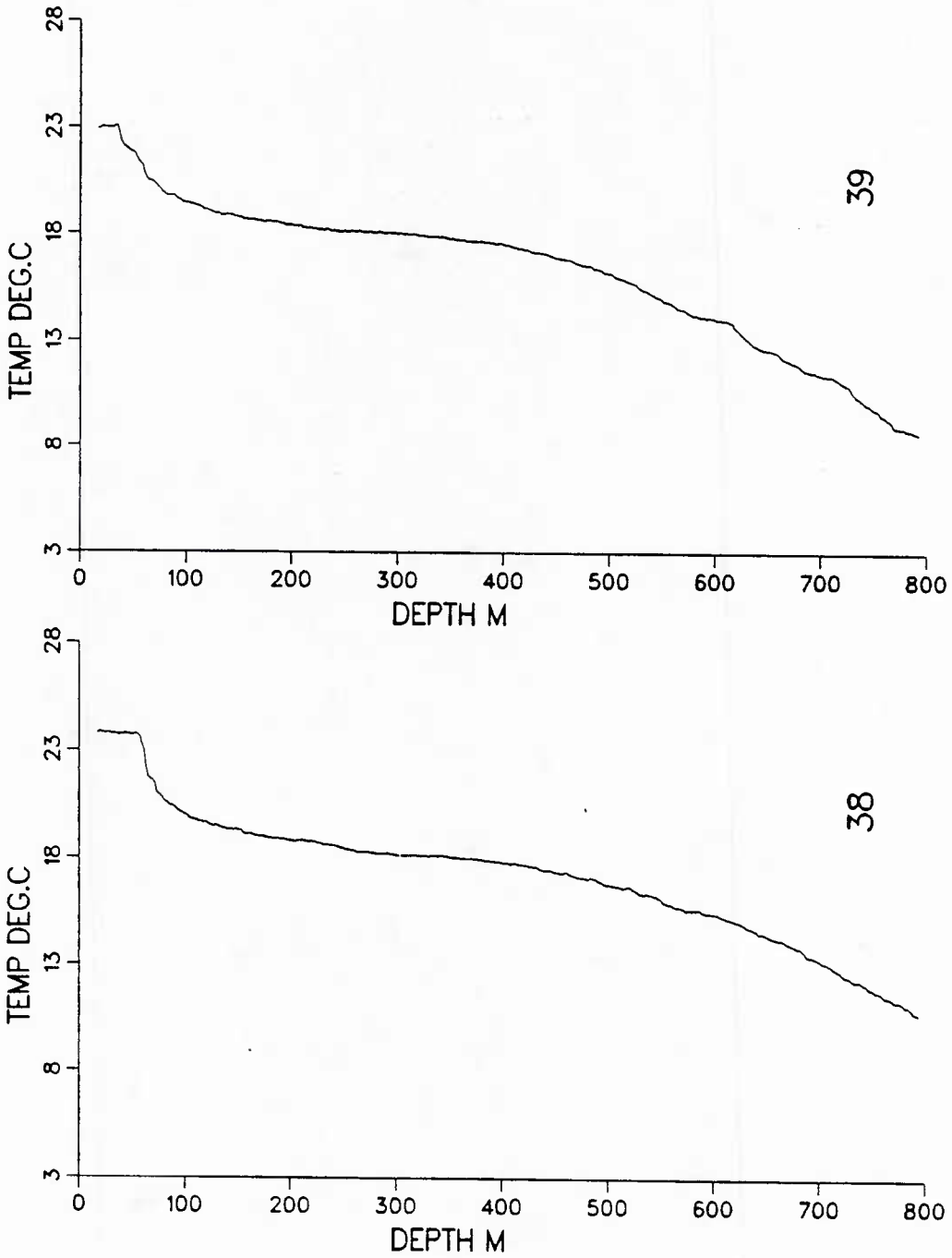

Figure 123. XBT profiles from IES recovery cruise.

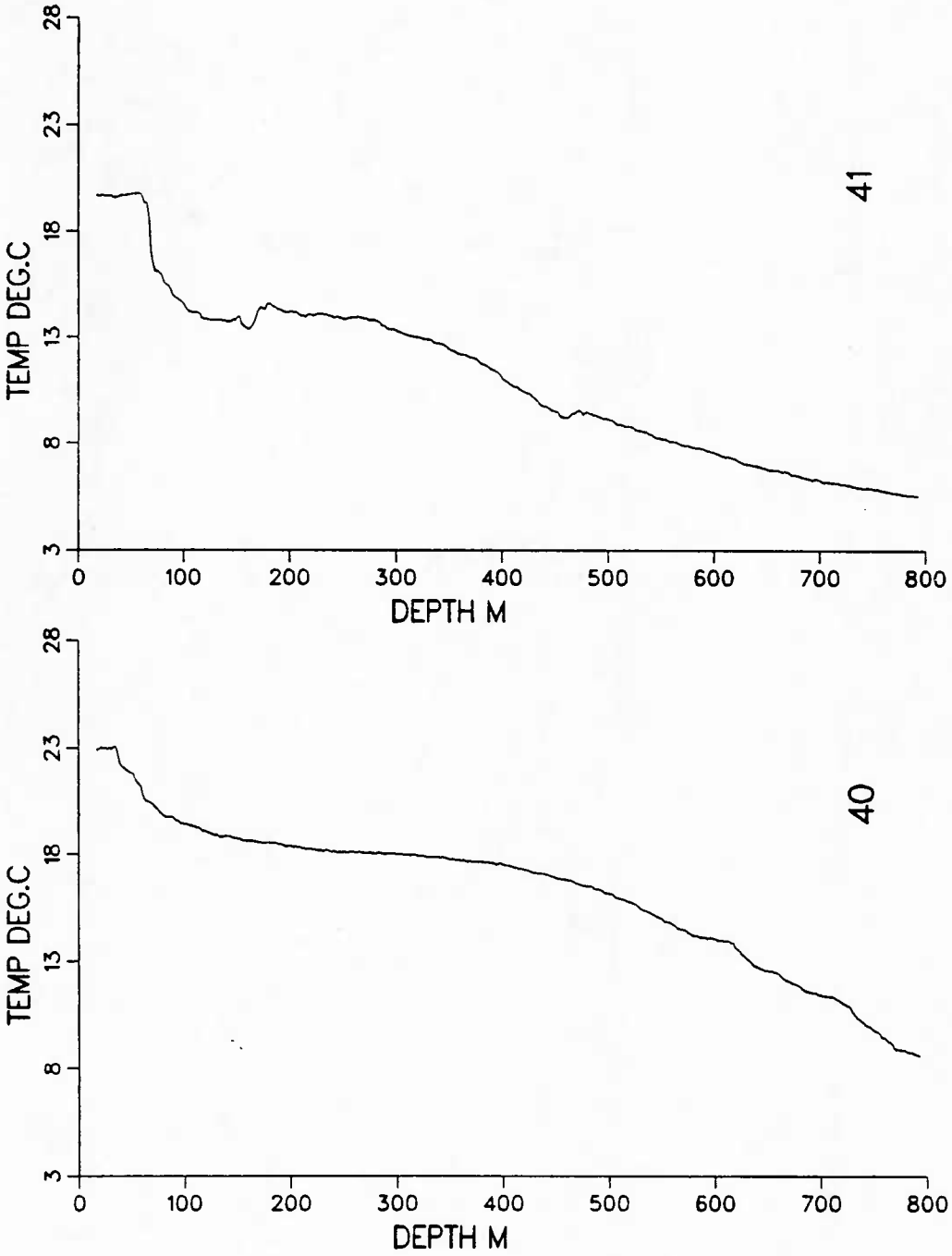

Figure 124. XBT profiles from IES recovery cruise.

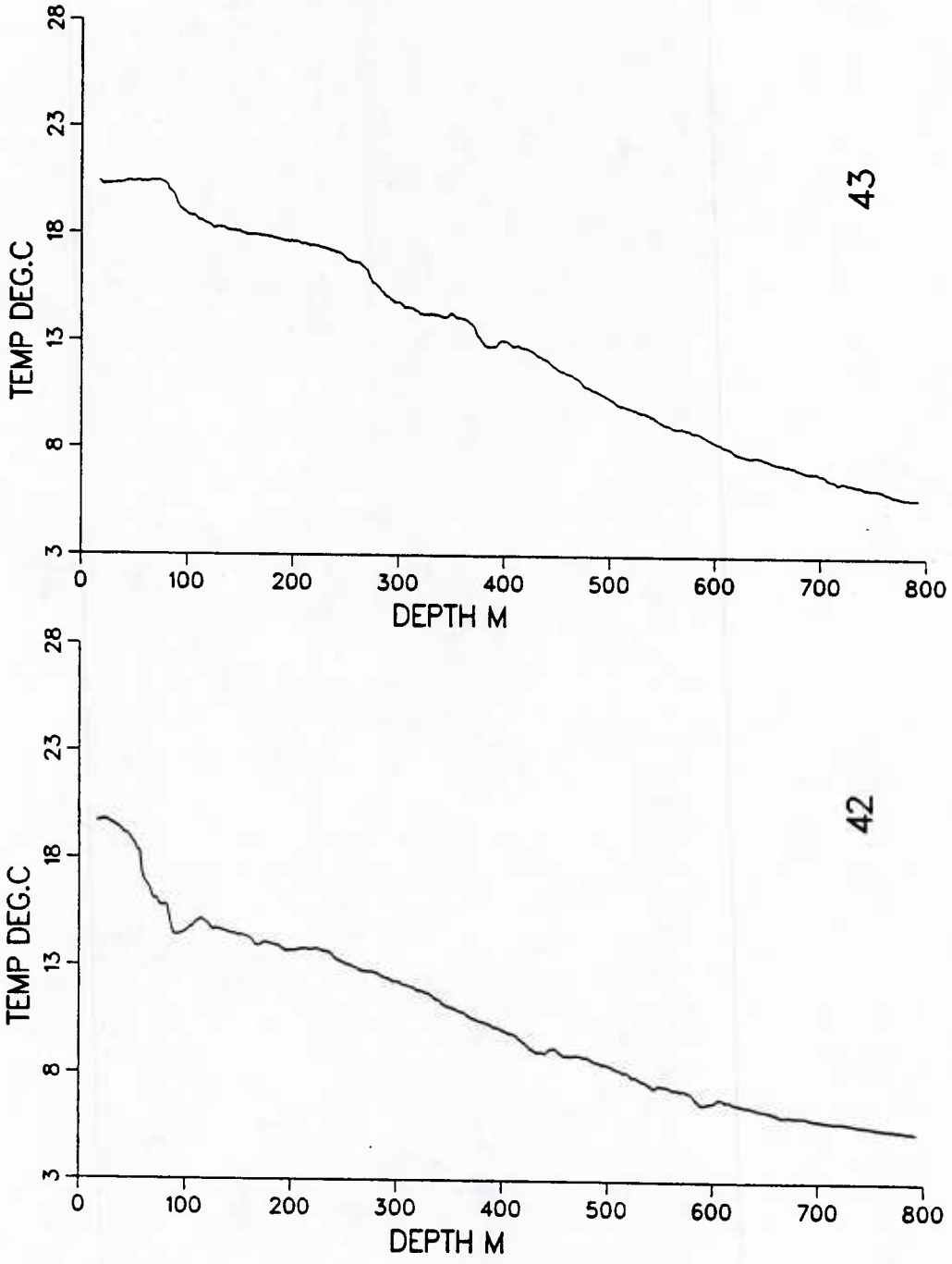

Figure 125. XBT profiles from IES recovery cruise.

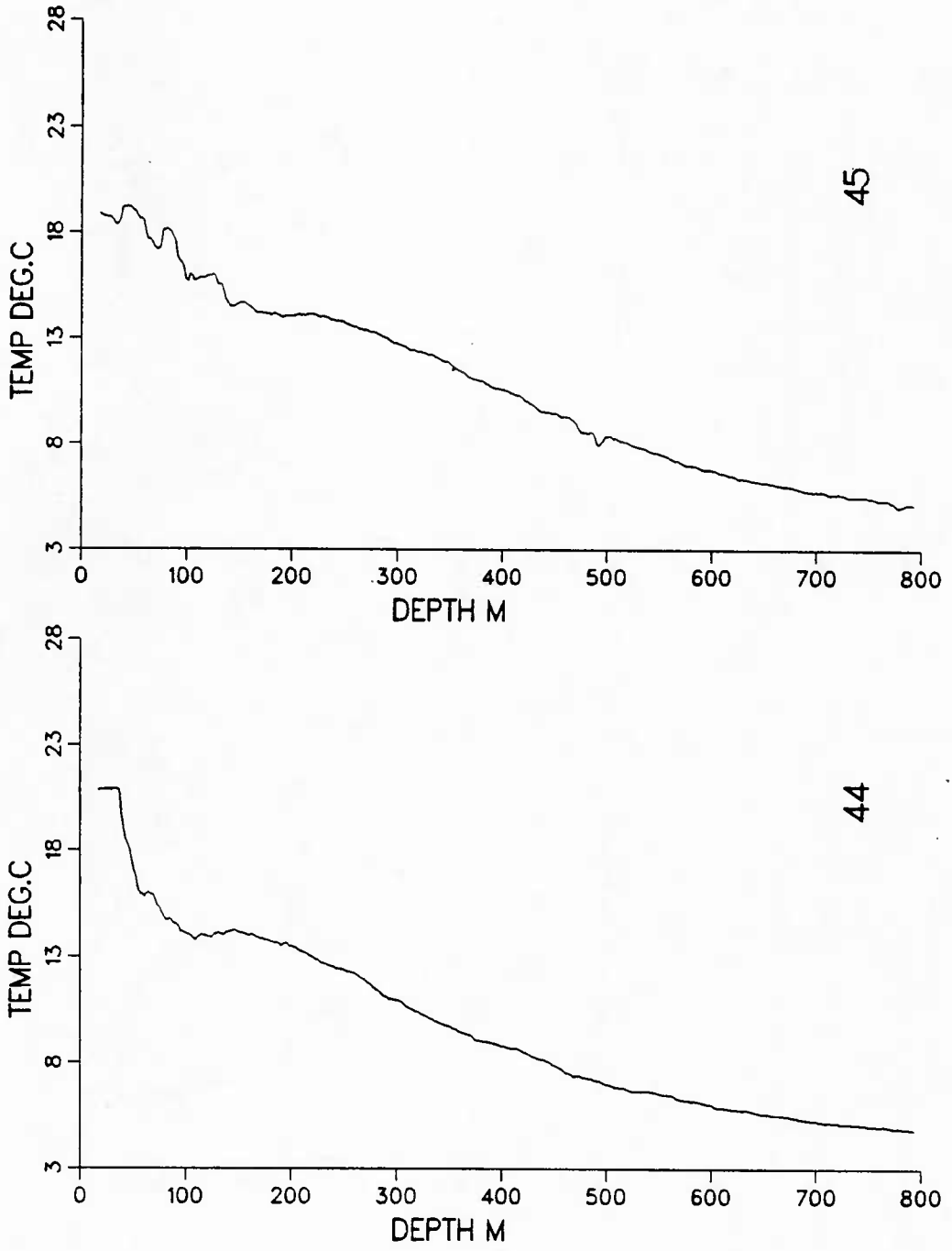

Figure 126. XBT profiles from IES recovery cruise.

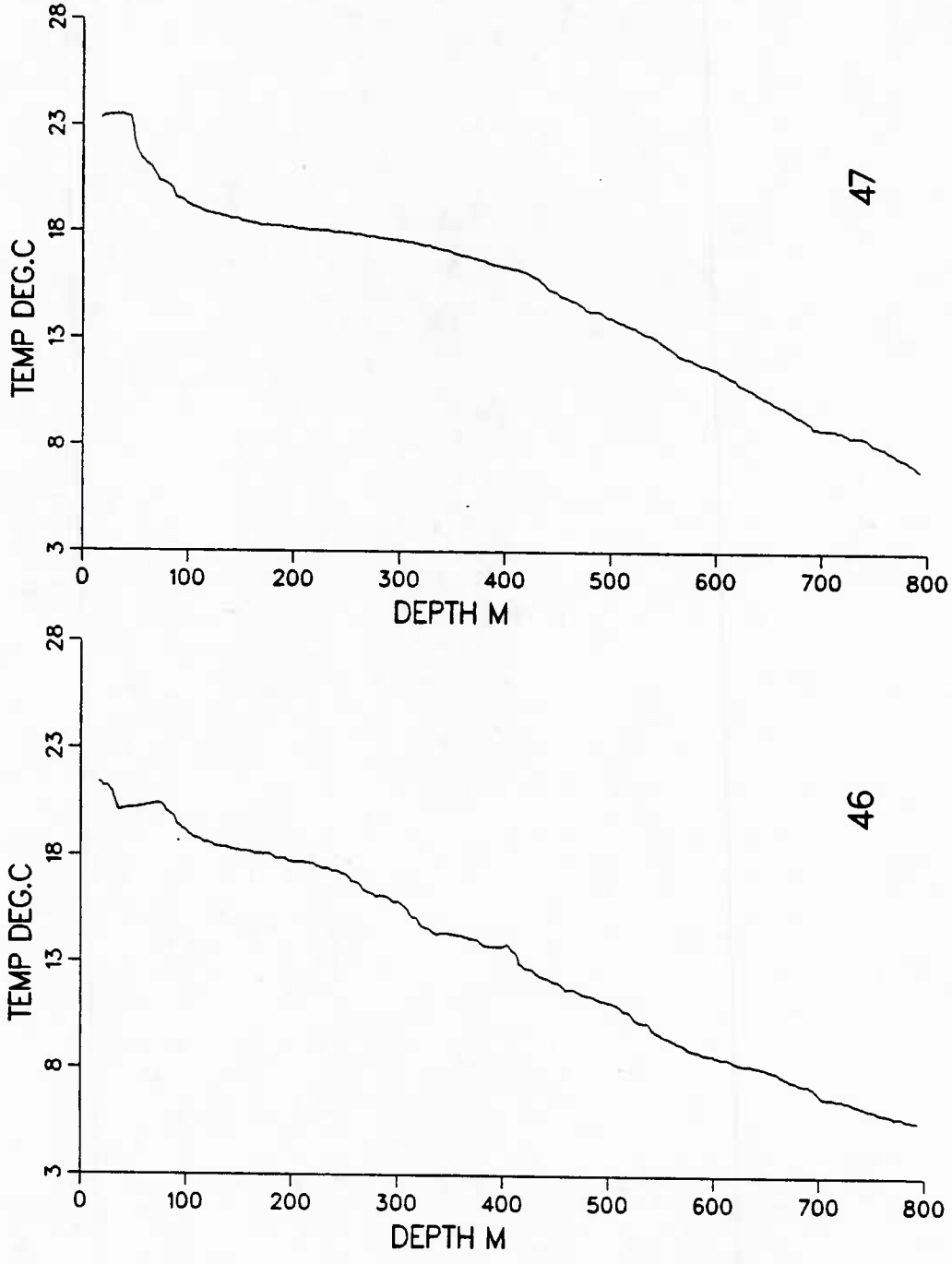

Figure 127. XBT profiles from IES recovery cruise.

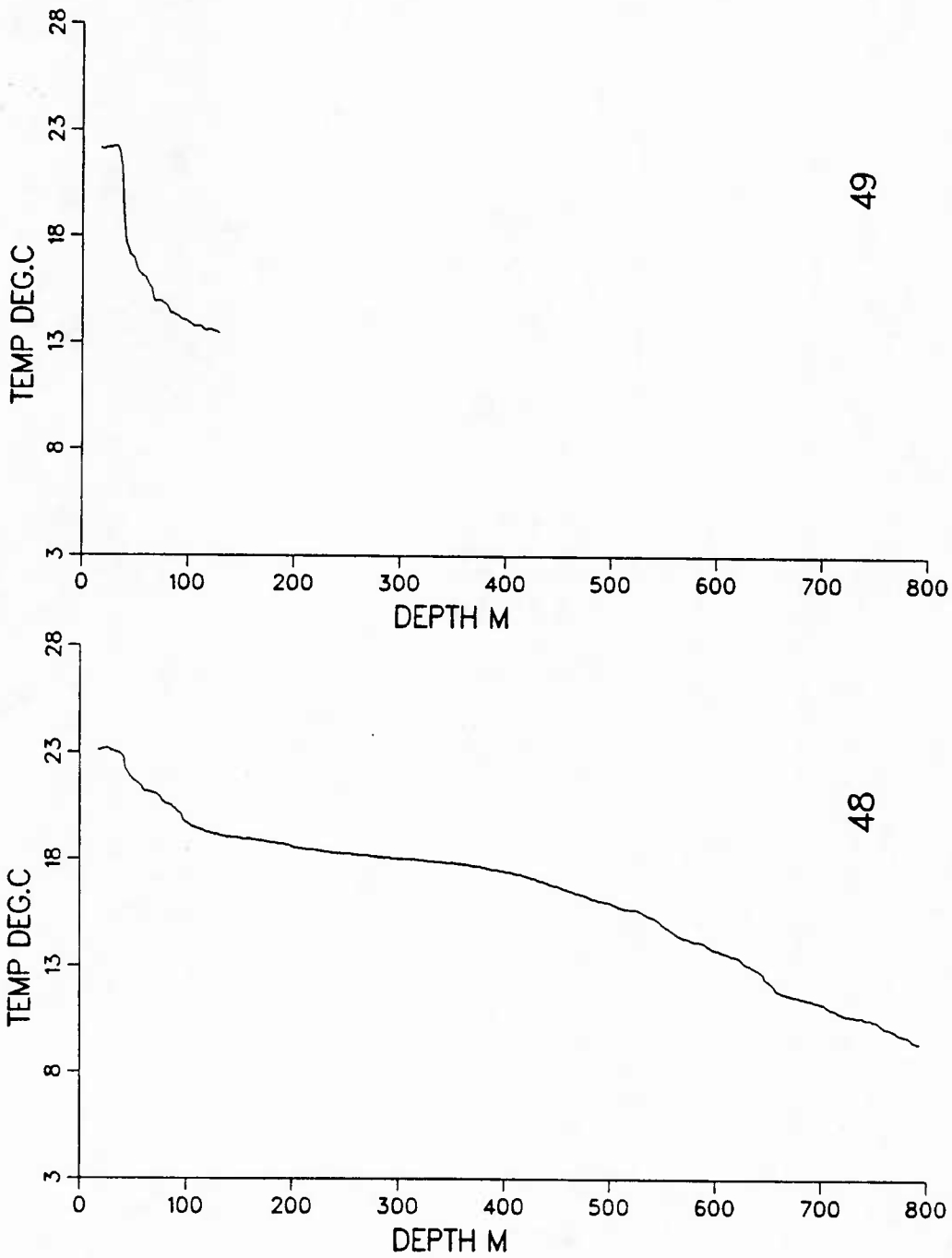

Figure 128. XBT profiles from IES recovery cruise.

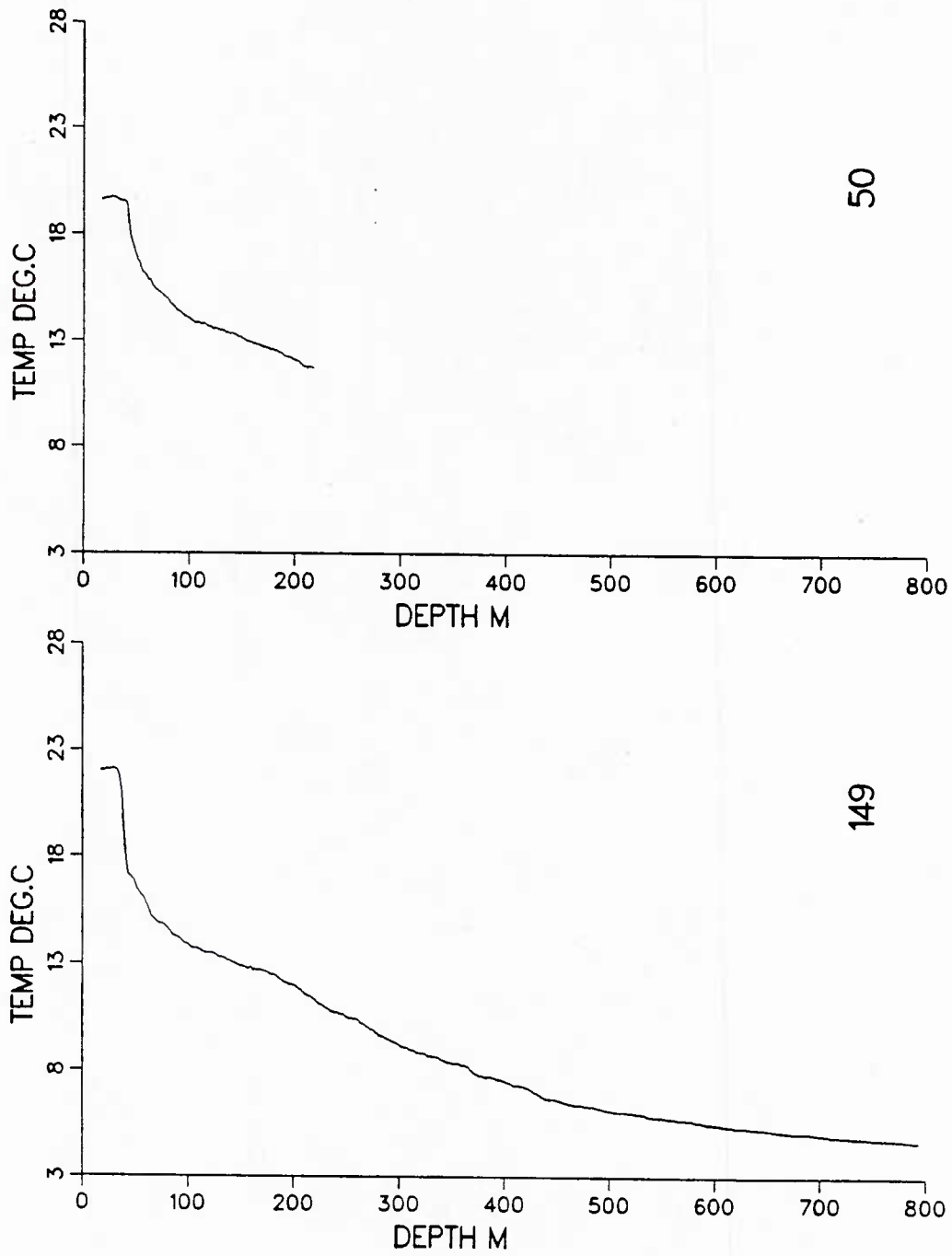

Figure 129. XBT profiles from IES recovery cruise.

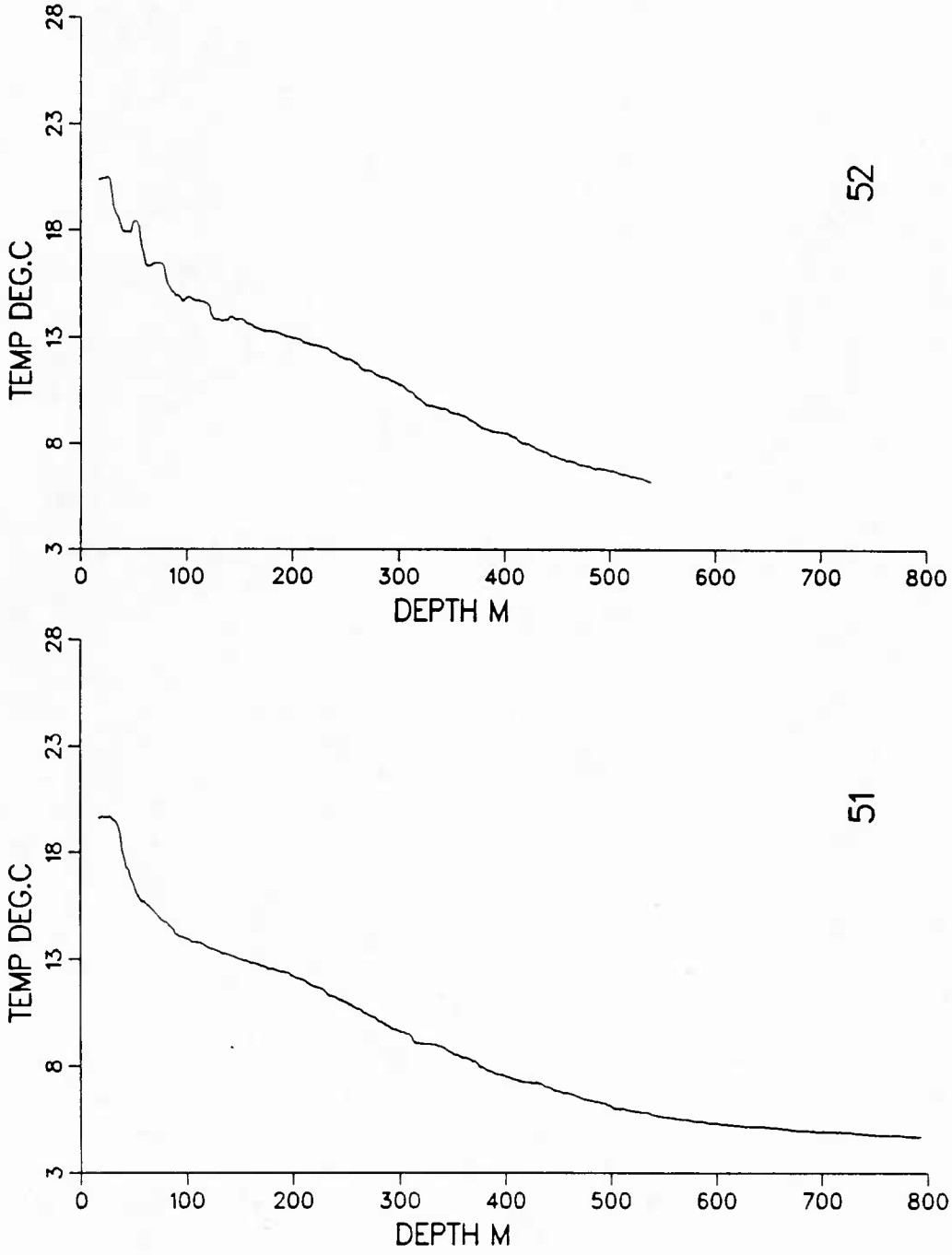

Figure 130. XBT profiles from IES recovery cruise.

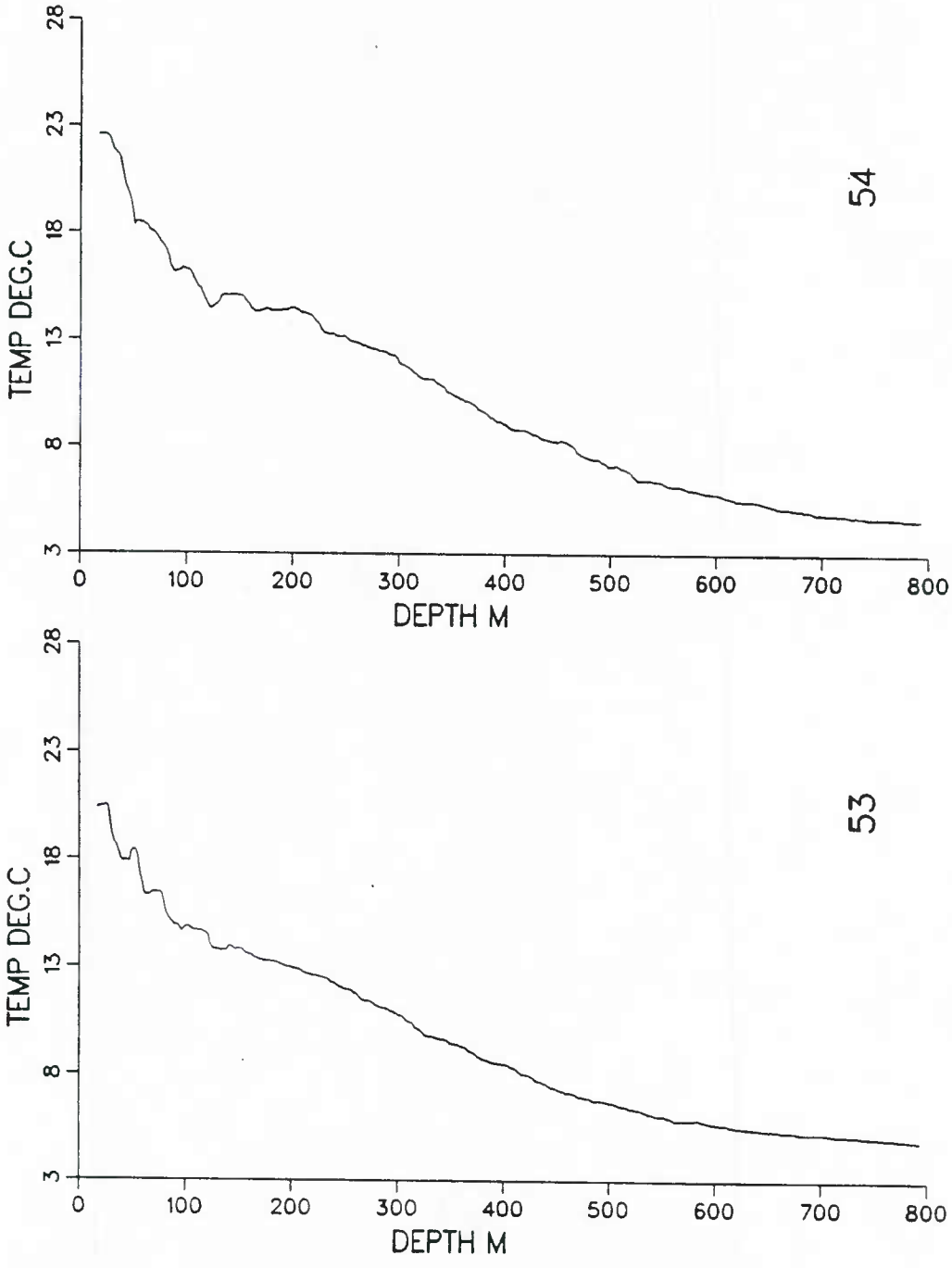

Figure 131. XBT profiles from IES recovery cruise.

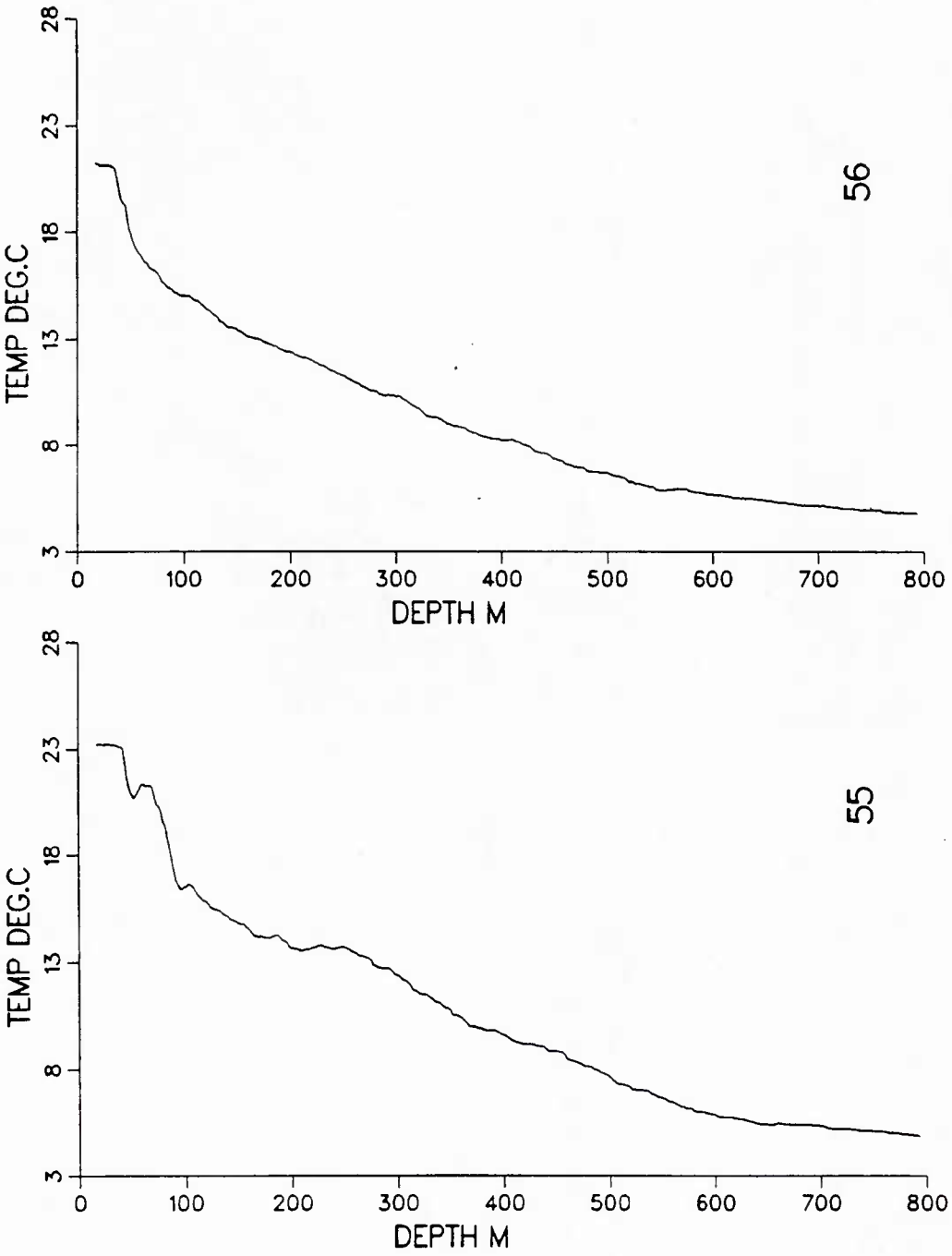

Figure 132. XBT profiles from IES recovery cruise.

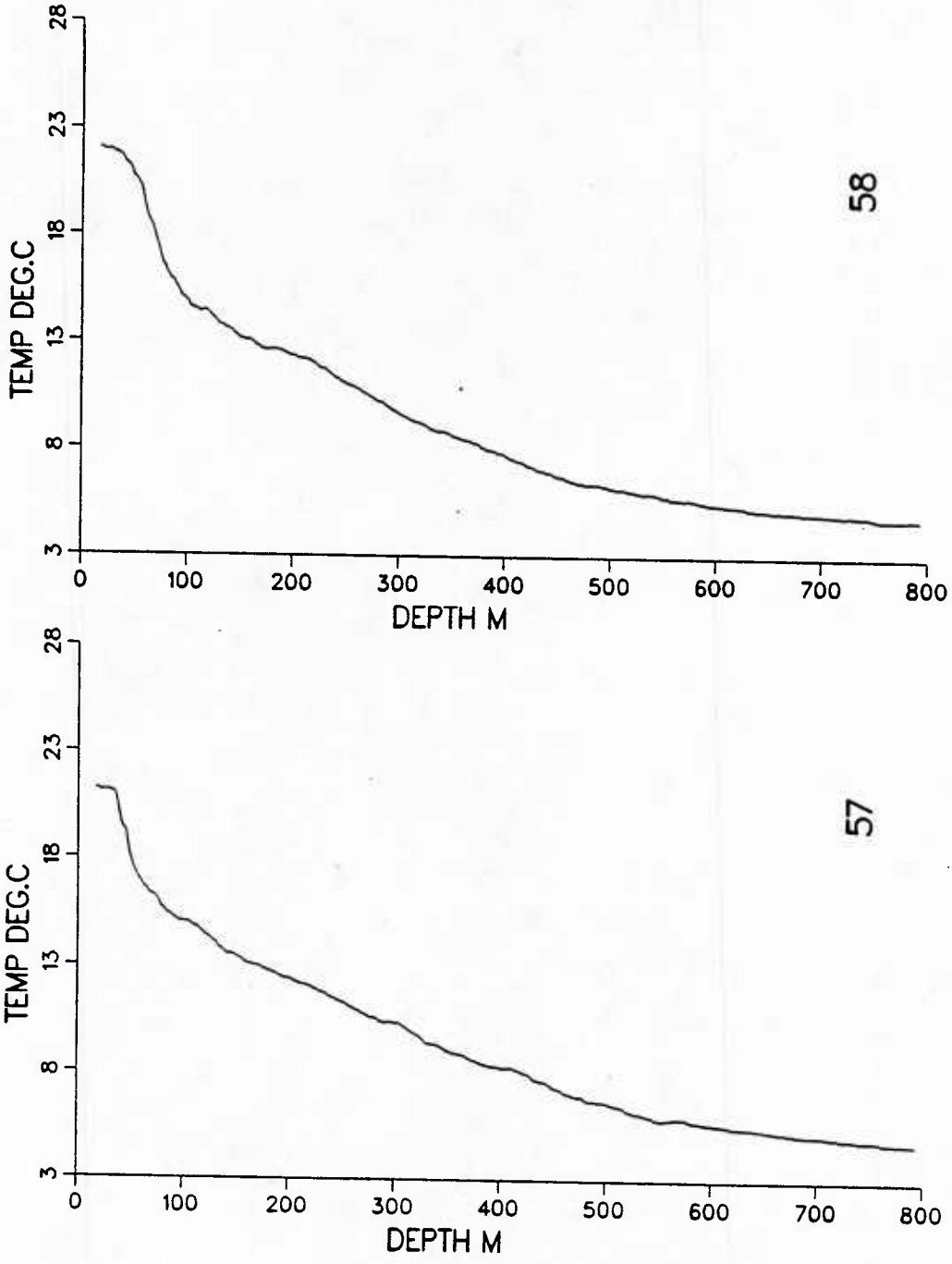

Figure 133. XBT profiles from IES recovery cruise.

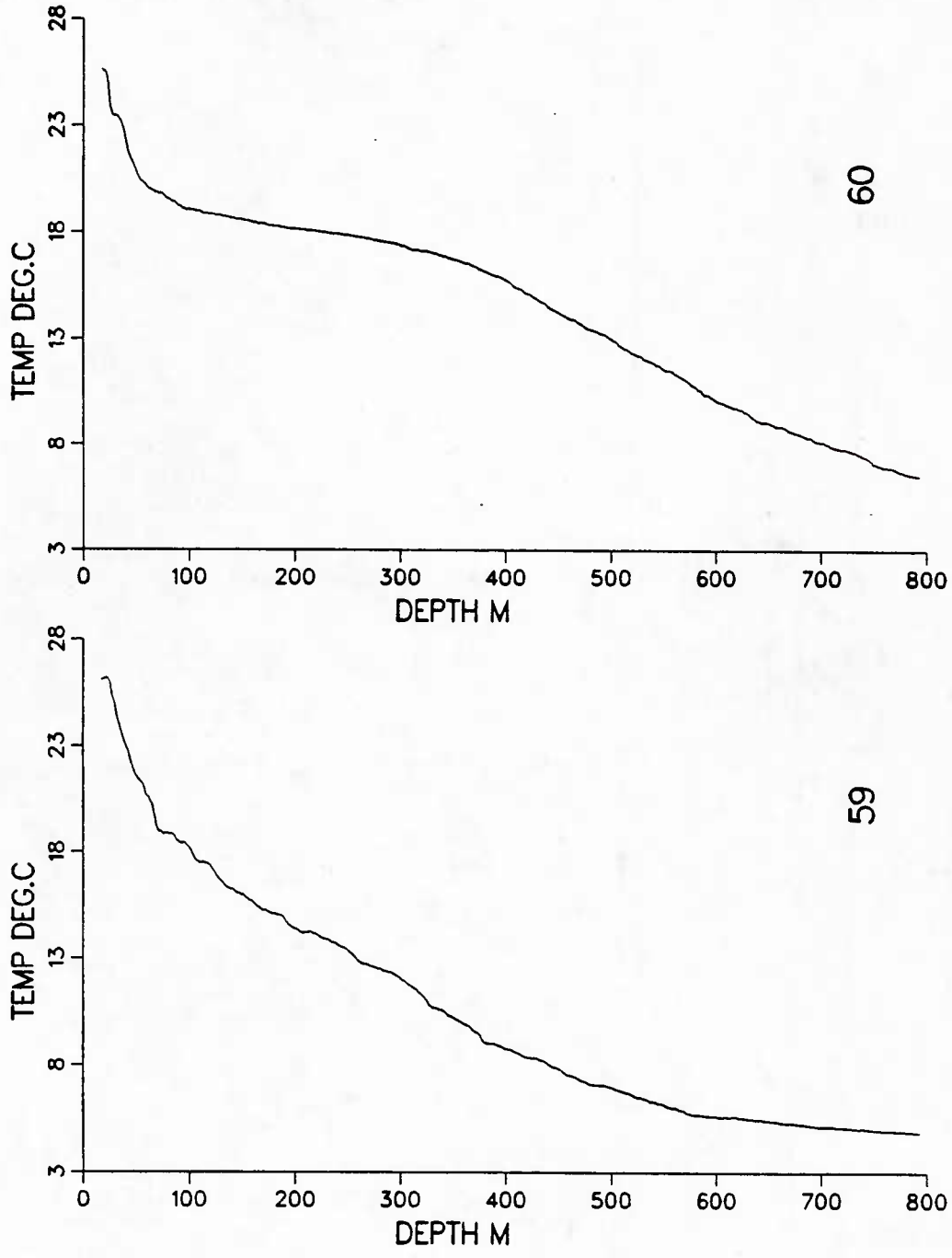

Figure 134. XBT profiles from IES recovery cruise.

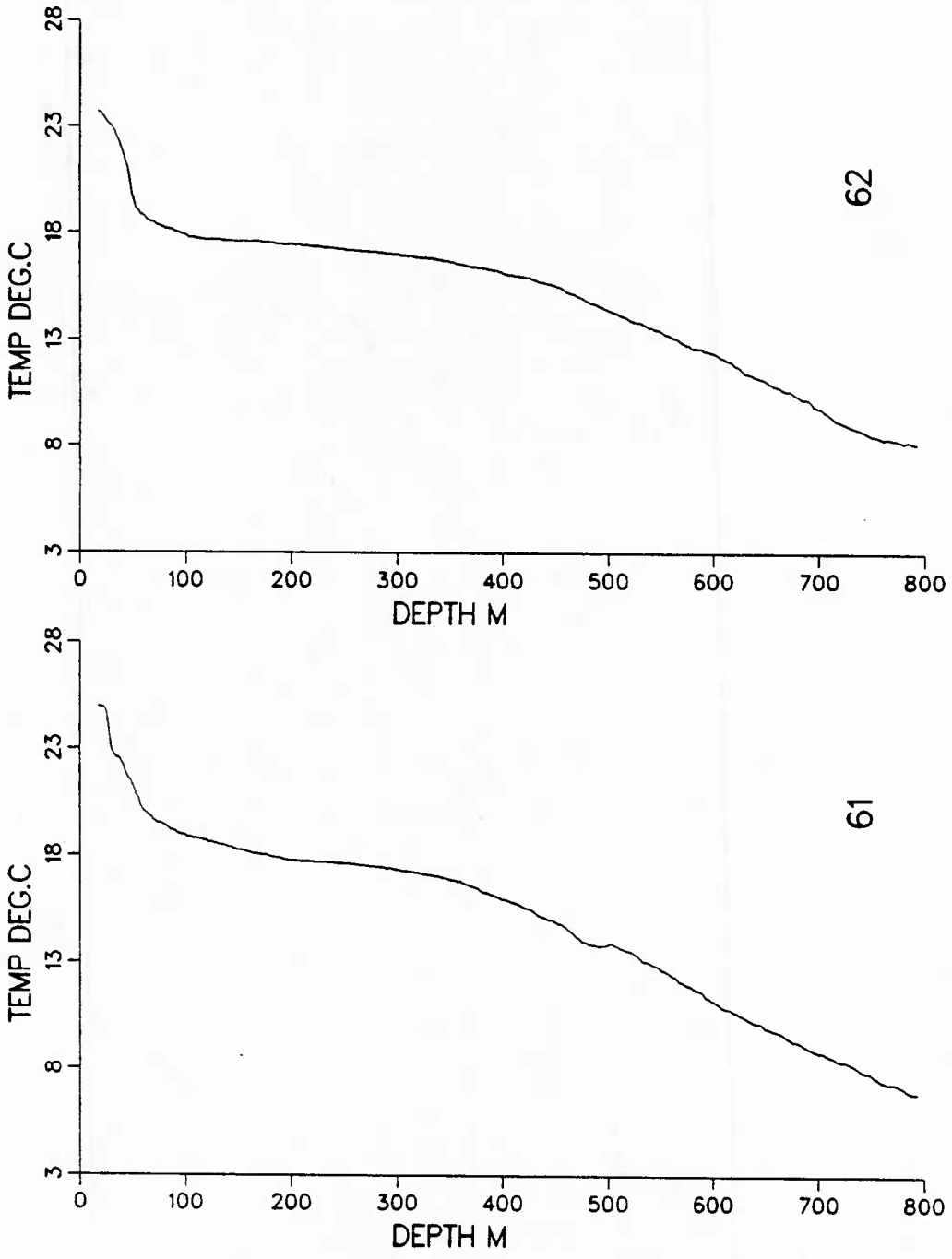

Figure 135. XBT profiles from IES recovery cruise.

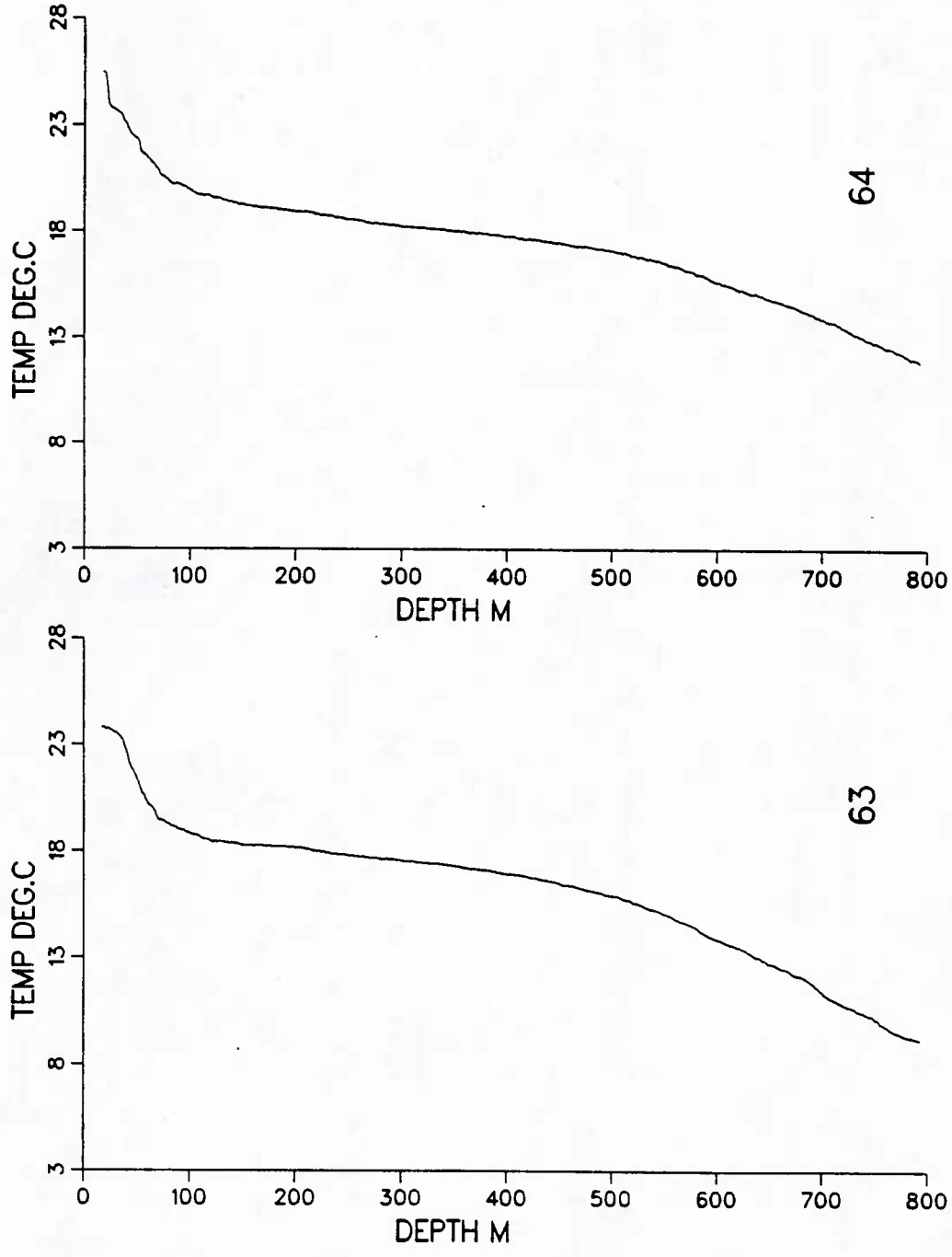

Figure 136. XBT profiles from IES recovery cruise.

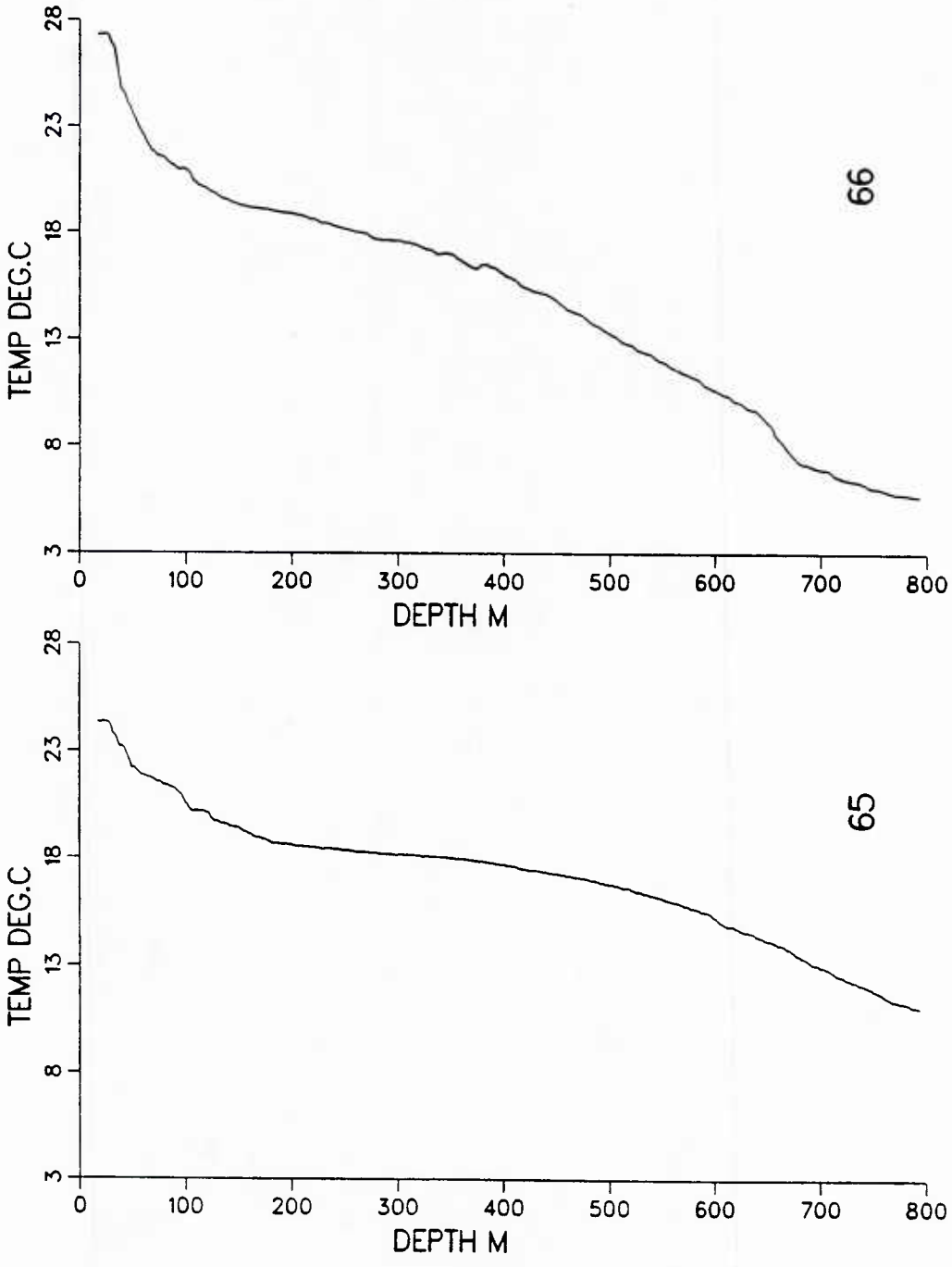

Figure 137. XBT profiles from IES recovery cruise.

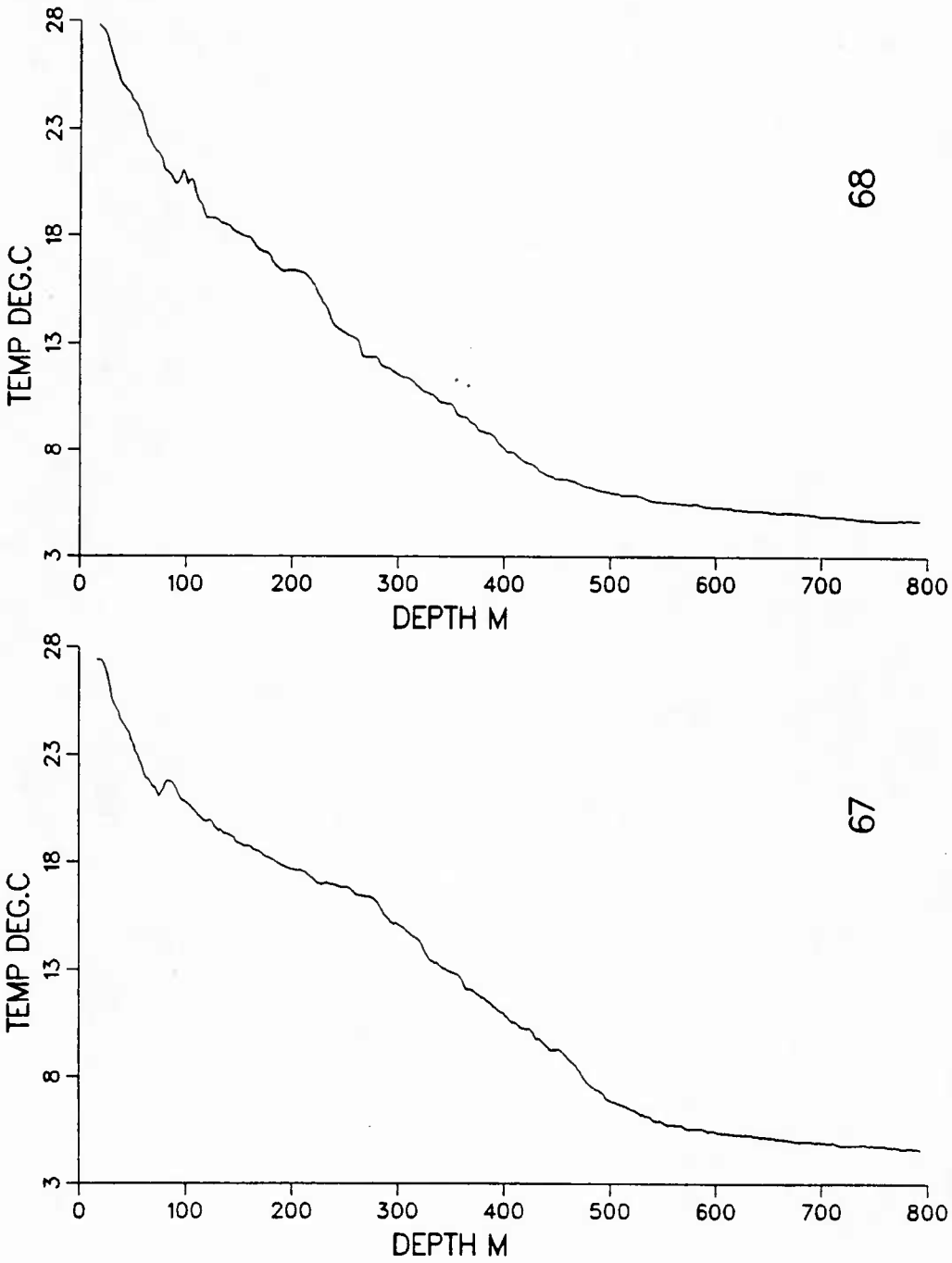

Figure 138. XBT profiles from IES recovery cruise.

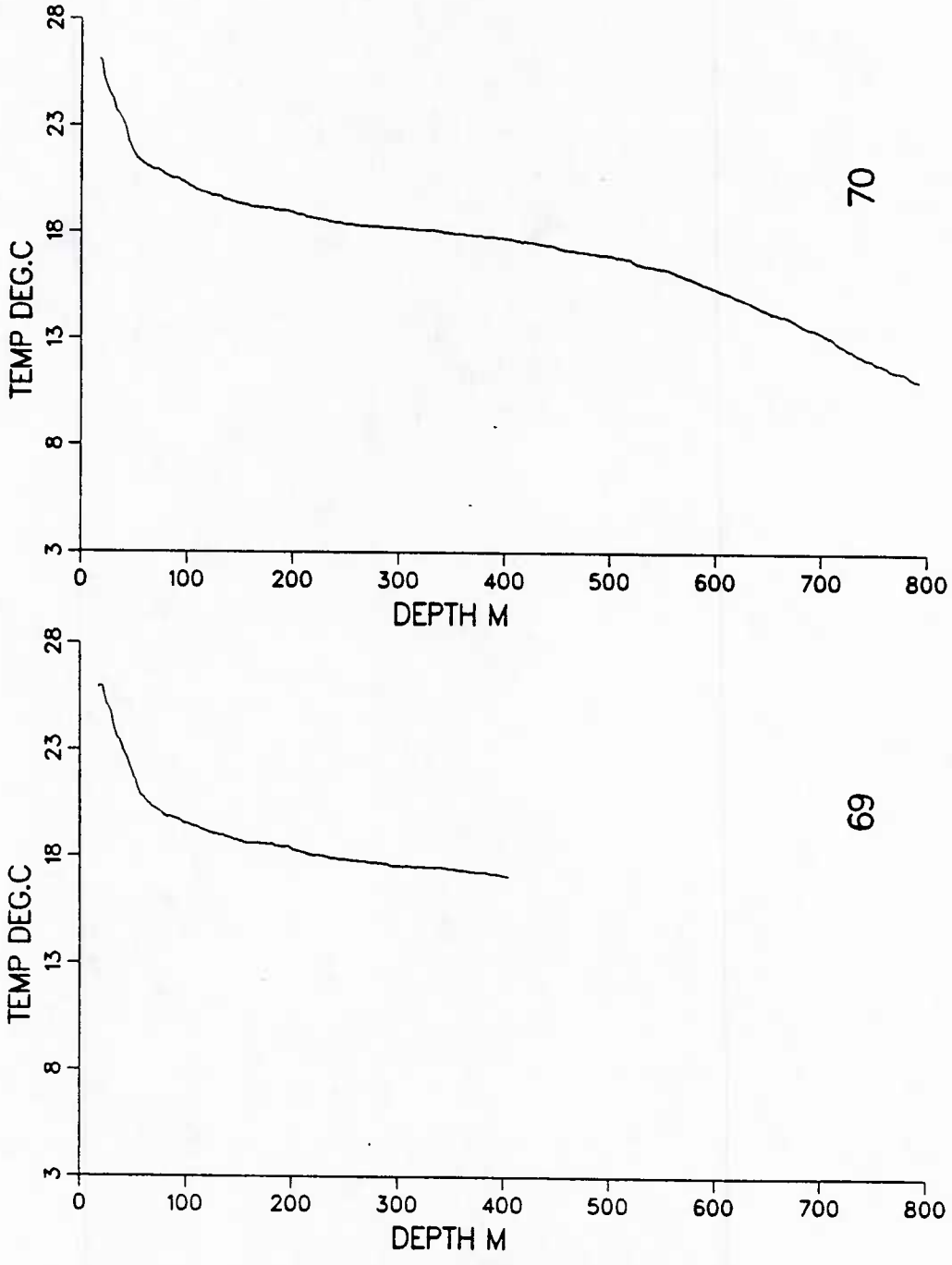

Figure 139. XBT profiles from IES recovery cruise.

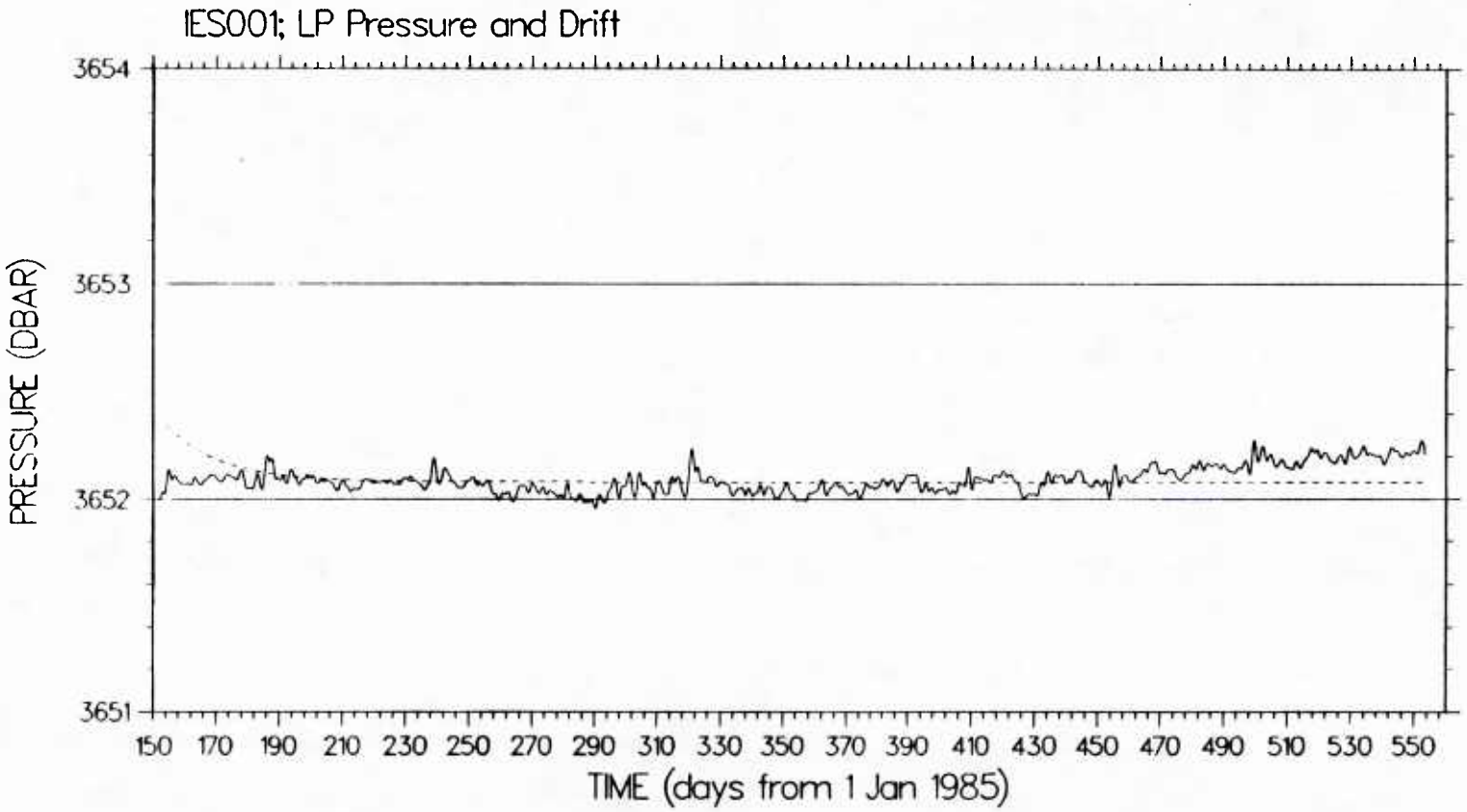

Figure 140. Pressure series (solid line) with periods shorter than 40 hours removed and exponential trend (dashed line) that was subtracted from the pressure series.

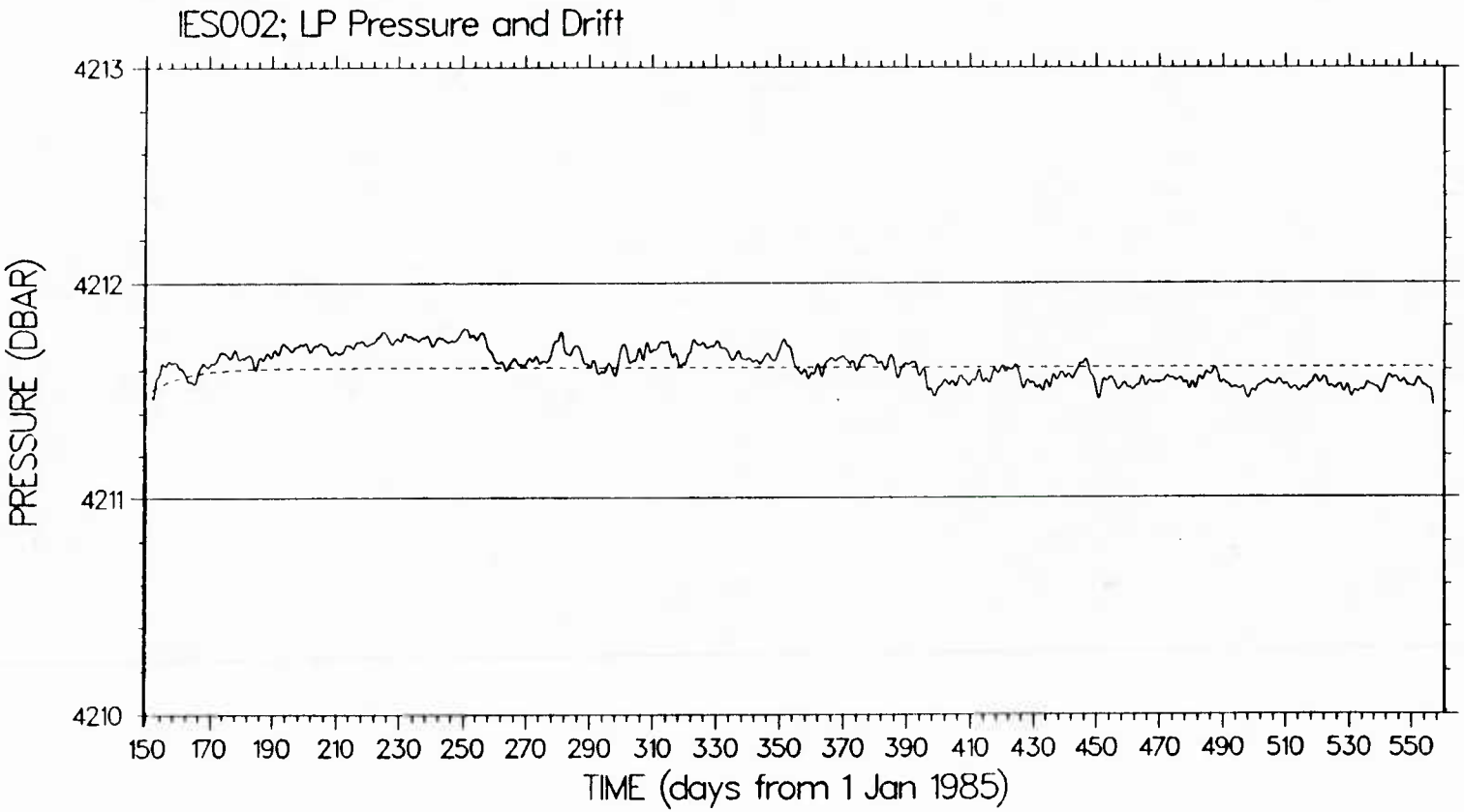

Figure 141. Pressure series (solid line) with periods shorter than 40 hours removed and exponential trend (dashed line) that was subtracted from the pressure series.

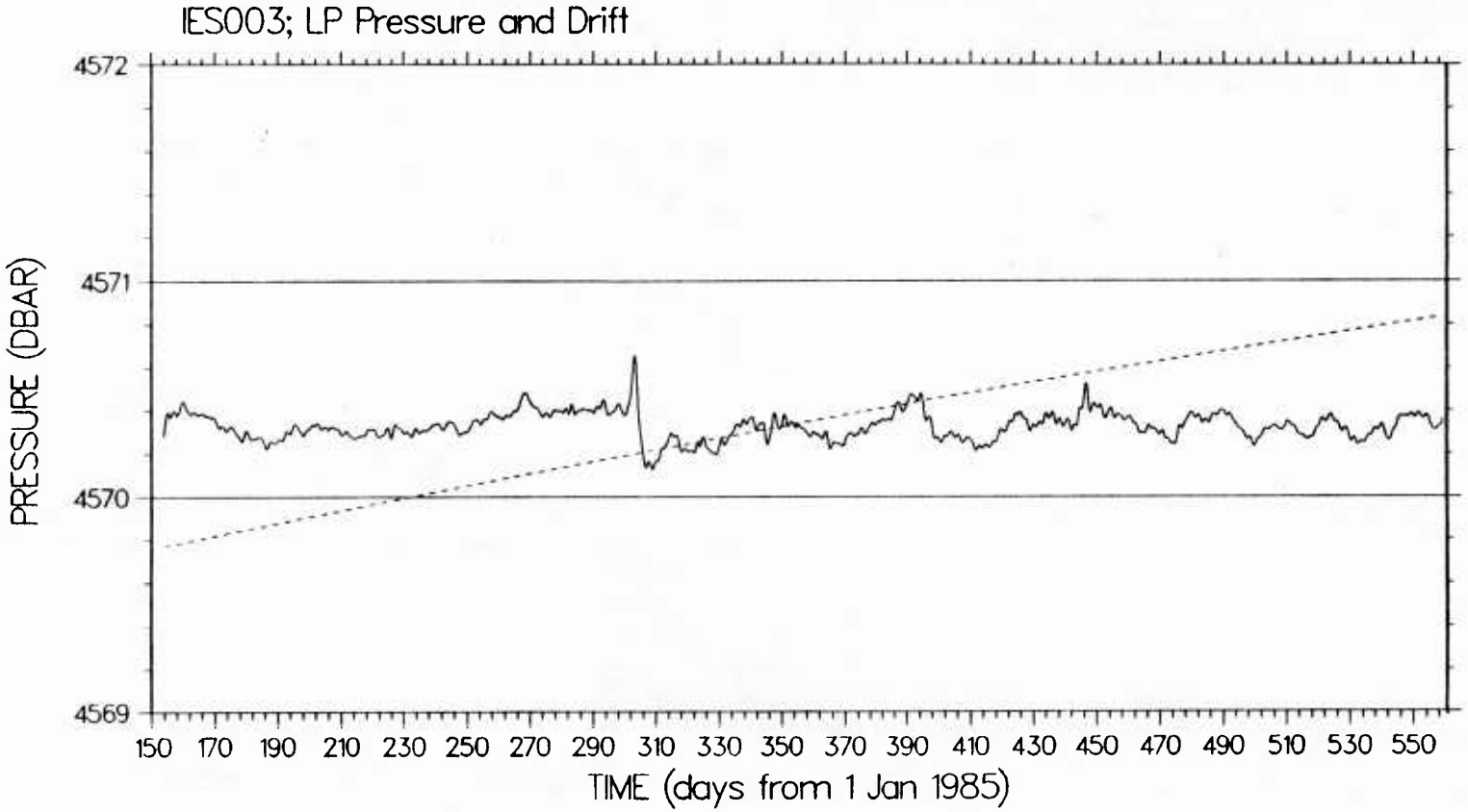

Figure 142. Pressure series (solid line) with periods shorter than 40 hours removed and exponential trend (dashed line) that was subtracted from the pressure series.

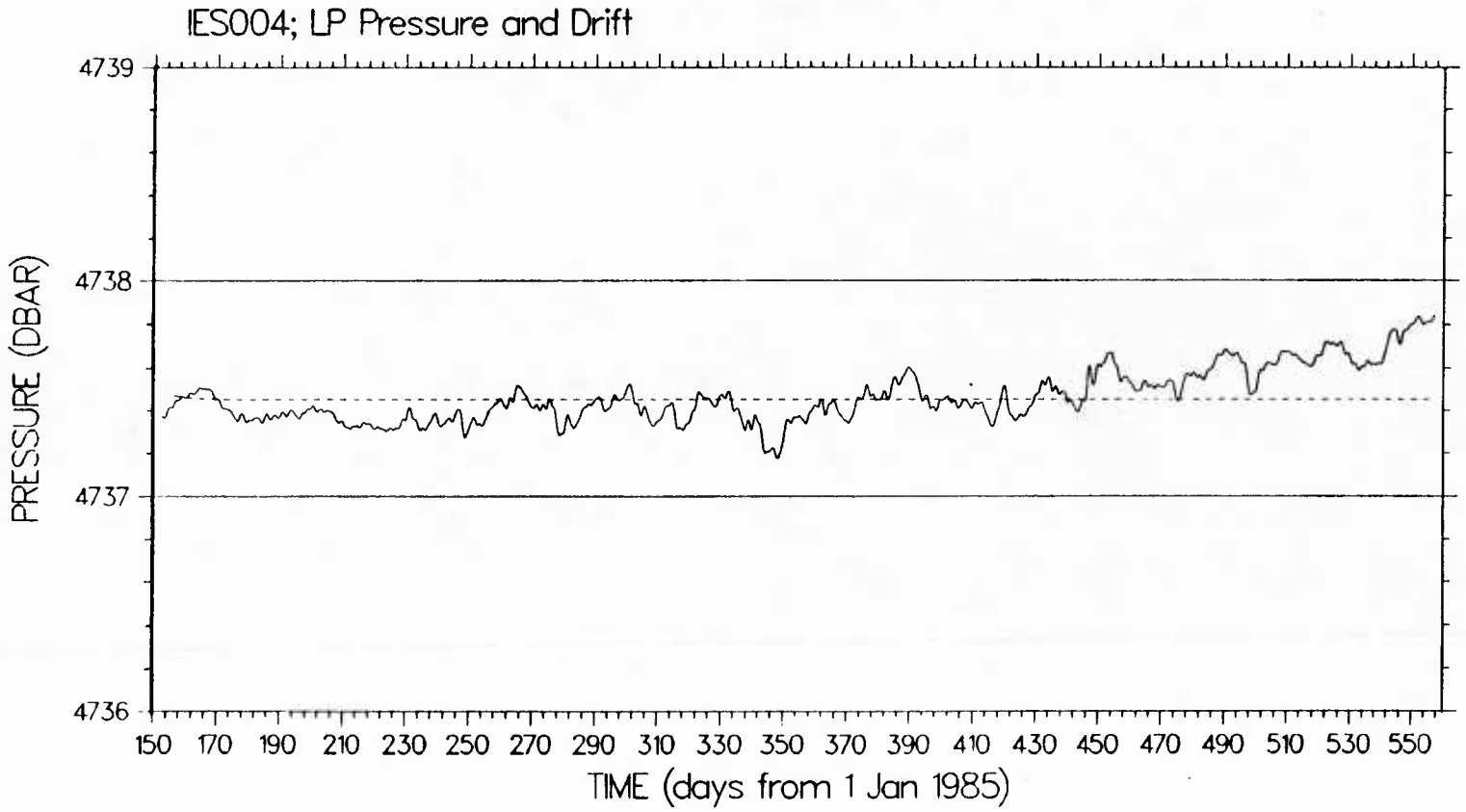

Figure 143. Pressure series (solid line) with periods shorter than 40 hours removed and exponential trend (dashed line) that was subtracted from the pressure series.

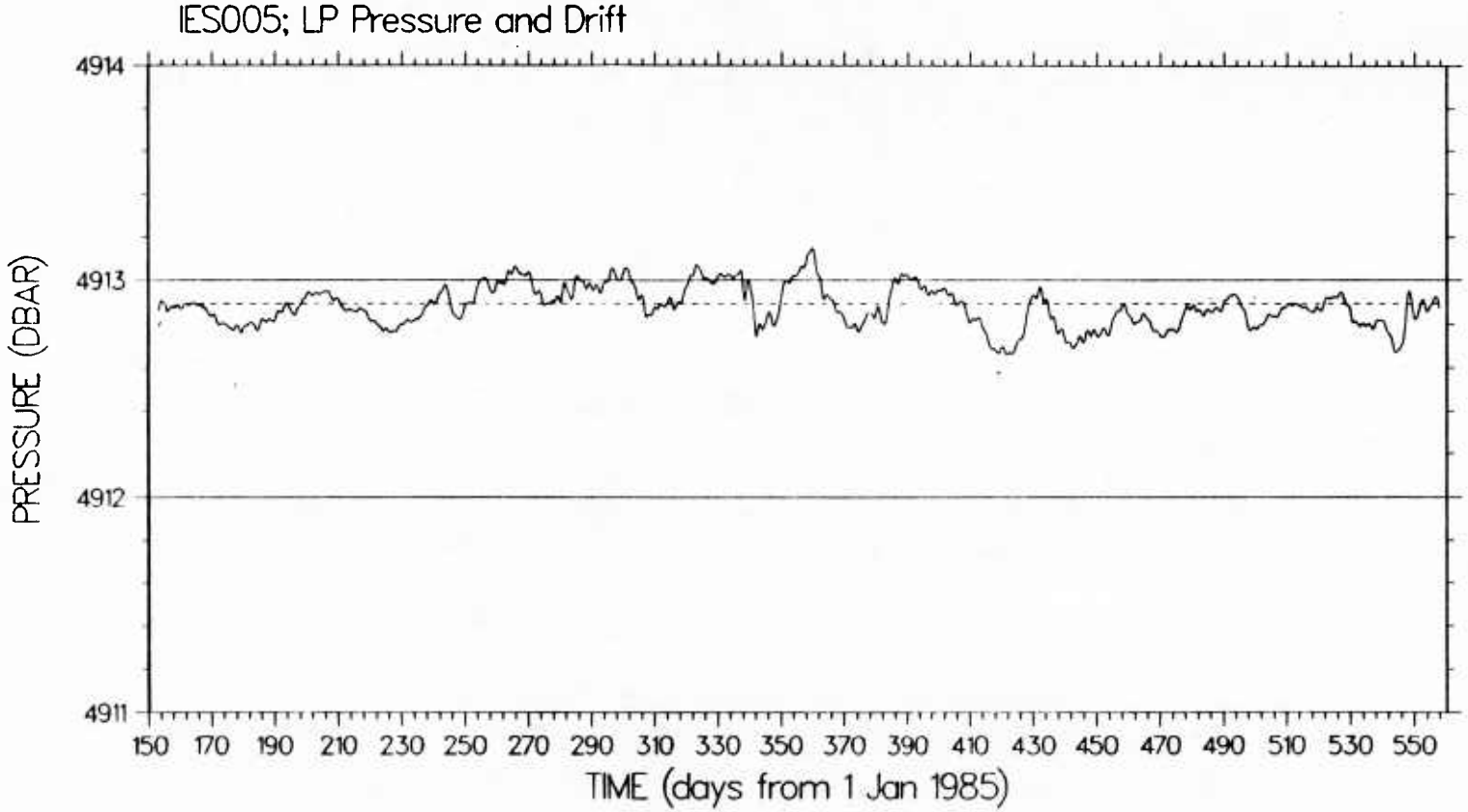

Figure 144. Pressure series (solid line) with periods shorter than 40 hours removed and exponential trend (dashed line) that was subtracted from the pressure series.

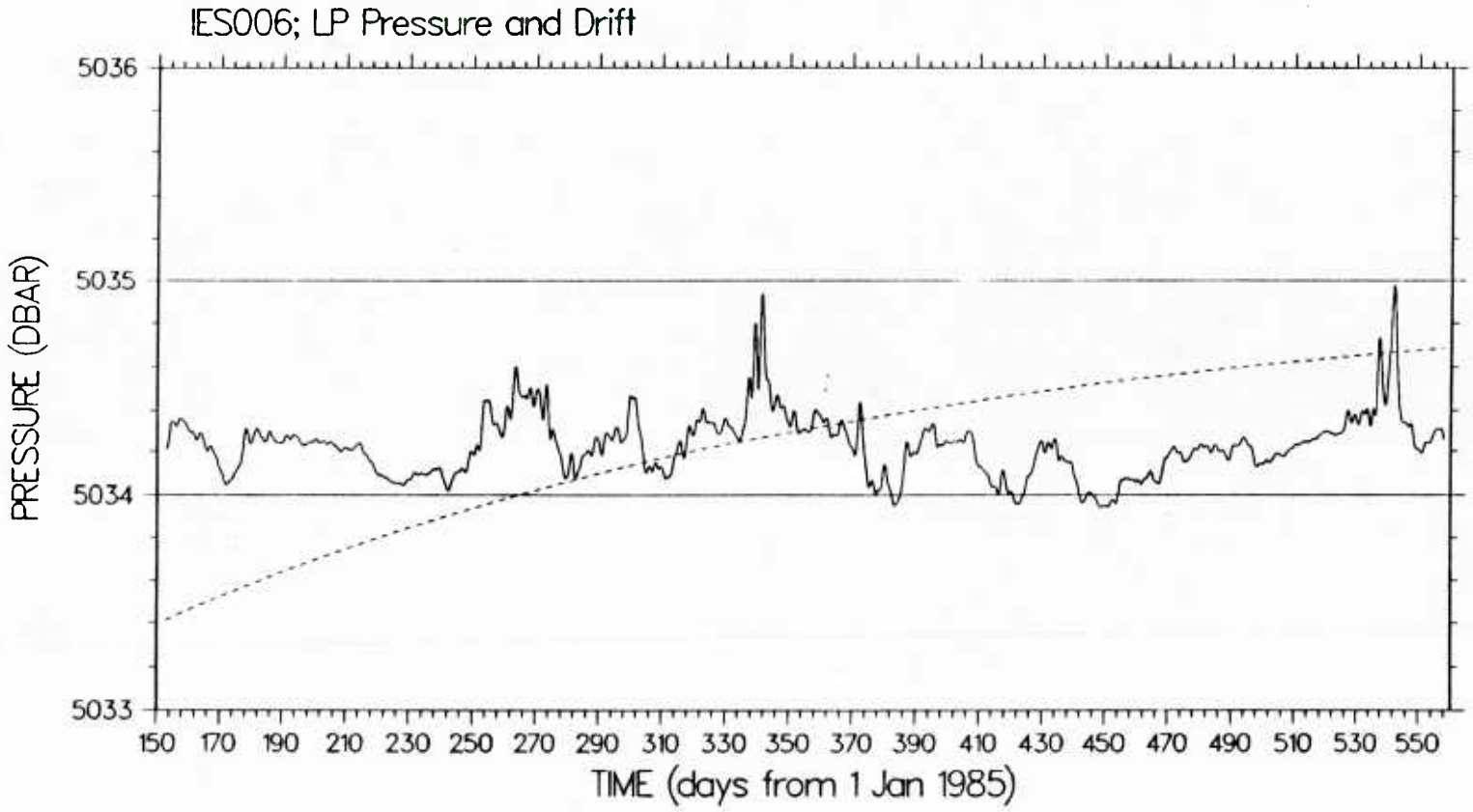

Figure 145. Pressure series (solid line) with periods shorter than 40 hours removed and exponential trend (dashed line) that was subtracted from the pressure series.

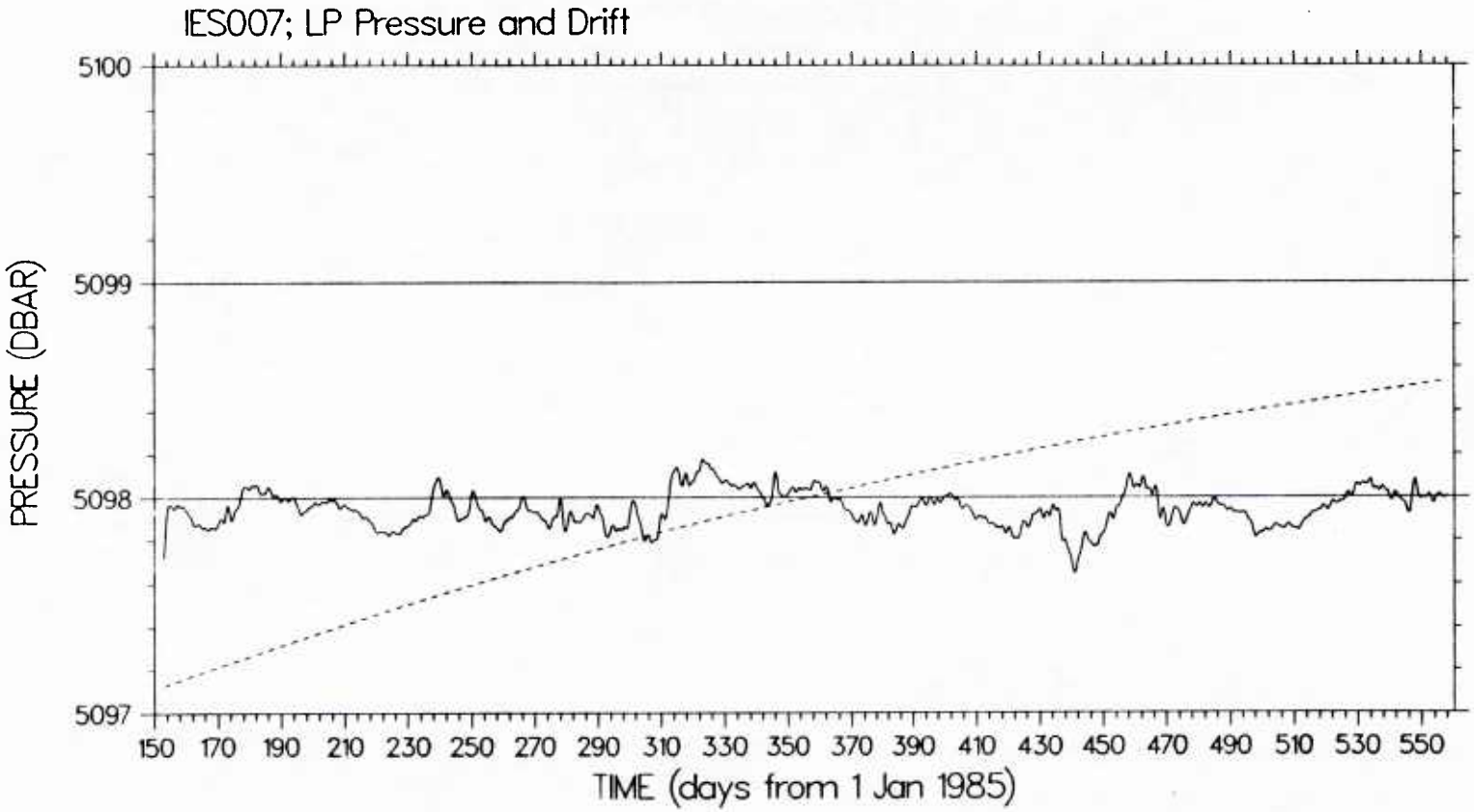

Figure 146. Pressure series (solid line) with periods shorter than 40 hours removed and exponential trend (dashed line) that was subtracted from the pressure series.

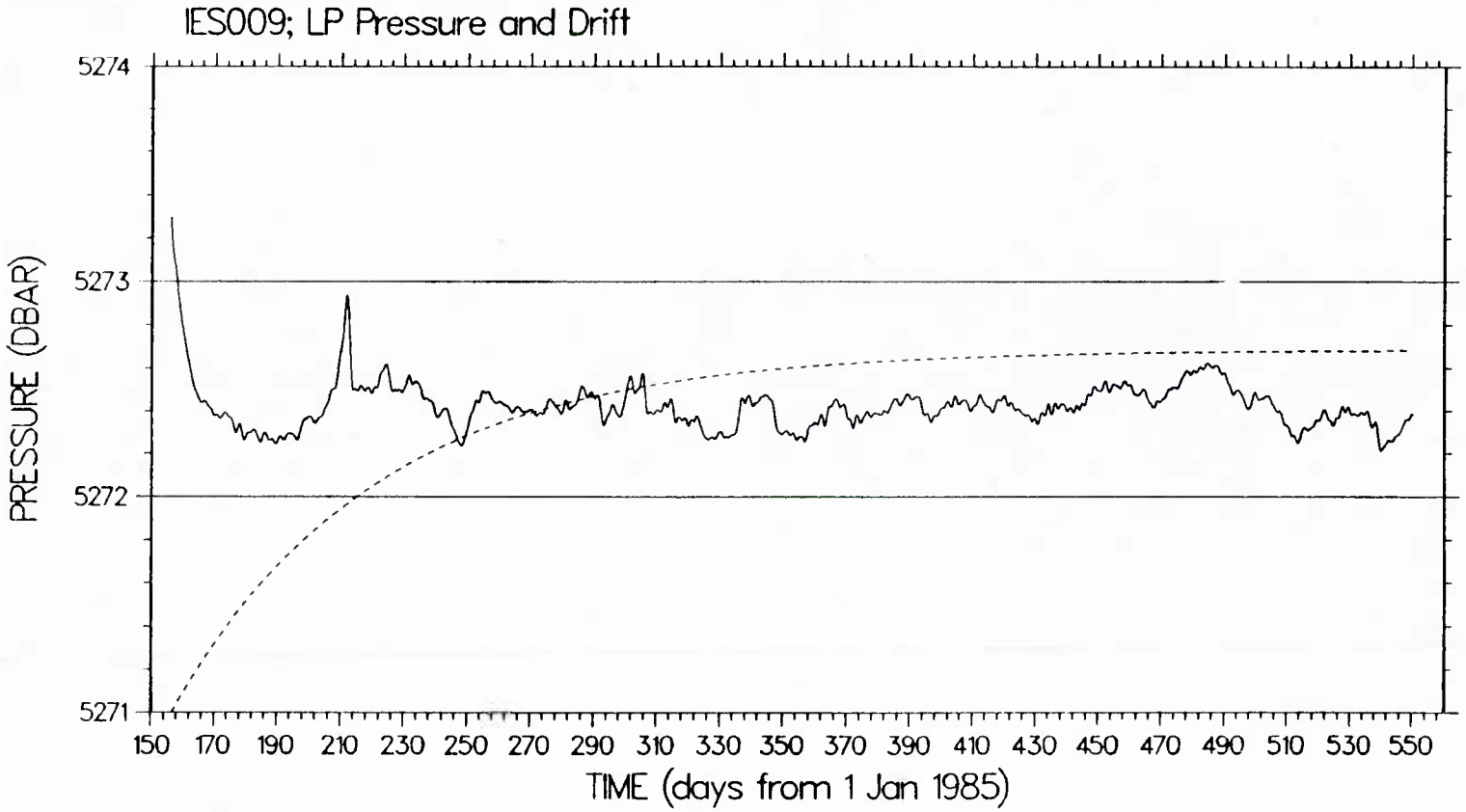

Figure 147. Pressure series (solid line) with periods shorter than 40 hours removed and exponential trend (dashed line) that was subtracted from the pressure series.

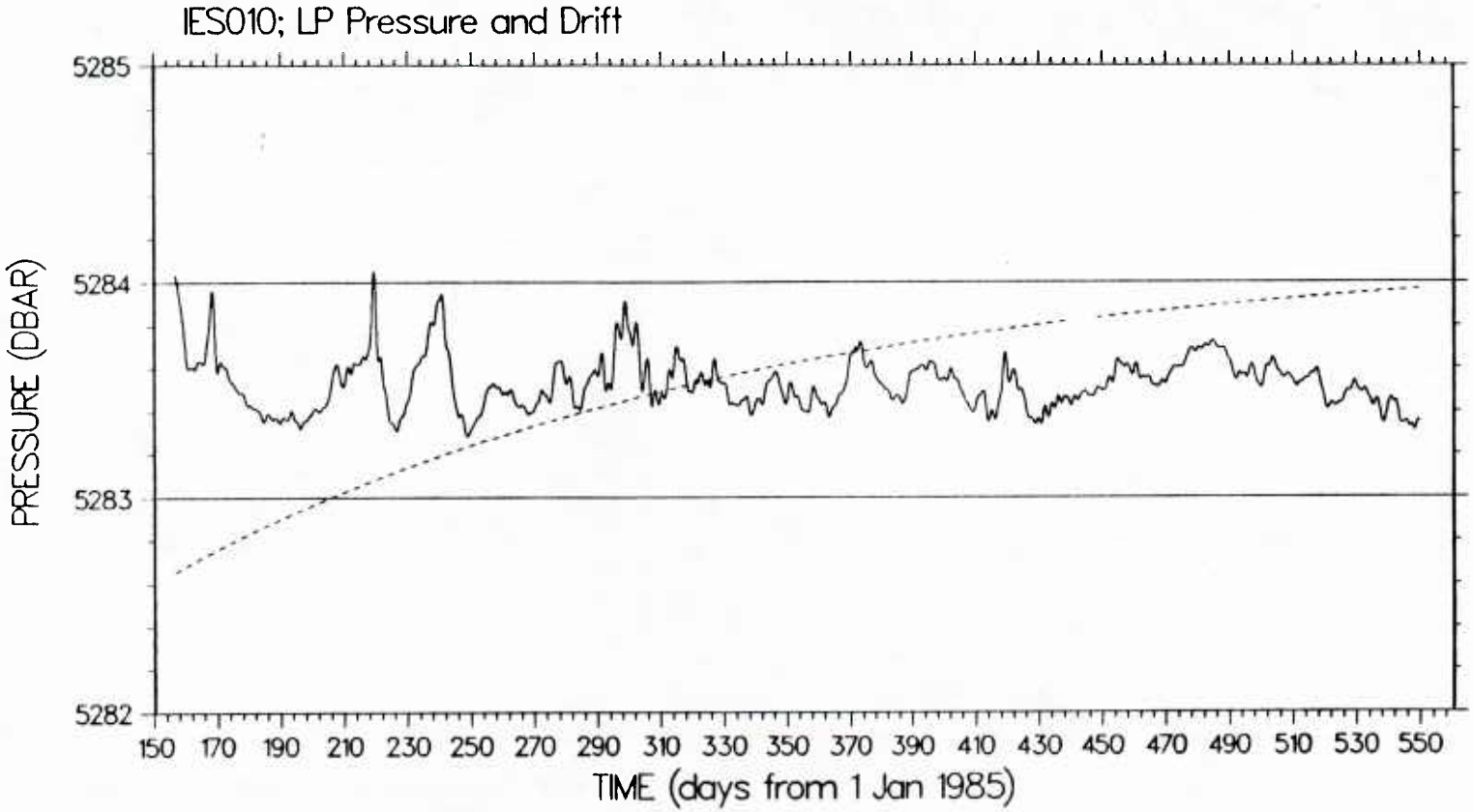

Figure 148. Pressure series (solid line) with periods shorter than 40 hours removed and exponential trend (dashed line) that was subtracted from the pressure series.

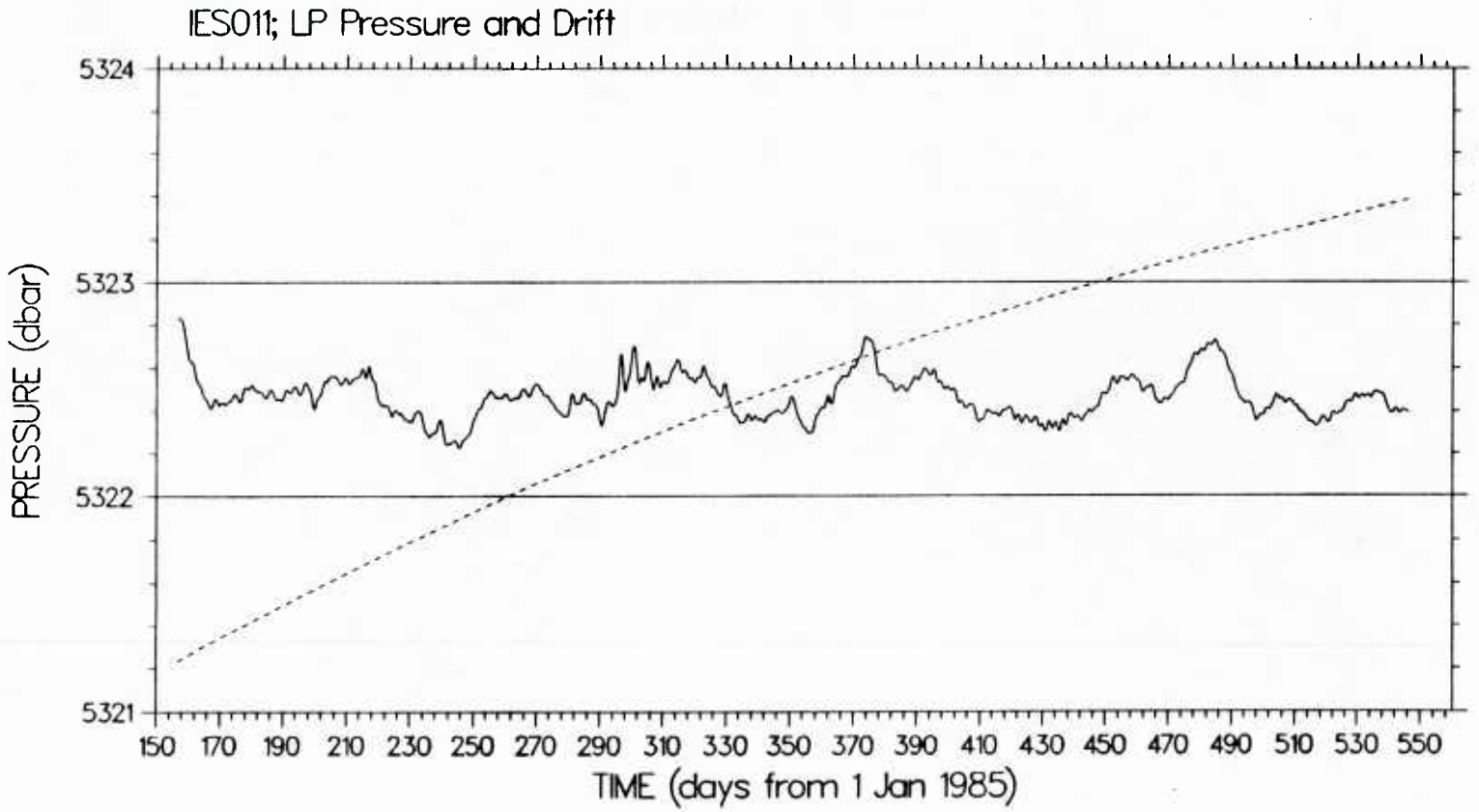

Figure 149. Pressure series (solid line) with periods shorter than 40 hours removed and exponential trend (dashed line) that was subtracted from the pressure series.

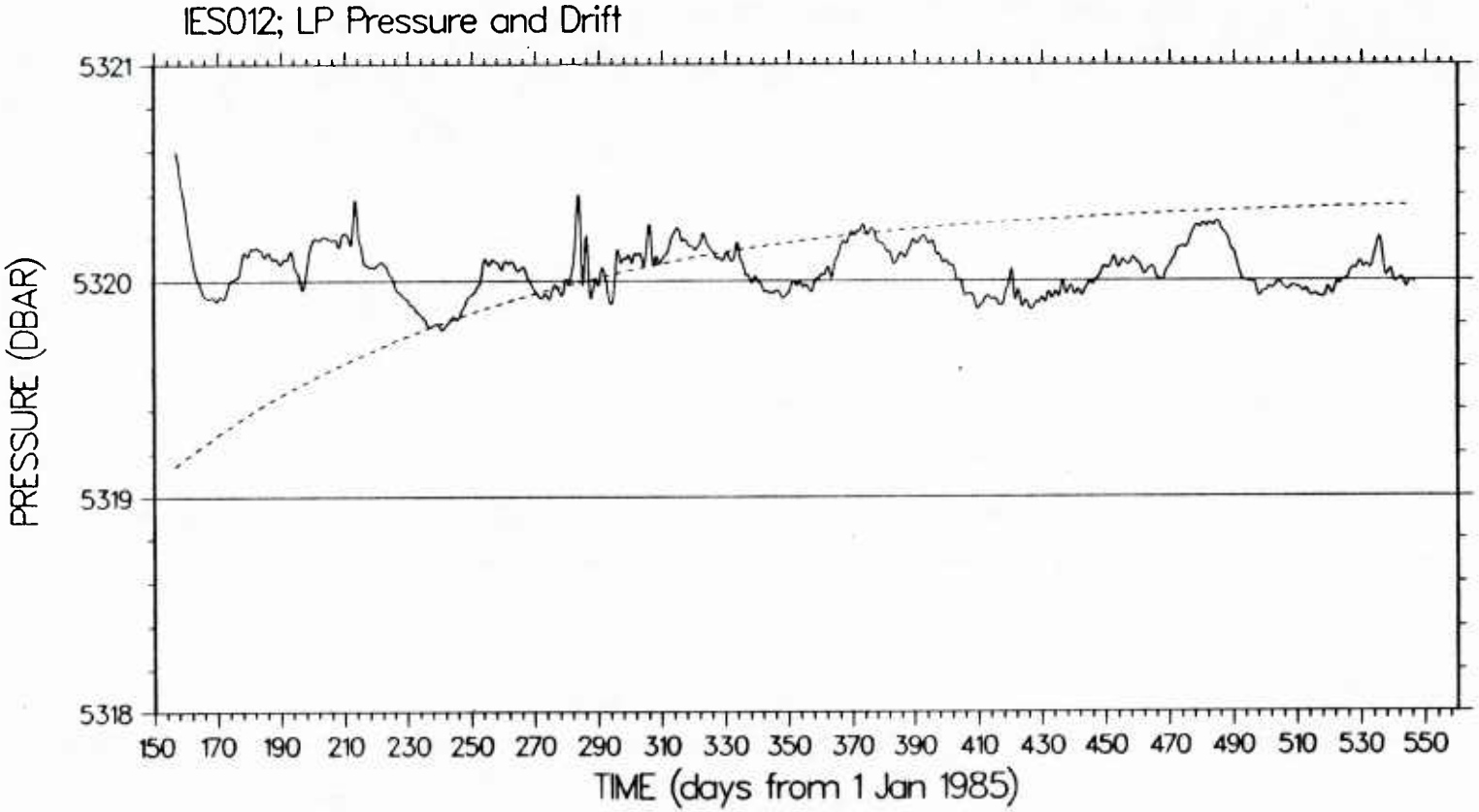

Figure 150. Pressure series (solid line) with periods shorter than 40 hours removed and exponential trend (dashed line) that was subtracted from the pressure series.

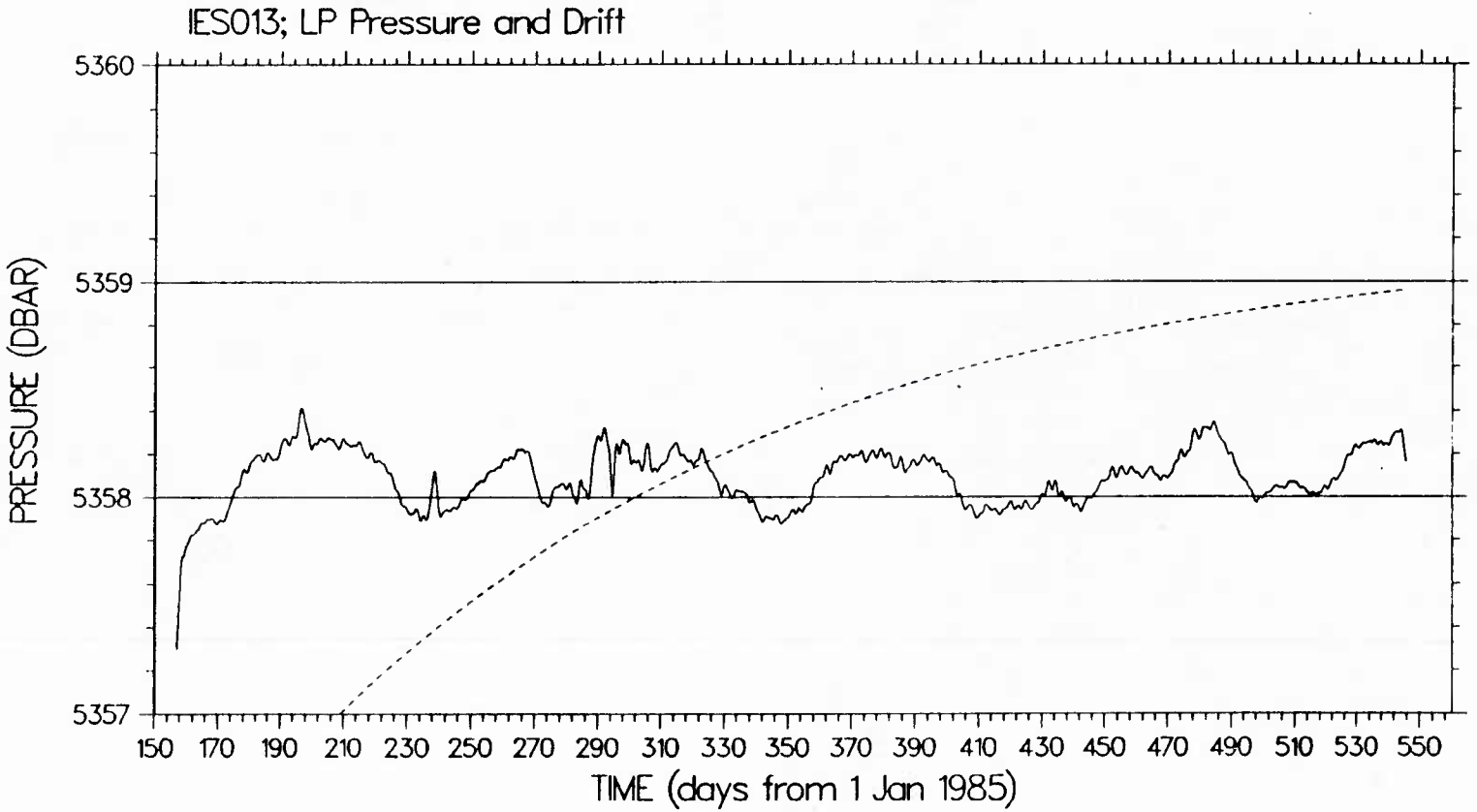

Figure 151. Pressure series (solid line) with periods shorter than 40 hours removed and exponential trend (dashed line) that was subtracted from the pressure series.

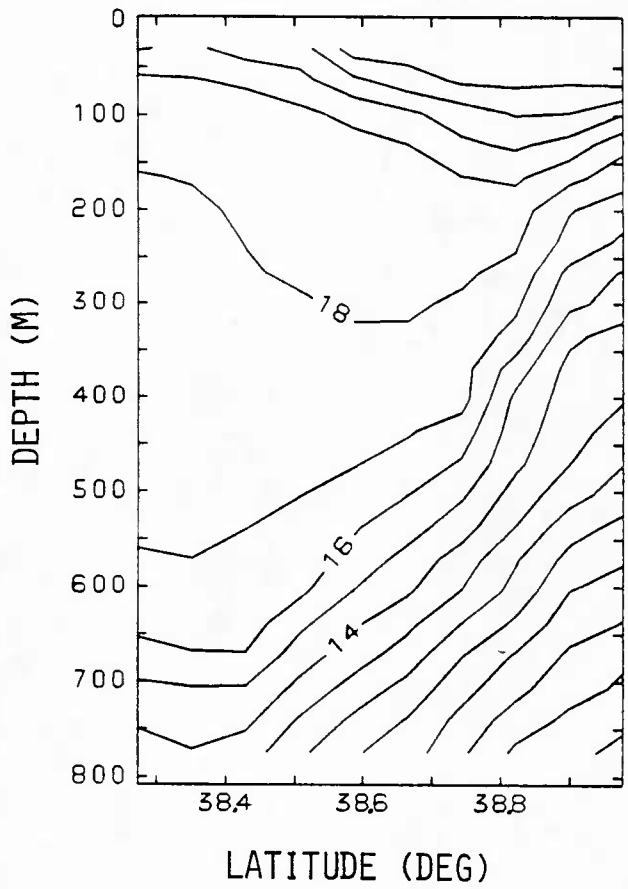

Figure 152. XBT section 1 (deployment cruise).

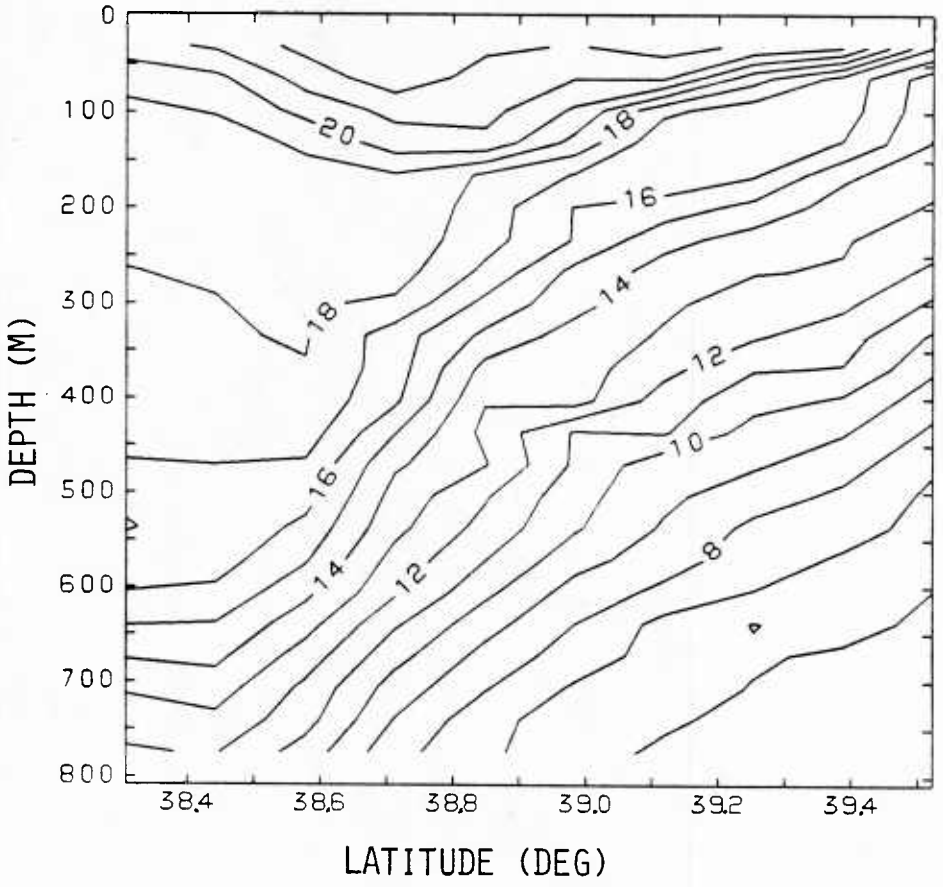

Figure 153. XBT section 2 (deployment cruise).

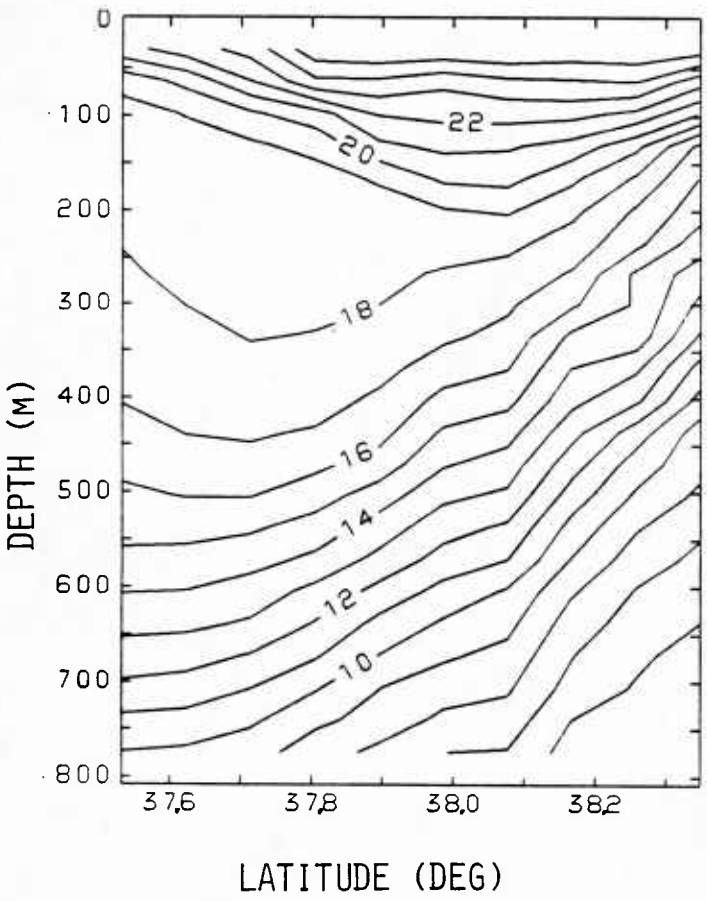

Figure 154. XBT section 3 (deployment cruise).

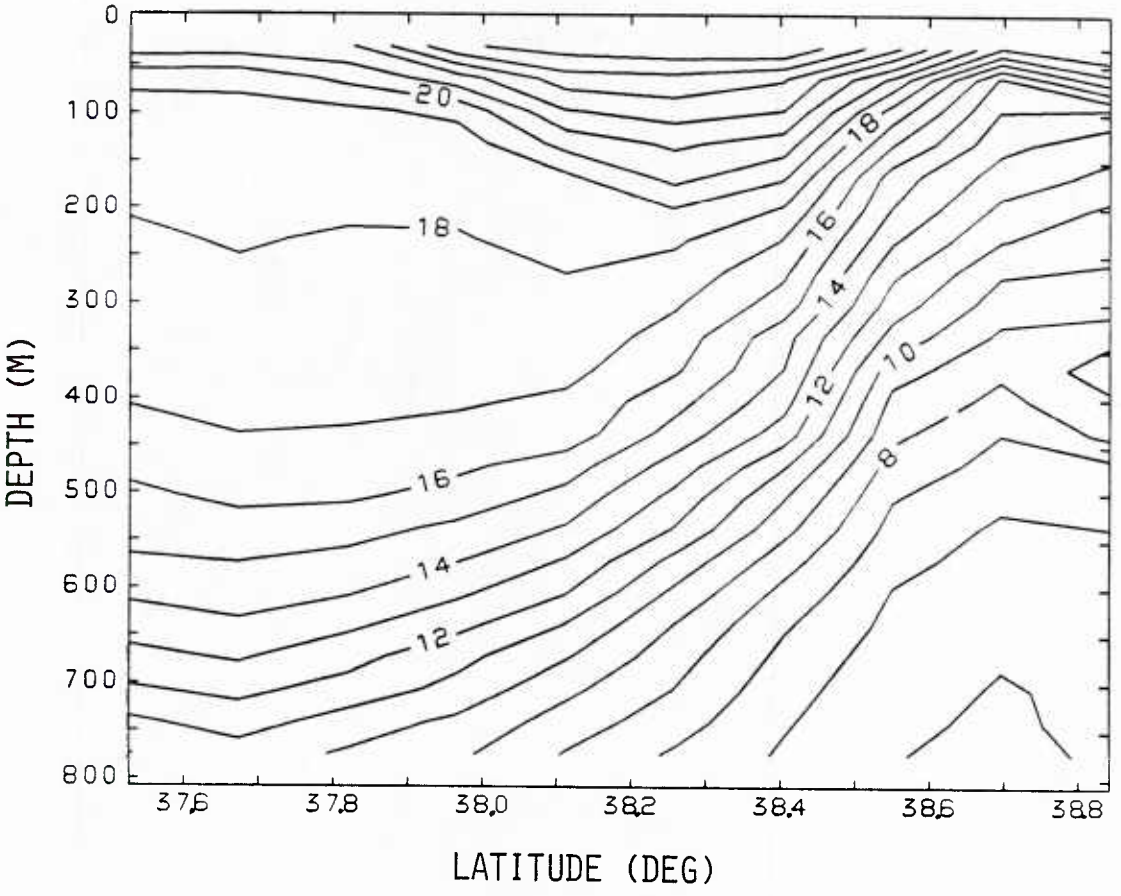

Figure 155. XBT section 4 (deployment cruise).